LANGLEY RESEARCH CENTER
3 1176 00504 3238

NASA-CR-167,041

NASA CR-167841
GDC-NAS-82-002

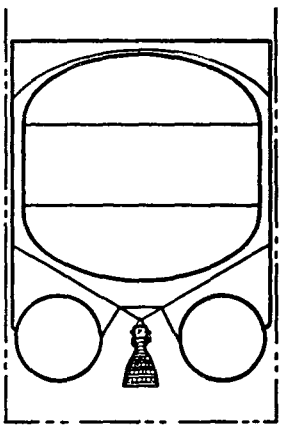

NASA-CR-167841
19820016412

LOW-THRUST CHEMICAL PROPULSION SYSTEM PROPELLANT EXPULSION AND THERMAL CONDITIONING STUDY

LIBRARY COPY

NF02679

GENERAL DYNAMICS
Convair Division

NASA CR-167841
GDC-NAS-82-002

LOW-THRUST CHEMICAL PROPULSION SYSTEM PROPELLANT EXPULSION AND THERMAL CONDITIONING STUDY

APRIL 1982

Prepared by

F Merino
I Wakabayashi
R L Pleasant
M Hill

for

National Aeronautics and Space Administration
LEWIS RESEARCH CENTER
21000 Brookpark Road
Cleveland, Ohio 44135

Under
Contract NAS3-22650

GENERAL DYNAMICS CONVAIR DIVISION
P O Box 80847
San Diego, California 92138

N82-24288#

1 Report No	2 Government Accession No	3 Recipient's Catalog No
CR 167841		

4 Title and Subtitle	5 Report Date
LOW-THRUST CHEMICAL PROPULSION SYSTEM PROPELLANT EXPULSION AND THERMAL CONDITIONING STUDY	April 1982
	6 Performing Organization Code
7 Author(s)	8 Performing Organization Report No
F Merino, I. Wakabayashi, R L. Pleasant, M. Hill	GDC-NAS-82-002
	10 Work Unit No
9 Performing Organization Name and Address	
General Dynamics Convair Division P O. Box 80847 San Diego, CA 92138	11 Contract or Grant No NAS3-22650
	13 Type of Report and Period Covered Contractor Report
12 Sponsoring Agency Name and Address	
NASA Lewis Research Center Cleveland, OH 44135	14 Sponsoring Agency Code

15 Supplementary Notes

Project Manager, J. C. Aydelott
Lewis Research Center, Cleveland, OH 44135

16 Abstract

Thermal conditioning systems for satisfying engine net positive suction pressure (NPSP) requirements, and propellant expulsion systems for achieving propellant dump during a return-to-launch-site (RTLS) abort were studied for LH_2/LO_2 and LCH_4/LO_2 upper stage propellant combinations A state-of-the-art thermal conditioning system employing helium injection beneath the liquid surface showed the lowest weight penalty for LO_2 and LCH_4. A new technology system incorporating a thermal subcooler (heat exchanger) for engine NPSP resulted in the lowest weight penalty for the LH_2 tank A preliminary design of two state-of-the-art and two new technology systems indicated a weight penalty difference too small to warrant development of a LH_2 thermal subcooler Analysis results showed that the LH_2/LO_2 propellant expulsion system is optimized for maximum dump line diameters, whereas the LCH_4/LO_2 system is optimized for minimum dump line diameter (LCH_4) and maximum dump line diameter (LO_2) The primary uncertainty is the accurate determination of two-phase flow rates through the dump system, experimentation was not recommended because this uncertainty is not considered significant

17 Key Words (Suggested by Author(s))	18 Distribution Statement
Heat Transfer, Pressurization, Propellant Expulsion, Thermodynamics, Venting	Unclassified - Unlimited

19 Security Classif (of this report)	20 Security Classif (of this page)	21 No of Pages	22 Price*
UNCLASSIFIED	UNCLASSIFIED	209	

* For sale by the National Technical Information Service Springfield Virginia 22161

NASA-C-168 (Rev 10-75)

This Page Intentionally Left Blank

FOREWORD

The following final report summarizes the technical effort conducted under Contract NAS3-22650 by the General Dynamics Convair Division from August 1980 to January 1982. The contract was administered by the National Aeronautics and Space Administration, Lewis Research Center, Cleveland, Ohio.

NASA/LeRC Program Manager - J. C. Aydelott

Convair Program Manager - F. Merino

Assisting - I. Wakabayashi, R. L. Pleasant, M. Hill

All data are presented with the International System of Units as the primary system and English Units as the secondary system. The English system was used for the basic calculations.

This Page Intentionally Left Blank

TABLE OF CONTENTS

Section			Page
1	INTRODUCTION		1-1
	1.1	SCOPE	1-1
	1.2	THERMAL CONDITIONING SYSTEM ANALYSES	1-3
	1.2.1	Tasks I and III	1-3
	1.2.2	Task II	1-3
	1.3	PRELIMINARY DESIGN/TECHNOLOGY REQUIREMENTS	1-3
	1.4	GROUND RULES	1-5
	1.4.1	Vehicle Configurations	1-5
	1.4.2	Vehicle Missions	1-5
	1.4.3	Main Engine Requirements	1-5
	1.4.4	Thermal Conditioning Systems Assumptions	1-7
	1.4.4.1	Propellant Settling	1-7
	1.4.4.2	Tank Pressure Control	1-7
	1.4.5	Abort Dump Systems Assumptions	1-8
	1.4.5.1	Shuttle/Centaur Experience	1-8
2	HELIUM PRESSURIZATION		2-1
	2.1	SYSTEM DESCRIPTION	2-1
	2.2	BACKGROUND/CAPABILITIES	2-1
	2.2.1	Propellant Heating Analysis	2-1
	2.2.1.1	Analytical	2-2
	2.2.1.2	Empirical	2-2
	2.2.2	Subsystem Development	2-3
	2.2.2.1	Analytical	2-3
	2.2.2.2	Empirical	2-3
	2.3	HELIUM PRESSURIZATION TECHNIQUES	2-3
	2.3.1	Bubbler Pressurization Mechanism	2-5
	2.3.1.1	Liquid Evaporation Model	2-6
	2.3.2	Bubbler Comparison with Ullage Injection	2-8
	2.4	AMBIENT/CRYOGENIC HELIUM STORAGE	2-9
	2.4.1	Mission Helium Usages	2-10

TABLE OF CONTENTS (CONT)

Section			Page
	2.4.1.1	Main Engine Start	2-10
	2.4.1.2	Engine Burn	2-12
	2.4.1.3	Pressurization System Weight	2-13
	2.5	TYPICAL MISSION ANALYSIS	2-13
	2.5.1	LH_2 Tank System Analysis	2-13
	2.5.1.1	LH_2 Propellant Vapor Pressures	2-13
	2.5.1.2	LH_2 Tank Peak Pressures	2-17
	2.5.1.3	Hydrogen Vent Masses	2-17
	2.5.1.4	Hydrogen Vapor Residuals	2-19
	2.5.1.5	Total Helium Pressurization Thermal Conditioning System Weight Penalty	2-19
	2.5.2	LO_2 Tank System Analysis	2-19
	2.5.2.1	LO_2 Propellant Vapor Pressures	2-19
	2.5.2.2	LO_2 Tank Peak Pressures	2-22
	2.5.2.3	Oxygen Vent Masses	2-22
	2.5.2.4	Oxygen Vapor Residuals	2-22
	2.5.2.5	Total System Weight Penalty	2-22
	2.5.3	LCH_4 Tank System Analysis	2-22
	2.5.3.1	Total System Weight Penalty	2-25
3	THERMAL SUBCOOLERS		3-1
	3.1	SYSTEM DESCRIPTION	3-1
	3.2	SUBCOOLER SIZING	3-1
	3.2.1	Subcooler Configurations	3-1
	3.2.1.1	Elliptical Aft Bulkhead	3-3
	3.2.1.2	Toroidal Tank	3-3
	3.2.2	Heat Removal Requirements	3-3
	3.2.2.1	Elliptical Bulkhead Subcooler Sizing Approach	3-5
	3.2.3	Cold-Side Flow Requirements	3-14
	3.2.3.1	Coolant Dump Option	3-16
	3.2.3.2	Coolant Return to Liquid	3-19
	3.2.3.3	Coolant Return to Ullage	3-21

TABLE OF CONTENTS (CONT)

Section			Page
	3.3	TYPICAL MISSION ANALYSIS	3-21
	3.3.1	LH_2 Tank System Analysis	3-24
	3.3.1.1	LH_2 Propellant Vapor Pressures	3-24
	3.3.1.2	Peak Tank Pressures	3-27
	3.3.1.3	Hydrogen Vent Mass	3-27
	3.3.1.4	Hydrogen Vapor Residuals	3-27
	3.3.1.5	Total Thermal Subcooler Thermal Conditioning System Weight Penalties	3-27
	3.3.2	LO_2 and LCH_4 Tank System Analyses	3-30
	3.3.2.1	Subcooler Influence Upon Ventage and Vapor Residuals	3-30
	3.3.2.2	Total System Weight Penalty	3-30
4	AUTOGENOUS PRESSURIZATION		4-1
	4.1	ENGINE START PRESSURIZATION	4-1
	4.1.1	Ambient Helium Storage	4-1
	4.1.2	Cryogenic Helium Storage	4-2
	4.1.3	Thermal Subcooler for Engine Start	4-2
	4.2	TYPICAL MISSION ANALYSIS	4-3
	4.2.1	LH_2 Tank System Analysis	4-3
	4.2.1.1	LTPS Mission Propellant Vapor Pressure	4-3
	4.2.1.2	Hydrogen Vent Masses	4-5
	4.2.1.3	Hydrogen Vapor Residuals	4-6
	4.2.1.4	Total Autogenous Thermal Conditioning System Weight Penalties	4-6
	4.2.2	LO_2 and LCH_4 Tank System Analyses	4-7
	4.2.2.1	Total System Weight Penalties	4-9
	4.2.2.2	Liquid-Ullage Coupling for LH_2 Tank Autogenous Pressurization	4-11
5	THERMAL CONDITIONING SYSTEMS COMPARISON		5-1
	5.1	LH_2 THERMAL CONDITIONING SYSTEMS	5-1
	5.1.1	State-of-the-Art Systems	5-1

TABLE OF CONTENTS (CONT)

Section			Page
	5.1.2	New Technology Systems	5-1
	5.1.3	Recommended Systems	5-2
	5.2	LO_2 THERMAL CONDITIONING SYSTEMS	5-2
	5.3	LCH_4 THERMAL CONDITIONING SYSTEMS	5-4
	5.4	LTPS RECOMMENDATIONS	5-4
6	PRELIMINARY DESIGN OF SELECTED THERMAL CONDITIONING SYSTEMS		6-1
	6.1	SYSTEMS SELECTION	6-1
	6.1.1	LO_2 Tank System	6-2
	6.1.2	LH_2 Tank Systems	6-2
	6.2	THERMAL CONDITIONING SYSTEM 1	6-2
	6.2.1	System Design	6-3
	6.2.1.1	Vehicle-Mounted Hardware	6-3
	6.2.2	System Weight Penalties	6-4
	6.2.2.1	Hardware Weight	6-4
	6.2.2.2	Helium Supply System Weight	6-4
	6.2.2.3	Ventage and Vapor Residuals	6-4
	6.2.2.4	Total Weight Penalty	6-4
	6.2.3	LTPS Weight Penalty at Zero NPSP	6-4
	6.3	THERMAL CONDITIONING SYSTEM 2	6-8
	6.3.1	System Schematic	6-8
	6.3.1.1	Vehicle-Mounted Hardware	6-9
	6.3.2	System Weight Penalties	6-9
	6.4	THERMAL CONDITIONING SYSTEM 3	6-10
	6.4.1	System Design	6-10
	6.4.1.1	Vehicle-Mounted Hardware	6-14
	6.4.1.2	Thermal Subcooler	6-14
	6.4.2	System Weight Penalties	6-18
	6.5	THERMAL CONDITIONING SYSTEM 4	6-18
	6.5.1	System Design	6-18
	6.5.2	System Weight Penalties	6-18
	6.6	THERMAL CONDITIONING SYSTEMS COMPARISON	6-20

TABLE OF CONTENTS (CONT)

Section		Page
7	LTPS ABORT PRESSURIZATION REQUIREMENTS	7-1
	7.1 ABORT GUIDELINES AND REQUIREMENTS	7-1
	7.1.1 LTPS/Shuttle Abort Modes	7-1
	7.1.2 Analytical Tools	7-3
	7.1.3 Shuttle Operational and Safety Requirements	7-3
	7.1.4 Return to Launch Site (RTLS) Abort Requirements	7-5
	7.1.5 LTPS Abort Dump Fluid Systems	7-5
	7.1.5.1 Helium Pressurization System	7-5
	7.1.5.2 Abort Propellant Dump System	7-5
	7.2 ABORT PROPELLANT EXPULSION	7-9
	7.2.1 Abort Pressurization Technique	7-10
	7.2.1.1 Helium Mass Requirements	7-10
	7.2.1.2 Abort Dump Flow Rates	7-15
	7.2.2 Dump System Selection	7-17
	7.2.2.1 Configuration 3 System Selection	7-19
	7.2.2.2 Configuration 1 System Selection	7-19
	7.3 POST-PROPELLANT DUMP HELIUM USAGES	7-19
	7.3.1 Propellant Tank Inerting	7-20
	7.3.2 Helium Purge Requirements	7-20
	7.4 TOTAL ABORT DUMP SYSTEM WEIGHT	7-20
8	TECHNOLOGY EVALUATION	8-1
	8.1 TECHNOLOGY REQUIREMENTS	8-1
	8.1.1 Thermal Conditioning Systems	8-1
	8.1.1.1 System 1	8-1
	8.1.1.2 System 2	8-2
	8.1.1.3 Systems 3 and 4	8-2
	8.1.2 Abort Expulsion Systems	8-3
	8.2 TECHNOLOGY PLAN	8-4
	8.2.1 Heat Exchanger Development	8-4
	8.2.1.1 Heat Exchanger Concept	8-4
	8.2.1.2 Zero-G Testing	8-7

TABLE OF CONTENTS (CONT)

Section		Page
	8.2.2 Systems Tests	8-7
	8.2.2.1 Engine Start Transient	8-7
	8.2.2.2 Engine Inlet NPSP Controls	8-7
9	SUMMARY OF RESULTS	9-1
10	CONCLUSIONS AND RECOMMENDATIONS	10-1
11	SYMBOLS	11-1
12	REFERENCES	12-1
Appendix		
A	HYPRS COMPUTER PROGRAM	A-1

LIST OF FIGURES

Figure		Page
1-1	Representative LTPS Vehicle Configuration	1-2
1-2	Tasks I and III Interaction Required Concurrent Scheduling	1-4
2-1	Helium Pressurization System	2-2
2-2	LO_2 Tank Bubbler Injection	2-4
2-3	LH_2 Tank Ullage Injection	2-4
2-4	Less Helium is Required by Using a Bubbler Beneath the LO_2 Surface	2-5
2-5	Bubbler Pressurization Versus Ullage Injection Helium Mass Usage Comparison	2-9
2-6	LH_2 Tank Mission Helium Usages for Ullage Injection . . .	2-11
2-7	LO_2 Tank Engine Start Total Helium Usage (Vapor at TVS Inlet)	2-12
2-8	Total Mission Helium Usages for LO_2 Tank and LCH_4 Tank Bubbler Pressurization	2-14
2-9	Total Pressurization System Weights for Helium Pressurization	2-16
2-10	Ambient Helium Pressurization System Influence Upon LH_2 Vapor Pressure (Configuration 1)	2-16
2-11	Peak LH_2 Tank Pressure During LTPS Mission for Helium Pressurization	2-18
2-12	LH_2 Tank Helium Pressurization System Weight Penalties (Configuration 1)	2-18
2-13	NPSP Influence Upon LO_2 Vapor Pressure During Mission (Configuration 1)	2-20
2-14	Bubbler Pressurization System and Space Heating Influence Upon LO_2 Vapor Pressure (Configurations 3 and 4)	2-21
2-15	Peak LO_2 Tank Pressure During LTPS Missions for Helium Bubbler Pressurization	2-23
2-16	LO_2 Tank Bubbler Pressurization System Weight Penalties (Configuration 1)	2-23
2-17	LO_2 Tank Bubbler Pressurization System Weight Penalties (Configuration 4)	2-24
2-18	Bubbler Pressurization System and Space Heating Influence Upon LCH_4 Vapor Pressures (Configurations 3 and 4) . . .	2-24
2-19	LCH_4 Tank Bubbler Pressurization System Weight Penalties (Configuration 3)	2-25

LIST OF FIGURES (CONT)

Figure		Page
2-20	LCH_4 Tank Bubbler Pressurization System Weight Penalties (Configuration 4)	2-26
3-1	The Thermal Subcooler Supplies Subcooled Propellants to the Engines	3-2
3-2	Throttling Provides the Low Temperature Fluid for the Heat Exchanger	3-2
3-3	General Dynamics Subcooler Design Used as Basis for Elliptical Bulkhead Subcoolers of this Study	3-4
3-4	Toroidal Tank Subcooler Located in Outlet Tubing	3-4
3-5	Fin Efficiency in LH_2 Subcooler (Hot-Side Flow Radially Outwards)	3-6
3-6	LH_2 Subcooler Hot-Side Heat Transfer Coefficient (Flow Radially Outward)	3-9
3-7	LH_2 Subcooler Hot-Side Heat Transfer Coefficient, Flow Radially Inward, Passage Height H = 0.25 cm (0.10 in.)	3-9
3-8	Integrated Heat Transfer Coefficient x Area (Including Fin Contribution), LH_2 Flow Radially Inward, Passage Height H = 1.72 cm (0.50 in.)	3-10
3-9	Thermal Subcooler Coolant Flow Rates for LTPS Missions	3-17
3-10	Thermal Subcooler Fuel Tank Coolant Dump Mass for LTPS Mission	3-18
3-11	Thermal Subcooler LO_2 Tank Coolant Dump Mass for LTPS Mission	3-18
3-12	Subcooler Heat Transfer and Pump Power Are Added to Cold-Side Fluid	3-20
3-13	Propellant Heating Rates Caused by Coolant Return Flow Rates	3-22
3-14	Engine NPSP Can Benefit From Thermal Subcooler Having Coolant Return to Ullage	3-23
3-15	Subcooler Influence Upon LH_2 Vapor Pressure (Configuration 1)	3-25
3-16	Subcooler Influence Upon LH_2 Vapor Pressure (Coolant Return-to-Ullage, Configuration 1)	3-25
3-17	NPSP Influence Upon LH_2 Vapor Presure During Burn No. 9 (Subcooler)	3-26
3-18	Peak LH_2 Tank Pressure During LTPS Mission for Thermal Subcoolers	3-28

LIST OF FIGURES (CONT)

Figure		Page
3-19	LH_2 Tank Subcooler System Weight Penalties (Coolant Dump, Configuration 1)	3-28
3-20	LH_2 Tank Subcooler System Weight Penalties (Coolant Return to Liquid, Configuration 1)	3-29
3-21	LH_2 Tank Subcooler System Weight Penalties (Coolant Return to Ullage, Configuration 1)	3-29
3-22	Thermal Subcooler System Influence Upon LH_2 Tank Ventage and Vapor Residuals (Configuration 1)	3-31
3-23	Thermal Subcooler System Influence Upon LO_2 Tank Ventage and Vapor Residuals (Configuration 3)	3-31
3-24	Thermal Subcooler System Influence Upon LCH_4 Tank Ventage and Vapor Residuals (Configuration 3)	3-32
3-25	Thermal Subcooler System Influence Upon LO_2 Tank Ventage and Vapor Residuals (Configuration 4)	3-32
3-26	Thermal Subcooler System Influence Upon LCH_4 Tank Ventage and Vapor Residuals (Configuration 4)	3-33
3-27	LO_2 Tank Subcooler System Weight Penalties (Coolant Dump, Configuration 3)	3-33
3-28	LO_2 Tank Subcooler System Weight Penalties (Coolant Return to Liquid, Configuration 3)	3-34
3-29	LO_2 Tank Subcooler System Weight Penalties (Coolant Return to Ullage, Configuration 3)	3-34
3-30	LO_2 Tank Subcooler System Weight Penalties (Coolant Return to Liquid, Configuration 4)	3-35
4-1	Autogenous Pressurization System (with Helium for Engine Start Pressurization)	4-2
4-2	Autogenous Pressurization System Influence Upon LH_2 Vapor Pressure (Ullage Injection/Autogenous, Configuration 1)	4-4
4-3	Autogenous Hydrogen Temperature Influence Upon Vent Mass	4-6
4-4	Autogenous Hydrogen Temperature Influence Upon Vapor Residual	4-7
4-5	LH_2 Tank Autogenous System Weight Penalties (Ullage Injection/Autogenous, Configuration 1)	4-8
4-6	LH_2 Tank Autogenous System Weight Penalties (Subcooler/Autogenous, Configuration 1)	4-8
4-7	Autogenous Pressurization System Influence Upon LO_2 Vapor Pressure (Bubbler/Autogenous, Configuration 3)	4-9

LIST OF FIGURES (CONT)

Figure		Page
4-8	LO_2 Tank Autogenous System Weight Penalties (Bubbler/ Autogenous, Configuration 3)	4-10
4-9	LO_2 Tank Autogenous System Weight Penalties (Bubbler/ Autogenous, Configuration 4)	4-10
4-10	LCH_4 Tank Autogenous System Weight Penalties (Bubbler/ Autogenous, Configuration 3)	4-12
4-11	LCH_4 Tank Autogenous System Weight Penalties (Bubbler/ Autogenous, Configuration 4)	4-12
4-12	Uniform Ullage Temperatures Were Assumed in Determining Ullage-to-Liquid Heat Rates	4-13
4-13	Comparison of Free Convection Versus Conduction Heating at LH_2 Surface	4-15
4-14	Vapor Pressure Rise Due to LH_2 Surface Heating	4-15
5-1	Comparison of LH_2 Tank Thermal Conditioning Systems (Configuration 1)	5-2
5-2	Comparison of LO_2 Tank Thermal Conditioning Systems (Configuration 1)	5-3
5-3	Comparison of LO_2 Tank Thermal Conditioning Systems (Configuration 4)	5-3
5-4	Comparison of LCH_4 Tank Thermal Conditioning Systems (Configuration 3)	5-5
5-5	Comparison of LCH_4 Tank Thermal Conditioning Systems (Configuration 4)	5-5
5-6	Weight Penalties for Recommended LH_2/LO_2 Thermal Conditioning Systems (Configuration 1)	5-6
5-7	Weight Penalties for Recommended LCH_4/LO_2 Thermal Conditioning Systems (Configuration 3)	5-6
6-1	Thermal Conditioning System No. 1	6-5
6-2	Thermal Conditioning System 1 Weight Penalty (LO_2: Bubbler/LH_2: Helium)	6-9
6-3	Thermal Conditioning System No. 2	6-11
6-4	Thermal Conditioning System 2 Weight Penalties	6-13
6-5	Thermal Conditioning System No. 3	6-15
6-6	LH_2 Thermal Subcooler	6-17
6-7	Thermal Conditioning System 3 Weight Penalties	6-20
6-8	Thermal Conditioning System No. 4	6-21

LIST OF FIGURES (CONT)

Figure		Page
6-9	Thermal Conditioning System 4 Weight Penalties	6-24
6-10	Thermal Conditioning Systems Weight Penalty Comparison . .	6-20
7-1	Our Centaur-in-Shuttle Study Resolved All Interface Problems Related to Centaur/Shuttle Abort	7-2
7-2	Propellant Settling During RTLS Abort Will Be Provided by SSME Thrust	7-2
7-3	Abort Dump Helium Pressurization System for Shuttle/ Centaur	7-4
7-4	Abort Propellant Dump System for Shuttle/Centaur	7-4
7-5	Abort Dump Analysis Employed Realistic Shuttle G-Levels .	7-6
7-6	Hydrogen Dump Line Schematic	7-7
7-7	Oxygen Dump Line Schematic	7-8
7-8	Abort Propellant Line Weights Were Included in a Total System Optimization Analysis	7-9
7-9	Helium Bubbler Pressurization Influence Upon LO_2 Vapor Pressure During Abort Dump	7-11
7-10	Abort Dump Helium Mass Usages	7-11
7-11	LCH_4 and LO_2 Tank Abort Dump System Weight Optimization (Configuration 3)	7-13
7-12	LO_2 Abort Dump System Optimization (Configuration 1) . . .	7-13
7-13	LH_2/LO_2 Abort Dump System Optimization (Configuration 1) .	7-14
7-14	Line Diameter Requirements for Propellant Dump	7-17
7-15	Abort Dump Line Weights	7-18
8-1	Phase Distribution of the Evaporating Process is Affected by Curved Channels	8-5
8-2	Phase Distributions in a Two-Phase Flow in a Curved Channel	8-6
A-1	Flow Chart of Subroutines Used by HYPRS	A-4

This Page Intentionally Left Blank

LIST OF TABLES

Table		Page
1-1	Low-Thrust Propulsion System (LTPS) Configurations	1-6
1-2	LTPS Mission Engine Burn and Coast Durations	1-7
2-1	Helium System Weight for Propellant Tank Pressurization	2-15
3-1	Subcooler Required Heat Removal Rate	3-6
3-2	Required LH_2 Single-Pass Subcooler Radius for Elliptical Aft Bulkhead Tanks	3-12
3-3	Required LH_2 Multiple-Pass Subcooler Radius for Elliptical Aft Bulkhead Tanks	3-12
3-4	Torus Tank Subcooler Length	3-14
3-5	Selected Thermal Subcooler Weights	3-15
6-1	Selected Thermal Conditioning Systems	6-1
6-2	Pressurization System Hardware Weights	6-7
6-3	System 1 Helium Supply Weights	6-8
6-4	System 2 Helium Supply Weights	6-10
6-5	Cryogenic Helium Storage Conditions	6-13
6-6	System 3 Helium Supply Weights	6-19
6-7	Hydrogen Thermal Subcooler Weights (Coolant Dump Configuration)	6-19
6-8	Hydrogen Thermal Subcooler Weights (Coolant Return-to-Ullage)	6-23
6-9	LTPS Fill, Dump, Drain and Ground Vent System Weights	6-25
7-1	Procedure for Determining Abort Helium Pressurization System Weight	7-12
7-2	Weight Tabulation of Abort Dump Line Components for Shuttle/Centaur	7-18
7-3	Tank Inerting Sequence of Events	7-21
7-4	RTLS Abort Helium Mass Usage Requirement	7-21
7-5	LTPS Abort Dump System Total Weights	7-22
A-1	Namelist TANK Input	A-5
A-2	Namelist TNKDIM Input	A-9
A-3	Namelist GASPRP Input	A-13
A-4	Namelist CASE Input	A-14
A-5	Namelist HELIUM Input	A-18
A-6	Namelist PHASE Input	A-21

This Page Intentionally Left Blank

SUMMARY

This study determined preferred techniques for providing abort pressurization and engine feed system net positive suction pressure (NPSP) for low-thrust chemical orbit-to-orbit propulsion systems (LTPS). The relative benefits and weight penalties of each technique and any required technology advances were determined. There were two major study areas: propellant expulsion systems for achieving propellant dump during a return-to-launch-site (RTLS) abort, and thermal conditioning systems for satisfying engine NPSP requirements.

Thermal conditioning techniques considered for providing main engine NPSP during engine start and steady-state operation included a) helium pressurization, b) thermal subcoolers (heat exchangers), and c) autogenous pressurization for steady-state engine burn with helium pressurization or thermal subcoolers for start-up. Parametric analyses were performed to obtain pressurant mass, hardware weights, ventage, and vapor residuals as a function of engine NPSP. Total system weight penalties were obtained for two LH_2/LO_2 stages with multi-layer insulation (MLI) and two LCH_4/LO_2 stages, one with MLI and the other with spray-on foam insulation (SOFI).

Major results include the following:

1. A state-of-the-art system, incorporating bubbler (helium injection beneath liquid surface) pressurization, was found to be the best for LO_2 and LCH_4, regardless of technology. It showed the lowest system weight penalty over the entire engine NPSP range.

2. A new technology system incorporating a subcooler for engine NPSP resulted in the lowest weight penalty for the liquid hydrogen tank.

3. Vent mass penalties due to the higher heating rates of a SOFI system were significantly greater than for the MLI system.

Following the parametric analysis, four systems, listed below, were selected for a preliminary design effort. Weight penalties were determined for NPSP levels up to 6.9 kpa (1.0 psid) and 13.8 kpa (2.0 psid), respectively, for the LH_2 and LO_2 sides. A weight penalty difference of 18 to 32 kg (40 to 70 lb) was found between state-of-the-art (1 and 2) and new technology (3 and 4) systems.

Thermal Conditioning Systems Selected for Preliminary Design

System	LO_2 Tank Engine Start/Engine Burn	LH_2 Tank Engine Start/Engine Burn
1	Bubbler/Bubbler	Helium/Autogenous
2	Same as 1, except for cryogenic storage of helium	
3	Bubbler/Bubbler	Subcooler/Autogenous
4	Bubbler/Bubbler	Subcooler/Subcooler

The only new technology identified for thermal conditioning systems was the heat exchanger portion of the LH_2 thermal subcooler. It was recommended that LH_2 thermal subcooler development not be pursued because the potential weight gain at low engine NPSPs is not significant. This recommendation is based on the premise that a low NPSP engine system is an achievable goal.

Propellant dump during Shuttle/LTPS abort modes was studied for purposes of identifying an LTPS propellant expulsion system, which consists of a helium pressurization system and an abort propellant dump system. Helium pressurization for propellant expulsion was the only technique considered for this analysis. Analysis results show that the LH_2/LO_2 system is optimized for minimum pressurization ΔP levels, which means increasing dump system line sizes to the maximum diameter possible. For the LCH_4/LO_2 system, the LO_2 side optimized at the minimum tank ΔP while the LCH_4 side optimized at the maximum tank ΔP. It was determined that the LCH_4/LO_2 total system mass would be about 182 kg (400 lb) lighter than the LH_2/LO_2 system mass of 584 kg (1288 lb).

An assessment of the propellant expulsion system revealed that the primary uncertainty is whether "shifting" equilibrium or "frozen" equilibrium conditions will exist as propellant is dumped to a near-vacuum condition. An experimental program was not recommended because this uncertainty should not have a major impact upon LTPS performance.

1

INTRODUCTION

Space missions planned for the mid-1980s and beyond will require increased Space Shuttle upperstage capability for placing Large Space Systems (LSS) in orbit. In concept, a lightweight structure will consist of a space platform on which would be mounted solar cells, antenna elements, computer systems and sensors appropriate to a specific mission. These LSS generate orbital transfer vehicle requirements considerably different from those for current vehicles. For example, transfer of an already assembled LSS from orbit-to-orbit requires a very low acceleration propulsion system, approximately 0.05 g compared to the nearly 5 g maximum acceptable for current payloads. These low acceleration requirements can be met with low-thrust chemical propulsion systems (LTPS) having multiple-burn capability.

Recent studies (References 1-1 and 1-2) have been conducted to define and size LTPS configurations. Emphasis was placed on describing general vehicle requirements rather than on detailed evaluations of specific subsystems. The purpose of this study was to perform such a detailed evaluation of LTPS propellant expulsion and thermal conditioning subsystems. Specifically, the primary study objective was to determine preferred techniques for providing abort pressurization and engine feed system net positive suction pressure (NPSP) for LTPS. The relative benefits of each technique and any required technology advances would be identified during the 12-month study period. A representative LTPS vehicle configuration (identified by the Reference 1-1 study) is given in Figure 1-1.

1.1 SCOPE

This study was conducted in two phases consisting of six major tasks. During phase one parametric analyses were performed to obtain pressurant mass, hardware weights, residuals and other payload penalties associated with each propellant expulsion and thermal conditioning system. At the completion of this phase, the NASA-LeRC selected four thermal conditioning systems for preliminary design.

The second phase of this study required that a preliminary design be performed on each of the selected thermal conditioning systems. Hardware size and weight was estimated from these designs for a final subsystem comparison. Additionally, a technology evaluation was performed for each system.

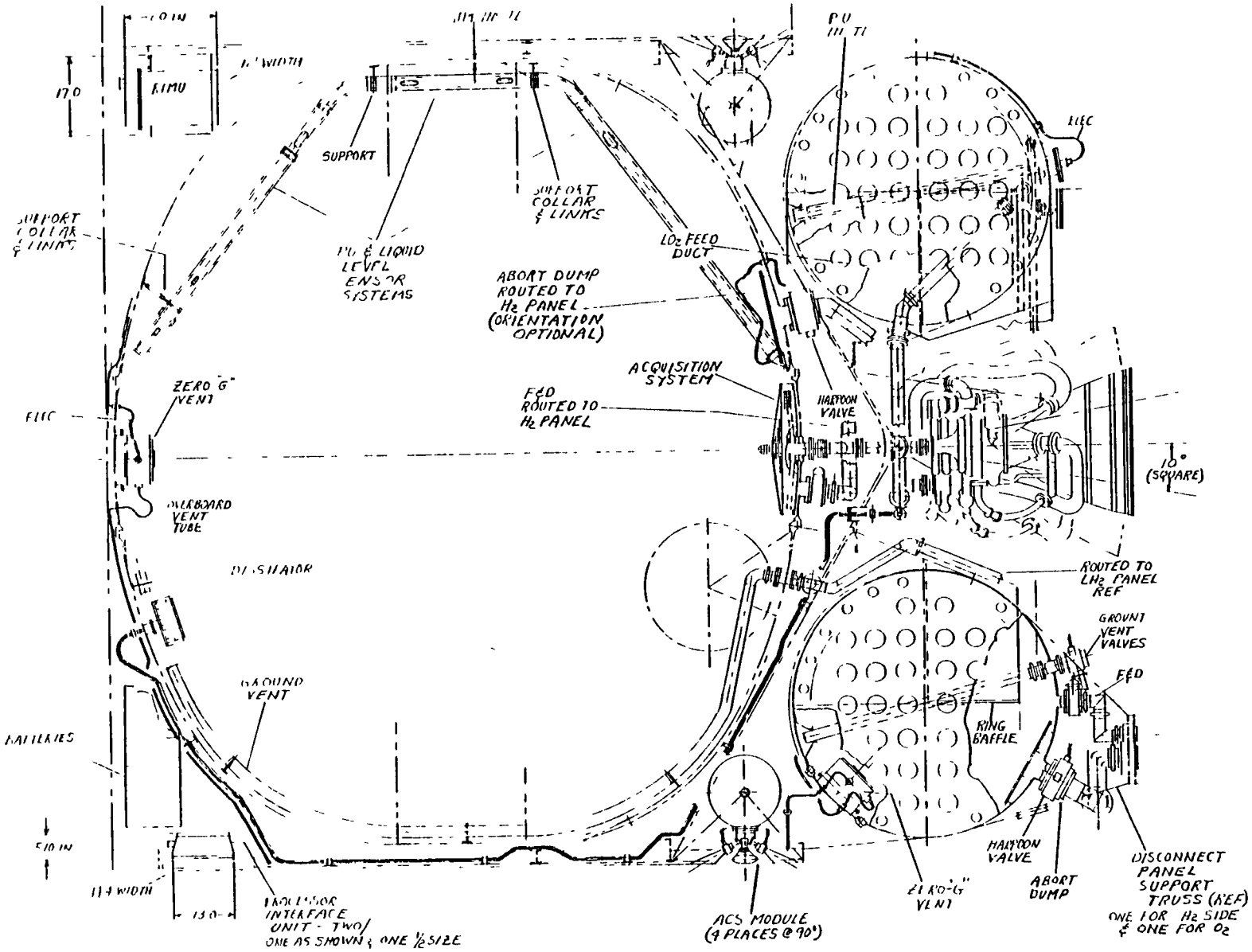

Figure 1-1. Representative LTPS Vehicle Configuration.

1.2 THERMAL CONDITIONING SYSTEM ANALYSES

The three major analysis tasks of this first study phase included:

Task I - Propellant heating analysis.

Task II - Pressurant requirements for abort propellant dump.

Task III - Comparative analysis of pressurization techniques and thermal subcoolers.

The interaction between Tasks I and III necessitated concurrent scheduling, Figure 1-2. In contrast, Task II was performed independently, with only minimal influence from the vehicle-mounted thermal conditioning system.

1.2.1 TASKS I AND III. In Task I we performed propellant tank thermodynamic analyses to establish tank pressure and propellant temperature histories as a function of time during a typical mission. Tankage configurations, heating rates and mission profiles were provided by NASA (Section 1.4). The LTPS mission conditions of low acceleration during engine burns, low propellant flow rates and long engine burn durations were analyzed to assess the influence of each upon vapor residuals and vapor vent masses.

Because it was known that the method of thermal conditioning could have an even greater influence on the propellant thermodynamic state than tank heating, Tasks I and III were conducted concurrently. The thermal conditioning techniques considered for providing main engine NPSP during engine start and steady-state operation included:

a. Helium pressurization (ambient and cryogenic temperature).

b. Thermal subcoolers (heat exchangers).

c. Autogenous pressurization (cryogenic temperature, 277.8K (500R) and 555.6K (1000R) for steady-state engine burn with helium pressurization (ambient and cryogenic temperature) for start-up.

d. Autogenous pressurization for steady-state engine burn with thermal subcoolers for start-up.

1.2.2 TASK II. In this task we determined helium pressurant mass required to expel LTPS propellants and perform tank inerting during return-to-launch-site (RTLS) emergency operating conditions for Shuttle. We weight optimized the abort dump system, which consisted of propellant dump lines and a shuttle-mounted helium supply system. Helium pressurization for propellant expulsion was the only technique considered in this task.

1.3 PRELIMINARY DESIGN/TECHNOLOGY REQUIREMENTS

Following NASA Project Manager approval of the four pressurization/thermal conditioning systems, General Dynamics performed a preliminary design of each complete system (Task IV). System design was patterned after the criteria

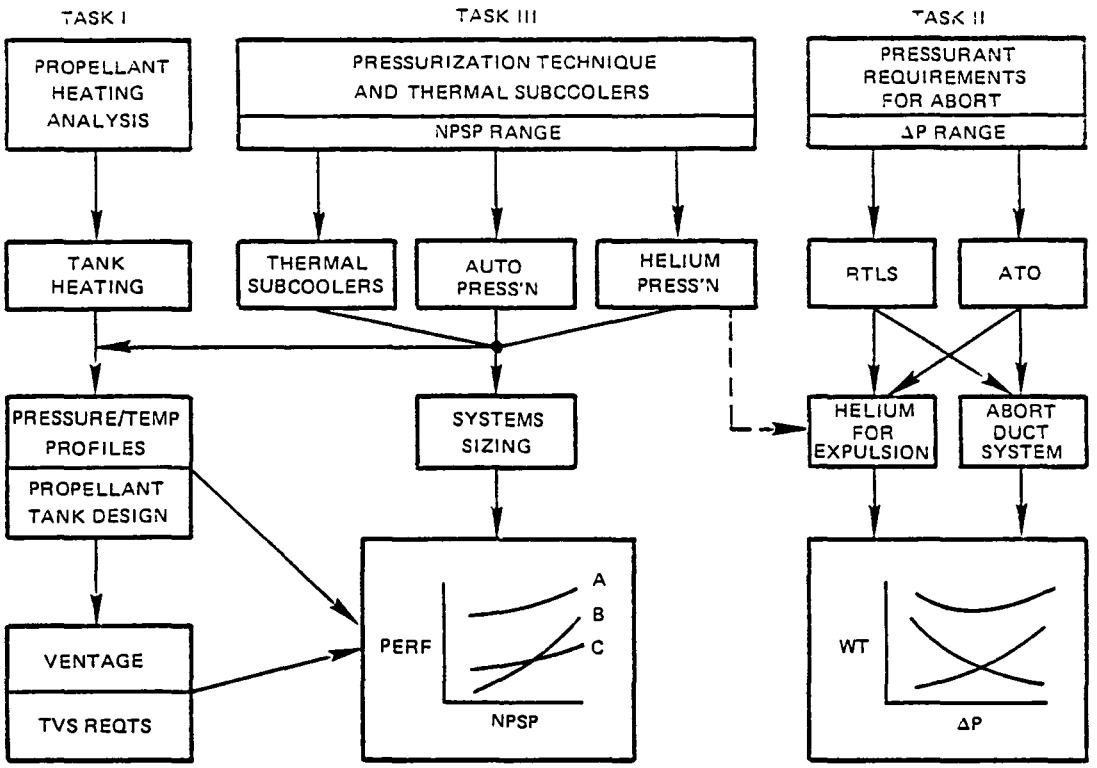

Figure 1-2. Tasks I and III Interaction Required Concurrent Scheduling.

established for the Shuttle/Centaur program. This criteria requires two-failure tolerancy for systems that function while in the Shuttle cargo bay and single-failure tolerancy for vehicle systems activated following deployment from the Shuttle. From these designs, size and weight estimates were made of the required components. These weights were combined with propellant vent masses, vapor residuals and other penalties to derive the final LTPS weight penalty for each of the selected systems and are reported in Section 6.

Although abort system weights were estimated in Task II, a preliminary design of the shuttle-mounted abort system was beyond the scope of this study. A preliminary design was performed on the LTPS-mounted abort system fluid lines (propellant dump and helium pressurization lines). For these fluid lines and associated valves/disconnects, sizing, line routings and weights were estimated and are reported in Section 7.

1.4 GROUND RULES

The ground rules established for subsystem analysis included those imposed by the NASA Program Manager (vehicle configuration, mission profile, etc) and a few imposed for convenience/simplicity. These latter ground rules did not significantly impact study results.

1.4.1 VEHICLE CONFIGURATIONS. The thermal conditioning and propellant expulsion subsystem analyses were performed for LTPS configurations and multiple-burn missions identified in a previous study, Reference 1-2. Details of the LTPS configurations are given in Table 1-1. Two LO_2/LH_2 stages and two LO_2/LCH_4 stages were selected. Note that the stages for each propellant combination are similarly sized. The major exception for the LO_2/LH_2 stages is a toroidal LO_2 tank (Configuration 1) versus an elliptical LO_2 tank (Configuration 2). Despite this difference, the configurations were virtually identical from a thermodynamic standpoint, which made the results of one configuration directly applicable to the other configuration. In contrast, although the LO_2/LCH_4 tank configurations were identical, the different insulation systems (MLI for Configuration 3 and SOFI for Configuration 4) resulted in a substantial thermodynamic dissimilarity. It was necessary, therefore, to analyze both LTPS configurations during the course of this study.

1.4.2 VEHICLE MISSIONS. The selected mission profiles are given in Table 1-2 for each vehicle configuration. These mission profiles reflect a vehicle thrust level of 2.24 kN (500 lb), which accounts for burn durations totaling 28,200 seconds to 33,482 seconds. Note that the same set of coast durations was imposed upon each mission profile.

1.4.3 MAIN ENGINE REQUIREMENTS. The main engine requirements given below, include flow rates, thrust level and engine NPSP:

NPSP Levels - 0.0 to 82.7 kpa (0.0 to 12 psid)

These levels apply to main engine start and steady-state operation and are maintained constant during engine burn. Flow pressure losses are quite small for both operations; consequently, NPSP provided at the propellant tank outlets was assumed equal to engine NPSP.

Thrust Level - 2.24 kN (500 lb)

Propellant Flow Rates

LH_2 = 0.074 kg/sec (0.162 lb/sec) } Isp = 440
LO_2 = 0.442 kg/sec (0.974 lb/sec) } Mixture ratio = 6 to 1

LCH_4 = 0.135 kg/sec (0.298 lb/sec) } Isp = 356.5
LO_2 = 0.501 kg/sec (1.104 lb/sec) } Mixture ratio = 3.7 to 1

Table 1-1. Low-Thrust Propulsion System (LTPS) Configurations

		CONF.1 (LO_2/LH_2)	CONF.2 (LO_2/LH_2)	CONF.3 (LO_2/LCH_4)	CONF.4 (LO_2/LCH_4)
		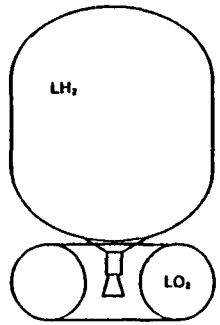	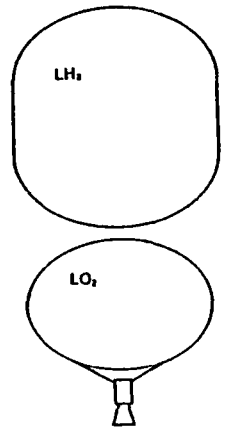	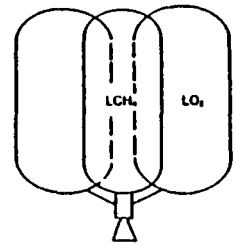	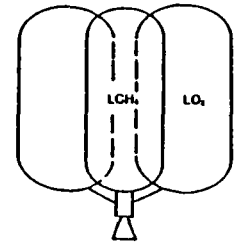
TANK VOLUME, M^3 (ft^3)	OXID.	14.4 (507.4)	14.2 (501.8)	7.3 (259.1)	7.8 (275.3)
	FUEL	39.9 (1407.8)	41.2 (1453.6)	5.4 (191.2)	5.7 (202.7)
TANK MASS, kg (lb)	OXID.	92.0 (202.9)	58.8 (129.7)	36.5 (80.4)	38.6 (85.1)
	FUEL	165.4 (364.7)	163.6 (360.6)	30.7 (67.7)	32.5 (71.6)
NO. OF TANKS		ONE EACH	ONE EACH	TWO EACH	TWO EACH
INSULATION		MLI	MLI	MLI	SOFI
SPACE HEATING RATES, WATTS (Btu/hr)	OXID.	142.7 (487)	142.3 (486)	131.6 (449)	819.5 (2797)
	FUEL	216.8 (740)	218.0 (744)	119.8 (409)	564.9 (1928)

Table 1-2. LTPS Mission Engine Burn and Coast Durations

VEHICLE CONFIG. / EVENT	No. 1 and 2	No. 3	No. 4	All
Burn Number	Duration, Sec	Duration, Sec	Duration, Sec	Coast Duration, Sec
1	3,820	3,787	3,614	6,024
2	3,538	3,447	3,273	6,990
3	3,277	3,137	2,963	8,255
4	3,035	2,855	2,679	9,972
5	2,810	2,597	2,422	12,424
6	2,602	2,363	2,187	16,198
7	2,409	2,150	1,973	22,426
8	2,230	1,956	1,778	22,278
9	9,759	8,125	7,311	-
TOTALS	33,480	30,417	28,200	104,567

Note: Vehicle Thrust = 224 kN (500 lb)

1.4.4 THERMAL CONDITIONING SYSTEMS ASSUMPTIONS. The following assumptions were applicable to the thermal conditioning systems analyses:

1.4.4.1 Propellant Settling. An attitude control system will provide thrust for collecting propellants following each zero-g coast period. Thus a surface tension screen acquisition system is not included as an element of the LTPS. Propellant tank pressurization is simplified because pressurant can be injected directly into the ullage or liquid, as required, since propellant distribution is known.

1.4.4.2 Tank Pressure Control. An initial propellant vapor pressure of 124 kpa (18 psia) was selected for all propellant combinations. It was also assumed that propellant tank venting would reduce tank pressure to 124 kpa (18 psia) at the end of each coast. A thermodynamic vent system (TVS) was used for zero-g venting.

1.4.5 ABORT DUMP SYSTEMS ASSUMPTIONS. The following assumptions were imposed upon abort pressurization requirements analysis:

1.4.5.1 Shuttle/Centaur Experience. It was found convenient to adopt a number of configurations, conditions and procedures developed during the Shuttle/Centaur study (Reference 1-3). These are given below.

Helium supply system. Helium is stored in ambient bottles at 27580 kpa (4000 psia) and 300K (540R).

Propellant dump lines. Employ the configuration developed for Shuttle/Centaur.

Propellant dump. Simultaneous dump of propellants in 250 seconds.

Vehicle Purges. Employ Shuttle/Centaur insulation system and engine system purge data.

2

HELIUM PRESSURIZATION

Helium pressurization systems that provide main engine NPSP requirements for engine start and steady-state conditions have been operational for many years. These systems have been thoroughly tested for both cryogens and earth storable propellants and are considered to be highly reliable. As such, a helium pressurization system can be treated as a baseline configuration to which all other configurations are compared on the basis of weight, performance and reliability.

2.1 SYSTEM DESCRIPTION

A schematic of an ambient helium pressurization system is given in Figure 2-1. This system meters helium to the propellant tanks through orifices to satisfy main engine NPSP requirements. Tank pressure control is maintained through on-off commands of the pressurization solenoid valves that can either maintain tank pressure at an absolute level, at a fixed differential pressure, or at a given differential pressure relative to a continuously changing liquid vapor pressure. Tank pressure control is maintained throughout a mission via a digital computer unit (DCU) that continuously monitors outputs from high-accuracy tank pressure transducers. Pre-programmed logic defines the desired pressure levels throughout flight. LH_2 will be pressurized with helium flow into the ullage because the alternative of liquid injection will require considerably more helium. Helium will be introduced into LO_2 (or CH_4) through a pressurization manifold beneath the liquid surface because substantially less helium is required than for ullage injection. These alternatives are discussed in greater detail in Section 2.3.

2.2 BACKGROUND/CAPABILITIES

General Dynamics Convair has more than 20 years experience in selecting, designing and qualifying helium pressurization systems for cryogenic vehicles (the Atlas vehicle and Centaur upper stages for Atlas and Titan vehicles). Experimental and operational Centaur missions have provided an extensive empirical data base for understanding the thermodynamics and fluid mechanics behavior of cryogenic propellants in space. This experience, combined with computer programs developed to support the Centaur program, was employed in the helium pressurization system parametric analyses for LTPS.

2.2.1 PROPELLANT HEATING ANALYSIS. Thermodynamic analyses of the LTPS propellants were performed for each engine firing and low-g coast phase of the multi-burn mission. Propellant pressure and temperature histories were determined as a function of time for each LTPS configuration. Vent mass requirements for maintaining tank pressure control during the long zero-g

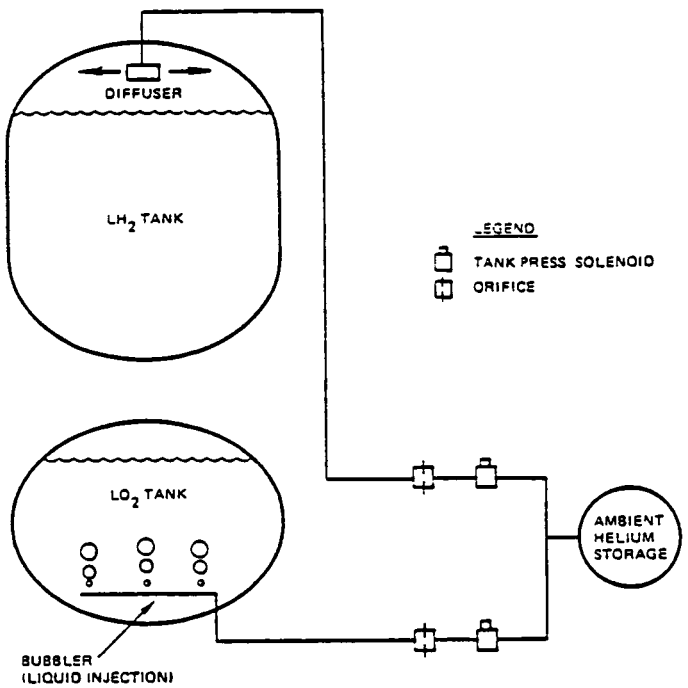

Figure 2-1. Helium Pressurization System.

coast periods and final vapor residuals were also determined for each configuration. Since it was difficult to isolate space heating effects from the thermal conditioning influence upon tank pressures, vent masses and vapor residuals, propellant heating analyses were performed for each of the thermal conditioning systems.

2.2.1.1 Analytical. An existing computer program, HYPRS (developed for the Centaur hydrogen tank and oxygen tank), was employed in this study. With this tool, all pertinent variables were considered during analysis, including propellant outflow rates, pressurant inflow rates, space heating (distributed to liquid and ullage), liquid-ullage coupling and tank wall-ullage influence. The HYPRS program has been used extensively for a variety of Centaur-related studies. It was modified, under IRAD, to accept methane thermo-physical properties. A brief description of HYPRS is given in Appendix A.

2.2.1.2 Empirical. Considerable normal- and low-g flight and ground test experience has been accumulated which was applicable to this study. There is extensive flight data relating to cryogenic propellant tank thermodynamics and fluid distribution during extended zero-g coast periods. This type of data was employed to establish realistic conditions and assess analytical results when analyzing engine burn and propellant tank pressure control.

The zero-g coast data was useful in determining if thermal equilibrium conditions will exist between engine burns of the LTPS mission. Flight data (propellant tank pressures) have shown that near-thermal equilibrium conditions existed in the Centaur liquid hydrogen and liquid oxygen tanks during coast periods of three or more hours in duration. The LTPS tanks will have a greater tendency toward thermal equilibrium than did the Centaur propellant tanks because LTPS heating rates are greatly reduced and the aluminum tanks are highly conductive. Consequently, thermal equilibrium conditions were assumed for the LTPS coast periods.

2.2.2 SUBSYSTEM DEVELOPMENT. Pressurization systems have been designed and developed for ambient and cryogenically stored helium, for helium introduced directly into the ullage or into liquid propellant. Methods have been devised and subsequently flight-demonstrated for low-g pressurization. This included developing an energy dissipator for ullage injection of ambient helium that enables rapid pressurization without excessive loss of energy to the cold tank walls or liquid surface.

2.2.2.1 Analytical. Two computer programs, developed for Centaur, were used for Task III pressurization system analysis. These programs are HYPRS and MULTBOT. MULTBOT can be used separately or as a subroutine of HYPRS. When employed separately, MULTBOT predicts helium storage bottle pressures and temperatures throughout a mission. Computer simulations include the effects of space radiation, conduction and helium usages for purges and pressurization.

The HYPRS computer program is capable of providing simulations of a variety of pressurization techniques, including helium injection into the ullage and helium bubbled through liquid. Validity of the helium pressurization routines has been demonstrated by flight data.

2.2.2.2 Empirical. A wealth of flight experience is available on helium pressurization systems which was directly applicable to this LTPS study. For example, Figures 2-2 and 2-3 represent a compilation of Centaur liquid hydrogen and liquid oxygen tank low-gravity pressurization data for a range of ullage volumes. These curves were used to determine pressurization helium usages for the tank and propellant combinations specified in Section 2.4.1.

2.3 HELIUM PRESSURIZATION TECHNIQUES

Two pressurization techniques were evaluated for providing engine start and steady-state LTPS mission pressures. The first technique is that of introducing helium directly into the ullage. This is the most common and well-understood pressurization method for cryogens and earth-storable propellants. The second technique is that of injecting (or bubbling) helium beneath the liquid surface. This technique of "bubbler" pressurization has been successfully employed for pressurizing the Centaur LO_2 propellant tank. Tests have demonstrated that less helium is required for pressurization during engine

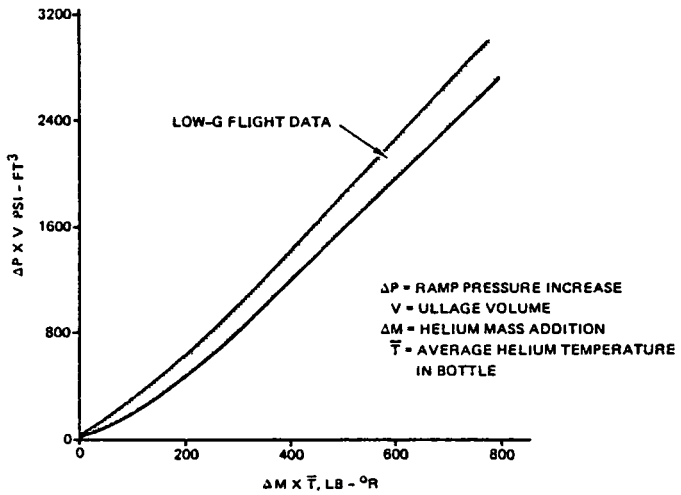

Figure 2-2. LO_2 Tank Bubbler Injection

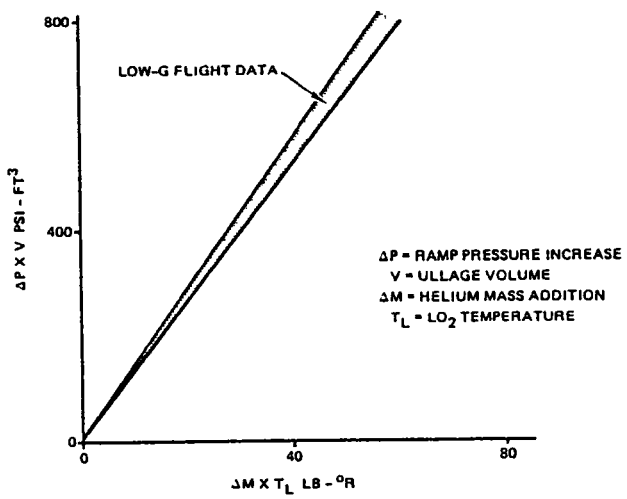

Figure 2-3. LH_2 Tank Ullage Injection

start and steady-state engine operation when helium is "bubbled" through LO_2, Figure 2-4. It was expected, therefore, that the LO_2 tank would use "bubbler" pressurization. Analyses were conducted to determine if this technique should also be selected for LH_2 and LCH_4 pressurization.

The mechanics of "bubbler" pressurization are described in Section 2.3.1. A comparison with the ullage injection technique is given in Section 2.3.2.

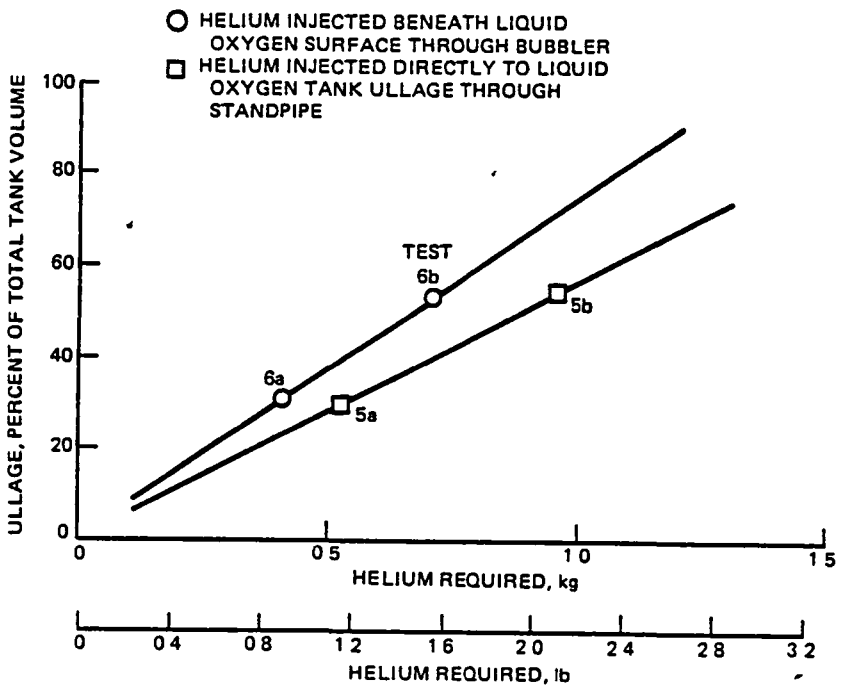

Figure 2-4. Less Helium is Required by Using a Bubbler Beneath the LO_2 Surface

2.3.1 BUBBLER PRESSURIZATION MECHANISM. The advantage of introducing helium beneath the liquid oxygen surface for pressurization is that less helium is required than if it is injected directly into the ullage. Less helium is needed for pressurization because liquid will readily evaporate into the helium bubbles and contribute to the pressurization process. Propellant evaporation into the bubbles will continue until partial pressure of the gas and vapor pressure of the liquid become equal. This mechanism is analytically described below.

2.3.1.1 Liquid Evaporation Model. The sketch below shows a pure helium bubble immersed in liquid. Initial conditions are described:

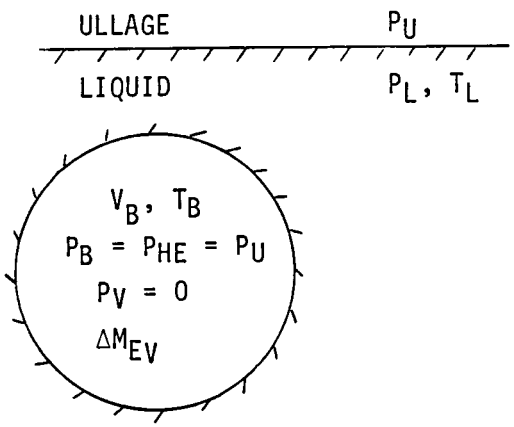

V_B = Bubble volume
T_B = Bubble temperature
P_B = Bubble pressure
P_{HE} = Helium pressure in bubble
P_U = Ullage pressure
P_V = Partial pressure of vapor in bubble
P_L = Liquid vapor pressure
T_L = Liquid temperature
ΔM_{EV} = Mass of liquid evaporated into bubble
$\Delta M_{EV} > o$ when $P_L > P_V$

The following condition exists when a bubble achieves equilibrium with liquid before entering the ullage:

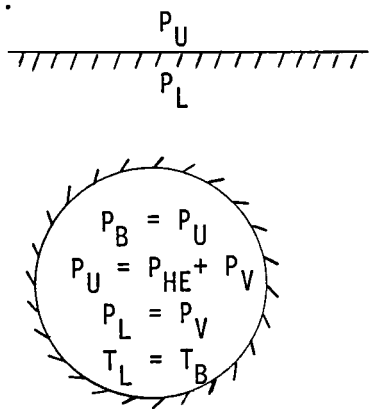

From a mass balance,

$$\frac{\Delta M_{HE}}{\Delta M_V} = \frac{\rho_{HE} \times V_B}{\rho_V \times V_B} = \left(\frac{P}{RT}\right)_{HE} \times \left(\frac{ZRT}{P}\right)_V \qquad (2\text{-}1)$$

where ΔM_{HE} = Bubble helium mass
ΔM_V = Bubble vapor mass
ρ_{HE} = Helium density within bubble
ρ_V = Vapor density within bubble
Z_V = Vapor compressibility factor
R_V = Vapor gas constant

Since $P_U = P_V + P_{HE}$ and $T_{HE} = T_V = T_B$, then

$$\frac{\Delta M_{HE}}{\Delta M_V} = \frac{(P_U - P_V)}{P_V} \cdot \frac{(ZR)_V}{R_{HE}} \tag{2-2}$$

But, since $P_V = P_L$ at equilibrium,

$$\frac{\Delta M_{HE}}{\Delta M_V} = \frac{(P_U - P_L)}{P_L} \cdot \frac{(ZR)_V}{R_{HE}} \tag{2-3}$$

Or,

$$\frac{\Delta M_V}{\Delta M_{HE}} = \frac{P_L}{(P_U - P_L)} \cdot \frac{R_{HE}}{(ZR)_V} \tag{2-4}$$

Equation 2-4 describes two important characteristics of bubbler pressurization. First, the mass ratio of vapor to helium is influenced by ullage pressure and liquid vapor pressure in such a way that considerably more mass is evaporated when $(P_U - P_L) \rightarrow 0$. Second, this mass ratio is also affected by the ratio of helium to vapor gas constant. Thus considerably more oxygen than hydrogen will evaporate into a helium bubble because of their respective gas constants, whereas more methane than oxygen will evaporate for the same reason. This idealized evaluation indicates that oxygen and methane will benefit more than hydrogen from bubbler pressurization. Since flight and test data demonstrate that LO_2 bubbler pressurization requires less helium than ullage injection of helium, it is concluded that the methane tank should also employ bubbler pressurization. A similar conclusion cannot be made regarding bubbler pressurization for the LH_2 tank. The bubble mass balance must be combined with an ullage energy balance in order to assess bubbler pressurization.

From an energy balance

$$\Delta E_U = \Delta Q + (\Delta M c_p T)_{HE} + (\Delta M\ h_s)_V \tag{2-5}$$

where ΔE_U = Ullage mass internal energy change

$\Delta Q = 0$ = Heat input to ullage

$c_{P_{HE}}$ = Helium constant pressure heat capacity

T_{HE} = Helium temperature = T_L

h_{sV} = Saturated vapor enthalpy

But, $\Delta E_U \approx \Delta(MC_VT)_U = \Delta(PVC_V/R)_U = (VC_V/R)_U\ \Delta P_U$ (2-6)

Combining (2-5) and (2-6) and rearranging terms,

$$(VC_V/R)_U \, \Delta P_U = (\Delta M \, c_p T)_{HE} \left[1 + \frac{\Delta M_V}{\Delta M_{HE}} \, \frac{h_{sV}}{c_p T_{HE}} \right] \tag{2-7}$$

Finally, combining (2-4) and (2-7) and recognizing that $T_{HE} = T_L$,

$$(V \, C_V/R)_U \, \Delta P_U = (\Delta M \, c_p)_{HE} \, T_L \left[1 + \frac{P_L}{(P_U - P_L)} \cdot \frac{R_{HE}}{(ZR)_V} \cdot \frac{h_{sV}}{c_{pHE} \, T_L} \right] \tag{2-8}$$

which gives the influence of fluid properties, ullage pressure and liquid vapor pressure upon ullage pressure rise with bubbler pressurization.

2.3.2 BUBBLER COMPARISON WITH ULLAGE INJECTION. Equation 2-8 can be used as an aid in identifying conditions under which bubbler pressurization is more advantageous than ullage injection. This is accomplished by comparing (2-8) to its ullage injection equivalent, which is,

$$(V \, C_V/R)_U \, \Delta P_U = (\Delta M \, c_p)_{HE} \, T_{HE} \tag{2-9}$$

where T_{HE} = Helium temperature in supply bottles.

Now, dividing (2-9) by (2-8),

$$1 = \frac{T_{HE}}{T_L \left[1 + \frac{P_L}{(\overline{P}_U - P_L)} \cdot \frac{R_{HE}}{(ZR)_V} \cdot \frac{h_{sV}}{c_{pHE} \, T_L} \right]} \tag{2-10}$$

where $\overline{P}_U$ = average ullage pressure during pressurization.

Equation 2-10 determines the helium temperature required for ullage injection that produces the same ullage pressure rise for bubbler pressurization with the same helium mass addition. The results of (2-10) are plotted in Figure 2-5 for LH_2, LO_2 and LCH_4. Figure 2-5 indicates that bubbler pressurization is preferred for the LO_2 and LCH_4 tanks over the entire NPSP range. LH_2 tank bubbler pressurization will be beneficial only at NPSP levels less than 11.1 kpa (1.6 psid). For this phase of the study, it was decided to employ LO_2 and LCH_4 tank bubbler pressurization and LH_2 tank ullage injection of helium. The advantage of LH_2 tank bubbler pressurization at NPSP levels below 11.1 kpa (1.6 psid) was not considered sufficient to warrant a separate analysis.

2.4 AMBIENT/CRYOGENIC HELIUM STORAGE

Helium storage at cryogen temperatures has the advantage of greater pressurant availability per pound of hardware weight. A weight benefit is derived for bubbler pressurization of LO_2 and LCH_4 because usage requirements will be the same regardless of storage temperature conditions. If, however, ullage injection of helium is required for the LH_2 tank, any advantage due to helium storage at cryogen temperatures will be lost; the increased helium mass storage capability will be offset by increased helium mass requirements for pressurization. Furthermore, the additional helium in the propellant tank could raise its partial pressure enough to greatly increase vent mass requirements.

It is possible that cryogenically stored helium may be advantageous for LH_2 tank pressurization if a heat exchanger is used to increase helium temperature as it flows to the LH_2 tank. However, a heat exchanger would complicate this particular thermal conditioning system. For the LO_2 and LCH_4 propellant tanks, cryogenic helium storage will afford a weight benefit over ambient

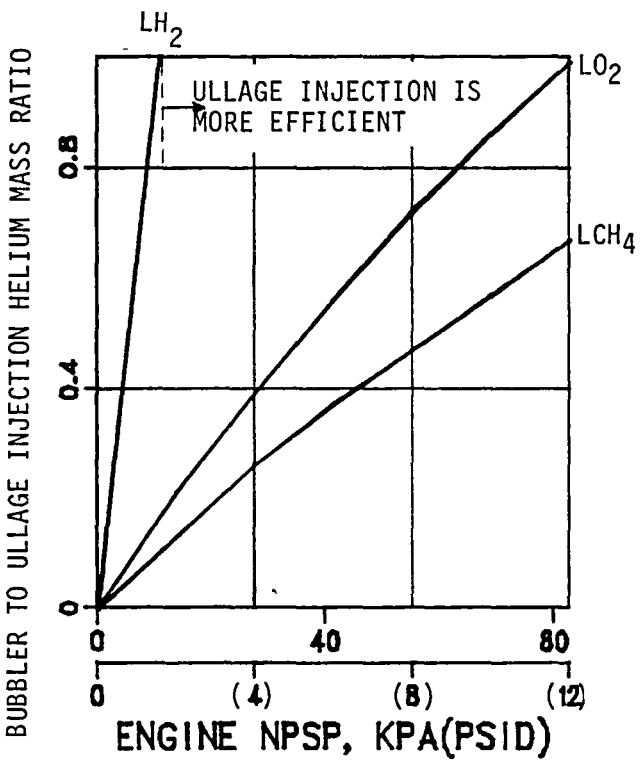

NOTES:

1. For ullage injection, T_{HE} = 250K (450R)
2. For bubbler pressurization, $T_{HE} = T_{LIQUID}$
3. Propellant initially saturated at 124.1 kpa (18 psia)

Figure 2-5. Bubbler Pressurization Versus Ullage Injection Helium Mass Usage Comparison.

storage. It was thought, however, that the benefit would not be significant for the parametric evaluation. The decision was made to analyze this cryogenic storage option in Phase II of the study only if bubbler pressurization was found to be one of the preferred thermal conditioning techniques.

2.4.1 MISSION HELIUM USAGES. Mission helium usages were determined for each vehicle configuration for the ambient temperature helium storage supply system. Usages were determined separately for main engine start and for steady-state engine firing conditions. Engine start helium mass requirements were based upon the empirical data of Figures 2-2 and 2-3. Helium usage requirements for each engine burn were determined from the HYPRS computer program.

2.4.1.1 Main Engine Start. Helium mass usages for main engine start were determined from the empirical data of Figures 2-2 and 2-3 which was also contained within program HYPRS. The empirical data shows that

$\Delta M = f(\Delta P, V, T)$, where:

ΔM = Helium mass usage

ΔP = Pressurization ΔP

V = Ullage volume

T = Average helium temperature entering ullage during pressurization period

Ullage volume for each vehicle configuration was readily determined for each mission. ΔP and T calculations depended upon whether ullage injection or bubbler pressurization was employed.

<u>LH_2 tank pressurization</u>. Since helium is injected directly into the ullage, T is taken to be helium temperature at the storage bottles. From previous Centaur flight experience, it was judged that a reasonable average helium temperature for the LTPS mission would be 250K (450R). This value was used both for main engine start pressurization and pressurization during steady-state operation.

Tank pressurization ΔP for each engine start was selected as the NPSP requirement. This was done because the helium accumulated during the mission would not be sufficient to realize a significant helium partial pressure. The total hydrogen tank helium mass requirement as a function of engine NPSP is given in Figure 2-6 for Configuration 1. Configuration 2 helium usages were not computed because they should be similar to those of Configuration 1.

<u>LO_2 and LCH_4 tank pressurization</u>. Helium storage temperature for bubbler pressurization is of no consequence because helium will always enter the ullage at liquid temperature. Furthermore, near-thermal equilibrium tank conditions will be maintained by bubbler pressurization during engine burn.

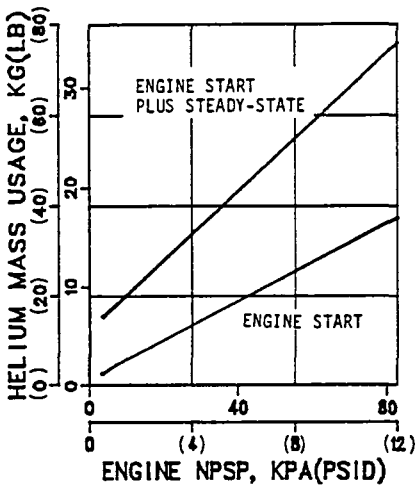

NOTES:

1. Usages apply to Configurations 1 and 2.

Figure 2-6. LH_2 Tank Mission Helium Usages for Ullage Injection

Tank pressurization ΔP for each engine start will be less than the NPSP requirements and could be zero for thermal equilibrium conditions. With bubbler pressurization, the partial pressure of helium during engine burn will be equal to engine NPSP. This relationship will also be maintained at MECO for thermal equilibrium conditions, as shown below:

$$P_T = P_{VP} + P_{NPSP}$$

But it is also known that

$$P_T = P_G + P_{HE}$$

For thermal equilibrium, $P_G = P_{VP}$.

Therefore, $P_{HE} = P_{NPSP}$ at MECO,

where

P_T = Tank pressure

P_{VP} = Liquid vapor pressure

P_{NPSP} = Engine NPSP

P_G = Propellant vapor partial pressure

P_{HE} = Helium partial pressure

It is expected that thermal equilibrium conditions will be maintained throughout each coast period due to fluid mixing provided by the zero-g vent system. This means that $P_{HE} = P_{NPSP}$ during each coast period. Now equality between

P_{HE} and P_{NPSP} for the entire mission will depend upon the vent option selected for tank pressure control. Two vent options evaluated for the TVS were:

a. Gas vent - helium and propellant vapor enter the TVS during each tank vent cycle.

b. Liquid vent - only liquid propellant enters the TVS during each tank vent cycle.

No helium is vented with option b and so, $P_{HE} = P_{NPSP}$ at the end of the coast period (end of venting). Consequently, helium pressurization is not required for the subsequent engine start because NPSP requirements are already satisfied.

With option a, $P_{HE} < P_{NPSP}$ at the end of tank venting and helium pressurization will be required for the subsequent engine starts. LO_2 tank engine start total helium usages are given in Figure 2-7 for Configurations 1, 2 and 3. Since helium usages for this option are significant, option b is preferred and the TVS should be positioned accordingly.

2.4.1.2 Engine Burn. Helium mass requirements for main engine burn are considerably greater than for engine start. Mass usages were determined from program HYPRS for each propellant tank and results include the effects of

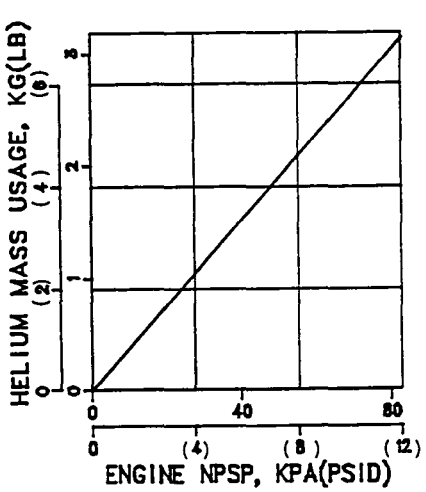

NOTES:

1. Bubbler pressurization
2. Usages apply to Configurations 1, 2 and 3
3. No helium required for engine restart for condition of liquid at TVS inlet

Figure 2-7. LO_2 Tank Engine Start Total Helium Usage (Vapor at TVS Inlet)

heat exchange between ullage and tank walls and between ullage and liquid surface. For LH_2, an entering helium temperature of 250K (450R) was imposed. For bubbler pressurization of LO_2 and LCH_4, helium will enter the ullage at liquid temperature. LH_2 tank mission helium usages are given in Figure 2-6 for Configuration 1. LO_2 tank and LCH_4 tank mission helium usages are given in Figure 2-8.

2.4.1.3 Pressurization System Weight. The weight of the pressurization system includes helium storage bottles and supports, helium mass, lines, fittings, LH_2 tank helium diffuser and bubbler manifolds for the LO_2 and/or LCH_4 tanks. Weights of the helium storage bottle and supports only are influenced by helium usage (or NPSP). All other hardware weights remain fixed whether engine requirements are 3.5 kpa (0.5 psid) or 82.7 kpa (12 psid) NPSP. Rationale for calculating total pressurization system weight is given in Table 2-1. These weights are summarized in Figure 2-9. It is seen that weights for LH_2 tank pressurization are considerably greater than for LO_2 or LCH_4 tank pressurization.

2.5 TYPICAL MISSION ANALYSIS

The influence of helium pressurization system and mission profile upon propellant tank thermodynamic conditions was different for the LH_2 tanks than for LO_2 and LCH_4 tanks. This difference was due to helium bubbler pressurization being employed for LO_2 and LCH_4, whereas ullage injection of helium was used for the LH_2 tank. It was found that the bubbler pressurization technique would maintain near-thermal equilibrium conditions throughout each main engine burn period. This caused minor pressure excursions due to thermal equilibrium mixing following each MECO.

NPSP had virtually no influence upon liquid vapor pressure (and temperature) histories during the mission. As expected, the substantially higher heating rates of a SOFI system had a major impact on pressures, vent masses and vapor residuals as compared to the MLI system.

2.5.1 LH_2 TANK SYSTEM ANALYSIS. The ullage injection pressurization system influence upon vent mass, vapor residuals and tank weight increase requirements is described in this section. It will be shown that ullage injection will maintain nonequilibrium fluid conditions throughout each engine burn, which will result in tank pressure excursions after MECO. These excursions could be increases (due to vapor generation from boiling at the tank walls) or decreases (due to ullage collapse caused by liquid-ullage mixing). It will also be shown that engine NPSP level will influence liquid vapor pressures (which affect peak tank pressures) and vent mass requirements. Finally, a total weight penalty for this thermal conditioning system will be compiled as a function of NPSP requirements. This total penalty will include pressurization system weight in addition to the above weight penalties.

2.5.1.1 LH_2 Propellant Vapor Pressures. Figure 2-10 gives Configuration No. 1 vapor pressure histories for the extremes of engine NPSP conditions considered for this study. The influence of engine NPSP upon propellant vapor pressure (and temperature) is evident. These effects are detailed below for the four major phases of the LTPS mission and are also applicable to Configuration No. 2.

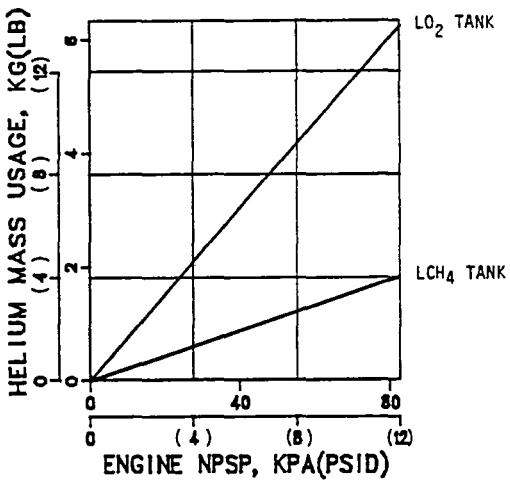

NOTES:

1. Data is based upon liquid at the TVS inlet
2. Usages are applicable to all propellant tank configurations

Figure 2-8. Total Mission Helium Usages for LO_2 Tank and LCH_4 Tank Bubbler Pressurization

Engine burn. Vapor pressure rise during engine burn will increase as NPSP is increased. The increased NPSP level will create warmer ullage temperatures during engine burn which, in turn, will increase ullage-to-liquid heat transfer rates. The subsequent increased liquid heating rate will cause liquid vapor pressure to rise during engine burn. It is noted that vapor pressure rise during each of the first eight burns will remain below about 3.4 kpa (0.5 psid), but that it will experience a substantial rise during the final engine burn. The rapid vapor pressure rise will occur as diminishing quantities of propellant absorb the high ullage-to-liquid heat rates during the 9759 second burn duration. This data illustrates a shortcoming in maintaining high NPSP levels with ullage injection, which is that propellant tank pressure levels will have to be elevated by the amount of the vapor pressure increase in order to maintain NPSP. A payload penalty must be assessed against this pressurization technique when tank weight increases are needed to withstand the increased propellant tank pressures.

Propellant mixing at MECO. The combination of main engine shutdown disturbances and zero-g coast environment will serve to create a thermal equilibrium condition in the tank following each MECO. The ullage mass and dry tank walls may be substantially warmer than liquid at MECO because of ambient helium pressurization. The thermal mixing of these mass quantities can result in liquid evaporation. But, depending upon MECO ullage pressure and temperature conditions, vapor pressure increase or decay will occur. Figure 2-10 shows that vapor pressure decays less than 2.1 kpa (0.3 psid) will occur for the minimum engine NPSP condition. Vapor pressure decays are due to liquid evaporation caused by ullage pressure collapse when liquid and vapor are mixed.

Table 2-1. Helium System Weight for Propellant Tank Pressurization.

Total System Weights = Helium Mass Usage + (Bottle + Supports + Helium Residual) + Plumbing

Helium Mass Usage (Σm) ≃ Based upon average helium temperature of 250K (450R)

$$\Sigma m = m_i - m_f = V(\rho_i - \rho_f) = V \rho_u$$

where

m_i = initial helium mass

m_f = final helium mass

V = total helium bottle volume

ρ_i = 2.45 lb/ft^3 (helium density at P = 4000 psia, T = 540R)

ρ_f = 0.485 lb/ft^3 (residual density at P = 400 psia, T = 300R)

ρ_u = $(\rho_i - \rho_f)$ = 1.965 lb/ft^3

Σm = 1.965 V or V = Σm/1.965

Bottle + Supports + Helium Residual (ΣW) = $(\rho_{BTL} + \rho_s + \rho_f)$ V

where ρ_{BTL} = 15.8 lb/ft^3 (kevlar outer wrap + aluminum liner)

ρ_s = 0.11 × ρ_{BTL} = 1.738 lb/ft^3 (bottle support density)

ΣW = (15.8 + 1.738 + 0.485) V = 18.023 V

Plumbing = 22 lb (valves, lines, fittings, disconnect, etc. for each propellant tank)

Total Weight (lb) = Σm + 18.023 (Σm/1.965) + 22 x 2 = $\boxed{10.172\ \Sigma m + 44}$

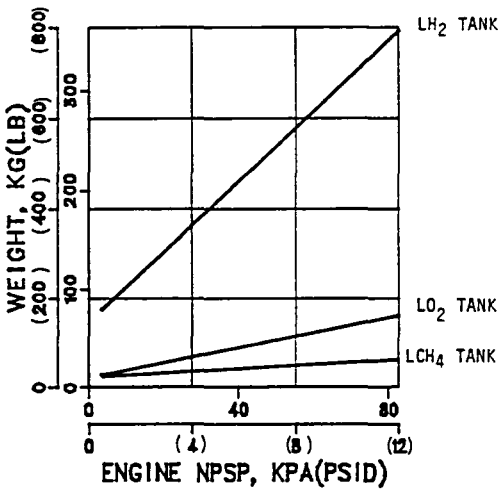

NOTES:

1. Data applicable to all LTPS configurations
2. System weights are based on Table 2-1

Figure 2-9. Total Pressurization System Weights for Helium Pressurization

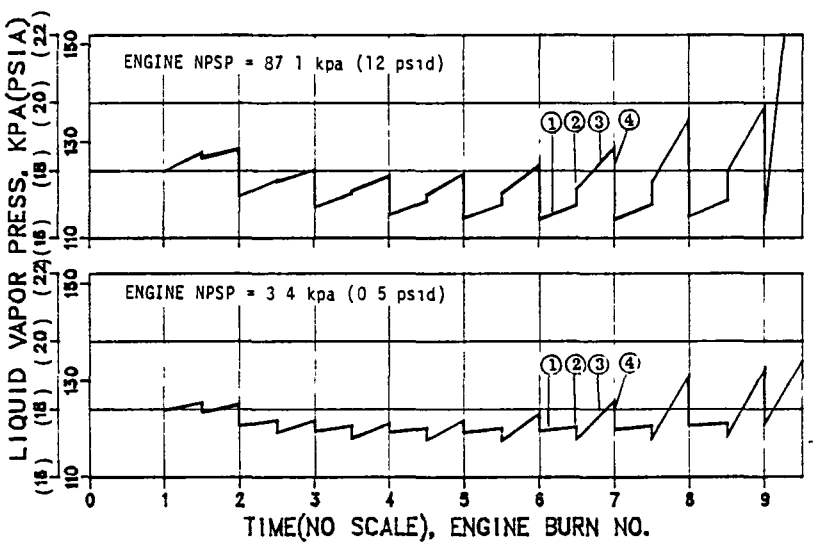

① Liquid vapor pressure rise during main engine burn

② Vapor pressure change caused by thermal equilibrium mixing following each MECO

③ Vapor pressure rise due to coast phase heating rate

④ Propellant tank vent down to a total pressure of 18 psia prior to each engine firing

Figure 2-10. Ambient Helium Pressurization System Influence Upon LH_2 Vapor Pressure (Configuration 1)

The maximum engine NPSP condition will create a vapor pressure decay following each of the first two burns, with vapor pressure increases occurring thereafter. Vapor pressure decay will occur for the reason given above. Vapor pressure rise will occur when the ullage mass and temperature conditions are such that energy is released, as vapor is chilled to liquid temperature during the mixing process and absorbed by the liquid with a subsequent vapor pressure rise. Vapor pressure rise can become as great as 6.2 kpa (0.9 psid) at MECO-8.

Coast phase. Coast phase pressure rise is affected by two variables only, heating rate and percent propellant in tank. Thus, neither pressurization method nor NPSP level will affect liquid vapor pressure increase. Figure 2-10 shows that i) coast phase vapor pressure increases are the same for both NPSP levels and ii) vapor pressure rise is greater for the last coast period than for any other coast period. This increased pressure is due in part to a longer coast duration but primarily to a reduced liquid mass in the propellant tank. Propellant tank heating rate was assumed to be constant at 0.217 kW (740 Btu/hr) throughout the mission.

End-of-coast vent. The propellant tank was vented down to 124.1 kpa (18 psia) at the end of each coast period. Figure 2-10 indicates that a maximum tank pressure decay of 11.7 kpa (1.7 psid) to 22.8 kpa (3.3 psid) can be expected, respectively, from the minimum and maximum NPSP conditions. The greater tank pressure decay is indicative of more vapor vented for the maximum NPSP condition.

Note that liquid vapor pressure will decay below 124.1 kpa (18 psia) following each vent. The difference between tank pressure and liquid vapor pressure is helium partial pressure, which increases with each main engine burn.

2.5.1.2 LH_2 Tank Peak Pressures. Figure 2-10 shows that liquid vapor pressure increase will be the greatest during burn No. 9 as a result of heat input to diminishing quantities of LH_2. Maximum tank pressures needed to maintain engine NPSP during this burn are given in Figure 2-11. Because the LTPS propellant tanks are designed for a maximum operating pressure of 165.5 kpa (24 psia), tank weight increases will be needed for engine NPSP conditions exceeding 20.7 kpa (3 psid), as shown in the figure. These weight increases, shown in Figure 2-12, are based upon the relationship of 1.0 kg/kpa (15.2 lb/psi) above an operating pressure of 165.5 kpa (24 psia). This relationship is taken as tank mass (Table 1-1) divided by operating pressure.

2.5.1.3 Hydrogen Vent Masses. The study ground rules required that propellant tanks be vented down to 124.1 kpa (18 psia) following each zero-g coast period. Figure 2-10 indicates i) that propellant tank venting will occur following each coast period and ii) that vent mass requirements increase for succeeding coast periods. The total vent mass for each NPSP condition is shown in Figure 2-12 and ranges between 45.4 kg (100 lbm) and 104.3 kg (230 lbm).

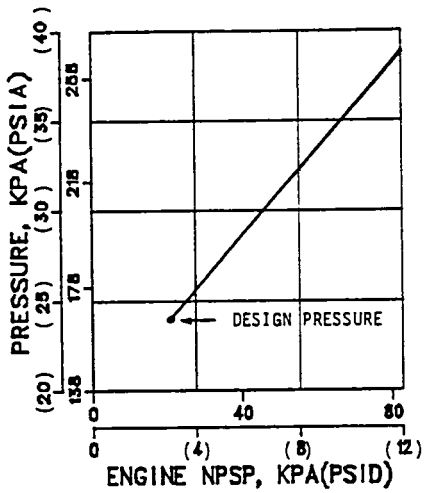

NOTES:

1. Maximum pressure occurs during Burn No. 9
2. Tank weight must be increased for pressures exceeding 165.5 kpa (24 psia)

Figure 2-11. Peak LH_2 Tank pressure During LTPS Mission for Helium Pressurization

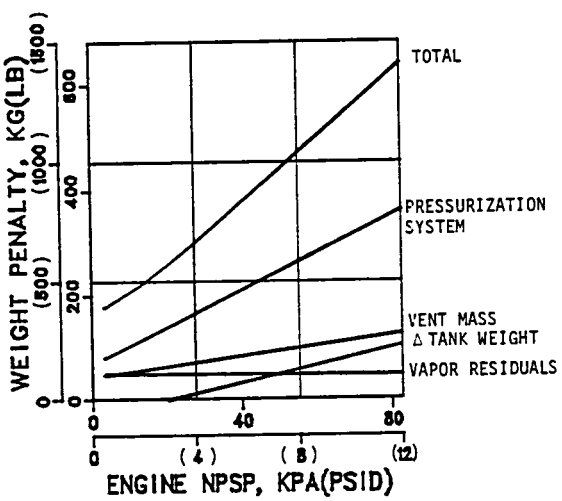

NOTES:

- Thermal equilibrium exists only during coast phase
- Weight penalties are similar for Configuration 2

Figure 2-12. LH_2 Tank Helium Pressurization System Weight Penalties (Configuration 1)

2.5.1.4 Hydrogen Vapor Residuals. The hydrogen vapor residuals given in Figure 2-12 are relatively insensitive to engine NPSP level. The influence of NPSP is less than 2.7 kg (6 lb) over the entire NPSP range under consideration.

2.5.1.5 Total Helium Pressurization Thermal Conditioning System Weight Penalty. The total weight penalty attributed to this thermal conditioning system includes the following weights: helium pressurization system, tank weight increase, vent mass and vapor residuals. The last three items must be included because, as will be shown in subsequent sections, each thermal conditioning system will affect these variables in different ways.

The total weight penalty is given in Figure 2-12. It is evident that helium pressurization system weight is the major component of the total weight penalty. It is also clear that a substantial weight penalty will be paid for high engine NPSP requirements. These results indicate that an attempt should be made to lower reliance upon helium pressurization. The weight penalties of Figure 2-12 also apply to Configuration No. 2.

2.5.2 LO_2 TANK SYSTEM ANALYSIS. Bubbler pressurization system influence upon components that comprise the total system weight penalty is described in this section. These are the same components identified for the LH_2 tank. The primary difference from the conditions described for LH_2 is that bubbler pressurization creates near-thermal equilibrium conditions that beneficially reduce all component weight penalties.

2.5.2.1 LO_2 Propellant Vapor Pressures. Figure 2-13 shows the propellant vapor pressure histories for the pressurization system using bubbler pressurization both prior to and during engine burn. Two vent options were considered for the thermodynamic vent system (TVS):

a. Gas vent - helium and propellant vapor enter the TVS throughout each tank vent-down cycle.

b. Liquid vent - only liquid propellant enters the TVS during each tank vent-down cycle.

With bubbler pressurization, near-equilibrium conditions will exist in the tank throughout the mission. For liquid vent, this results in helium partial pressure being equal to the desired NPSP level. The tank can then be vented down to 124.1 kpa (18 psia) + NPSP to assure a liquid vapor pressure of 124.1 kpa (18 psia) prior to each engine burn. For gas vent, helium is lost during each vent cycle. This causes the partial pressure of helium to be less than the desired NPSP level. If the tank is vented down to 124.1 kpa (18 psia) + NPSP using gas vent, then the liquid vapor pressure will increase above 124.1 kpa (18 psia) prior to engine burn as shown in Figure 2-13. The obvious advantages of option b resulted in its selection for TVS operation.

Engine burn. For the bubbler pressurization system, vapor pressure will decrease as the liquid propellant is cooled by the rising helium bubbles. There is little ullage-to-liquid heat transfer since propellants reside at

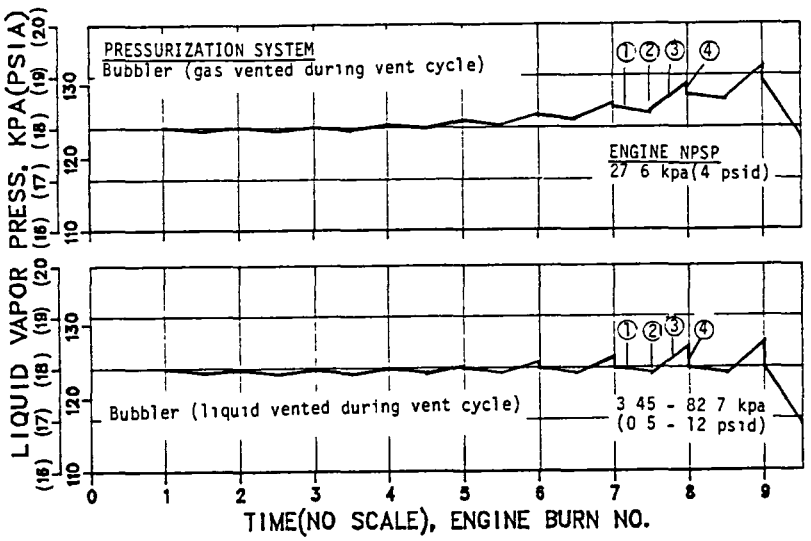

① Liquid vapor pressure decay during main engine burn

② Vapor pressure change caused by thermal equilibrium mixing following each MECO

③ Vapor pressure rise due to coast phase heating rate of 142 9 W (487 5 Btu/hr)

④ Tank vent down to 124.1 kpa (18 psia) + NPSP prior to each engine firing (for liquid vent)
Tank vent down to 151.7 kpa (22 psia) prior to each engine firing (for gas vent)

Figure 2-13. NPSP Influence Upon LO_2 Vapor Pressure During Mission (Configuration 1)

near-equilibrium conditions. Therefore, engine NPSP levels have little influence on propellant liquid vapor pressure. The type of insulation will have a significant impact upon propellant vapor pressure histories. Figure 2-14 gives a comparison between MLI and SOFI insulation for Configurations 3 and 4. Liquid vapor pressure for the MLI system will remain relatively constant throughout the mission, as was also predicted for Configurations 1 and 2. For the vehicle Configuration 4 (with SOFI), vapor pressure will increase. The high heating rate increases ullage temperature and the tank is no longer in thermal equilibrium. The increased propellant heating rates exceed cooling provided by the rising helium bubbles.

Propellant mixing at MECO. There is little change in pressure at MECO for the MLI configurations since tank propellants are at near-equilibrium conditions. With the SOFI configuration, however, vapor pressure will increase as shown in Figure 2-14 because energy absorbed by the tank walls and ullage during engine burn is transferred to the liquid when mixing occurs at MECO.

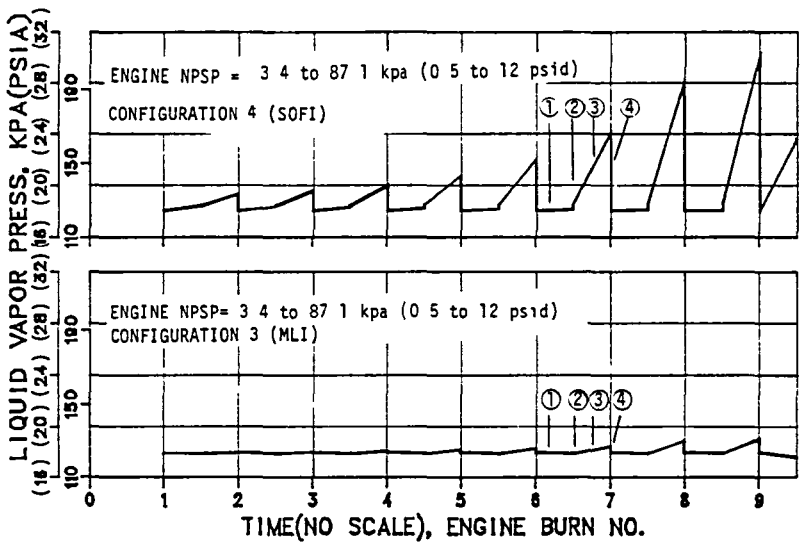

① ENGINE BURN
② MECO
③ COAST
④ TANK VENT

NOTES:

- For MLI, NPSP level has little influence upon liquid vapor pressure. Thermal equilibrium will exist during mission.
- Space heating effect (SOFI vs MLI) has substantial influence upon liquid vapor pressure and vent mass history.

Figure 2-14. Bubbler Pressurization System and Space Heating Influence Upon LO_2 Vapor Pressure (Configurations 3 and 4)

Coast phase. Coast phase vapor pressure rise is affected only by heating rate and percent propellant in the tank. The heating effect of SOFI is substantial, as indicated by Figure 2-14. Liquid vapor pressure increases are greater during the latter phases of the mission because less propellant is available to absorb heat input.

End of coast vent. For the MLI vehicle configurations, the tank was vented down to 124.1 kpa (18 psia) + NPSP. Since near-thermal equilibrium conditions exist throughout the mission, the liquid vapor pressure will be 124.1 kpa (18 psia) with the helium partial pressure equal to the NPSP level after the vent.

For the SOFI vehicle configuration, thermal equilibrium conditions will no longer exist during engine burn because of the high heating rate. Thus, helium partial pressure will be less than the NPSP level and it will no longer be possible to vent the tank down to 124.1 kpa (18 psia) + NPSP. Consequently, the tank was vented down to 124.1 kpa (18 psia) to assure that vapor pressure would not exceed that level.

2.5.2.2 LO_2 Tank Peak Pressures. Maximum tank pressures needed to maintain engine NPSP throughout the mission are given in Figure 2-15. These pressures are the same for all vehicle configurations with MLI. Tank weight increases for MLI configurations will be required for all engine NPSP levels that exceed 41.4 kpa (6 psid). The higher heating rates of the SOFI configuration will increase maximum tank pressures above that required for MLI configurations, as shown in Figure 2-15. The resulting tank weight increases are summarized in Figures 2-16 and 2-17 and are based upon the relationship of 0.56 kg/kpa (8.5 lb/psi) for Configuration 1 and 0.46 kg/kpa (7.0 lb/psi) for Configurations 2, 3 and 4.

2.5.2.3 Oxygen Vent Masses. The mass vented for bubbler pressurization systems having MLI is not affected by engine NPSP level. This is because the liquid vapor pressure history is the same for all engine NPSP levels. Figure 2-16 shows vent mass will remain constant at 109 kg (240 lbm) for all NPSP levels. Vent masses for the SOFI configuration also appear to be insensitive to engine NPSP level, as illustrated in Figure 2-18. However, the high heating environment will increase vent mass to about 1179 kg (2600 lbm).

2.5.2.4 Oxygen Vapor Residuals. Vapor residuals given in Figures 2-16 and 2-17 are relatively insensitive to engine NPSP level and tank heating rate. Vapor residual will be approximately 15 percent lower for the SOFI configuration (superheated vapor at final MECO) than for the MLI configurations (saturated vapor at final MECO).

2.5.2.5 Total System Weight Penalty. The total weight penalties attributed to the bubbler pressurization system are given in Figures 2-16 and 2-17 for the MLI and SOFI configurations, respectively. Unlike the LH_2 system, the LO_2 bubbler pressurization system weight is not a major component. This system also benefits from the reduced vapor residuals and vent mass quantities that result from the thermal equilibrium condition created by the bubbler process. Bubbler pressurization also represents current technology which has been demonstrated in a low gravity environment.

One further observation is that MLI may always provide a substantial performance benefit over SOFI. Although there are considerations, such as groundhold, that have not been evaluated, it seems unlikely that the benefits of SOFI could compensate for the performance differences shown between Figures 2-16 and 2-17.

2.5.3 LCH_4 TANK SYSTEM ANALYSIS. Bubbler pressurization for the LCH_4 propellant tanks will create conditions that are thermodynamically similar to the LO_2 tank configurations for all phases of flight, as seen by Figure 2-18. This is so because sub-surface injection of helium will assure near-thermal equilibrium conditions during the mission. Consequently, the LCH_4 system weight penalty analysis results are summarized only, rather than discussed for each phase of flight.

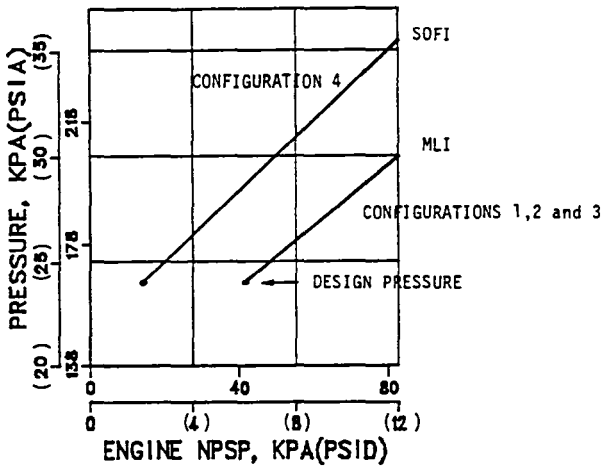

NOTES:

1. Maximum pressure occurs during Burn No. 9
2. Tank weight must be increased for pressures exceeding 165.5 kpa (24 psia)

Figure 2-15. Peak LO_2 Tank Pressure During LTPS Missions for Helium Bubbler Pressurization

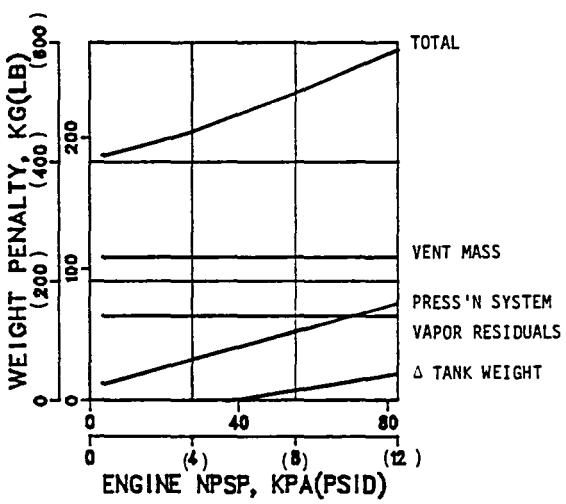

NOTES:

1. Thermal equilibrium exists throughout mission
2. Tank is vented down to 124 kpa (18 psia) + NPSP prior to each burn
3. Weight penalties for Configurations 2 and 3 are similar to Configuration 1

Figure 2-16. LO_2 Tank Bubbler Pressurization System Weight Penalties (Configuration 1)

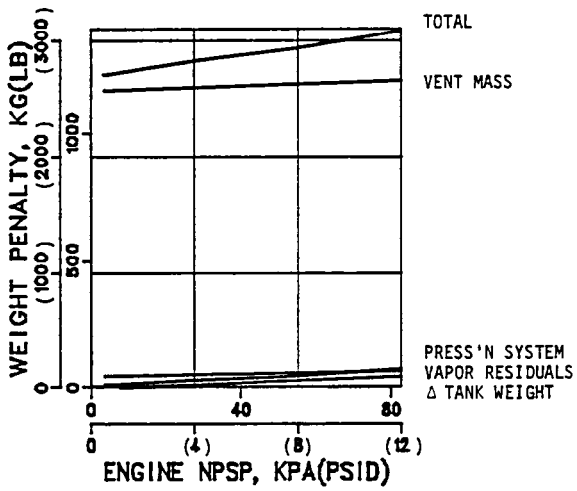

NOTES:

1. Greatly increased vent mass is caused by higher heating rates of SOFI insulation system
2. Thermal equilibrium occurs only during coast periods

Figure 2-17. LO_2 Tank Bubbler Pressurization System Weight Penalties (Configuration 4)

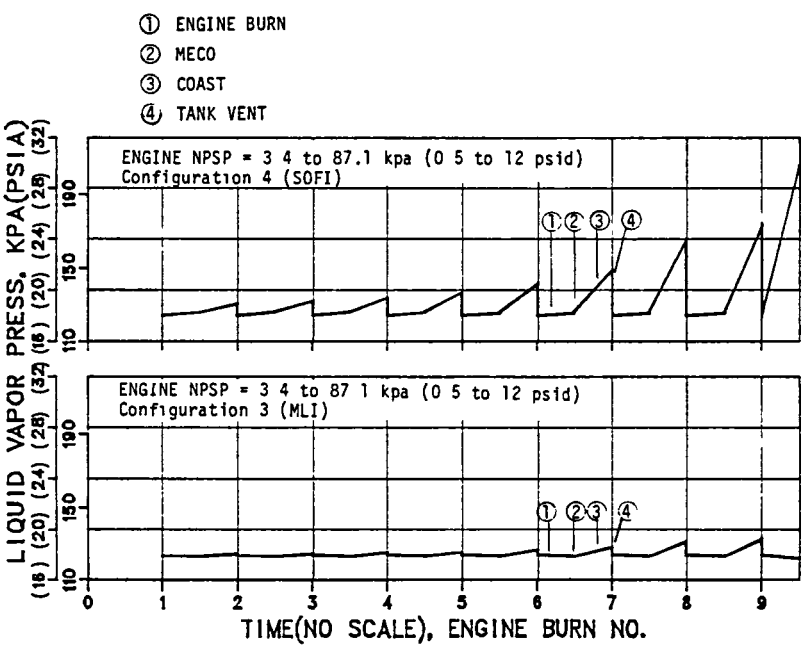

NOTES:

1. For MLI, NPSP level has little influence upon liquid vapor. Thermal equilibrium will exist during mission.
2. SOFI system heating rates have substantial influence upon liquid vapor pressure.

Figure 2-18. Bubbler Pressurization System and Space Heating Influence Upon LCH_4 Vapor Pressures (Configurations 3 and 4)

2.5.3.1 Total System Weight Penalty. The bubbler pressurization system total weight penalty is given in Figures 2-19 and 2-20 for the MLI and SOFI configurations, respectively. Similarities to the LO_2 tank system analysis are given below:

a. Helium supply system weights are not a significant percentage of the total.

b. Vapor residual and vent mass quantities are relatively insensitive to engine NPSP.

c. Tank weight increases to accommodate higher tank pressures are small.

d. The use of SOFI presents a significant weight penalty (a vent mass increase of about 188 kg (415 lb).

As with the LO_2 tank, bubbler pressurization represents current technology, although it has not been demonstrated with LCH_4.

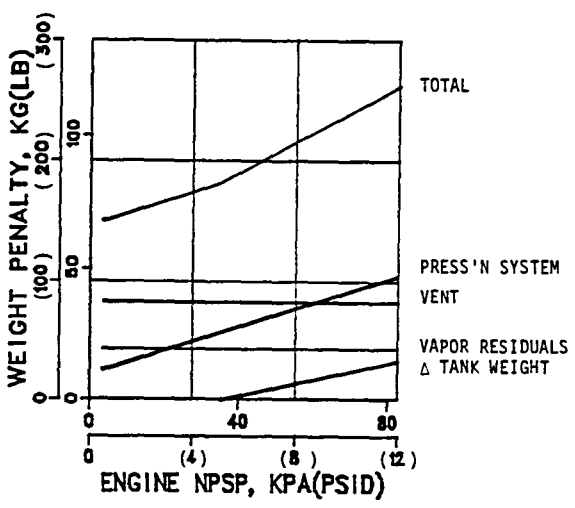

NOTES:

1. Thermal equilibrium exists throughout mission
2. Tank is vented down to 124 kpa (18 psia) + NPSP prior to each burn

Figure 2-19. LCH_4 Tank Bubbler Pressurization System Weight Penalties (Configuration 3)

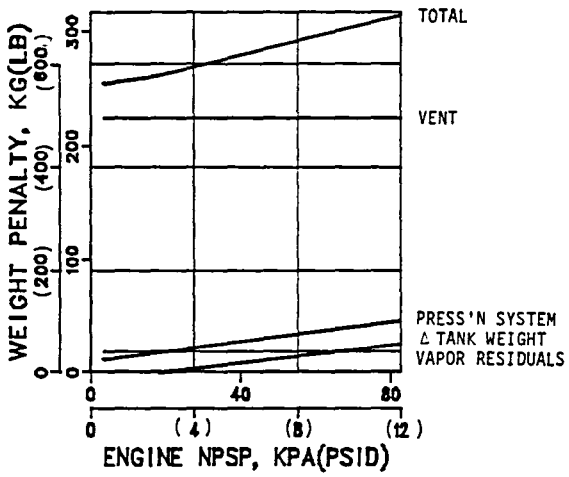

NOTES:

1. Greatly increased vent mass is caused by higher heating rates of SOFI system
2. Thermal equilibrium occurs only during coast periods.

Figure 2-20. LCH_4 Tank Bubbler Pressurization System Weight Penalties (Configuration 4)

3

THERMAL SUBCOOLERS

Thermal subcoolers (heat exchangers) can attain engine NPSP conditions thermodynamically rather than through the traditional approach of propellant tank pressurization. With the traditional approach engine inlet NPSP is satisfied when an ullage pressure increase subcools tank propellants. In contrast, thermal subcoolers will cool tank propellants as they flow to the main engine. Liquid vapor pressures decrease as propellants are cooled and, thus,engine inlet NPSP is achieved.

3.1 SYSTEM DESCRIPTION

Thermal subcoolers will provide NPSP by using throttled vent fluid to subcool the delivered propellant. This system is shown schematically in Figure 3-1 and thermodynamically in Figure 3-2. The cold-side fluid will experience a temperature drop as it is throttled to a low pressure. This fluid will boil as it absorbs heat from the hot-side fluid being delivered to the main engine. The hot-side fluid exits at the desired NPSP; the cold-side fluid, exiting at a high quality, can be either dumped overboard or returned to the tank. One of the two major subcooler tasks was to determine if the cold-side flow should be dumped or returned to the tank; the other was to size the heat exchangers.

3.2 SUBCOOLER SIZING

Two types of subcoolers were analyzed for the LTPS configurations; one for installation on the elliptical aft bulkheads of the LH_2, LO_2 and LCH_4 tanks, and the other for installation within a toroidal LO_2 tank. Each configuration was analyzed for NPSP requirements from 3.5 to 82.7 kpa (0.5 to 12 psid) and for each propellant. The two subcooler configurations are described in Section 3.2.1. Heat removal requirements and subcooler sizing are discussed in Section 3.2.2. Finally, the method for determining cold-side flow requirements is given in Section 3.2.3.

3.2.1 SUBCOOLER CONFIGURATIONS. The elliptical aft bulkhead subcooler configuration is based upon a concept previously analyzed at General Dynamics for high thrust vehicles (References 3-1 and 3-2). The same analysis techniques have been applied for this study. The toroidal LO_2 tank subcooler configuration had not been previously analyzed and, therefore, did not have an equivalent analysis data base.

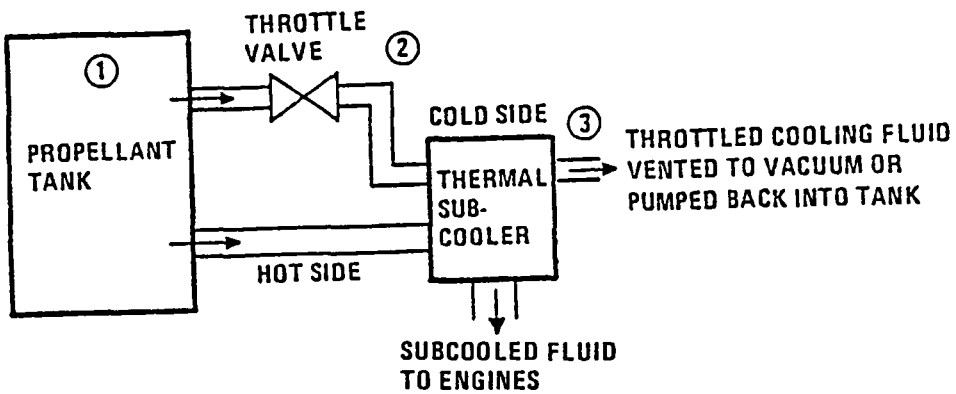

Figure 3-1. The Thermal Subcooler Supplies Subcooled Propellants to the Engines.

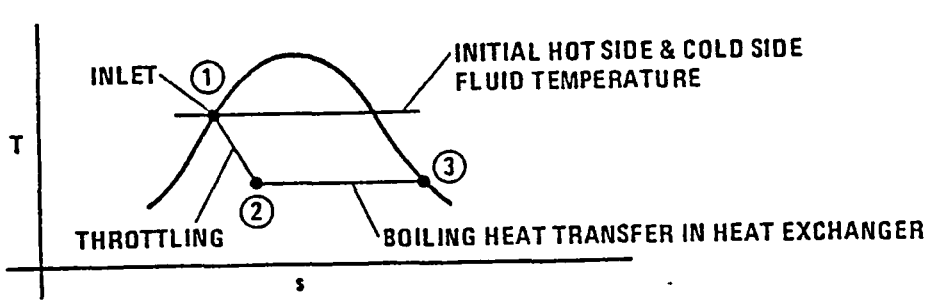

Figure 3-2. Throttling Provides the Low Temperature Fluid for the Heat Exchanger.

3.2.1.1 Elliptical Aft Bulkhead. The subcoolers of this analysis used in tanks with an elliptical aft bulkhead employ the concept shown in Figure 3-3 which was developed at General Dynamics for high-thrust vehicles. The propellant to be subcooled (hot side) enters the heat exchanger at the circumference and flows radially inward toward a 3.8-cm (1.5-inch) radius hole at the center. The cold-side propellant is expanded down to 34.5 kpa (5 psi) through a throttling valve located at the centerline and above the subcooler (not shown in Figure 3-3). Two-phase boiling cold-side fluid enters the subcooler top passage layer, is spiraled radially outward, passes through the hot-side layer in tubes near the circumference and is spiraled radially inward in the second cold-side layer. If multiple hot-side passes are required to achieve the necessary heat transfer area (four hot-side passes are seen in Figure 3-3), the sequence is repeated with both hot-and cold-side flow direction alternating with each pass. Radial fins in the hot-side passages augment heat transfer. A new set of fins starts at each radial location where fin spacing reaches 2.54 cm. (1.0 inch), doubling the number of fins from that point outward.

3.2.1.2 Toroidal Tank. The toroidal LO_2 tank contains a propellant acquisition device (a ring manifold) located at the bottom of the tank which supplies a single outlet to the engine as shown in Figure 3-4. The subcooler heat exchanger occupies a section of the outlet tubing within the tank. Cold-side propellant is spiraled around the tubing. Hot-side fins are located inside the tubing as shown in Figure 3-4. Tube diameters of 1.9, 2.5 and 3.8 cm (0.75, 1.0 and 1.5 inch) with four and eight fins were analyzed.

3.2.2 HEAT REMOVAL REQUIREMENTS. The required rate of heat removal from the delivered propellant to achieve a desired NPSP level is given by:

$$\dot{Q}_r = \dot{m} \frac{\Delta h}{\Delta P} (\text{NPSP} + \text{losses}) \qquad (3\text{-}1)$$

where

$\dot{Q}_r$ = required rate of heat removal

$\dot{m}$ = flow rate of liquid to engine

Δh = change in enthalpy from that of the saturated propellant entering the heat exchanger hot-side to the enthalpy of the delivered propellant

ΔP = change in saturation pressure corresponding to propellant conditions entering and leaving the heat exchanger hot side

NPSP = required engine inlet net positive suction pressure

losses = pressure drop within the subcooler. For the low-thrust flow rates of this study, these losses are negligible

Required heat removal rates are summarized in Table 3-1. These rates are based upon the engine flow rates given in Section 1.4.3.

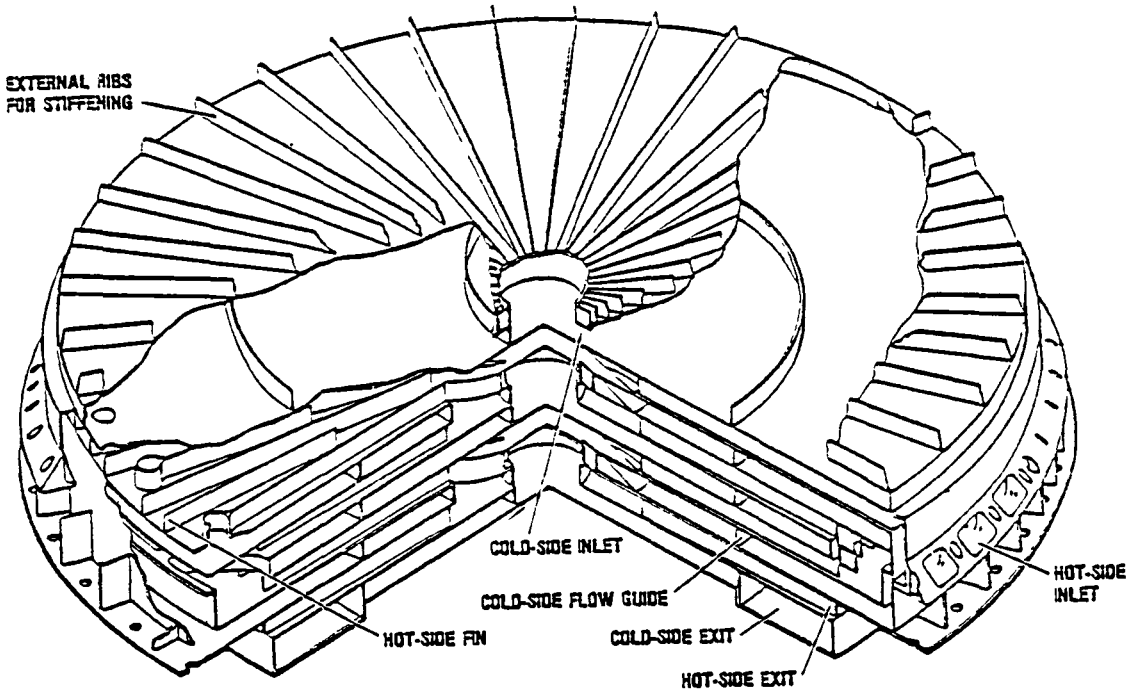

Figure 3-3. General Dynamics Subcooler Design Used as Basis for Elliptical Bulkhead Subcoolers of this Study.

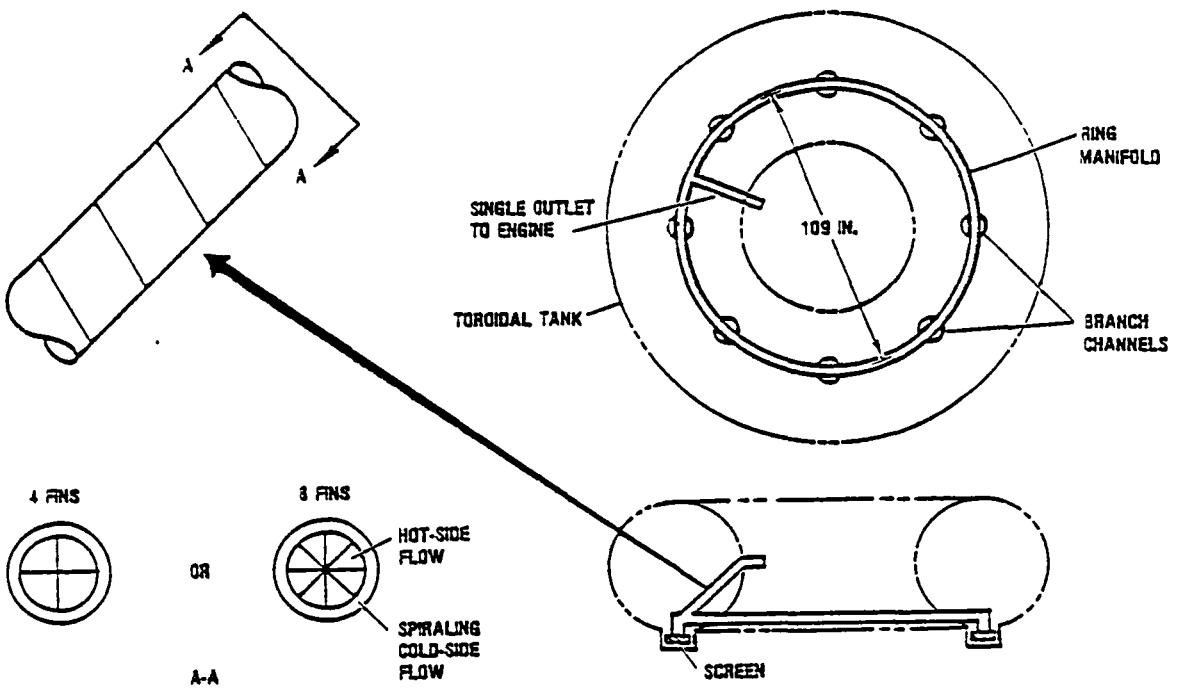

Figure 3-4. Toroidal Tank Subcooler Located in Outlet Tubing.

3.2.2.1 Elliptical Bulkhead Subcooler Sizing Approach. The objective of the sizing thermal analysis is to determine the size of subcooler which provides sufficient heat transfer area (primary + fin) to meet the required heat removal rates of Table 3-1. Heat removal rates are a function of propellant flow rate as well as required NPSP. Two sets of LO_2 requirements are given because the LH_2/LO_2 stage and LCH_4/LO_2 stage require different mass flow rates to the main engine. The resistance to heat flow is assumed to consist of the sum of convective film resistances on hot and cold sides of the separating wall (negligible resistance across the wall). Throttling the propellant from 124 kpa to 34.5 kpa (18 psi to 5 psi) results in the following hot side inlet-to-cold-side temperature differences to drive the heat transfer:

LH_2 = 3.86K (6.94R)

LO_2 = 11.1K (20.0R)

LCH_4 = 14.1K (25.3R)

The radially flowing hot-side propellant velocity changes significantly with radius because of the change in flow area. The hot-side heat transfer coefficient, h, therefore likewise varies with radius. It is thus necessary to integrate the product of local h times incremental heat transfer area to obtain the total effective hot-side hA. Fins contribute to the hot-side heat transfer area, but with an efficiency slightly less than one (Figure 3-5). Fin efficiency varies with passage height and h according to:

$$\eta = \frac{1}{mL_f} \tanh (mL_f), \text{ and } m = \sqrt{\frac{2h}{kw}} \qquad (3\text{-}2)$$

where

η = ratio of actual heat transferred to heat transferred if entire fin were at root temperature

L_f = fin length, root-to-tip = one-half passage height

w = fin width = 0.10 cm (0.04 inch)

k = material thermal conductivity

Fin efficiency increases with decreasing h and decreasing fin length (passage height) as shown in Figure 3-5. The net heat removal contribution of the fins decreases with decreasing passage height because of the reduction in surface area.

Fluid on the cold side undergoes nucleate boiling over the entire heat exchanger flow path and the cold side h can be considered uniform throughout.

Heat removal from the delivered propellant is given by:

$$\dot{Q}_r = \Sigma(h\Delta A)_h(T_h - T_w) \qquad \text{(hot side)} \qquad (3\text{-}3a)$$

$$\dot{Q}_r = (KA)_c(T_w - T_c)^{2.5} \qquad \text{(cold side)} \qquad (3\text{-}3b)$$

Table 3-1. Subcooler Required Heat Removal Rate, kW (Btu/sec).

Propellant	NPSP, kpa (psid)					
	3.4 (0.5)	6.9 (1.0)	13.8 (2.0)	27.6 (4.0)	55.2 (8.0)	82.7 (12.0)
LH_2	0.0692 (0.0730)	0.1385 (0.1461)	0.2769 (0.2921)	0.5770 (0.6086)	1.239 (1.307)	2.030 (2.141)
LO_2 (LH_2/LO_2)	(0.1755) (0.1851)	0.3694 (0.3896)	0.7664 (0.8084)	1.607 (1.695)	3.713 (3.916)	6.556 (6.915)
LO_2(LCH_4/LO_2)	0.1989 (0.2098)	0.4187 (0.4416)	0.8688 (0.9164)	1.821 (1.921)	4.208 (4.439)	7.432 (7.839)
LCH_4	0.1697 (0.1790)	0.3451 (0.3640)	0.6987 (0.7370)	1.406 (1.483)	3.050 (3.217)	5.336 (5.628)

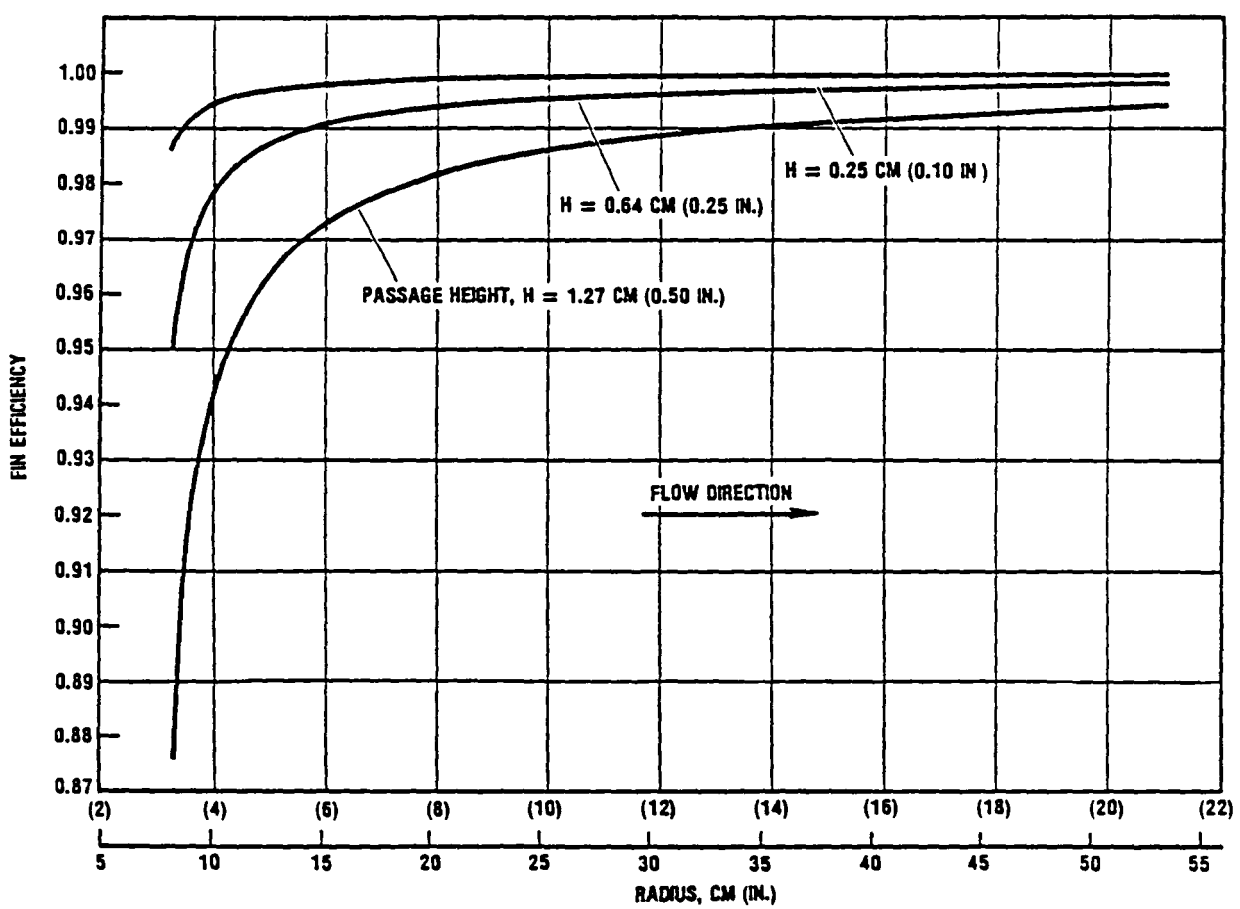

Figure 3-5. Fin Efficiency in LH_2 Subcooler (Hot-side Flow Radially Outwards).

where

$\dot{Q}_r$ = rate of heat removal from delivered propellant (heat removed from the hot side equals heat added to the cold side)

T_h = average of hot-side inlet and outlet temperatures

T_w = temperature of heat exchanger wall separating hot and cold sides

T_c = temperature of cold-side boiling propellant

$\Sigma(h\Delta A)_h$ = hot-side effective hA = local heat transfer coefficient times incremental primary heat transfer area, integrated from the center hole to the subcooler perimeter, $\Sigma(h\Delta A_p)$, plus fin efficiency, times local heat transfer coefficient, times incremental fin area integrated from the center hole to the subcooler perimeter, $\Sigma(\eta h\Delta A_f)$

$(KA)_c(T_w-T_c)^{2.5}$ = heat transferred from heat exchanger wall to the boiling cold fluid (see detailed description later)

Heat Transfer in Radially Outward Flow

In the hot-side passages, propellant flow is described by equations for flow over a flat plate. For radially outward flow, velocity v decreases as flow length L increases. At the low flow rates of this study, the product vL never reaches a value high enough for attainment of critical Reynold's number,

$$Re_c = \left(\frac{\rho vL}{\mu}\right)_c = 400{,}000.$$

Radially outward flow is therefore laminar for all three passage heights analyzed (1.25, 0.64 and 0.25 cm). The laminar heat transfer coefficient is given by:

$$h = 0.664\,\frac{k}{L}\left(\frac{\rho vL}{\mu}\right)^{1/2}(Pr)^{1/3} \qquad (3\text{-}4)$$

where

h = heat transfer coefficient

k = propellant thermal conductivity

L = flow distance downstream from entrance

ρ = propellant density

v = flow velocity

μ = propellant viscosity

Pr = propellant Prandtl number

Heat transfer coefficient for radially outward flow (Figure 3-6) is a simple function of radius since radius r and flow length L are directly related (see Figure 3-6 for h at each passage height analyzed). The jogs in h at 14.7 and 29.7 cm (5.8 and 11.7 inches) are caused by the start of a new set of fins which reduces flow area and increases velocity.

Heat Transfer in Radially Inward Flow

Heat transfer coefficient at a given radius for radially inward flow depends on subcooler inlet radius and flow length to that point. Parameters L and r are now measured in opposite directions and are no longer uniquely related. Further, flow can become turbulent at the higher velocities near the center since both v and L increase as flow approaches the center. The result is a family of h versus r curves typical of those seen in Figure 3-7 for a passage height of 0.25 cm (0.10 inch) [only subcoolers out to a radius of 20 cm (8 inches) are shown]. To obtain an integrated $h\Delta A$ over the hot-side area as a function of subcooler size, the following intermediate step is required. The integration of local h times the sum of primary and effective fin incremental areas is performed for each of a number of subcooler sizes. The result is the family of solid line curves seen in Figure 3-8. Connecting the end points of the solid curves gives the dashed line which relates the total hot-side convective factor, $\Sigma(h\Delta A)_h$, of Equation 3-3a to subcooler size (radius).

Cold Side Heat Transfer

On the subcooler cold side, the fluid is throttled to 34.5 kpa (5 psi). Cold-side flow rate is established by the requirement that the exit quality not exceed 0.9. This ensures that nucleate boiling heat transfer occurs throughout the subcooler at the design condition of 124 kpa (18 psia) tank pressure. The Kutateladze nucleate boiling heat transfer coefficients given by Equation 3-5 (Reference 3-3) were assumed.

$$\frac{\dot{Q}}{A_{SC}\,[0.555\,(\Delta T_{WC})]^{2.5}} = 1.547 \times 10^{-7}\left[\frac{112.3\,C_{P\ell C}}{(h_{sV} - h_{s\ell})\rho_{VC}}\right]^{1.5} \times \left[\frac{0.0173k_{\ell C}\,(0.01603\rho_{\ell C})^{1.282}\,(6.894\times10^{4}\,P_{Ci})^{1.75}}{(\sigma_{\ell C})^{0.906}\,(14.88\mu_{\ell C})^{0.626}}\right] \tag{3-5}$$

where

A_{SC} = total cold-side heat transfer surface area

$C_{P\ell C}$ = cold-side liquid specific heat

$\dot{Q}$ = heat transfer rate

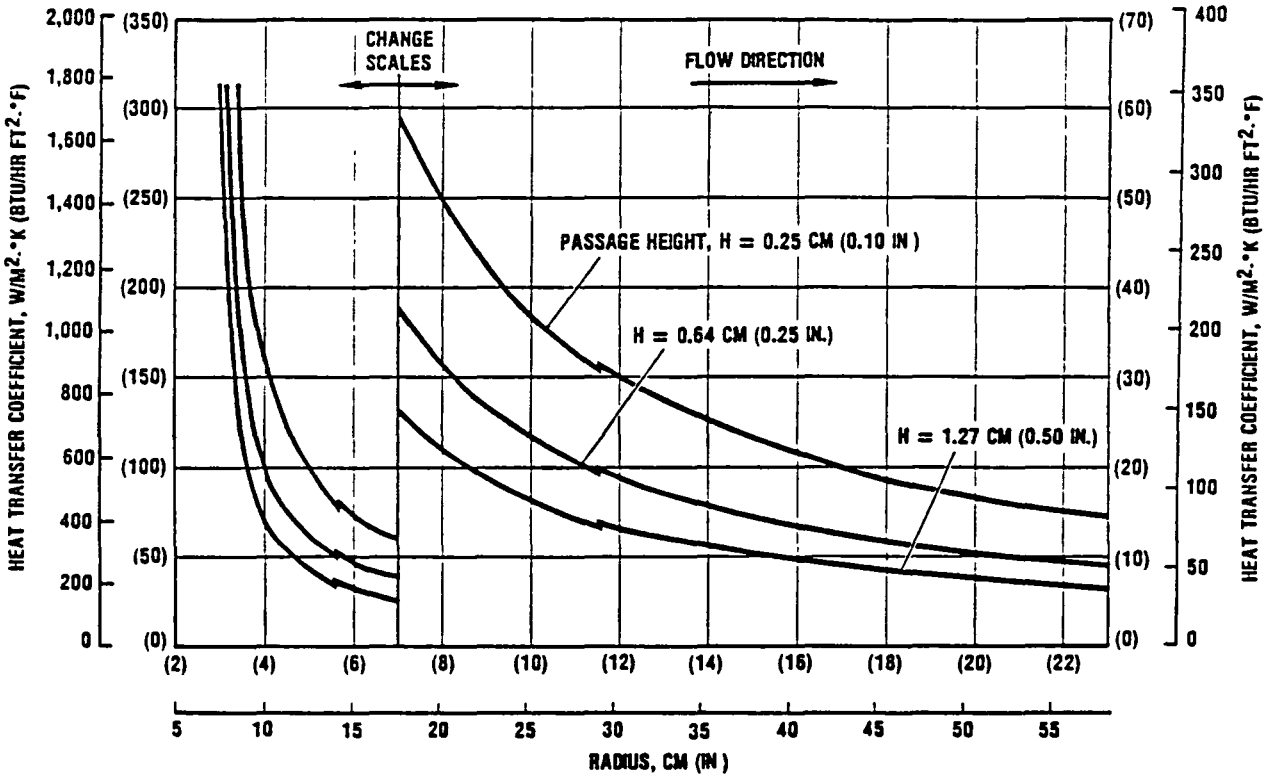

Figure 3-6. LH_2 Subcooler Hot-side Heat Transfer Coefficient (Flow Radially Outward).

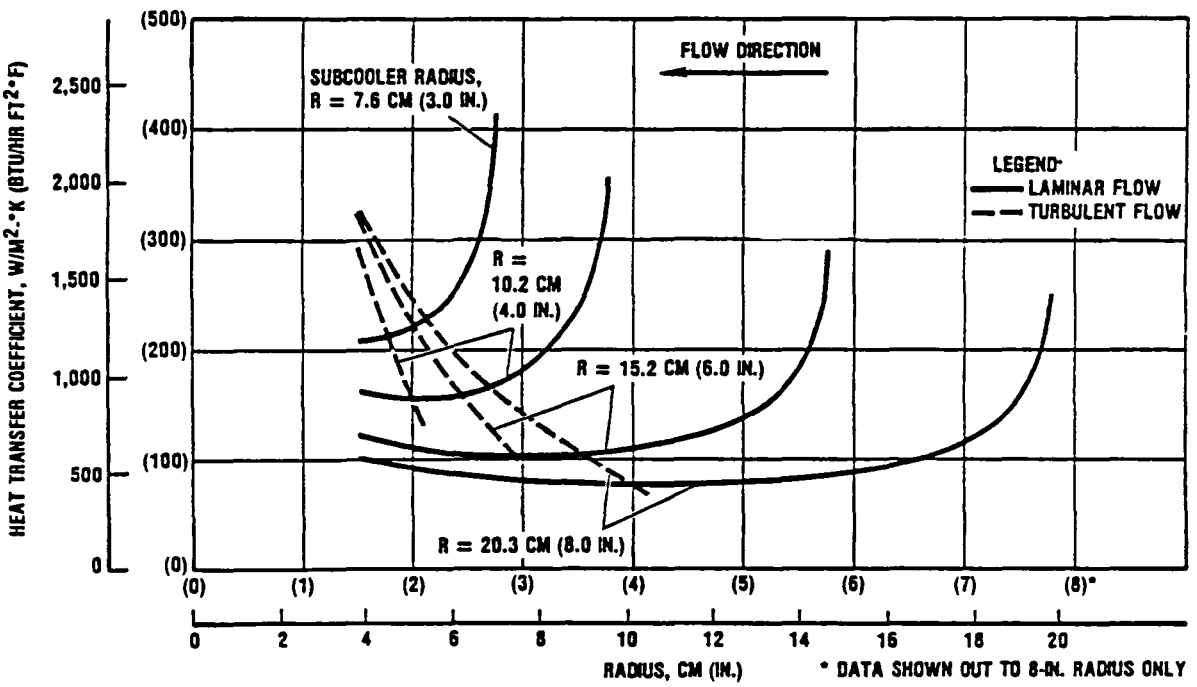

Figure 3-7. LH_2 Subcooler Hot-side Heat Transfer Coefficient, Flow Radially Inward, Passage Height H = 0.25 cm(0.10 in.).

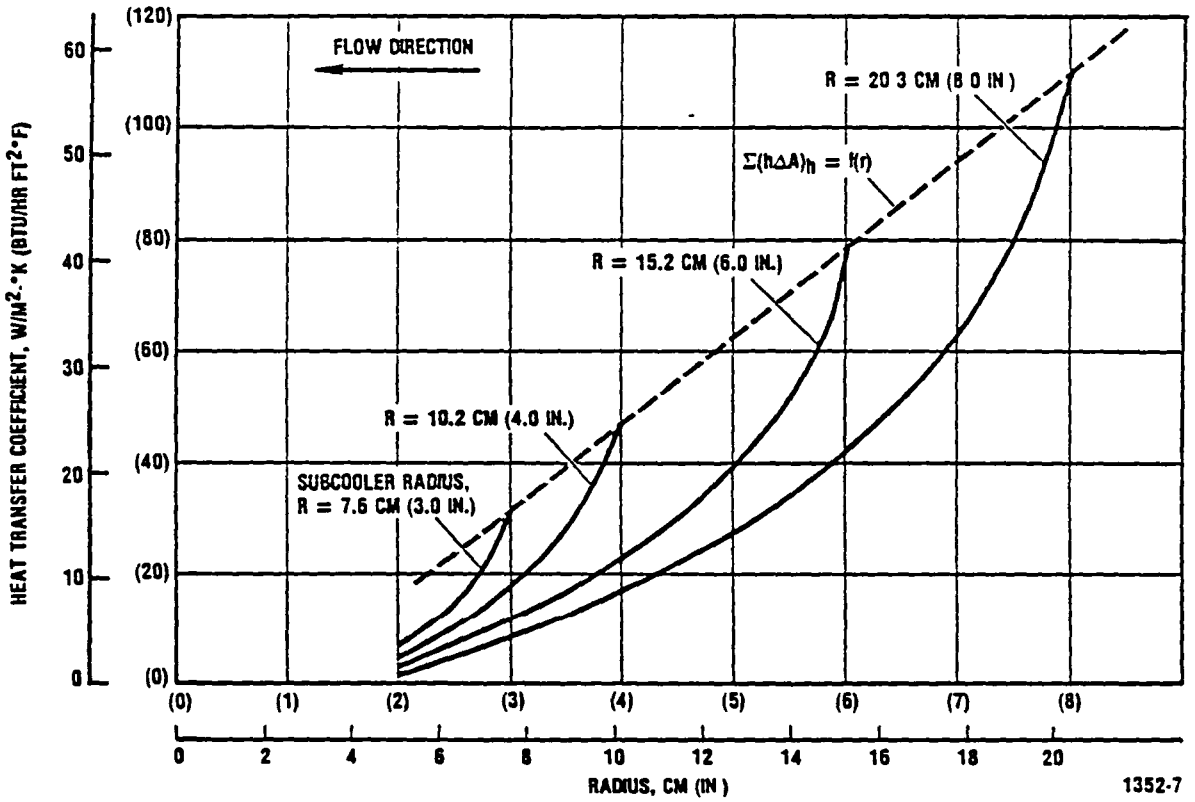

Figure 3-8. Integrated Heat Transfer Coefficient x Area (Including Fin Contribution), LH_2 Flow Radially Inward, Passage Height H = 1.72 cm (0.50 in.)

$k_{\ell C}$ = cold-side liquid thermal conductivity

P_{Ci} = cold-side inlet pressure

ΔT_{WC} = temperature difference between wall and cold-side fluid

h_{sV} = specific enthalpy of saturated vapor on cold side

$h_{s\ell}$ = specific enthalpy of saturated liquid on cold side

$\rho_{\ell C}$ = cold-side liquid density

$\sigma_{\ell C}$ = surface tension of cold-side liquid

$\mu_{\ell C}$ = cold-side liquid viscosity

Equation 3-5 reduces to the form $\dot{Q}_r = (KA)_c(T_w-T_c)^{2.5}$ for each propellant. Specific values for this equation are:

$$LH_2 \quad \dot{Q}_r/A = 12.05\ (T_w-T_c)^{2.5}$$

$$LO_2 \quad \dot{Q}_r/A = 115.6\ (T_w-T_c)^{2.5}$$

$$LCH_4 \quad \dot{Q}_r/A = 25.4\ (T_w-T_c)^{2.5}$$

Note that a heat transfer comparison for the three propellants cannot be made from the above equations alone. Overall hot-to-cold-side ΔTs (and also cold side ΔT, T_w-T_c) vary from 3.8K to 14.1K (6.9R to 25.3R) for the propellants as indicated earier.

Elliptical Bulkhead Subcooler Sizing Calculations

From the above equation development, Equations 3-3a and 3-3b can not be expressed in terms of two unknowns, wall temperature and subcooler radius ($\dot{Q}_r$, T_h and T_c are given or known). The equations were programmed and solved for single pass (one hot-side passage) radially inward flow at passage heights of 1.25, 0.64, 0.25 cm (0.5, 0.25, 0.1 inch) and LH_2, LO_2 and LCH_4 properties. LH_2 subcooler sizes (radii) which provide the heat removal rates of Table 3-1 were computed and are presented in Table 3-2. Reducing passage height increases velocity and heat transfer coefficient, but reduces fin area. The net result is a smaller radius heat exchanger as the passage height is reduced.

Single-pass subcooler radii calculated for NPSP levels of 55.2 and 82.7 kpa (8 and 12 psi) were too great to be practical. Multiple pass subcoolers were therefore analyzed. In this case Equation 3-3a incorporates $\Sigma(h\Delta A)$ versus r expressions which include the relationships for both outward and inward hot-side flow. Subcoolers of 2-pass and 4-pass configurations were sized to provide 55.2 kpa (8 psi) NPSP. Subcoolers of 4-pass and 6-pass configurations were sized to provide 82.7 kpa (12 psi) NPSP. Results are summarized in Table 3-3. As might be expected, increasing the number of passes reduces the required radius.

Heat transfer and sizing equations were similarly developed for LO_2 and LCH_4. Hot-side heat transfer coefficients were within 13% of the LH_2 values. Cold-side (boiling) heat transfer factors and the hot-to-cold-side temperature potentials noted earlier were introduced into Equations 3-3a and 3-3b. The resulting LO_2 and LCH_4 subcooler radii were found to be approximately 94% and 70% of the LH_2 subcooler radii, respectively. As might be expected, the required subcooler size is inverse to the hot-to-cold-side temperature potential for the three fluids considered for an 124 to 34.5 kpa (18 psi to 5 psi) expansion, i.e., the greater the ΔT, the smaller the required subcooler).

Table 3-2. Required LH_2 Single-Pass Subcooler Radius, cm (inches) for Elliptical Aft Bulkhead Tanks.

Hot-Side Passage Height cm (inches)	NPSP, kpa (psi)					
	3.5 (0.5)	6.9 (1.0)	13.8 (2.0)	27.6 (4.0)	55.2 (8.0)	82.7 (12.0)
0.25 (0.10)	5.99 (2.36)	8.31 (3.27)	12.85 (5.06)	23.01 (9.06)	*	*
0.64 (0.25)	7.04 (2.77)	10.69 (4.21)	18.01 (7.09)	34.54 (13.60)	*	*
1.27 (0.50)	7.32 (2.88)	11.56 (4.55)	19.96 (7.86)	40.39 (15.90)	*	*

* Too great to be practical

Table 3-3. Required LH_2 Multiple-Pass Subcooler Radius, cm (inches) for Elliptical Aft Bulkhead Tanks.

Hot-Side Passage Height cm (inches)	NPSP, kpa (psi)			
	55.2 (8.0)		82.7 (12.0)	
	Two-Pass	Four-Pass	Four-Pass	Six-Pass
0.25 (0.10)	47.32 (18.63)	25.65 (10.10)	53.49 (21.06)	37.44 (14.74)
0.64 (0.25)	54.10 (21.30)	29.13 (11.47)	60.93 (23.99)	42.49 (16.73)
1.27 (0.50)	56.44 (22.22)	30.30 (11.93)	63.53 (25.01)	44.20 (17.40)

Torus Tank Subcooler Sizing Thermal Analysis

As described earlier, the torus tank subcooler heat exchanger occupies a section of outlet tubing within the tank. Hot-side flow is described by equations for flow in tubes. Flow is turbulent for the three heat exchanger diameters analyzed: 1.90, 2.54 and 3.81 cm (0.75, 1.0 and 1.5 inches). Entrance effects aside, hot-side heat transfer coefficient is uniform over the heat exchanger length and is given by:

$$h = 0.23 \frac{k}{d} \left(\frac{\rho v d}{\mu} \right)^{0.8} Pr^{0.4} \qquad (3\text{-}6)$$

where

d = hydraulic diameter of each flow passage formed by dividing the tube cross-section into fourths or eighths

Fin efficiency is given by Equation 3-2. The hot-side primary area plus effective fin area is a linear function of the heat exchanger length, L. The hot-side convection factor $\Sigma(h\Delta A)_h$ of Equation 3-3a is therefore merely a constant, times L.

Cold-side heat transfer is again described by Equation 3-5 which reduces to the form of Equation 3-3b. Since cold-side heat transfer area is a constant times L, Equation 3-3b takes the form

$$\dot{Q}_r = K_1 L (T_w - T_c)^{2.5}$$

Equations 3-3a and 3-3b are now known in terms of heat exchanger length and wall temperature. The equations were programmed using LO_2 properties and the resulting computed lengths are summarized in Table 3-4. Reducing hot-side tubing diameter increases velocity and heat transfer coefficient but reduces fin area. The net result is a somewhat shorter heat exchanger as the diameter is reduced. Doubling the number of fins results in a 20% shorter heat exchanger. Since outlet tubing shown in Figure 3-5 is only approximately 76 cm (30 inches) in length, provisions such as doubling the tubing back on itself would have to be made for the longer heat exchangers required for 27.6 kpa (4 psi) NPSP. At NPSP levels of 55.2 and 82.7 kpa (8 and 12 psi), the required lengths are so great that this design concept seems impractical.

The subcoolers sized for the LTPS configurations are small (smaller than those analyzed for the high-thrust vehicles of References 3-1 and 3-2 for a given NPSP level). As a result, hardware weights are generally low. The selected hardware weights computed for the various LTPS configurations and propellant combinations are presented in Table 3-5. In addition to the heat exchanger surfaces, the weights include an inlet manifold, connecting passages, fins for rigidity and the expansion valve. No attempt was made to assess subcooler weight differences between the toroidal and elliptical bulkhead LO_2 tank designs. Thermodynamic considerations for the various thermal conditioning systems resulted in weight penalties which far exceed subcooler hardware weights.

Table 3-4. Torus Tank Subcooler Length, cm (inches)

Diameter cm (inches)	NPSP, kpa (psi) 3.5 (0.5)	6.9 (1.0)	13.8 (2.0)	27.6 (4.0)	55.2 (8.0)	82.7 (12.0)
4 Fins						
1.91 (0.75)	12.8 (5.05)	27.7 (10.9)	60.2 (23.7)	140.5 (55.3)	433.8* (170.8)	1336* (525.9)
2.54 (1.0)	13.3 (5.23)	28.7 (11.3)	62.0 (24.4)	143.5 (56.5)	433.1* (170.5)	1276* (502.5)
3.81 (1.5)	14.9 (5.87)	32.0 (12.6)	69.1 (27.2)	163.1 (64.2)	465.8* (183.4)	1300* (511.8)
8 Fins						
1.91 (0.75)	10.1 (3.96)	21.7 (8.55)	47.5 (18.7)	111.5 (43.9)	352.6* (138.8)	1129* (444.6)
2.54 (1.0)	10.7 (4.22)	23.1 (9.08)	50.0 (19.7)	116.8 (46.0)	357.6* (140.8)	1084* (426.9)
3.81 (1.5)	11.7 (4.60)	25.1 (9.89)	54.4 (21.4)	125.0 (49.2)	371.6* (146.3)	1061* (417.9)

* Probably too long to be practical

The major nonhardware weight penalties for subcoolers deal with 1) the mass of cold-side propellant dumped overboard or, if the cold-side propellant is recirculated back to the tank, 2) the detrimental effects of heat addition resulting from the high energy content of the cold-side fluid. These effects are discussed in the remainder of Section 3.

3.2.3 COLD-SIDE FLOW REQUIREMENTS. To provide subcooled propellants to the main engine a heat sink must accommodate the required rate of heat removal identified in Table 3-1. This heat sink is created by throttling tank propellant to a reduced pressure of 34.5 kpa (5 psi) within the subcooler. Subcooler sizing of Section 3.2.1 has been predicated upon an exit quality of 90%, which identifies the exiting fluid thermodynamic state. This fluid exit state coupled with Table 3-1 heat removal rates is sufficient to identify required cold-side flow rates.

Table 3-5. Selected Thermal Subcooler Weights, kg (lb)

NPSP kpa (psi)	LH_2 Tank kg (lb)	LO_2 Tank * kg (lb)	LCH_4 Tank kg (lb)
3.5 (0.5)	0.45 (1.0)	0.45 (1.0)	0.36 (0.8)
6.9 (1.0)	0.86 (1.9)	0.82 (1.8)	0.54 (1.2)
13.8 (2.0)	2.09 (4.6)	2.00 (4.4)	1.13 (2.5)
27.6 (4.0)	7.35 (16.2)	6.58 (14.5)	3.17 (7.0)
55.2 (8.0)	14.0 (30.8)	12.0 (26.5)	6.03 (13.3)
82.7 (12.0)	36.9 (81.4)	18.1 (40.0)	16.0 (35.2)

* Weight is for elliptical bulkhead design.

3.2.3.1 Coolant Dump Option. The temperature-entropy diagram below gives a thermodynamic description of the cold-side fluid as it flows through the subcooler:

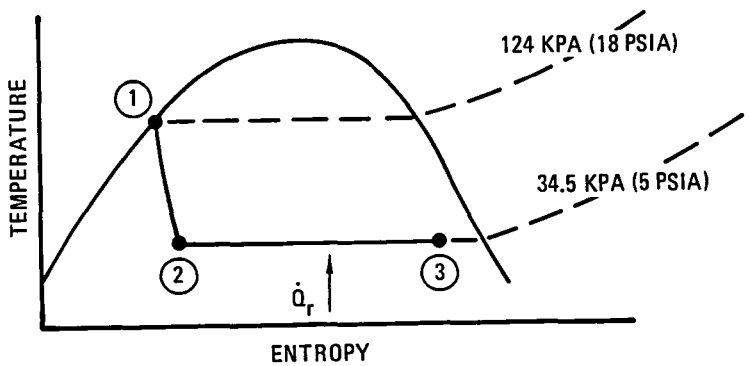

265 585-5

where

① = saturated liquid (at tank pressure) at subcooler inlet

② = two-phase fluid following constant enthalpy expansion process

③ = two-phase fluid at subcooler exit (90% quality) after absorbing energy at required heat removal rate, $\dot{Q}_r$.

This process is identified by the following equation,

$$\dot{Q}_r = \dot{m}_c (h_{3_c} - h_{2_c}) \tag{3-7}$$

or,

$$\dot{m}_c = \dot{Q}_r/(h_{3_c} - h_{2_c}) \tag{3-8}$$

where

$\dot{Q}_r$ = heat removal rate

$\dot{m}_c$ = cold-side flow rate

h_{3_c} = cold-side fluid enthalpy at subcooler exit

h_{2_c} = cold-side fluid enthalpy at subcooler entrance

Coolant flow rates are given in Figure 3-9 for each vehicle configuration.

One of three subcooler configuration options is to dump the cold-side fluid overboard during main engine burn. This is a simpler option than returning coolant to the propellant tank (which requires a pump). However, a substantial weight penalty will result because coolant is dumped for up to 9.3 hours of main engine burn (Table 1-2). Coolant mass dumped during the LTPS mission is given in Figure 3-10 for LH_2 and LCH_4 and in Figure 3-11 for LO_2. Note that up to 1360 kg (3000 lb) LO_2 can be dumped during the mission.

NOTES

1. Flow rates are based upon the following coolant thermodynamic state points:

   - subcooler inlet: liquid saturated at 124.1 kpa (18 psia)
   - subcooler outlet: fluid at 34.5 kpa (5 psia) and 0.9 quality

2. Hot-side (engine liquid enters subcooler saturated at 124.1 kpa (18 psia) and exits at a subcooled state.

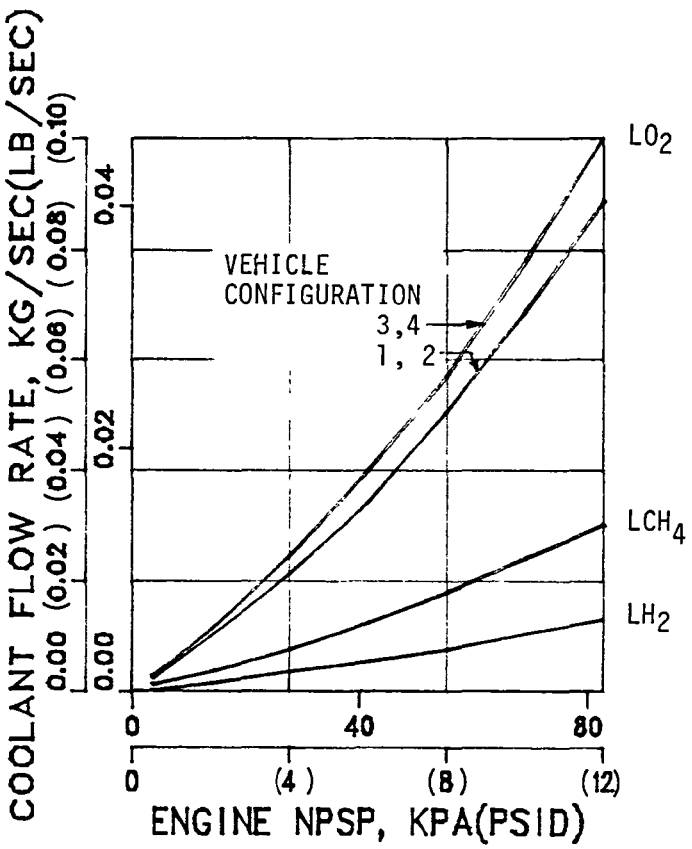

Figure 3-9. Thermal Subcooler Coolant Flow Rates for LTPS Missions.

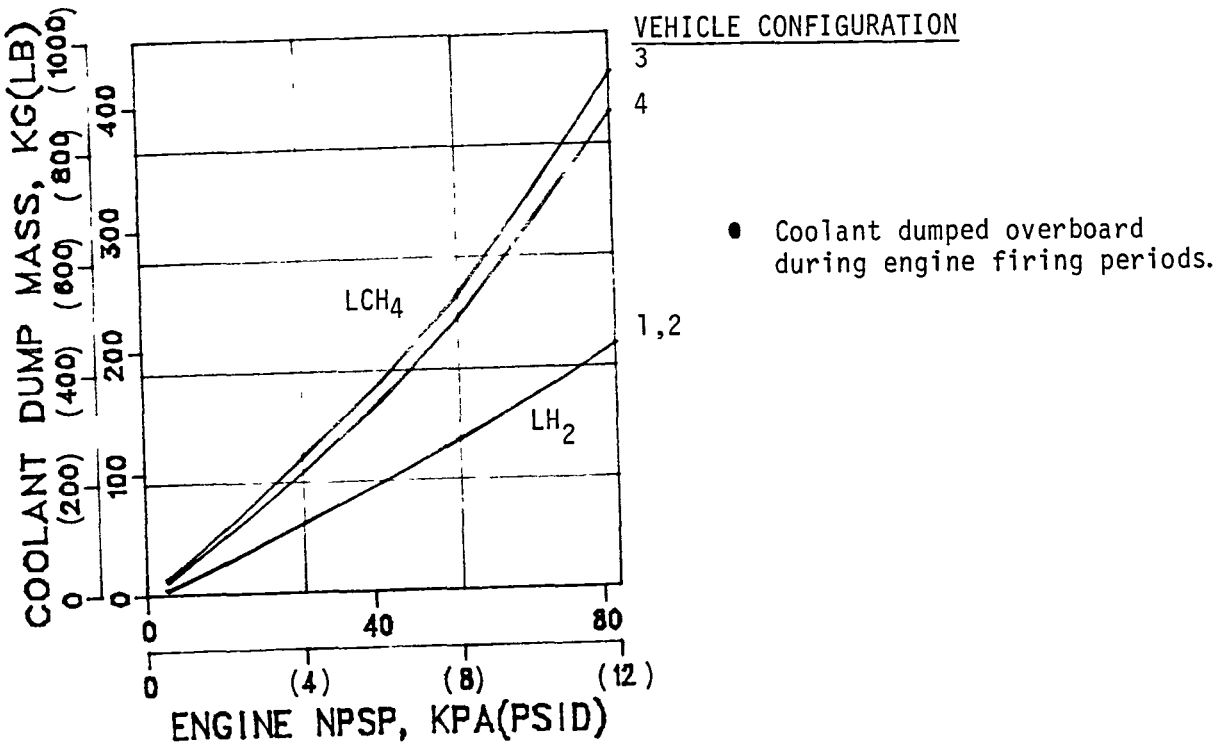

- Coolant dumped overboard during engine firing periods.

Figure 3-10. Thermal Subcooler Fuel Tank Coolant Dump Mass for LTPS Mission.

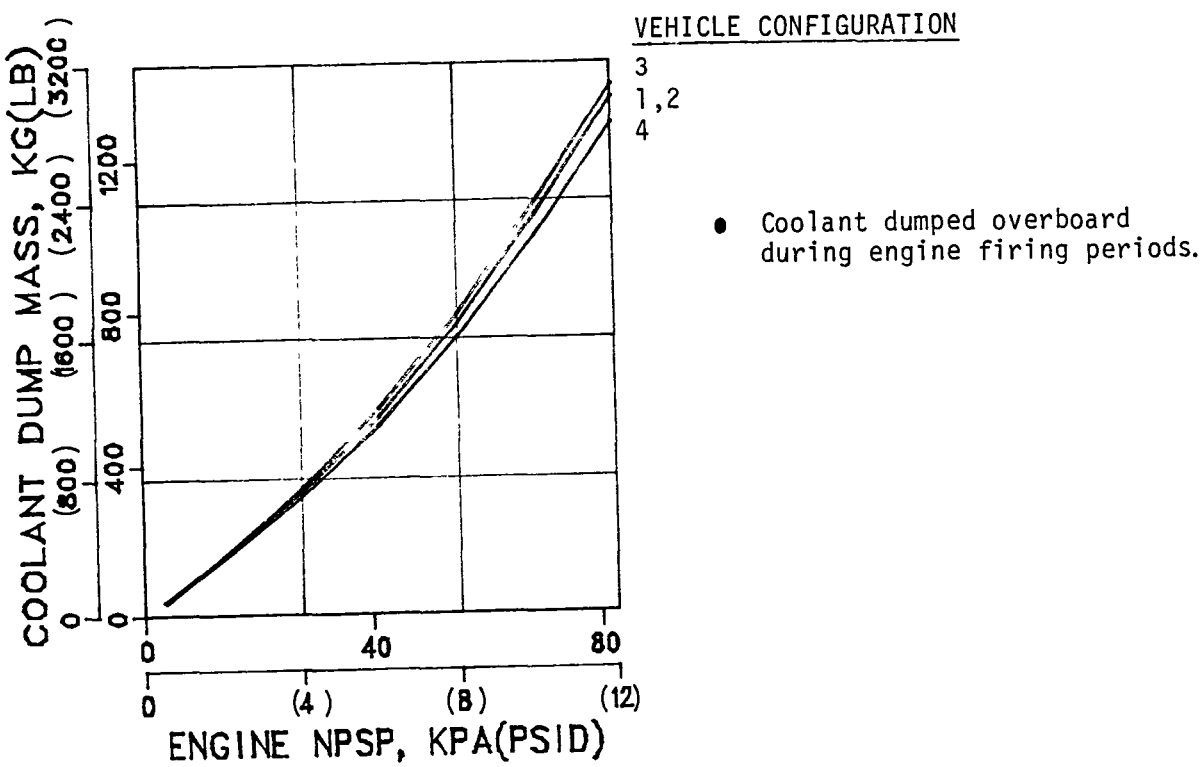

- Coolant dumped overboard during engine firing periods.

Figure 3-11. Thermal Subcooler LO_2 Tank Coolant Dump Mass for LTPS Mission.

3.2.3.2 Coolant Return to Liquid. Because of the high weight penalty inherent with coolant dump, consideration was given to returning the coolant to the propellant tank, beneath the liquid surface. Coolant flow rates will be the same as those calculated for coolant dump because flow requirements are a function only of hot-side NPSP requirements. A pump, motor, plumbing and electrical power will be required to effect coolant return, which represents a complexity over coolant dump. The advantage, of course, is that propellant is saved to provide useful impulse. A major disadvantage, however, is that the coolant will be reentering the tank at a higher energy level than when it entered the subcooler. Consequently, vapor residuals and propellant vent masses will be greater than for the coolant dump configuration. This influence will be discussed in Section 3.3.

A thermodynamic description of the cold-side fluid as it returns to the propellant tank is given below:

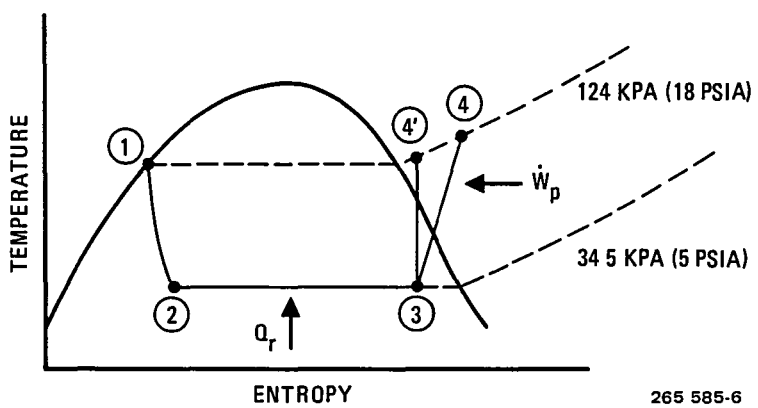

where state points ① ② and ③ were previously described for the coolant dump process. And,

④' = super-heated vapor returning to the tank following an isentropic compression (100 % efficiency).

④ = super-heated vapor returning to the tank along a path which includes the inefficiencies of compression.

This coolant return process is shown schematically in Figure 3-12.

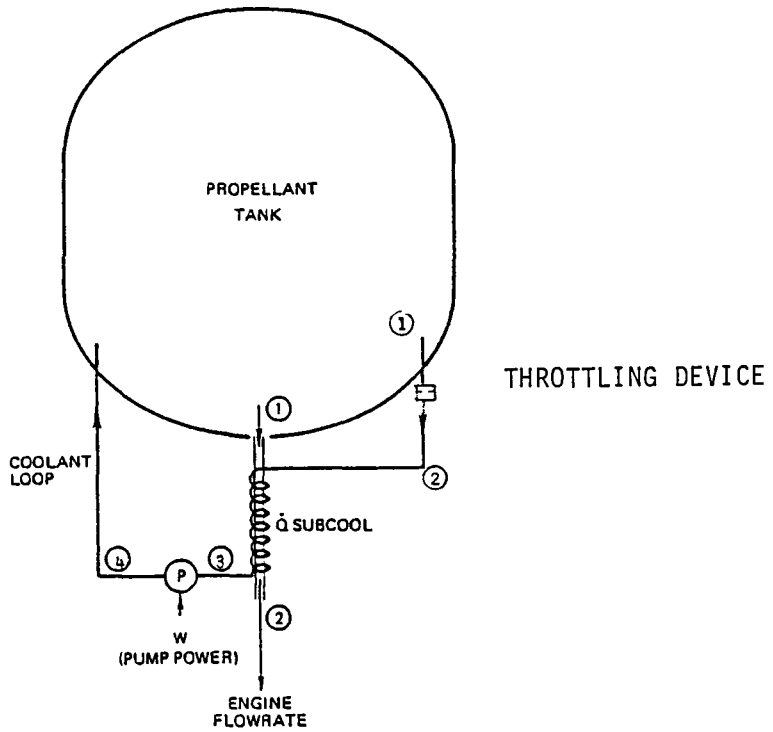

Figure 3-12. Subcooler Heat Transfer and Pump Power Are Added to Cold-Side Fluid.

The equations describing the process between states ③ and ④ are:

$$\dot{W}_p = (h_4 - h_3) \times \dot{m}_c \qquad (3\text{-}9)$$

and

$$\dot{W}_p = (h_{4'} - h_3) \times \dot{m}_c / \eta_p \qquad (3\text{-}10)$$

where h_4 = enthalpy of coolant returned to the tank

$\dot{W}_p$ = pump power absorbed by coolant

$h_{4'}$ = enthalpy of coolant returned to tank for 100% efficiency during compression process (constant entropy process).

η_p = pump compression efficiency (assumed to be 80%).

Heat addition to the propellant tank from coolant return is approximated by

$$\dot{Q}_c = \dot{Q}_r + \dot{W}_p = \dot{Q}_r + (h_{4'}-h_3) \times \dot{m}_c/\eta_p \qquad (3\text{-}11)$$

where $\dot{Q}_c$ = heat rate addition due to coolant return.

Now, all variables are known with the exception of $h_{4'}$, which can readily be calculated for an isentropic process. $\dot{Q}_c$ has been determined for each propellant tank; results are given in Figure 3-13. Note that $\dot{Q}_c$ can be nearly two orders of magnitude greater than space heating rates for MLI systems and more than one order of magnitude greater for SOFI systems. It is clear that vent masses for the LTPS mission will be greatly affected by these tank heating rate increases. This impact is explored in greater detail in Section 3.3.

3.2.3.3 Coolant Return to Ullage. Each of the two previously discussed subcooler options appear to suffer from major LTPS performance shortcomings. As a result, a third option was suggested by the NASA-LeRC Program Manager, that of returning the coolant (now in gaseous form) to the ullage.

Figure 3-14 describes the thermodynamic processes of this coolant return option. Coolant extracted from the propellant tank as liquid will be returned as a low temperature vapor once it has cooled propellant flow to the engine (point 1 to 2) and is pumped back to the tank. Thus the coolant will serve as a low temperature autogenous pressurant that can maintain tank pressure during engine burn.

Figure 3-14a shows that the total propellant NPSP at the engine inlet will be comprised of two terms: propellant subcooling and tank pressurization. Propellant subcooling will be accomplished, as before, with the subcooler. The coolant returned will provide for tank pressurization, as described above. Figure 3-14b shows how these terms can be combined to arrive at the total available NPSP. The results from the detailed analysis of this concept are included in the following section. Figure 3-14b indicates the advantage to be gained by this pressurization technique, that of a decreased coolant flow to provide the same NPSP as a thermal subcooler without coolant return. A reduction in coolant flow also decreases energy input to the tank which will result in reduced boiloff for the LTPS mission.

3.3 TYPICAL MISSION ANALYSIS

A thermal subcooler will influence LTPS mission performance. Vapor residuals, propellant ventage and coolant flow dumped overboard will be affected by the type of subcooler in use. Propellant tank weights must also be increased for mission pressures that exceed the design value of 165.5 kpa (24 psid). Three coolant flow options were evaluated for their effect upon propellant tank pressure profiles, vent masses and vapor residuals. For the first option, that of coolant dump, NPSP levels had no influence upon tank thermodynamic conditions. The major shortcoming of this option was that large propellant quantities would be dumped overboard during the mission, (Figures 3-10 and 3-11). For the second option, coolant return to the propellant, engine NPSP

- Heating rates are based upon the following thermodynamic state points.
  - subcooler inlet: liquid saturated at 124.1 kpa (18 psia).
  - subcooler outlet: fluid at 34.5 kpa (5 psia) and 0.9 quality.
  - pump (at 80% efficiency) return coolant to propellant tank.
- Hot-side (engine) liquid enters subcooler saturated at 34.5 kpa (18 psia) and exits at a subcooled state.

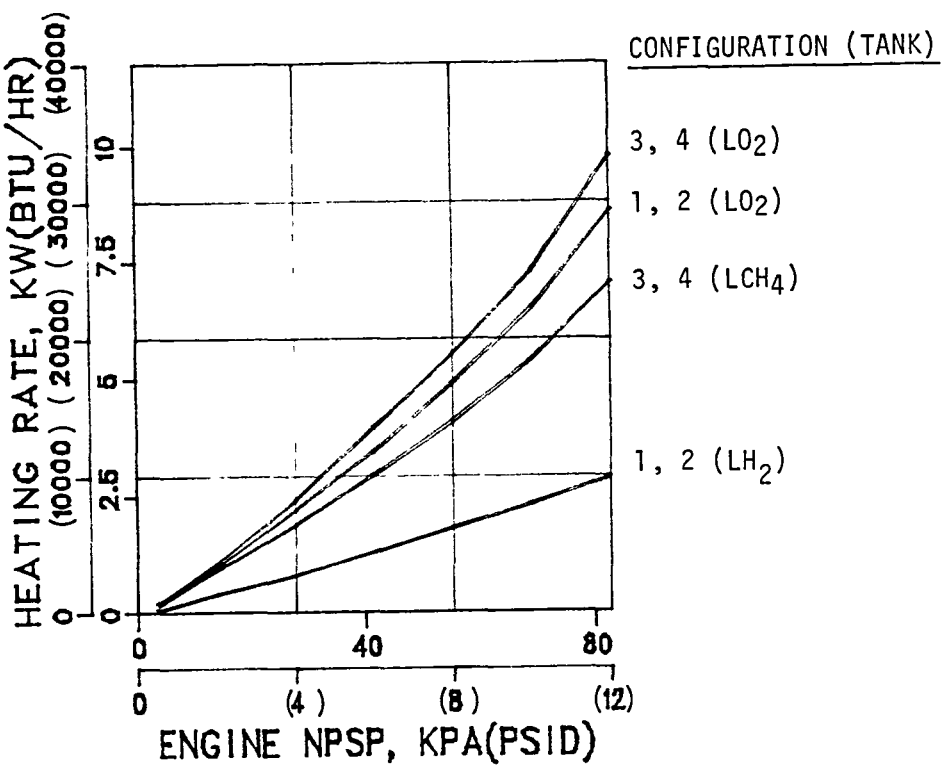

Figure 3-13. Propellant Heating Rates Caused by Coolant Return Flow Rates.

(a)

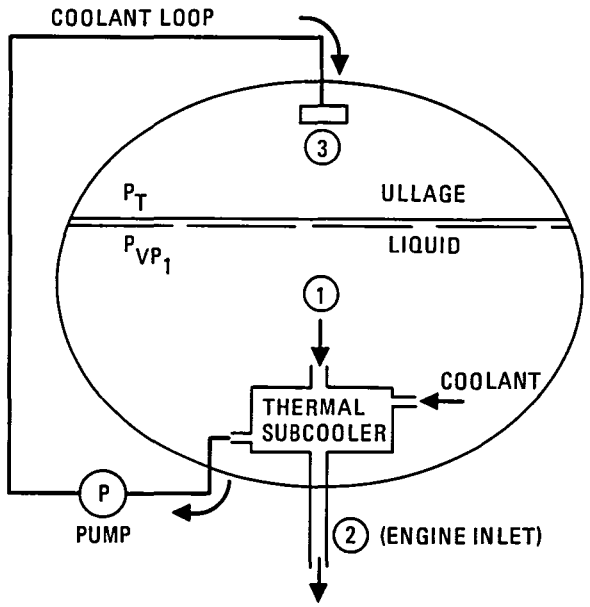

$$\Delta P_T = P_T - P_{VP_2}$$
$$= (P_T - P_{VP_1}) + (P_{VP_1} - P_{VP_2})$$
$$= \Delta P_u + \Delta P_s$$

ΔP_T = ENGINE NPSP

ΔP_u = ULLAGE PRESSURE RISE

ΔP_s = PROPELLANT SUBCOOLING ΔP

(b)

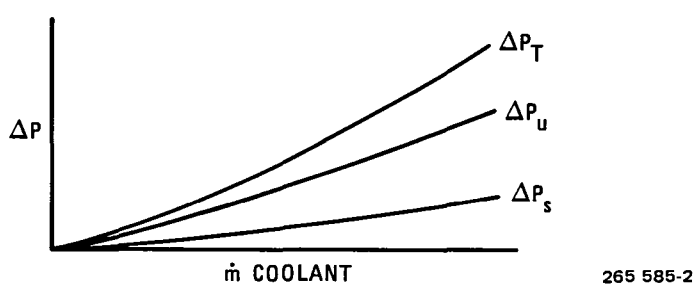

Figure 3-14. Engine NPSP Can Benefit from Thermal Subcooler Having Coolant Return to Ullage

levels had a substantial influence upon propellant temperatures and vapor pressures, vent masses and vapor residuals. This effect was caused by high heating rates indicated by Figure 3-13. The third option, that of coolant return to the ullage, proved to be the most promising candidate of the three. This option avoided coolant dump losses and benefited from the high energy state of the returned coolant which provided autogenous pressurant without suffering excessively from increased vent masses. A detailed discussion follows.

3.3.1 LH_2 TANK SYSTEM ANALYSIS. The thermal subcooler system influence upon LH_2 propellant tank thermodynamics is discussed in this section, with emphasis upon quantifying vapor residuals, vent mass and peak tank pressures. These quantities combined with coolant dump mass (where applicable) will enable a compilation of total system weight penalties.

3.3.1.1 LH_2 Propellant Vapor Pressures. Figures 3-15 and 3-16 give LH_2 vapor pressure histories for the ranges of NPSP levels and coolant flow options considered in this study. Propellant vapor pressure histories are independent of NPSP level for the coolant dump option. This is in contrast to the coolant return to liquid option which shows a substantial vapor pressure increase for high engine NPSP levels. Effects of the three options are detailed below for the four major phases of the LTPS mission.

Engine Burns. Liquid vapor pressure will decay during all engine burns of the coolant dump option as the propellant boils to self-pressurize the ullage. Propellant boiling will reduce liquid temperature, which in turn decreases liquid vapor pressure. Because the coolant is dumped overboard during engine burn, it will not influence propellant tank conditions, except for the amount of coolant dumped. This variation in coolant mass quantity will have an insignificant influence upon tank thermodynamic conditions.

When coolant from the thermal subcooler is returned to the propellants, it will add substantial heat to the propellants. This heat rate (given in Figure 3-13) is the sum of energies absorbed from the engine (or hot-side) propellant and the pump work required to return coolant to the propellant tank. The heat rate magnitudes indicate that the coolant return flow will be the dominant heat source for propellant tank heating at the high NPSP levels. This is evident in the vapor pressure history comparison of Figure 3-15. Note that engine firing vapor pressures rise during each main engine burn for coolant return-to-liquid, whereas vapor pressure decays are experienced for coolant dump. A substantial pressure increase will occur during burn Number 9. This increase in vapor pressure occurs because diminishing propellant quantities are available to absorb the coolant flow energy. Additional detail is provided by Figure 3-17. This data illustrates an advantage of the coolant dump option, which is that propellant tank pressure levels will not have to be elevated to maintain NPSP levels.

① ENGINE BURN
② MECO
③ COAST
④ TANK VENT

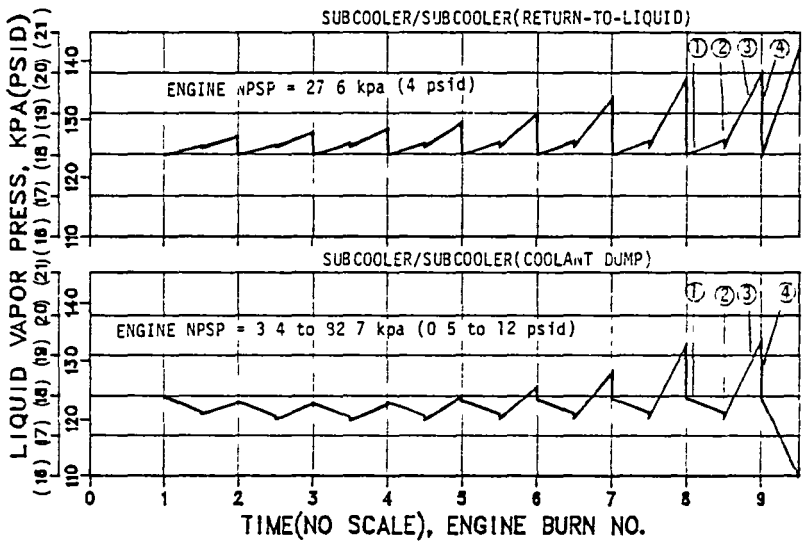

Figure 3-15. Subcooler Influence Upon LH_2 Vapor Pressure (Configuration 1)

① ENGINE BURN
② MECO
③ COAST
④ TANK VENT

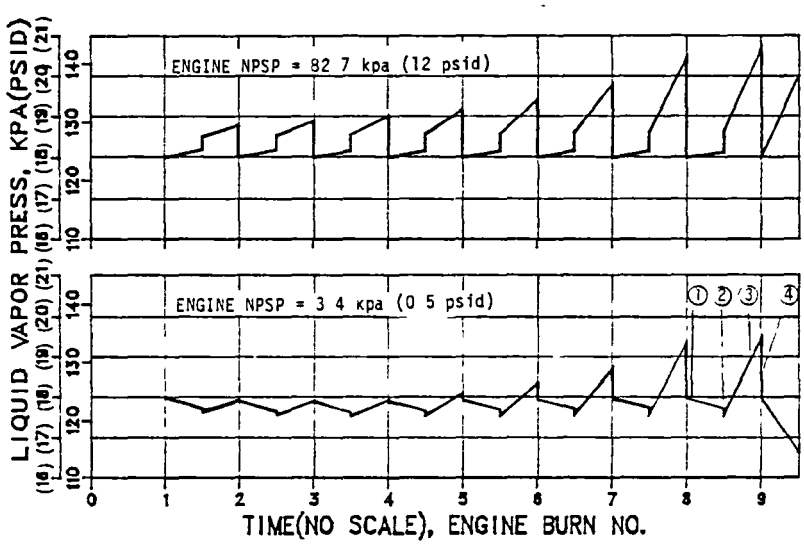

Figure 3-16. Subcooler Influence Upon LH_2 Vapor Pressure (Coolant Return-to-Ullage, Configuration 1)

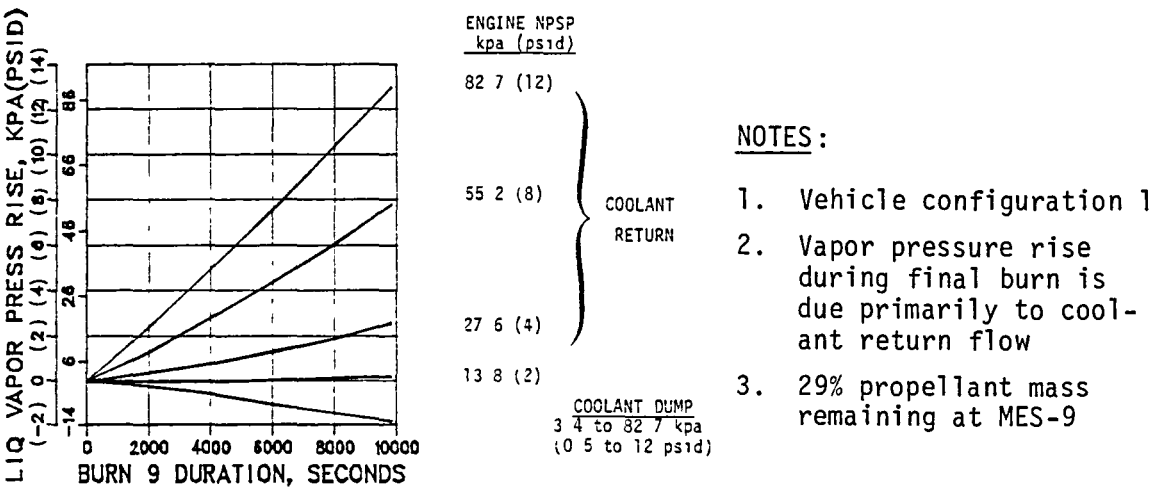

Figure 3-17. NPSP Influence Upon LH_2 Vapor Pressure During Burn No. 9 (Subcooler)

For the third option, that of coolant return to the ullage, vapor pressure histories will reside between those for coolant dump and coolant return to the liquid, Figure 3-16. Vapor pressures during engine burn periods will decay slightly at low engine NPSP conditions and rise slightly at high engine NPSP conditions.

Propellant Mixing at MECO. The combination of main engine shutdown disturbances and zero-g coast environment will serve to create a thermal equilibrium condition in the tank following each MECO. It is expected that near-equilibrium conditons will exist in the propellant tank during engine burn, except for option three. Consequently there will be little or no pressure change experienced after MECO. For the third option, a slight pressure decay is experienced following each MECO at low engine NPSPs and pressure increases are experienced at the higher NPSPs.

Coast Phase. Coast phase pressure rise is affected by two variables only, heating rate and percent propellant in tank. Thus, the coast phase pressure rise is independent of pressurization system and NPSP level.

End of Coast Vent. The propellant tank is vented down to 124.1 kpa (18 psia) at the end of each coast period. Figure 3-15 shows that the maximum NPSP condition for coolant return to the liquid will require propellant tank venting following each coast period. For the coolant dump option, however, venting will not be required until prior to engine burn Number 6. Figure 3-16 shows that venting requirements for coolant return to the ullage are, at high NPSPs, similar to those for coolant return to liquid; at low NPSPs, venting requirements are similar to those for coolant dump.

3.3.1.2 Peak Tank Pressures. Peak tank pressures occurring during the LTPS mission for the three subcooler options are given in Figure 3-18. For coolant dump, tank pressure never increased to the maximum design value of 165.4 kpa (24 psia). Consequently, a tank weight increase is not required and a weight penalty is not given in Figure 3-19. For coolant return-to-liquid, maximum design tank pressure is exceeded by 48.3 kpa (7.0 psid), which results in the maximum tank weight penalty of 48.2 kg (106 lb) given in Figure 3-20. Finally, for coolant return to ullage, a peak tank pressure of 167.5 kpa (24.3 psia) will be experienced. The corresponding maximum tank weight penalty shown in Figure 3-21 is 2.3 kg (5.0 lb).

3.3.1.3 Hydrogen Vent Mass. The propellant tanks will be vented down to 124.1 kpa (18 psia) following each zero-g coast period. Propellant vapor pressure will be greatest for the coolant return-to-liquid option because of the heat addition provided by the coolant flow rate. Consequently, more propellant vapor will be vented for this option. The total hydrogen mass vented is given in Figure 3-22 as a function of NPSP for the three subcooler options. As expected, the engine NPSP influence upon vent mass is substantial for both coolant return options and has no impact upon the coolant dump option.

3.3.1.4 Hydrogen Vapor Residuals. Vapor residuals exhibit the same trend as do vent masses relative to the influence of engine NPSP and coolant dump options. That is, residuals are greatest for coolant return to liquid and least for coolant dump. The residual mass difference at 82.7 kpa (12 psid) can be as great as 34.5 kg (76 lb).

3.3.1.5 Total Thermal Subcooler Thermal Conditioning System Weight Penalties. The weight penalty attributed to the thermal subcooler options includes the following: tank weight increase, subcooler weight, vent mass, vapor residuals and coolant dump mass. For the coolant dump option (Figure 3-19), it is seen that coolant dump mass represents approximately 70 percent of the total penalty of 354 kg (780 lb) at the maximum engine NPSP. The coolant dump mass appears to be excessive at high NPSPs, and an alternative should be considered.

One alternative to coolant dump is to return coolant to the liquid propellant. Figure 3-20, however, shows that an excessive coolant dump mass is replaced with what appears to be excessive vent mass. This vent mass represents about 48 percent of the total system penalty of 372 kg (820 lb) at the maximum engine NPSP. In fact, this option offers no advantage over coolant dump.

The final option of coolant return to ullage (Figure 3-21) offers a significant improvement over the other options at the high engine NPSP levels. This is due to the moderate vent mass quantities predicted for the LTPS mission. A weight savings as great as 136 kg (300 lb) will be experienced by using the coolant for autogenous pressurization.

The weight penalties of Figures 3-19 through 3-21 also apply to Configuration 2 because it is thermodynamically similar to Configuration 1.

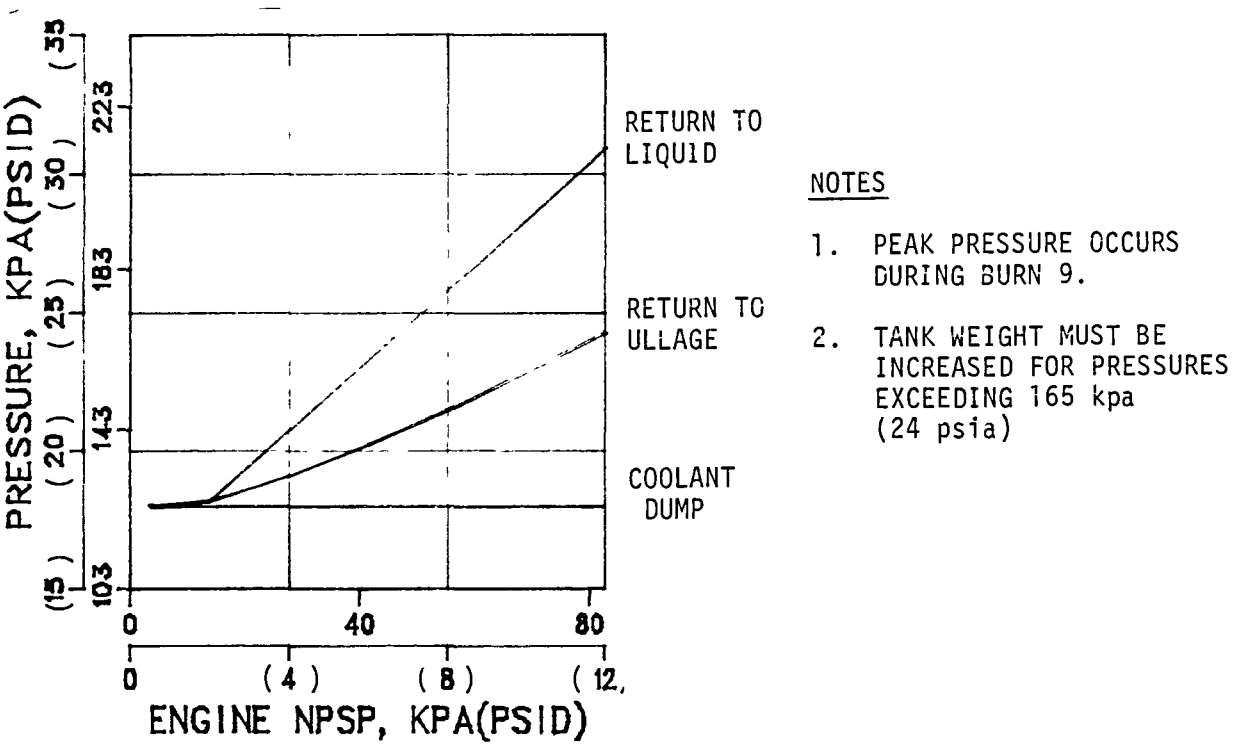

Figure 3-18. Peak LH_2 Tank Pressure During LTPS Mission for Thermal Subcoolers.

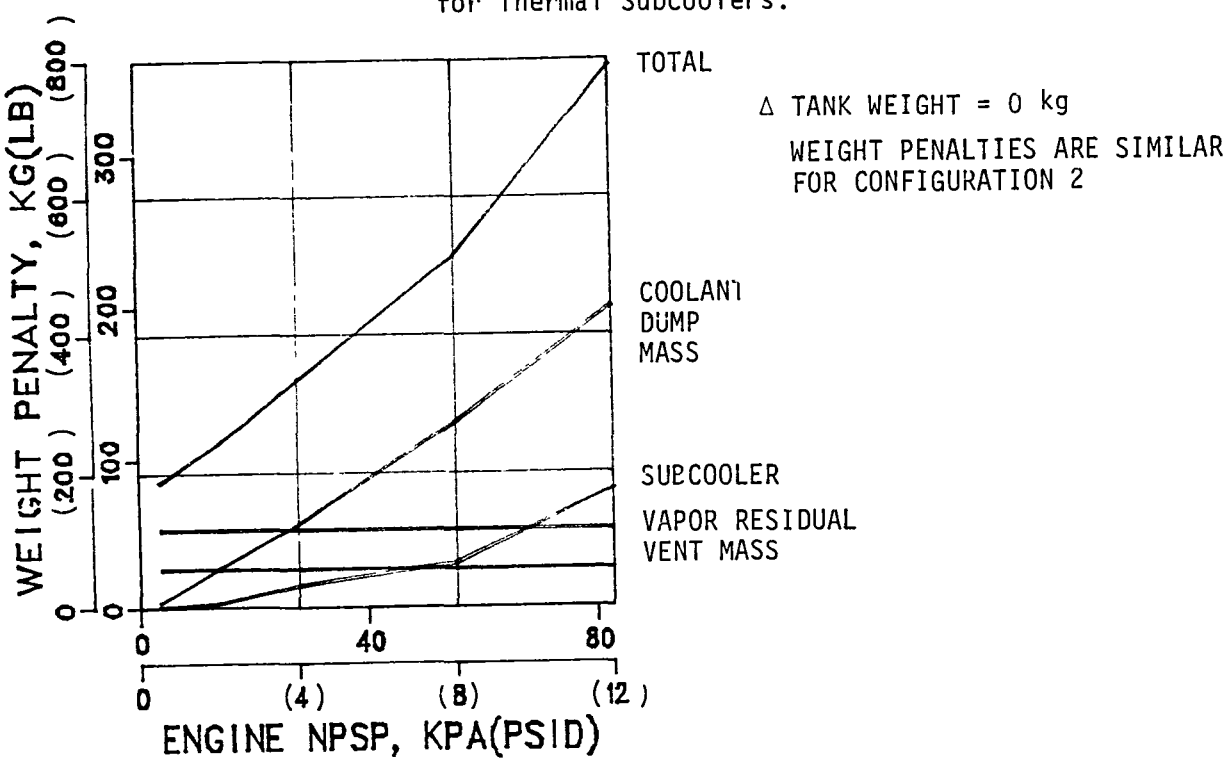

Figure 3-19. LH_2 Tank Subcooler System Weight Penalties (Coolant Dump, Configuration 1)

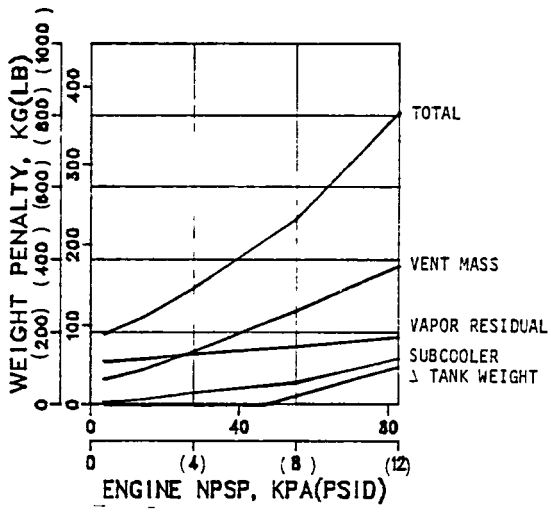

- WEIGHT PENALTIES ARE SIMILAR FOR CONFIGURATION 2

Figure 3-20. LH_2 Tank Subcooler System Weight Penalties (Coolant Return to Liquid, Configuration 1)

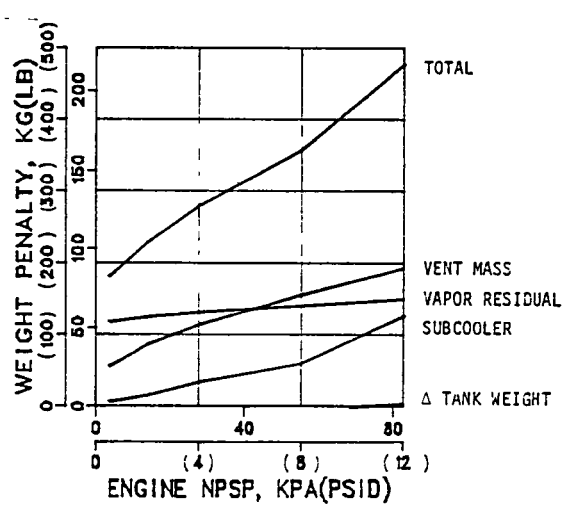

- THE LOWER COOLANT FLOW RATE SUBSTANTIALLY REDUCES VENT MASS IN COMPARISON TO COOLANT RETURN TO LIQUID
- WEIGHT PENALTIES ARE SIMILAR FOR CONFIGURATION 2

Figure 3-21. LH_2 Tank Subcooler System Weight Penalties (Coolant Return to Ullage, Configuration 1)

3.3.2 LO_2 AND LCH_4 TANK SYSTEM ANALYSES. The thermodynamic influence of subcoolers upon LO_2 and LCH_4 propellants is similar to that described for LH_2 during all phases of flight. Consequently, the LO_2 and LCH_4 analysis results are summarized only, rather than discussed for each phase of flight. Insulation system effects upon individual weight penalties will be addressed because the SOFI system of Configuration 4 yields substantially higher heating rates than the MLI system of Configuration 3.

3.3.2.1 Subcooler Influence Upon Ventage and Vapor Residuals. LTPS mission vent masses and vapor residuals versus engine NPSP are given in Figures 3-23 and 3-24 for Configuration 3. Configurations 1 and 2 data are not shown because results are similar to Configuration 3 data. Vapor vent masses and residuals for coolant return to liquid are substantially greater than for the other options due to the high energy content of the coolant. These quantities are lowest for the coolant dump option and remain relatively unaffected by NPSP.

Figures 3-25 and 3-26 summarize ventage and vapor residuals for Configuration 4 (which includes the SOFI system). The trends are similar to Configuration 3 data except that oxygen vent mass quantities are all increased by approximately 1130 kg (2500 lb) and methane vent quantities are increased by about 160 kg (350 lb). These higher vent mass quantities reflect the substantially higher vehicle heating rates of the SOFI system. As stated previously, the vent mass penalty suffered by a SOFI system appears to be unacceptably high, whatever its advantages.

It should be noted that data is not available for the methane tank coolant return to ullage option. There are two reasons for not generating the data. First, another thermal conditioning system had been identified that was clearly preferable to this option. Second, at this same time, less emphasis was being placed upon LO_2/LCH_4 stages by the customer. Consequently, it was concluded that the intent of the study would not be compromised by deleting this analysis.

3.3.2.2 Total System Weight Penalty. Total system weight penalties for the LO_2 tank subcooler options are summarized in Figures 3-27 through 3-30 for Configurations 3 and 4. As expected, the coolant return to ullage option for an MLI system (Figure 3-29) will result in a substantially lower weight penalty than the other options. Total system weight for the option varies from 181 to 490 kg (400 to 1080 lb) over the NPSP range, with vent mass (as the largest factor) representing about 40 percent of the total. For coolant dump (Figure 3-27), system weights are about 218 to 1905 kg (480 to 4200 lb), with the dump mass responsible for 20 to 75 percent of the total, depending upon NPSP level. The return to liquid option (Figure 3-28) shows system weights ranging from 218 to 1410 kg (480 to 3100 lb). Vent mass is the major weight penalty contributor, representing up to 77 percent of the total at high NPSP levels.

Figure 3-30 summarizes the total weight penalty for the coolant return-to-liquid option of Configuration 4. This figure illustrates the adverse effects of a SOFI system, which penalizes the total system by about 1130 kg (2500 lb)

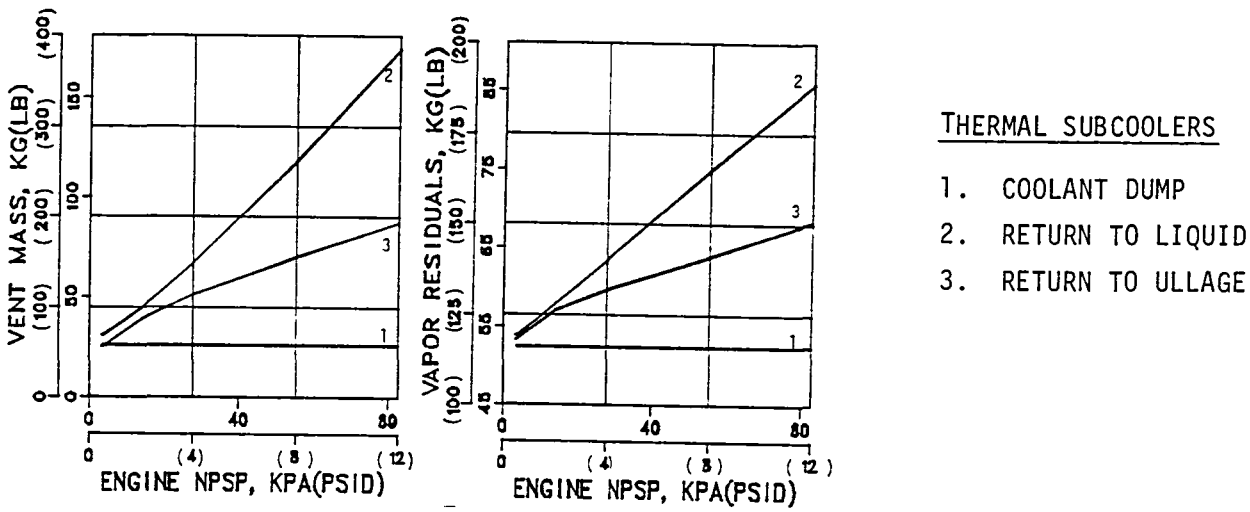

Figure 3-22. Thermal Subcooler System Influence Upon LH_2 Tank Ventage and Vapor Residuals (Configuration 1)

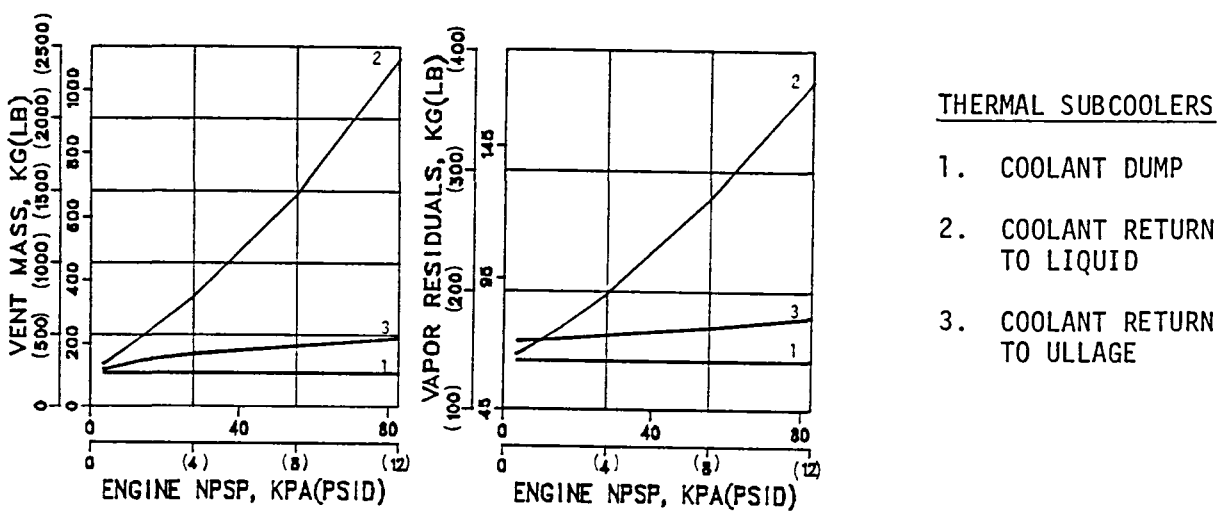

Figure 3-23. Thermal Subcooler System Influence Upon LO_2 Tank Ventage and Vapor Residuals (Configuration 3)

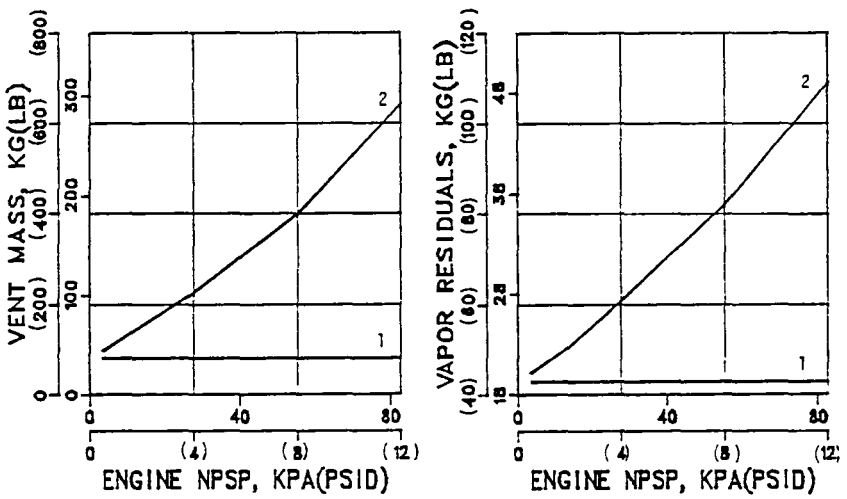

THERMAL SUBCOOLERS

1. COOLANT DUMP
2. COOLANT RETURN TO LIQUID

Figure 3-24. Thermal Subcooler System Influence Upon LCH_4 Tank Ventage and Vapor Residuals (Configuration 3)

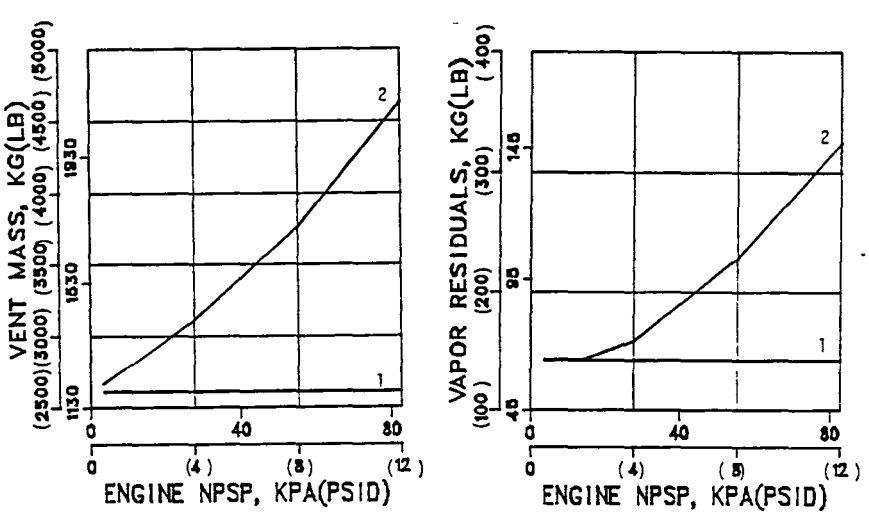

THERMAL SUBCOOLERS

1. COOLANT DUMP
2. COOLANT RETURN TO LIQUID

Figure 3-25. Thermal Subcooler System Influence Upon LO_2 Tank Ventage and Vapor Residuals (Configuration 4)

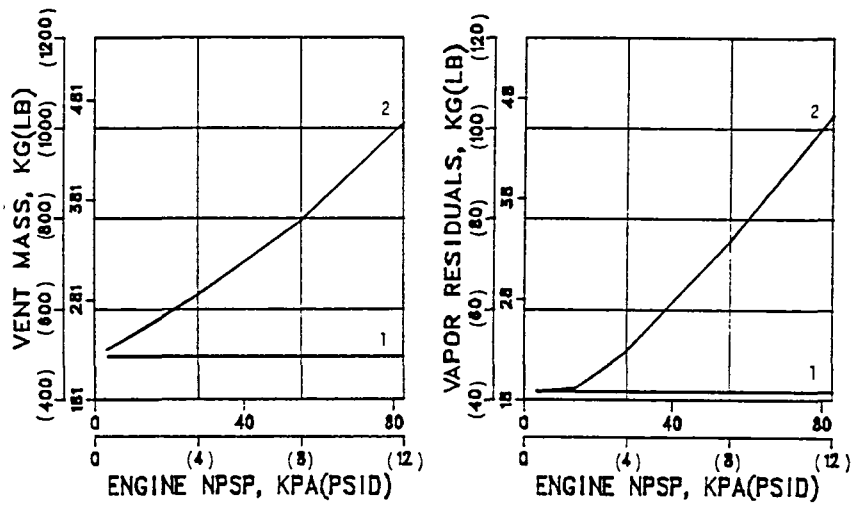

THERMAL SUBCOOLERS

1. COOLANT DUMP
2. COOLANT RETURN TO LIQUID

Figure 3-26. Thermal Subcooler System Influence Upon LCH_4 Tank Ventage and Vapor Residuals (Configuration 4)

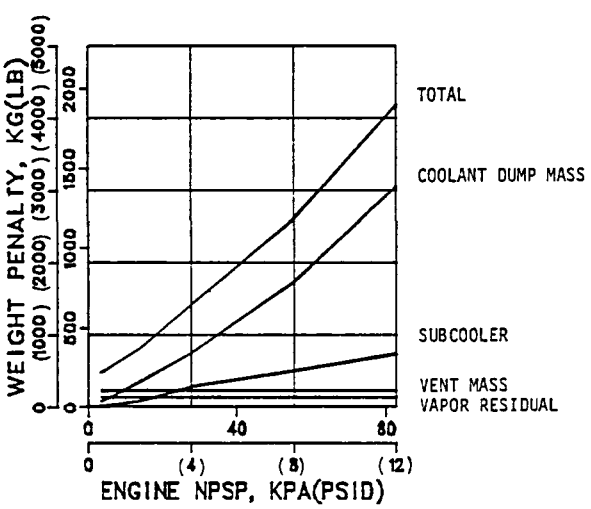

NOTES:

- COOLANT DUMP MASS PRESENTS A SUBSTANTIAL WEIGHT PENALTY
- WEIGHT PENALTIES ARE SIMILAR FOR CONFIGURATIONS 1 AND 2

Figure 3-27. LO_2 Tank Subcooler System Weight Penalties (Coolant Dump, Configuration 3)

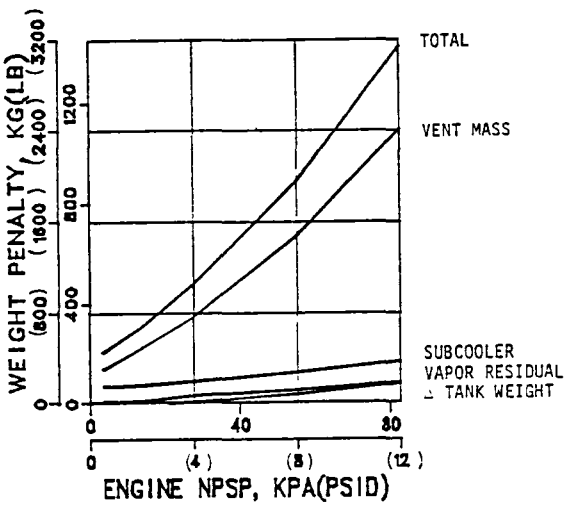

NOTES:

- WEIGHT PENALTIES ARE SIMILAR FOR CONFIGURATIONS 1 AND 2
- VENT MASS PRESENTS A SUBSTANTIAL WEIGHT PENALTY

Figure 3-28. LO_2 Tank Subcooler System Weight Penalties (Coolant Return to Liquid, Configuration 3)

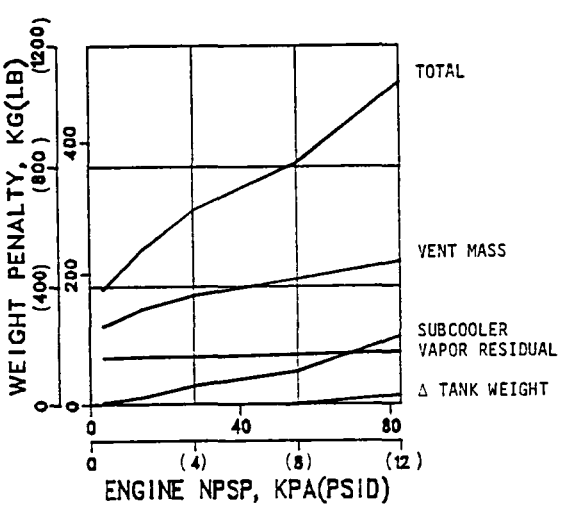

NOTES:

- THE LOWER COOLANT FLOW RATE SUBSTANTIALLY REDUCES VENT MASS IN COMPARISON TO COOLANT RETURN TO LIQUID
- WEIGHT PENALTIES ARE SIMILAR FOR CONFIGURATIONS 1 AND 2

Figure 3-29. LO_2 Tank Subcooler System Weight Penalties (Coolant Return to Ullage, Configuration 3)

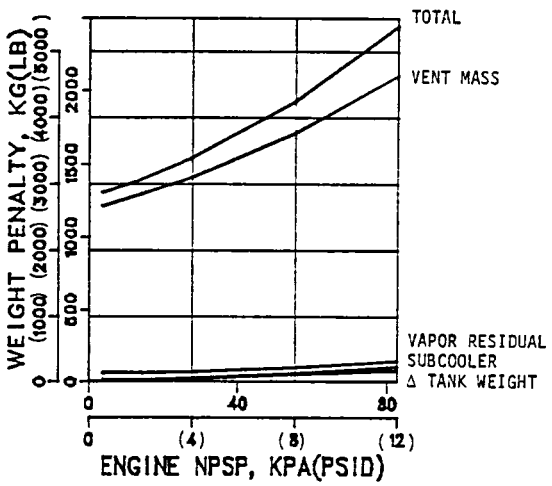

NOTES:

- WEIGHT PENALTIES ARE SIMILAR FOR CONFIGURATIONS 1 AND 2
- VENT MASS DUE TO THE HIGH SOFI HEATING RATES PRESENTS A SUBSTANTIAL WEIGHT PENALTY

Figure 3-30. LO_2 Tank Subcooler System Weight Penalties (Coolant Return to Liquid, Configuration 4)

relative to an MLI system. Since this weight delta also applies to the other options, total weight summaries are not given. Instead, the weight delta can be applied to Figures 3-27 and 3-28, if one wishes to obtain a total weight penalty for Configuration 4.

No LCH_4 system weight summaries are presented in this section for the reasons previously stated in Section 3.3.2.1. It is known, however, that coolant return-to-ullage is the preferred option. It was also known at the time that other thermal conditioning systems would experience even lower weight penalties than this subcooler option and so a decision was made not to pursue the subcooler analyses. Section 5, which compares all thermal conditioning systems, does show a final comparison to support this decision.

4

AUTOGENOUS PRESSURIZATION

A schematic of the autogenous pressurization system is given in Figure 4-1. This system will bleed high pressure gas from the main engine to pressurize propellant tanks. Tank pressure control is maintained through on-off commands of the autogenous pressurization solenoid valves. This system would represent the simplest hardware configuration for LTPS except that autogenous pressurant becomes available only after steady-state engine firing conditions are attained. Consequently, another pressurant source is required for tank pressurization to satisfy engine start NPSP requirements. The schematic of Figure 4-1 includes an ambient storage helium supply system for pressurization employing two techniques, ullage injection and liquid injection (or "bubbler" pressurization) of helium. Other alternatives for engine start pressurization include cryogenically stored helium, and a thermal subcooler. Each option is discussed later.

Aside from the option of selecting a supplementary pressurization system for main engine start, the only variables to consider with this system are autogenous gas temperature and engine NPSP. The influence of each variable upon propellant tank thermodynamic conditions was evaluated for the identified mission heating conditions and vehicle configurations. Neither variable will affect the weight of the autogenous bleed hardware. Only NPSP will influence the weight and selection of the supplementary pressurization system, as described below.

4.1 ENGINE START PRESSURIZATION

Alternative means for engine start pressurization are required to supplement autogenous pressurization during steady-state engine burn. It was expected that any type of system employed for engine start would have considerably less impact upon vapor residuals and mission vent mass than autogenous pressurization because of the time element. That is, autogenous pressurization will be active for up to nine hours during a mission, whereas the systems for engine start NPSP are active for only a matter of seconds during each engine start.

4.1.1 AMBIENT HELIUM STORAGE. This system will use ullage injection of helium for liquid hydrogen tank pressurization and liquid injection of helium pressurant (bubbler pressurization) for liquid oxygen and methane. These pressurization methods were selected for an all-helium pressurization system in Section 2 and that selection applies to this system as well.

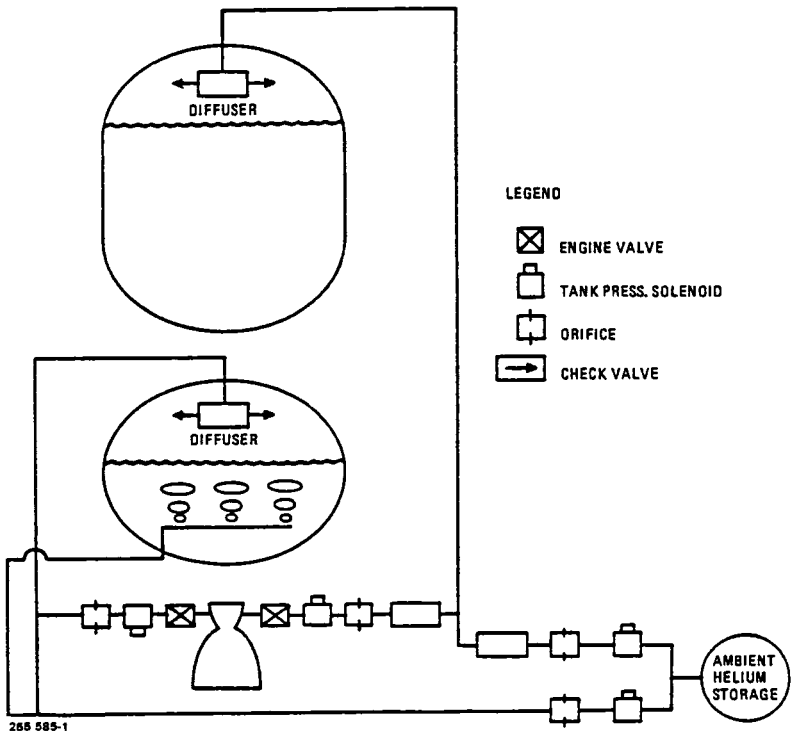

Figure 4-1. Autogenous Pressurization System (with Helium for Engine Start Pressurization)

4.1.2 CRYOGENIC HELIUM STORAGE. In Section 2 (Helium Pressurization), it was judged that the weight advantage of cryogenic over ambient helium storage Phase II of this study only if helium pressurization was found to be one of the preferred techniques. Because an even smaller weight advantage should exist for a helium/autogenous system, the same decision applies to this thermal conditioning system.

4.1.3 THERMAL SUBCOOLER FOR ENGINE START. The discussion of Section 3.3 identified potentially serious shortcomings with the thermal subcooler when used to provide NPSP during engine firing. It was determined that a) propellant tank pressures could become excessively high during engine firings, b) excessive quantities of coolant could be dumped during engine firings, or c) excessive propellant venting could occur during the coast periods. If, however, the subcooler is used for engine start pressurization only, the start-up helium pressurization hardware could be eliminated. Several benefits may be derived from this configuration. One is that the subcooler thermodynamic problems identified for main engine burn are not likely to exist for engine

start. Another benefit is that the adverse effects of helium upon zero-g coast propellant tank venting will be eliminated. An analysis was conducted to determine the benefits and performance penalties for this configuration.

4.2 TYPICAL MISSION ANALYSIS

The autogenous pressurization systems can have a significant impact upon LTPS mission performance, i.e., vapor residuals, propellant ventage and propellant tank weight increases. It was determined that propellant temperatures and resulting vapor pressure histories could be substantially affected by engine NPSP, especially during final engine burn. Vent mass quantities were greatly affected by NPSP, while vapor residuals remained relatively insensitive to this variable. Autogenous temperature was found to have little impact upon the propellant thermodynamic state.

A determination was made that the propellant state was not significantly influenced by either helium pressurization or a thermal subcooler for engine start. This is particularly true for the LO_2 and LCH_4 propellant tanks, where ventage and vapor residuals were about the same for either thermal conditioning system. A general discussion of the tank propellants thermodynamic state is given below for the LH_2 tank (Configuration 1 mission). This description is applicable to all propellants and vehicle configurations, with the exception of Configuration 4. As before, the substantially higher heating rates of a SOFI system create a major deviation from the other configurations.

Specific details for the remaining LTPS propellant combinations are provided in Section 4.2.2.

4.2.1 LH_2 TANK SYSTEM ANALYSIS. Analyses were conducted on configuration 1 to determine weight penalties for these thermal conditioning systems. Vapor residuals, ventage and tank weight increases were combined with pressurization system and subcooler weights (determined using the methods described in Sections 2 and 3). The total weight penalties computed for Configuration 1 also apply to Configuration 2.

4.2.1.1 LTPS Mission Propellant Vapor Pressure. Figure 4-2 gives vapor pressure histories for the extremes of engine NPSP conditions considered for this study. The influence of engine NPSP upon propellant vapor pressure (and temperature) can readily be seen by comparing the 82.7 kpa (12 psid) with the 3.4 kpa (0.5 psid) condition. These effects are detailed below for the four major phases of the LTPS mission and are similar for both autogenous pressurization options.

Engine Burn. Vapor pressure rise during engine burn will increase as NPSP is increased. The increased NPSP level will create warmer ullage temperatures during engine burn which, in turn, will increase ullage-to-liquid heat transfer rates. The subsequent increased liquid heating rate will cause liquid vapor pressure to increase during engine burn. Note that vapor pressure rise during each of the first eight burns will remain below about 3.4 kpa (0.5 psid) but that it will experience a substantial rise during the final engine burn.

① ENGINE BURN

② MECO

③ COAST

④ TANK VENT

- ULLAGE-TO-LIQUID HEAT RATES CAUSE HIGH LIQUID VAPOR PRESSURES DURING BURN NO. 9
- SUBCOOLER/AUTOGENOUS PRESSURE HISTORIES ARE EQUIVALENT TO ULLAGE INJECTOR/AUTOGENOUS PRESSURE HISTORIES.

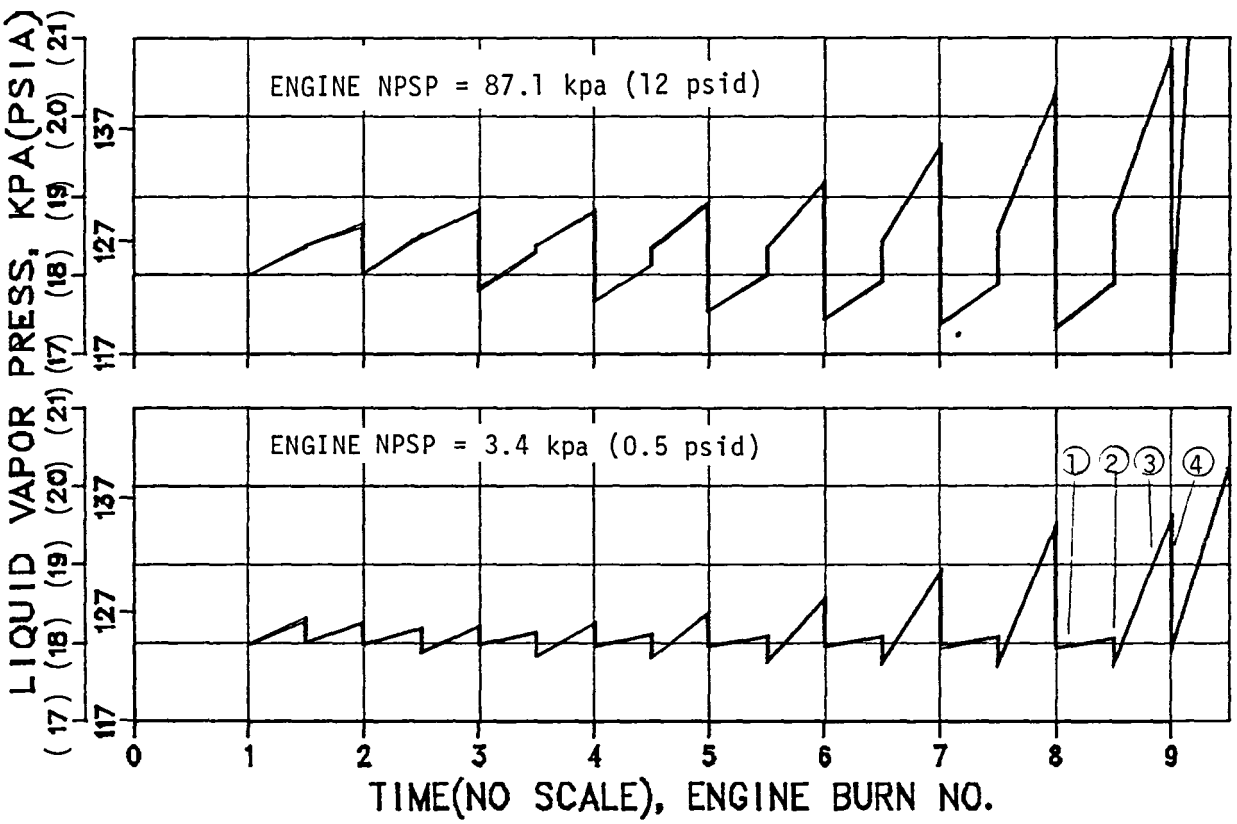

Figure 4-2. Autogenous Pressurization System Influence Upon LH_2 Vapor Pressure (Ullage Injection/Autogenous, Configuration 1).

The rapid vapor pressure rise will occur as diminishing quantities of propellant absorb the high ullage-to-liquid heat rates during the 9759-second burn duration. This data illustrates a shortcoming in maintaining high NPSP levels with autogenous pressurization which is that propellant tank pressure levels will have to be elevated by the amount of the vapor pressure increase in order to maintain NPSP levels. A payload penalty must be assessed against this pressurization technique if tank weight increases are needed to withstand the increased propellant tank pressures. This phenomenon is discussed in greater detail in Section 4.2.2.2.

Propellant Mixing at MECO. The combination of main engine shutdown disturbances and zero-g coast environment will serve to create a thermal equilibrium condition in the tank following each MECO. The ullage mass and dry tank walls may be substantially warmer than liquid at MECO because of autogenous pressurization. The thermal mixing of these mass quantities can result in vapor condensation, liquid evaporation or no phase change at all, depending upon ullage pressure and temperature conditions. Figure 4-2 shows that vapor pressure decays of about 2.1 kpa (0.3 psid) will occur for the minimum engine NPSP condition. Vapor pressure decays are due to liquid evaporation caused by ullage pressure collapse when liquid and vapor are mixed.

The maximum engine NPSP condition will create a vapor pressure rise following propellant mixing. Energy released as vapor is condensed during the mixing process will be absorbed by the liquid with a subsequent vapor pressure rise. Note that vapor pressure rise for the mission ranged between 0 kpa (0 psid) and 6.2 kpa (0.9 psid).

Coast Phase. Coast phase pressure rise is affected by two variables only, heating rate and percent propellant in tank. Thus, neither autogenous pressurization nor NPSP level will affect liquid vapor pressure increase. Figure 4-2 shows that i) coast phase vapor pressure increases are the same for both NPSP levels and ii) vapor pressure rise is greater for the last coast period than for any other coast period. This increased pressure is due in part to a longer coast duration but primarily to a reduced liquid mass in the propellant tank. Propellant tank heating rate was assumed to be constant at 0.217 kW (740 Btu/hr) throughout the mission.

End-of-Coast Vent. The propellant tank was vented down to 124.1 kpa (18 psia) at the end of each coast period. Figure 4-2 indicates that a maximum tank pressure decay of 11.7 kpa (1.7 psid) to 24.1 kpa (3.5 psid) can be expected, respectively, from the minimum and maximum NPSP conditions. The greater tank pressure decay is indicative of more vapor vented for the maximum NPSP condition.

Note that liquid vapor pressure will decay below 124.1 kpa (18 psia) following each vent. The difference between tank pressure and liquid vapor pressure is helium partial pressure, which increases following each pre-MES helium pressurization period.

4.2.1.2 Hydrogen Vent Masses. The total hydrogen mass vented during the mission is given in Figure 4-3 for helium/autogenous pressurization as a

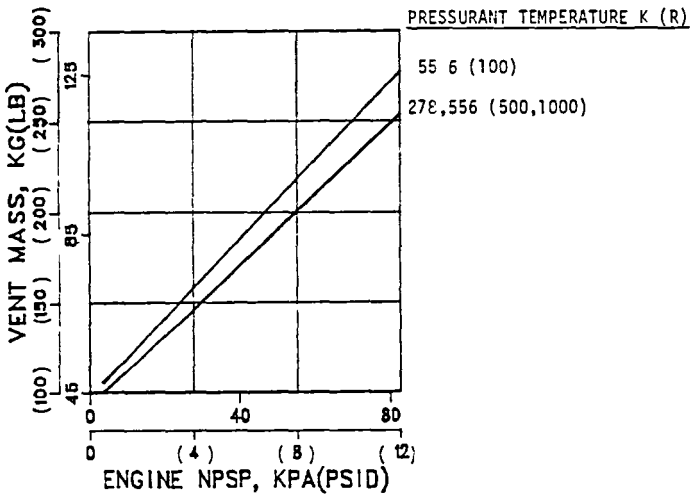

NOTES:

- VEHICLE CONFIGURATION 1
- VENT MASS IS INSENSITIVE TO AUTOGENOUS TEMPERATURES ABOVE 278K (500R). RESULTS ARE SIMILAR FOR LO_2 AND LCH_4 PROPELLANT TANKS
- A TEMPERATURE OF 278K (500R) WAS SELECTED FOR REMAINDER OF STUDY

Figure 4-3. Autogenous Hydrogen Temperature Influence Upon Vent Mass

function of engine NPSP and pressurant gas temperature conditions. The vent mass will be relatively insensitive to autogenous gas temperature. This is particularly true at temperatures above 278K (500R). As expected engine NPSP influence upon vent mass quantities is substantial.

Hydrogen vent masses for the subcooler option were about 18 kg (40 lb) lower than those indicated by Figure 4-3. This difference is due to the helium partial pressure effect which increases tank pressure and, therefore, increases tank venting.

4.2.1.3 Hydrogen Vapor Residuals. Hydrogen vapor residuals, given in Figure 4-4, are seen to be relatively insensitive to NPSP and autogenous gas temperature levels. Vapor residuals will be independent of temperature for levels above 278K (500R). The influence of NPSP is less than 2.7 kg (6 lb). Thus, for practical considerations, vapor residuals will be independent of NPSP and temperature.

Vapor residuals for the subcooler/autogenous option were computed to be the same as for the helium/autogenous option.

It is clear from Figures 4-3 and 4-4 that the selected pressurant temperature should remain well above cryogen temperatures. An evaluation of the LO_2 and LCH_4 tanks gave similar results. A temperature of 278K (500R) was selected for the remainder of this study.

4.2.1.4 Total Autogenous Thermal Conditioning System Weight Penalties. Weight penalties attributed to the autogenous options include the following: tank weight increase, vent mass, vapor residuals, pressurization system and subcooler weight (for the subcooler option only). For the helium pressurization option

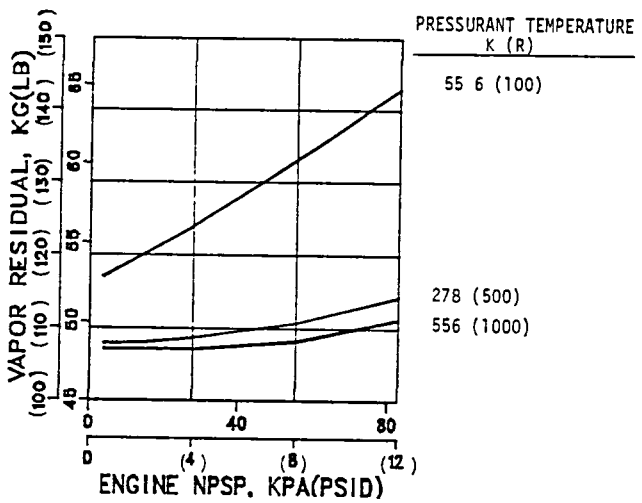

NOTES:

- o VEHICLE CONFIGURATION 1
- o VAPOR RESIDUAL IS RELATIVELY INSENSITIVE TO NPSP AND TEMPERATURE
- o A TEMPERATURE OF 278K (500R) WAS SELECTED FOR REMAINDER OF STUDY

Figure 4-4. Autogenous Hydrogen Temperature Influence Upon Vapor Residual

(Figure 4-5) it is seen that pressurization system weight represents a major portion of the total weight penalty for NPSP levels greater than about 10.3 kpa (1.5 psid). This weight is significant considering that helium is used only for main engine start. Pressurization system weights were determined with the methods described in Section 2. Delta tank weight is zero for NPSP levels less than 20.7 kpa (3 psid) because peak tank pressure remains below 165 kpa (24 psia). For higher NPSP levels, delta tank weight increase can be significant. This increase is caused by the high ullage-to-liquid heat rate during the final engine burn.

Total weight penalties for the subcooler/autogenous option are given in Figure 4-6. Component weights for this option are similar to those given in Figure 4-5, except that subcooler weights are substantially lower than the helium pressurization system weights they have replaced. Thus, total weight penalties for this subcooler/autogenous option are about 36 to 136 kg (80 to 300 lb) lighter than the helium pressurization/autogenous option.

4.2.2 LO_2 AND LCH_4 TANK SYSTEM ANALYSES. The thermodynamic influence of autogenous pressurization upon LO_2 and LCH_4 is somewhat similar to the description given for LH_2. Figure 4-7 shows that ullage-to-liquid heat transfer rates will have a major influence upon tank propellant vapor pressure rise during final main engine burn. Unlike the LH_2 tank, vapor pressure rise will not be excessive because of the substantial propellant thermal masses.

Analyses showed that the total weight differences were minor between helium pressurization and subcooler options for engine start. Ventage, vapor residuals and delta tank weights were the same; weight differences were small between pressurization system and subcooler weights.

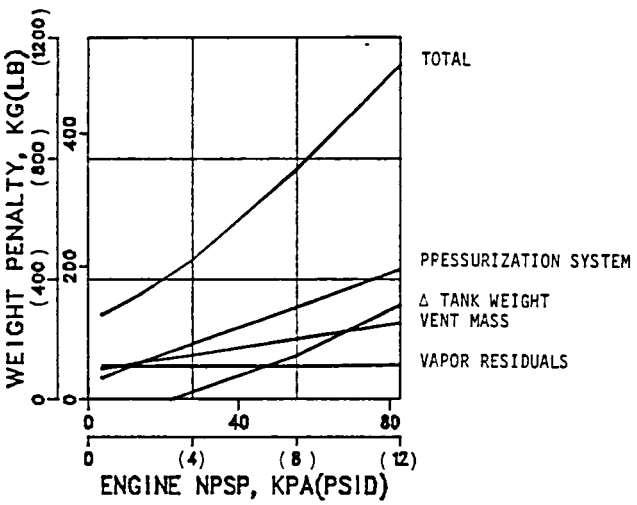

NOTES:

1 Δ TANK WEIGHT BECOMES SUBSTANTIAL AT HIGH NPSPs AS A RESULT OF HIGH ULLAGE-TO-LIQUID HEAT RATES DURING THE FINAL ENGINE BURN

2 WEIGHT PENALTIES ARE SIMILAR FOR CONFIGURATION 2

Figure 4-5. LH_2 Tank Autogenous System Weight Penalties (Ullage Injection/Autogenous, Configuration 1)

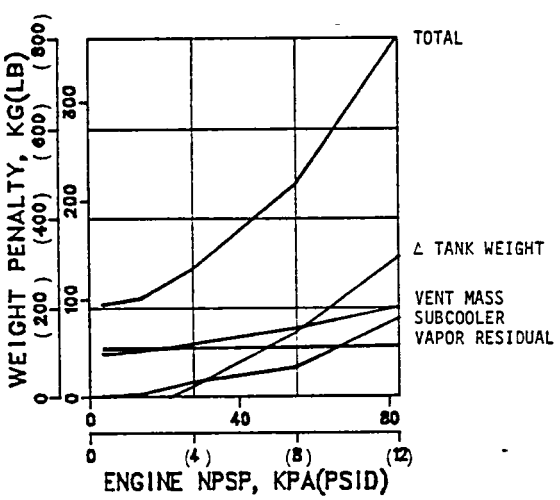

NOTES:

1 Δ TANK WEIGHT BECOMES SUBSTANTIAL AT HIGH NPSPs AS A RESULT OF HIGH ULLAGE-TO-LIQUID HEAT RATES DURING THE FINAL ENGINE BURN

2 WEIGHT PENALTIES ARE SIMILAR FOR CONFIGURATION 2

Figure 4-6. LH_2 Tank Autogenous System Weight Penalties (Subcooler/Autogenous, Configuration 1)

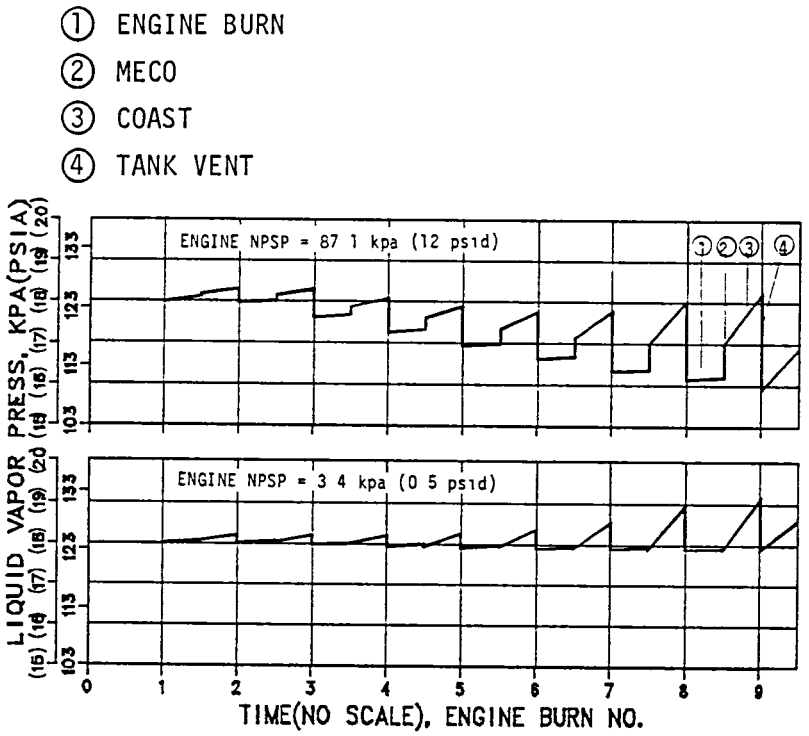

- SUBCOOLER/AUTOGENOUS PRESSURE HISTORIES ARE EQUIVALENT TO BUBBLER/ AUTOGENOUS PRESSURE HISTORIES
- CONFIGURATIONS 1 AND 2 RESULTS ARE SIMILAR TO THOSE OF CONFIGURATION 3

Figure 4-7. Autogenous Pressurization System Influence Upon LO_2 Vapor Pressure (Bubbler/Autogenous, Configuration 3)

Because of similarities between LO_2 and LCH_4 with the LH_2 discussion of Section 4.2.1, LO_2 and LCH_4 results will be summarized only rather than discussed for each phase of flight. Insulation system effects will be addressed because the SOFI system for Configuration 4 yields substantially higher heating rates than the MLI system for Configuration 3.

4.2.2.1 Total System Weight Penalties. Total and component weight penalties for LO_2 tank (Configuration 3) helium bubbler/autogenous pressurization are given in Figure 4-8. Vent mass is the major contributor the the total, representing 60 to 70 percent. The high vent mass reflects the adverse effects of autogenous pressurization, which is that the energy content of the pressurant results in considerable venting during the mission. Vapor residuals are seen to be somewhat insensitive to NPSP level. Pressurization system and delta tank weights together comprise less than 20 percent of the total system weight. Total system weight varies between 218 to 426 kg (480 to 940 lb) over the NPSP range, which is about the same total as for the subcooler/autogenous option.

The influence of the higher SOFI system heating rates upon weight penalty is shown in Figure 4-9. Total weight is about 1000 kg (2200 lb) greater than for the MLI system and this increase is due almost solely to the vent mass increase. Thus the SOFI system has about the same influence on autogenous pressurization as it has on the other thermal conditioning systems analyzed in Section 2 and 3.

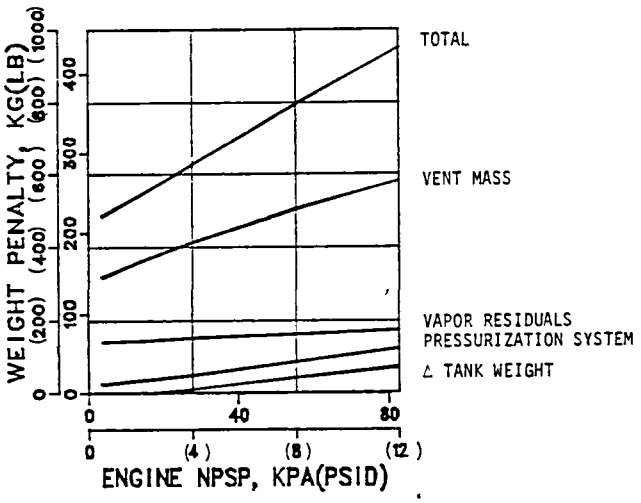

NOTES:

1 TOTAL WEIGHT PENALTIES ARE THE SAME FOR THE SUBCOOLER/AUTOGENOUS OPTION

2 WEIGHT PENALTIES ARE SIMILAR FOR CONFIGURATIONS 1 AND 2

Figure 4-8. LO_2 Tank Autogenous System Weight Penalties (Bubbler/Autogenous, Configuration 3)

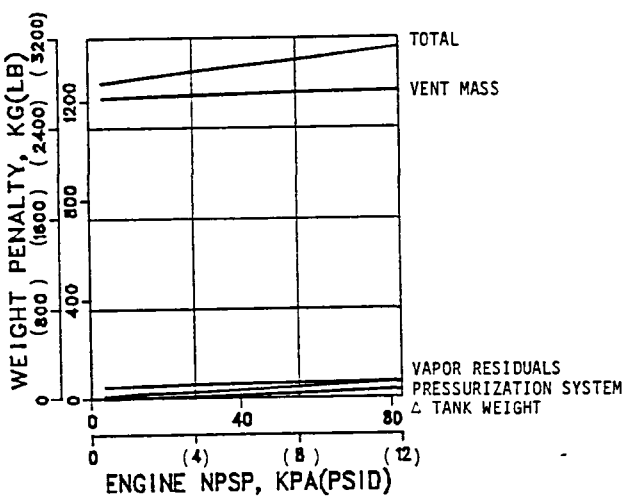

NOTES:

1 INCREASED HEATING RATES OF SOFI SYSTEM ARE RESPONSIBLE FOR THE WEIGHT DELTA BETWEEN CONFIGURATIONS 3 AND 4

2 TOTAL WEIGHT PENALTIES ARE THE SAME FOR THE SUBCOOLER/AUTOGENOUS OPTION

Figure 4-9. LO_2 Tank Autogenous System Weight Penalties (Bubbler/Autogenous, Configuration 4)

The LCH_4 weight summaries are given in Figures 4-10 and 4-11, respectively, for Configurations 3 and 4. Component weight breakdowns are similar to that given for LO_2 in Figures 4-8 and 4-9, the only difference being that pressurization system weight is the smallest component for LCH_4, whereas delta tank weight is the smallest component for LO_2. Vent mass again represents the major contributor to total weight penalty. Also, the higher weight totals for Configuration 4 are casued by the SOFI system higher heating rates.

As with all of the thermal conditioning systems that were analyzed, total system weight penalties will increase substantially as engine NPSP levels increase.

4.2.2.2 Liquid-Ullage Coupling for LH_2 Tank Autogenous Pressurization. One of the shortcomings identified for autogenous pressurization was that ullage-to-liquid heat transfer could be appreciable during the long burn periods of the LTPS mission. This shortcoming was especially evident with liquid hydrogen during burn No. 9 for Configuration 1. Vapor pressure increases as great as 75.8 kpa (11 psid) can occur as a result of ullage-to-liquid heating. In order to maintain a constant engine NPSP condition, it became necessary to increase propellant tank pressure in accordance with the vapor pressure increase. The resulting increase in propellant tank weight represented a performance penalty against autogenous pressurization, Figure 4-5.

It is believed that the ullage-to-liquid heat transfer rates calculated by program HYPRS are excessively high. This is because a uniform ullage temperature was assumed throughout burn No. 9 rather than to incorporate ullage and liquid temperature gradients (Figure 4-12). Figure 4-12a shows an ullage temperature increase during pressurization that is due primarily to the heat of compression caused by the tank pressure increase. The ullage temperature will continue to increase during engine burn as hot autogenous pressurant is introduced. The high ullage temperature at the liquid surface is responsible for a high heat transfer rate to liquid which results in a substantial temperature increase of the bulk liquid.

Figure 4-12b indicates two significant differences with Figure 4-12a: autogenous pressurization affects ullage temperature only in the upper regions of the tank; and temperature gradients will exist above and below the liquid surface. The hot GH_2 entering the ullage during burn No. 9 will remain localized because of low velocities at the diffuser exit. (This condition has been experienced on Centaur flights.) Consequently, vapor near the liquid surface is expected to reside at the MES9 temperatures throughout the final burn duration. This vapor mass will be influenced only by conduction (and some convection) heat transfer to the liquid surface.

Pure conduction was selected as an acceptable representation of the interfacial heat transfer that will occur during the final LTPS burn period. The influence of buoyancy in both liquid and vapor phase will serve to suppress free convection. Furthermore, the low vehicle acceleration (<0.02 g's) will tend to decrease fluid circulation near the liquid surface.

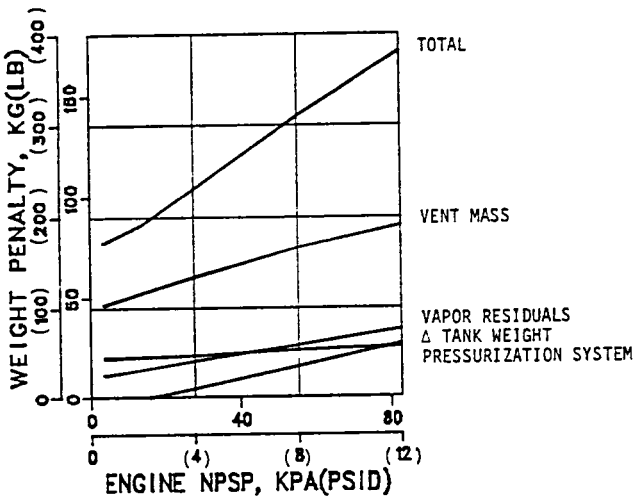

NOTE:

TOTAL WEIGHT PENALTIES ARE THE SAME FOR THE SUBCOOLER/ AUTOGENOUS OPTION

Figure 4-10. LCH_4 Tank Autogenous System Weight Penalties (Bubbler/Autogenous, Configuration 3)

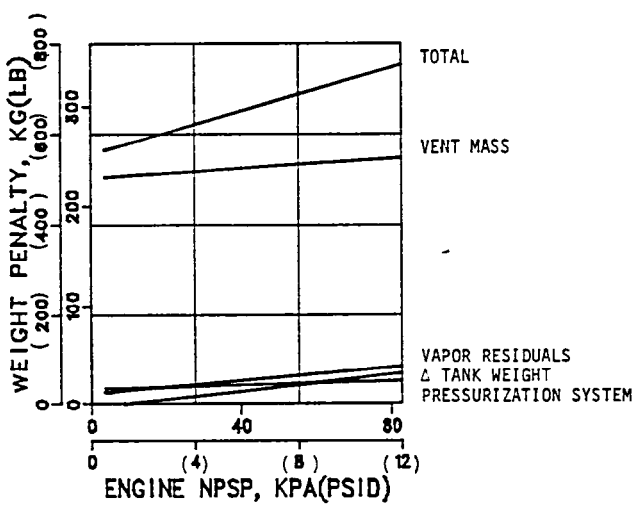

NOTES:

1 INCREASED HEATING RATE OF SOFI SYSTEM IS RESPONSIBLE FOR THE WEIGHT DELTA BETWEEN CONFIGURATIONS 3 AND 4

2 TOTAL WEIGHT PENALTIES ARE THE SAME FOR THE SUBCOOLER/AUTOGENOUS OPTION

Figure 4-11. LCH_4 Tank Autogenous System Weight Penalties (Bubbler/Autogenous, Configuration 4)

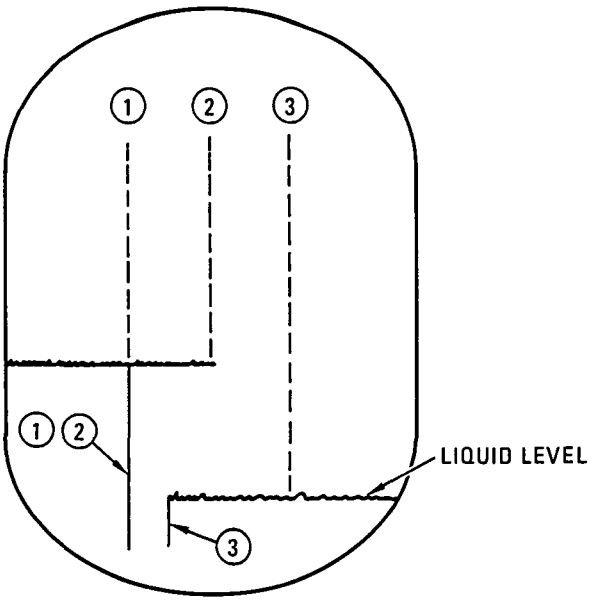

4-12a A UNIFORM ULLAGE TEMPERATURE IS ASSUMED FOR TANK THERMODYNAMIC COMPUTER PROGRAM

---- ULLAGE TEMPERATURE GRADIENT

—— LIQUID TEMPERATURE GRADIENT

(1) UNIFORM TEMPERATURE PRIOR TO TANK PRESSURIZATION

(2) TEMPERATURE GRADIENT AT END OF PRESSURIZATION (MES 9)

(3) TEMPERATURE GRADIENT PRIOR TO MECO 9

NOTE

AUTOGENOUS PRESSURIZATION DURING ENGINE BURN

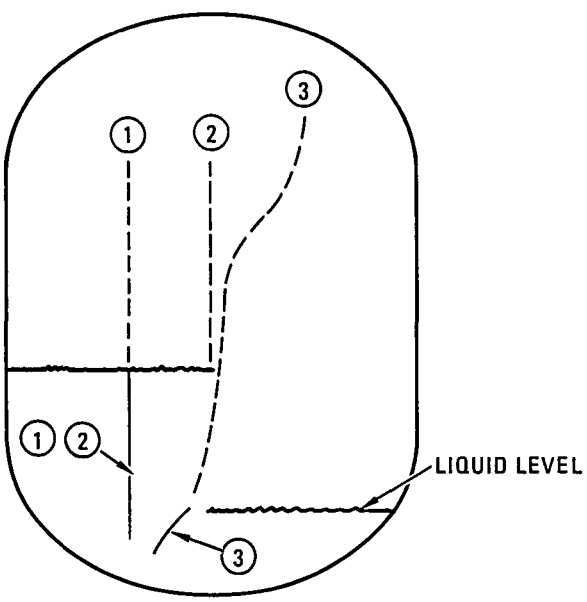

4-12b A MORE REALISTIC MODEL WOULD INCLUDE ULLAGE AND LIQUID TEMPERATURE GRADIENTS NEAR LIQUID SURFACE

265 585-7

Figure 4-12. Uniform Ullage Temperatures Were Assumed in Determining Ullage-to-Liquid Heat Rates

A comparison of free convection to conduction heating of the LH_2 surface is given in Figure 4-13. It is seen that total convective heating to the liquid is about four times greater than for conduction. The resulting vapor pressure increases during burn No. 9 are given in Figure 4-14 and the difference can be as great as 52.4 kpa (7.6 psid) for a 82.7 kpa (12 psid) NPSP condition. It was concluded that maximum LH_2 tank pressures for Configuration 1 could be decreased by the pressure differentials indicated in Figure 4-14. Autogenous pressurization system weight penalties would also be decreased as tank masses are reduced to reflect lower mission peak pressures. These changes were implemented in the Section 5 systems weight comparison for both the helium/autogenous and thermal subcooler/autogenous systems.

The impact of interfacial heat transfer was evaluated for LO_2 and LCH_4 with autogenous pressurization. The vapor pressure differential between convection and conduction was determined to be as great as 6.9 kpa (1.0 psid) during burn No. 9. The greater LO_2 and LCH_4 thermal masses are primarily responsible for the small differential and, as a result, corrections were not necessary for these propellants.

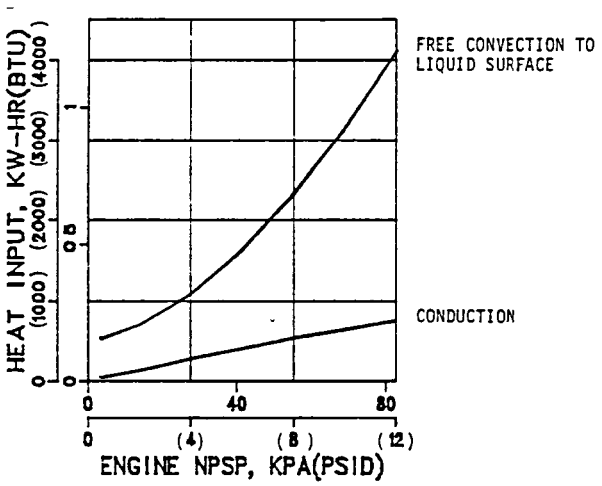

NOTES:

- CONFIGURATION 1, BURN NO. 9
- AUTOGENOUS PRESSURIZATION
- LH_2 BULK INITIALLY SATURATED AT 124 KPA (18 PSIA)
- FREE CONVECTION DATA DETERMINED FROM HYPRS PROGRAM

Figure 4-13. Comparison of Free Convection Versus Conduction Heating at LH_2 Surface

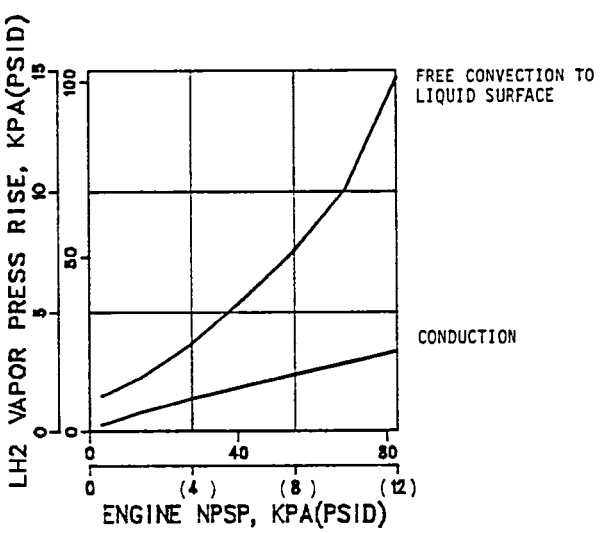

NOTES:

- CONFIGURATION 1, BURN NO. 9
- AUTOGENOUS PRESSURIZATION
- LH_2 BULK INITIALLY AT 124 KPA (18 PSIA)

Figure 4-14. Vapor Pressure Rise Due to LH_2 Surface Heating

5

THERMAL CONDITIONING SYSTEMS COMPARISON

In this section the analysis results of sections 2, 3 and 4 are compared over the entire NPSP range in order to recommend thermal conditioning systems for further study. These results were compared on the basis of total weight penalty, although consideration was given to state-of-the-art. It was thought that no one system would exhibit an advantage over the entire NPSP range. The recommended systems, however, do show an advantage over much of the NPSP range. In general, it was found that for systems at the low end of the NPSP scale, there was little or no weight differentiation.

5.1 LH_2 THERMAL CONDITIONING SYSTEMS

Configurations 1 and 2 are thermodynamically identical because initial propellant loads are nearly the same and MLI systems are similar. Consequently, the data presented for Configuration 1 applies in every respect to Configuration 2. Of the six systems evaluated, two were state-of-the-art (helium and autogenous pressurization) with a wealth of empirical data to support predictions. These two systems also show the maximum weight penalty. The four remaining systems include variations of a thermal subcooler which represents a totally new technology. These systems also show the lowest weight penalties. Consequently, comparisons must include a trade between state-of-the-art and performance gain.

5.1.1 STATE-OF-THE-ART SYSTEMS. Figure 5-1 gives a weight penalty comparison of the six thermal conditioning system options. Of the two state-of-the-art systems, helium pressurization (engine start)/autogenous (engine burn) is the lightest weight system over helium pressurization alone by approximately 50 to 213 kg (110 to 470 lb) lighter over the NPSP range. Also, both systems are equivalent on a state-of-the-art basis since both are flight-proven. Consequently, the helium/autogenous system is selected for comparison to the new technology systems.

5.1.2 NEW TECHNOLOGY SYSTEMS. Figure 5-1 shows weight penalty differences of less than 13.6 kg (30 lb) for the four subcooler options at NPSP levels less than 13.8 kpa (2 psid). Weight differences will increase to 150 kg (330 lb) at the maximum NPSP of 82.7 kpa (12 psid). The return-to-ullage option exhibits the best performance, i.e., lowest weight penalty, over the entire NPSP range. However, it does require a pump for returning coolant vapor to the ullage. Furthermore, tank pressure controls during engine burn are more complicated than for other options because coolant rates must be decreased as autogenous pressurization ΔPs increase.

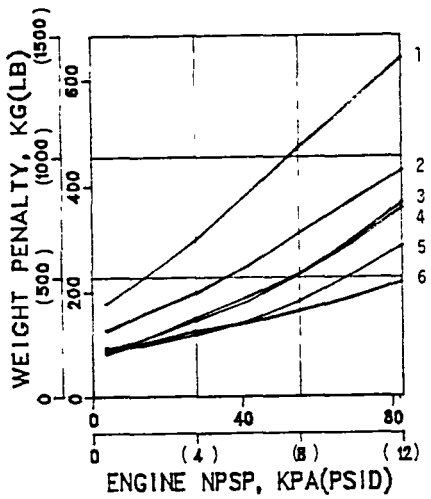

THERMAL CONDITIONING SYSTEMS (ENGINE START/ENGINE BURN)

1 ULLAGE INJECTION/ULLAGE INJECTION

2 ULLAGE INJECTION/AUTOGENOUS

3 SUBCOOLER/SUBCOOLER (RETURN TO LIQUID)

4 SUBCOOLER/SUBCOOLER (COOLANT DUMP)

5 SUBCOOLER/AUTOGENOUS

6 SUBCOOLER/SUBCOOLER (RETURN TO ULLAGE)

- CONFIGURATION 2 RESULTS ARE SIMILAR TO THOSE OF CONFIGURATION 1.

Figure 5-1. Comparison of LH_2 Tank Thermal Conditioning Systems (Configuration 1)

The least complicated subcooler options are coolant dump and subcooler/autogenous. Neither one requires a pump, nor is tank pressure control a concern. The advantage rests with the latter option because it exhibits the second best performance over the NPSP range.

The subcooler selection process can also be influenced by the design NPSP level. If, for example, an engine is developed for NPSP levels of 13.8 kpa (2.0 psid) or less, then the coolant dump option might represent the best compromise. Its weight penalty at low NPSPs is within about 6.8 kg (15 lb) of the return-to-ullage option penalty. It would also be slightly less complicated than the subcooler/autogenous option.

5.1.3 RECOMMENDED SYSTEMS. The systems recommended for preliminary design were the subcooler/subcooler (return-to-ullage) and subcooler/autogenous options. The former was recommended because of lower weight penalties over the NPSP range. The latter recommendation was i) for the second lowest weight penalties over the NPSP range and ii) because it is a less complicated system.

5.2 LO_2 THERMAL CONDITIONING SYSTEMS

LO_2 tank thermal conditioning system weight comparisons are shown in Figures 5-2 and 5-3 for all vehicle configurations. The bubbler pressurization system is the obvious choice of all thermal conditioning systems studied. It has every advantage: state-of-the-art, simplicity and minimum weight penalty.

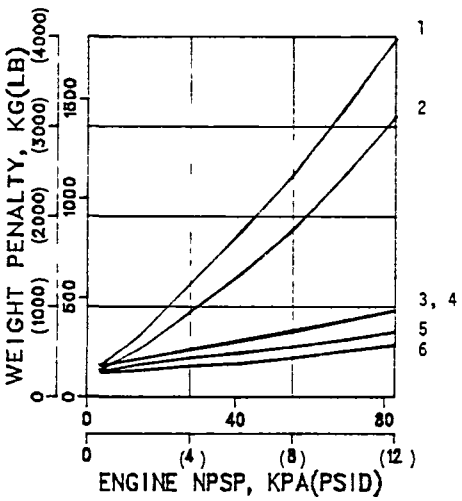

THERMAL CONDITIONING SYSTEMS (ENGINE START/ENGINE BURN)

1 SUBCOOLER/SUBCOOLER (COOLANT DUMP)

2 SUBCOOLER/SUBCOOLER (RETURN TO LIQUID)

3 SUBCOOLER/AUTOGENOUS

4 BUBBLER/AUTOGENOUS

5 SUBCOOLER/SUBCOOLER (RETURN TO ULLAGE)

6 BUBBLER/BUBBLER

NOTE: CONFIGURATIONS 2 AND 3 ARE SIMILAR TO THOSE OF CONFIGURATION 1.

Figure 5-2. Comparison of LO_2 Tank Thermal Conditioning Systems (Configuration 1)

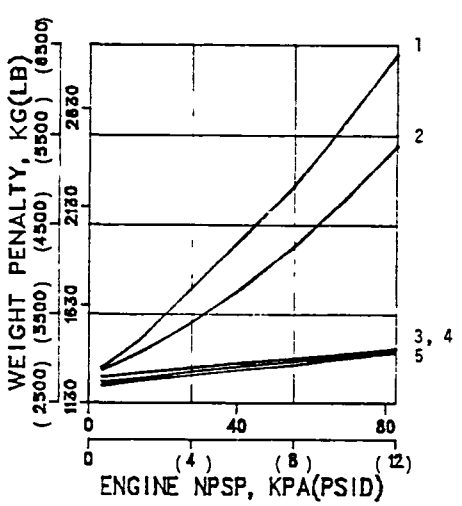

THERMAL CONDITIONING SYSTEMS (ENGINE START/ENGINE BURN)

1 SUBCOOLER/SUBCOOLER (COOLANT DUMP)

2 SUBCOOLER/SUBCOOLER (RETURN TO LIQUID)

3 BUBBLER/AUTOGENOUS

4 SUBCOOLER/AUTOGENOUS

5 BUBBLER/BUBBLER

Figure 5-3. Comparison of LO_2 Tank Thermal Conditioning Systems (Configuration 4)

Regarding the first benefit, bubbler pressurization is the system developed for the Centaur vehicle. It has been flight demonstrated for low-g operation over a wide range of ullage volume conditions. It has also been ground-test demonstrated. Bubbler pressurization is the simplest of the thermal conditioning systems evaluated; no pump/motor unit, heat exchanger nor autogenous pressurization are required. Finally, Figures 5-2 and 5-3 show that this system will experience the lowest weight penalty over the entire NPSP band.

A second, or backup, thermal conditioning system was not recommended for the LO_2 tank because the primary system is clearly superior. Its ranking remains unaffected by choice of insulation system, as evidenced by comparing Figures 5-2 and 5-3.

5.3 LCH_4 THERMAL CONDITIONING SYSTEM

Bubbler pressurization is recommended for both LCH_4 tanks for the same reasons as given for the LO_2 tanks: state-of-the-art, simplicity and minimum weight penalty. Figures 5-4 and 5-5 show that this thermal conditioning system will experience the lowest weight penalty of all systems considered. Although this pressurization technique has not been attempted with LCH_4, it is expected that system performance will be, in every way, similar to what has been experienced with LO_2.

Note that there is no data for the subcooler return-to-ullage option. Analyses were not performed on that option because at that time it was clear that bubbler pressurization would be the only recommendation. Even if the return-to-ullage technique matched the low weight penalty of bubbler pressurization, it would not be recommended because new technology would be required. Furthermore, it is believed that weight penalties for the bubbler pressurization system will be lower than for the subcooler return-to-ullage system.

5.4 LTPS RECOMMENDATIONS

A total of three thermal conditioning systems were recommended for the four LTPS configurations, two for the LH_2/LO_2 configurations and one for the LCH_4/LO_2 configurations. Weight penalties for the combined fuel/oxidizer systems are given in Figures 5-6 and 5-7.

The recommended systems for the LH_2/LO_2 vehicle stages are:

1. LH_2 side - subcooler return-to-ullage

   LO_2 side - bubbler pressurization

2. LH_2 side - subcooler/autogenous

   LO_2 side - bubbler pressurization

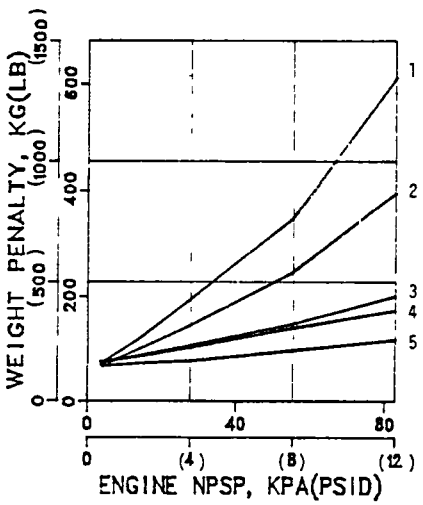

THERMAL CONDITIONING SYSTEMS (ENGINE START/ENGINE BURN)

1 SUBCOOLER/SUBCOOLER (COOLANT DUMP)

2 SUBCOOLER/SUBCOOLER (RETURN TO ULLAGE)

3 SUBCOOLER/AUTOGENOUS

4 BUBBLER/AUTOGENOUS

5 BUBBLER/BUBBLER

Figure 5-4. Comparison of LCH_4 Tank Thermal Conditioning Systems (Configuration 3)

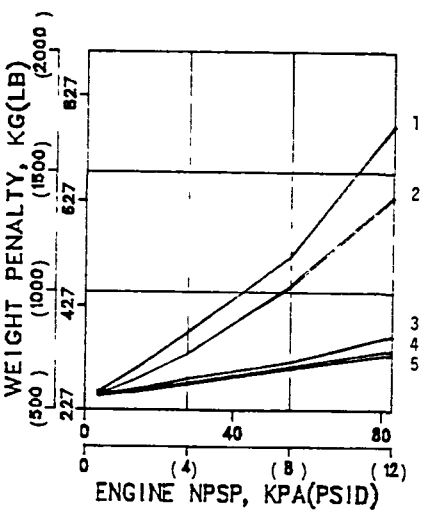

THERMAL CONDITIONING SYSTEMS (ENGINE START/ENGINE BURN)

1 SUBCOOLER/SUBCOOLER (COOLANT DUMP)

2 SUBCOOLER/SUBCOOLER (RETURN TO ULLAGE)

3 BUBBLER/AUTOGENOUS

4 SUBCOOLER/AUTOGENOUS

5 BUBBLER/BUBBLER

Figure 5-5. Comparison of LCH_4 Tank Thermal Conditioning Systems (Configuration 4)

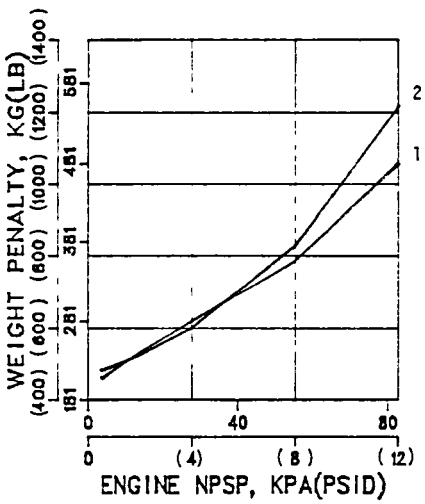

RECOMMENDED SYSTEMS

1 LH_2 SIDE - SUBCOOLER/SUBCOOLER (RETURN TO ULLAGE)

LO_2 SIDE - BUBBLER/BUBBLER

2 LH_2 SIDE - SUBCOOLER/AUTOGENOUS

LO_2 SIDE - BUBBLER/BUBBLER

NOTE: RECOMMENDATION ALSO APPLIES TO CONFIGURATION 2.

Figure 5-6. Weight Penalties for Recommended LH_2/LO_2 Thermal Conditioning Systems (Configuration 1)

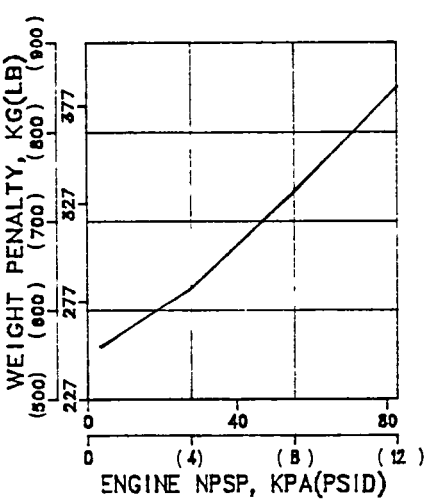

RECOMMENDED SYSTEMS

LCH_4 SIDE - BUBBLER/BUBBLER

LO_2 SIDE - BUBBLER/BUBBLER

NOTE: RECOMMENDATION ALSO APPLIES TO CONFIGURATION 4.

Figure 5-7. Weight Penalties for Recommended LCH_4/LO_2 Thermal Conditioning Systems (Configuration 3)

Figure 5-6 shows that these systems are equivalent from 3.4 to 41.4 kpa (0.5 to 6.0 psid). A significant weight difference exists only at the upper end of the NPSP band. It is possible that System 2 could be preferred over System 1 at low NPSPs because of a less complex hydrogen system. Detailed analyses beyond the scope of this study would be required before such an assessment could be made.

Only one thermal conditioning system was recommended for the LCH_4/LO_2 stages. This system included bubbler pressurization for both propellants. Total weight penalty is shown in Figure 5-7. A second system was not recommended because it offers no possibility for trading system strengths and weaknesses.

6

PRELIMINARY DESIGN OF SELECTED THERMAL CONDITIONING SYSTEMS

Following the completion of Tasks I and III, General Dynamics recommended the three LTPS thermal conditioning systems identified in Section 5 for further study. The NASA project manager approved both LH_2/LO_2 LTPS systems and selected two additional LH_2/LO_2 systems for the Task IV preliminary design rather than the recommended LCH_4/LO_2 system. All preliminary designs were to be performed on vehicle Configuration 1. Hardware size and weights were estimated from the designs. These weights were added to propellant ventage and residuals and all other identifiable weight penalties. A final weight penalty comparison was made of the four thermal conditioning systems.

6.1 SYSTEM SELECTION

System characteristics and operating conditions for Task IV were specified by the NASA project manager. Table 6-1 lists the four systems selected for preliminary design effort on vehicle Configuration 1.

Table 6-1. Selected Thermal Conditioning Systems

System	LO_2 Tank Engine Start/Engine Burn	LH_2 Tank Engine Start/Engine Burn
1	Bubbler/Bubbler	Helium/Autogenous
2	Same as 1, except for cryogenic storage of helium	
3	Bubbler/Bubbler	Subcooler (coolant dump)/ Autogenous
4	Bubbler/Bubbler	Subcooler/Subcooler (coolant return to ullage)

Three engine NPSP design points were considered for each system:

Engine Design	LO_2 Side kpa(psid)	LH_2 Side kpa(psid)
Zero NPSP	0	0
Low NPSP	6.9 (1.0)	3.4 (0.5)
Moderate NPSP	13.8 (2.0)	6.9 (1.0)

The low NPSP levels imposed upon the preliminary design activity are significant because, as shown in Section 5, weight penalty differences become small in this NPSP range. A comment should be made regarding the zero NPSP design point. It is generally accepted that development costs and, perhaps, engine weight and complexity will increase as engine NPSP levels approach zero. Furthermore, it is known that thermal conditioning system weight penalties will decrease as NPSP levels approach zero. Consequently, the weight penalties provided by this study can be used to show potential LTPS mission performance gains as engine complexity and cost are increased.

6.1.1 LO_2 TANK SYSTEM. Bubbler pressurization was selected for all four vehicle thermal conditioning systems. It is a simpler state-of-the-art technique than the other systems. Ambient storage of helium was selected for System 1 and cryogenic storage for the other systems. The thermodynamic effects of ambient versus cryogenically stored helium are trivial for bubbler pressurization, but there is a helium supply system weight benefit for cryogenic storage.

6.1.2 LH_2 TANK SYSTEMS. Systems 1 and 2 are helium/autogenous pressurization, one with ambient helium storage and the other with cryogenically stored helium. The comparisons of Section 5 (Figure 5-1) showed significant weight penalty differences between state-of-the-art and new technology options at the maximum NPSP level. These differences reduced to about 45 kg (100 lb) at the low NPSP range, and can serve as a basis for trading weight versus technology for thermal conditioning systems.

Thermal conditioning Systems 1 and 2 are identical except for helium storage temperature. In Section 2 it was stated that cryogenic storage of helium would reduce weight penalties under certain conditions, and that this option would be evaluated if bubbler pressurization was selected for further analysis. This evaluation is performed for System 2; weight penalties are developed in Section 6.2.2.

6.2 THERMAL CONDITIONING SYSTEM 1

This system reflects today's technology. Bubbler pressurization for the LO_2 tank represents the best thermal conditioning system, regardless of technology, at all NPSP levels. The hydrogen tank system of helium (engine start)/autogenous (engine burn) pressurization will suffer a greater weight penalty than the subcooler systems. System weight penalty may not be excessive because of the low NPSP requirements.

6.2.1 SYSTEM DESIGN. A preliminary design drawing of this thermal conditioning system is given in Figure 6-1. The schematic reflects the philosophy adopted for the Shuttle/Centaur vehicle relative to component failure and safety considerations. Rationale for the use of multiple pneumatic components is given below.

6.2.1.1 Vehicle-Mounted Hardware. In general two-failure tolerancy is required for operations in the Shuttle and single-failure tolerancy is required for post-deployment operations.

Pressurization valves. Four valves (two each in parallel) are required to satisfy the requirement for single-failure tolerancy during the vehicle mission. That is, failure of one valve to open or close must not fail the mission. For example, if in Figure 6-1 a LO_2 tank pressurization valve in Branch 1 fails to open for pressurization, the valves in Branch 2 would be commanded open. Alternatively, if a Branch 1 valve failed to close during a pressurization sequence, the second valve in series would be commanded closed to terminate flow. Two-failure tolerancy of this system is not required while in the Shuttle cargo-bay because it will remain inactive until after deployment.

GH_2 engine bleed line check valves. Check valves are installed to prevent the backflow of high pressure helium through the engine system during abort dump. Since this system must be two-failure tolerant during abort, three check valves in series are required.

Fill, drain, dump and ground tank vent lines. The schematics do not show a parallel set of valves that are mounted on the LTPS deployment adapter. It has been determined (with concurrence from JSC and RI) that the parallel sets of valves on Centaur, combined with the deployment adapter-mounted valves, will satisfy Shuttle safety requirements. Consequently, this configuration is employed for LTPS. These lines are considered to be part of the LTPS baseline configuration rather than of a thermal conditioning system. As a result, line weights will be listed separately in Table 6-9 rather than as part of the thermal conditioning weight summary.

Helium charge line check valves. Four check valves (two each in parallel) were selected to provide single failure tolerancy during the pre-launch helium charge activities. This configuration allows for the failure of a check valve to open in the flow direction without impacting pre-launch operations.

Tank pressurization diffusers. The LH_2 tank is pressurized through a diffuser mounted off the forward bulkhead. Helium enters the propellant tank for abort propellant dump and engine start pressurization. Autogenous GH_2 enters the propellant tank during engine burn.

The LO_2 tank is pressurized with helium through a ring-manifold during abort, engine start and engine burn.

Helium supply bottle. The helium supply bottle and mounting bracketry is the only hardware affected by engine NPSP requirements. Size and weight are calculated from helium mass requirements, employing the procedure identified by Table 2-1.

6.2.2 SYSTEM WEIGHT PENALTIES. Total system weight includes hardware (pressurization system) weight identified in Section 6.2.1, initial helium load, in addition to the thermodynamic weight penalties of vent mass and vapor residual.

6.2.2.1 Hardware Weight. The number and weights of pressurization system components are given in Table 6-2. Helium bottle and support bracketry weights are not included in this compilation as they are affected by engine NPSP and reported separately in Section 6.2.2.2. This vehicle-mounted weight total is 32.4 kg (71.4 lb)

6.2.2.2 Helium Supply System Weight. Table 6-3 gives the helium supply system weight as a function of engine NPSP. LO_2 tank and LH_2 tank helium usages are tabulated and were obtained from the work reported in Section 2. Helium bottle and support weights are based upon the technique of Table 2-1. Total weights are 17.4 and 29.6 kg (38.3 and 65.3 lb) for the design engine NPSP requirements.

6.2.2.3 Ventage and Vapor Residuals. Vent and vapor residual masses are shown in Figure 6-2 for the design engine NPSP requirements. Masses are plotted against LO_2 side NPSP. The corresponding LH_2 side NPSP is one-half the LO_2 NPSP. Analyses indicate that a vent mass weight reduction will occur for autogenous pressurization systems at zero NPSP. For these systems, vent mass is determined by the amount of energy added to the tanks during burn and coast periods. This energy comes from mission heating rates and the pressurant gas added to the ullage during an engine start and burn.

During engine burn at zero NPSP, the LH_2 boils as tank pressure decreases during propellant outflow. The energy from the mission heating rate adds to the propellant boil-off at zero NPSP. When pressurant gas is injected into the ullage to provide some engine NPSP level, the boil-off is suppressed. The mission heating rate will now go into raising the liquid vapor-pressure throughout the engine burn. More pressurant gas will also be required to compensate for the increasing liquid vapor pressure. The energy in the pressurant gas required to suppress propellant boil-off causes the step change in vent mass at near-zero NPSP for the autogenous pressurization systems.

6.2.2.4 Total Weight Penalty. System 1 component and total weight penalties are given in Figure 6-2. These weights are 250 and 265 kg (551 and 584 lb) for the low and moderate NPSP levels, respectively. There is no penalty shown for tank weight increase because peak tank pressures will not exceed design allowables of 165.5 kpa (24 psia).

6.2.3 LTPS WEIGHT PENALTY AT ZERO NPSP. An alternative to thermal conditioning systems is to develop a low-thrust engine that requires zero NPSP. The benefit of a zero NPSP engine would be a reduced system weight penalty. The weight penalty would not, however, drop to zero because the combination of ventage and vapor residuals is nonzero. Furthermore, there is a minimum hardware weight (Table 6-2) required for RTLS pressurization during abort propellant dump. Individual and total system weight penalties are given in Figure 6-2; the total penalty is 201 kg (443 lb). At zero NPSP, the tank weight delta and helium supply system weight will be zero. This zero

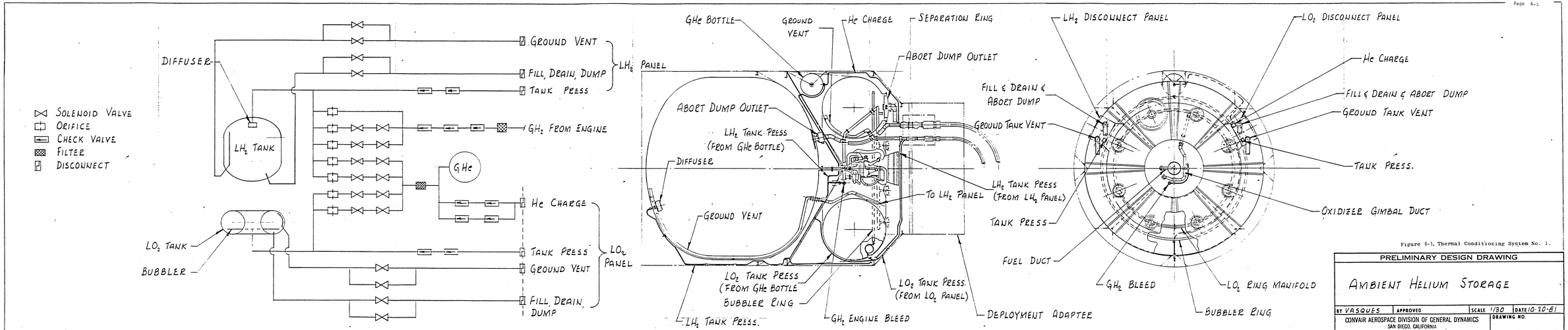

Figure 6-1. Thermal Conditioning System No. 1.

PRELIMINARY DESIGN DRAWING			
AMBIENT HELIUM STORAGE			
BY VASQUES	APPROVED	SCALE 1/30	DATE 10-20-61
CONVAIR AEROSPACE DIVISION OF GENERAL DYNAMICS SAN DIEGO, CALIFORNIA		DRAWING NO.	

6549 (9-7)

This Page Intentionally Left Blank

Table 6-2. Pressurization System Hardware Weights

Thermal Conditioning System Configuration	Helium Disconnects	Solenoid Valves	Orifices	Check Valves	Filters	Bubbler Ring	Diffuser	Tubing Fittings etc	Press'n Line Gimbal Joints	Wiring	Total Weight
Weight, kg(lb)/item	0 45(1.0)	0 45 (1 0)	0 14(0 3)	0 23(0 5)	0 14(0 3)	3 2(7 1)	1 6(3 5)	-	0 45(1 0)	-	-
1 Number	3	12	7	11	2	1	1	-	3	-	-
Weight, kg(lb)	1 4 (3 0)	5 4 (12 0)	1 0 (2 1)	2 5 (5 5)	0 3 (0 6)	3 2(7 1)	1 6(3.5)	12 5(27 6)	1 4 (3 0)	1 6(3.5)	32 4(71 4)
2 Number	3	12	7	11	2	1	1	-	3	-	-
Weight, kg(lb)	1 4 (3.0)	5 4 (12 0)	1 0 (2 1)	2 5 (5 5)	0 3 (0 6)	3 2(7 1)	1 6(3 5)	12 5(27 6)	1 4 (3 0)	1 6(3.5)	32 4(71 4)
3 Number	3	8	5	11	2	1	1	-	3	-	-
Weight, kg(lb)	1 4 (3 0)	3 6 (8 0)	0 7 (1 5)	2 5 (5 5)	0 3 (0 6)	3 2(7 1)	1 6(3 5)	11 3(25 0)	1 4 (3 0)	1 1(2 4)	27 0(59 6)
4 Number	3	4	2	8	1	1	1	-	3	-	-
Weight, kg(lb)	1 4 (3 0)	1 8 (4 0)	0 3 (0 6)	1 8 (4 0	0.14(0 3)	3 2(7 1)	1 6(3 5)	9 6(21 2)	1 4 (3 0)	0 5(1 2)	20 1(44 4)
(1) Zero NPSP											
Number	2	0	0	4	0	1	1	-	2	0	
Weight, hg(lb)	0 9 (2 0)	0	0	0 9 (2 0)	0	3 2(7 1)	1 6(3 5)	7 5(16 6)	0 9 (2 0)	0	15 1(33 2)

(1) A thermal conditioning system is not required for zero NPSP Pressurization system hardware is still needed for RTLS abort dump pressurization

Table 6-3. System 1 Helium Supply Weights

	(1) Low Engine NPSP		(2) Moderate Engine NPSP	
	LO_2 Tank	LH_2 Tank	LO_2 Tank	LH_2 Tank
Mission Helium Usages, kg (lb)	0.5 (1.1)	1.2 (2.7)	1.0 (2.1)	2.0 (4.3)
Initial Helium Mass, kg (lb)	2.1 (4.7)		3.6 (8.0)	
Helium Bottle Weight kg (lb)	13.7 (30.3)		23.4 (51.6)	
Bottle Supports(3) kg (lb)	1.5 (3.3)		2.6 (5.7)	
Total Weight kg (lb)	17.4 (38.3)		29.6 (65.3)	

(1) LH_2 side NPSP = 3.4 kpa (0.5 psid)
LO_2 side NPSP = 6.9 kpa (1.0 psid)

(2) LH_2 side NPSP = 6.9 kpa (1.0 psid)
LO_2 side NPSP = 13.8 kpa (2.0 psid)

(3) Supports = 0.11 x Bottle weight

NPSP weight penalty is applicable to all thermal conditioning systems analyzed in Section 6. Tank weight penalty is also zero for the three remaining systems.

6.3 THERMAL CONDITIONING SYSTEM 2

This system is identical to System 1 except that helium will be stored cryogenically. Most of the weight penalties between Systems 1 and 2 are identical. Consequently, only the system differences are discussed below.

6.3.1 SYSTEM SCHEMATIC. A system preliminary design drawing is given in Figure 6-3. The vehicle helium bottle is mounted inside the LO_2 tanks. Again, ambient helium from the deployment adapter is available in the event of an abort mode. Thus, the RTLS hardware requirements will be identical to those identified for System 1.

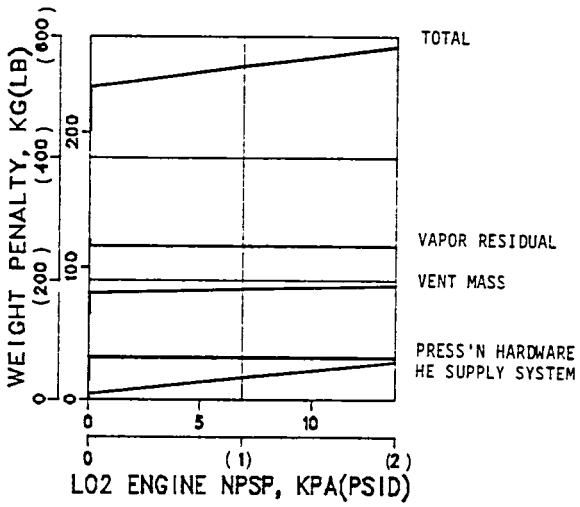

NOTES:

1. LH_2 NPSP = 1/2 x LO_2 (NPSP)
2. A SHARP WEIGHT PENALTY REDUCTION OCCURS BETWEEN ZERO AND NEAR-ZERO NPSP

Figure 6-2. Thermal Conditioning System 1 Weight Penalty (LO_2: Bubbler/LH_2: Helium)

6.3.1.1 Vehicle-Mounted Hardware. The helium supply bottle will be mounted within the LO_2 tank. All other hardware requirements are identical to System 1. The decision to store helium in the LO_2 tank rather than the LH_2 tank was based upon a desire to decrease helium mass usages for LH_2 tank engine start pressurization and decrease vent mass. These decreases will more than offset the helium supply bottle weight increase.

6.3.2 SYSTEM WEIGHT PENALTIES. Total system weight includes hardware (pressurization system) weight identified in Section 6.3.1, initial helium load, in addition to the thermodynamic weight penalties of vent mass and vapor residual. The vehicle-mounted weight (Figure 6-2) totals 33.4 kg (71.4 lb) which is the same as for System 1.

Table 6-4 gives helium supply system weight versus engine NPSP. LO_2 tank helium usages are the same as for System 1. LH_2 tank usages are greater than System 1 usages because entering helium temperature during engine start pressurization is only 93K (168R). Total weights are 11.5 and 22.5 kg (25.3 and 49.5 lb) for the design engine NPSP requirements. These totals are approximately 6 kg (14 lb) less than ambient helium storage system weights.

Vent and vapor residual masses are given in Figure 6-4 for the design engine NPSP requirements. These mass quantities are virtually identical to the System 1 masses.

Table 6-4. System 2 Helium Supply Weights

	Low Engine NPSP		Moderate Engine NPSP	
	LO_2 Tank	LH_2 Tank	LO_2 Tank	LH_2 Tank
Mission Helium Usages, kg (lb)	0 5 (1 1)	1 5 (3 2)	1 0 (2 1)	2 9 (5 3)
Initial Helium Mass,(1) kg (lb)	2 3 (5 2)		4 6 (10 1)	
Helium Bottle Weight(1) kg (lb)	8 2 (18 1)		16 1 (35 5)	
Bottle Supports(2) kg (lb)	0 9 (2 0)		1 8 (3 9)	
Total Weight kg (lb)	11 5 (25 3)		22 5 (49 5)	

(1) From Table 6-5.

(2) Supports = 0.11 x Bottle weight

System 2 component and total weight penalties are given in Figure 6-4. The totals given are approximately 6 kg (14 lb) lower than the System 1 totals. This difference represents the lower weight of the cryogenically stored helium supply system.

6.4 THERMAL CONDITIONING SYSTEM 3

This system represents new technology since the hydrogen side will employ a thermal subcooler for engine start. However, autogenous pressurization for engine burn and bubbler pressurization for the LO_2 tank are current methods of propellant thermal conditioning. The weight penalties for this system will be lower than for either Systems 1 or 2. Penalties are not expected to be significantly lower than for System 2, however, because the only weight improvement will be in eliminating the LH_2 tank helium supply system, which is not significant.

6.4.1 SYSTEM DESIGN. A preliminary design drawing is given in Figure 6-5 for this thermal conditioning system. The LO_2 tank pressurization system is identical to that for System 2, including the helium bottle mounted inside the LO_2 tank. LH_2 tank engine start pressurization has been replaced with a thermal subcooler (coolant dump configuration). The thermal subcooler eliminates the need for (4) solenoid valves, (2) orifices and some tubing, wiring and clips. Much of the System 2 LH_2 tanks pressurization system remains, as indicated by Table 6-2, because of RTLS pressurization requirements.

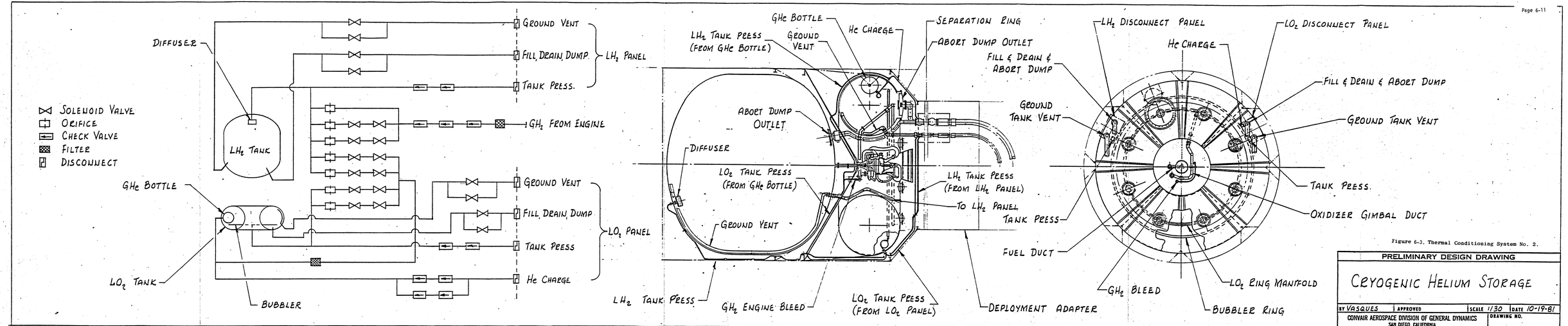

Figure 6-3. Thermal Conditioning System No. 2.

PRELIMINARY DESIGN DRAWING

CRYOGENIC HELIUM STORAGE

BY VASQUES	APPROVED	SCALE 1/30	DATE 10-19-81

CONVAIR AEROSPACE DIVISION OF GENERAL DYNAMICS
SAN DIEGO, CALIFORNIA

DRAWING NO.

6549 (9-71)

This Page Intentionally Left Blank

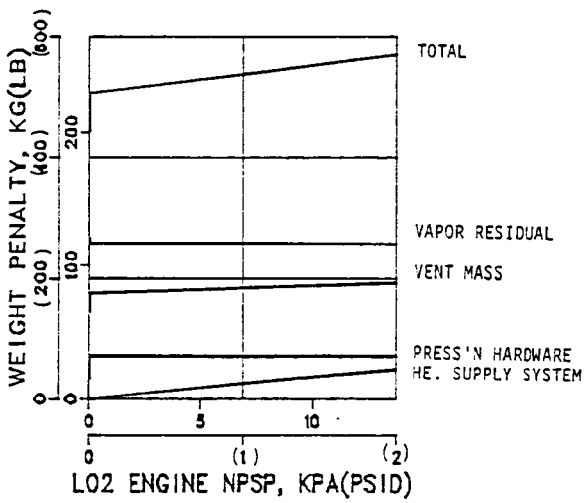

NOTES:

1. LH_2 NPSP = 1/2 x (LO_2 NPSP)
2. A SHARP WEIGHT PENALTY REDUCTION OCCURS BETWEEN NEAR-ZERO AND ZERO NPSP

Figure 6-4. Thermal Conditioning System 2 Weight Penalties

Table 6-5. Cryogenic Helium Storage Conditions

ρ_{BTL} = Bottle density (1) (bottle weight/storage volume)

= 1420 kg/m^3 (18.24 lb/ft^3)

ρ_i = Initial helium density at 21370 kpa and 93K (4000 psia and 168R)

= 404 kg/m^3 (5.19 lb/ft^3)

ρ_R = Residual helium density for mission at 2137 kpa and 93K (400 psia and 168R)

= 66.6 kg/m^3 (0.856 lb/ft^3)

ρ_u = $(\rho_i - \rho_R)$ = Usable density for mission

= 337 kg/m^3 (4.334 lb/ft^3)

$\frac{\text{Initial helium mass}}{\text{Mission helium usage}} = \rho_i/\rho_u = 1.198$

$\frac{\text{Helium bottle weight}}{\text{Initial helium mass}} = \rho_{BTL}/\rho_i = 3.514$

(1) Bottle construction is 301 stainless steel, low silicon

6.4.1.1 Vehicle-Mounted Hardware. The vehicle-mounted hardware is the same as described for System 2, with the minor exceptions indicated above for eliminating engine start helium pressurization.

6.4.1.2 Thermal Subcooler. A preliminary design drawing of the LH_2 thermal subcooler is shown in Figure 6-6. This drawing gives some detail of the subcooler installation over the tank outlet and the hot-side and cold-side heat exchanger passages. A description of subcooler components and its operation follows.

Pressure Regulator. The pressure regulator is mounted external to the LH_2 tank and a tank penetration is provided for tubing for flowing cold-side propellant from the tank to the pressure regulator and from the regulator to the subcooler inlet, Section A-A. The regulator is mounted external to the tank because of ready access and a benign thermal environment. The function of a pressure regulator is to throttle the tank liquid to a 28 - 34 kpa (4-5 psia) pressure level from a tank vapor pressure level of about 124 kpa (18 psia). A corresponding temperature drop will be experienced as the liquid is throttled and this lower temperature will provide the sink for heat exchange with the hot-side liquid.

The cold-side fluid enters the upper heat exchanger passage at the center, Section B-B. The fluid then spirals outward in the direction of five tubes located at the periphery of the upper passage. The fluid is then carried through the tubes to the lower heat exchanger passage. The fluid at the lower passage spirals inward, is collected near the center and ducted overboard through small diameter tubing. Although not shown, restricting orifices/ nozzles will be installed to provide a back pressure of approximately 21-28 kpa (3-4 psia) to avoid freezing of the vent fluid.

The hot-side fluid to the main engine will enter its heat exchanger passage through twenty slots located at the circumference, Section C-C. Vanes will direct the LH_2 radially inward to a 3.8 cm (1.5-inch) diameter outlet at the center. The LH_2 will be cooled due to heat transfer with the cold-side fluid flowing through the upper and lower heat exchanger passages. The LH_2 is now subcooled as it enters the engine feedlines, Section A-A.

The pressure regulator was selected over a throttling orifice because it represents a proven approach with greater flow control capability. A pressure regulator was previously tested for a liquid hydrogen thermodynamic vent system (Reference 6-1) which served the same function and had approximately the same mass flow rate control capability as required for the thermal subcooler.

Heat Exchanger Passage Screens. Screens are needed across the upper cold-side passage (Section B-B) and hot-side passages (Section C-C) so that the fluid may spread to encompass the total flow passage area. The pressure loss experienced by fluid flow across the screen will cause spreading to occur downstream of each screen surface. Without these screens the cold-side and hot-side fluid spreading would cover only a portion of the fluid flow area

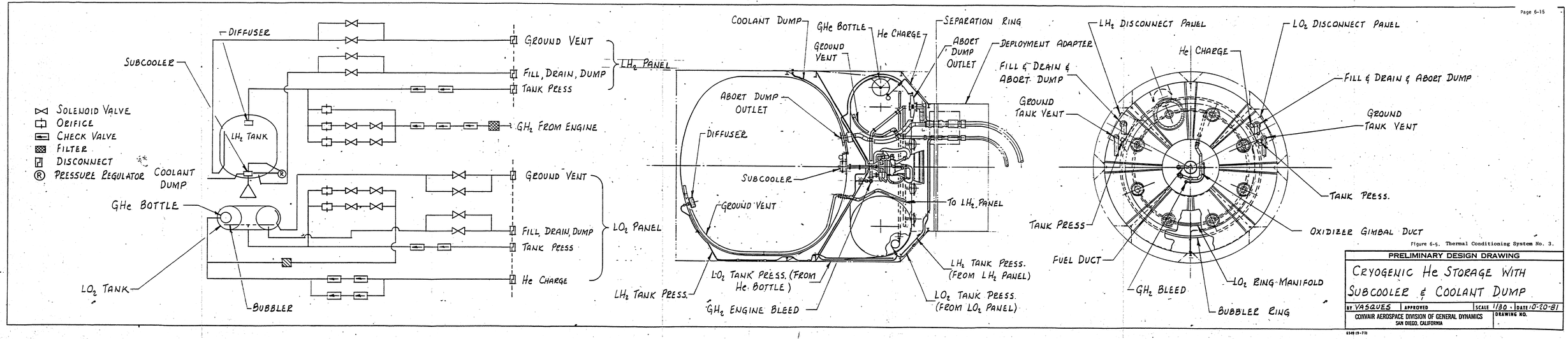

Figure 6-5. Thermal Conditioning System No. 3.

PRELIMINARY DESIGN DRAWING

CRYOGENIC He STORAGE WITH SUBCOOLER & COOLANT DUMP

BY VASQUES | APPROVED | SCALE 1/30 | DATE 10-20-81

CONVAIR AEROSPACE DIVISION OF GENERAL DYNAMICS
SAN DIEGO, CALIFORNIA

DRAWING NO.

6549 (9-73)

This Page Intentionally Left Blank

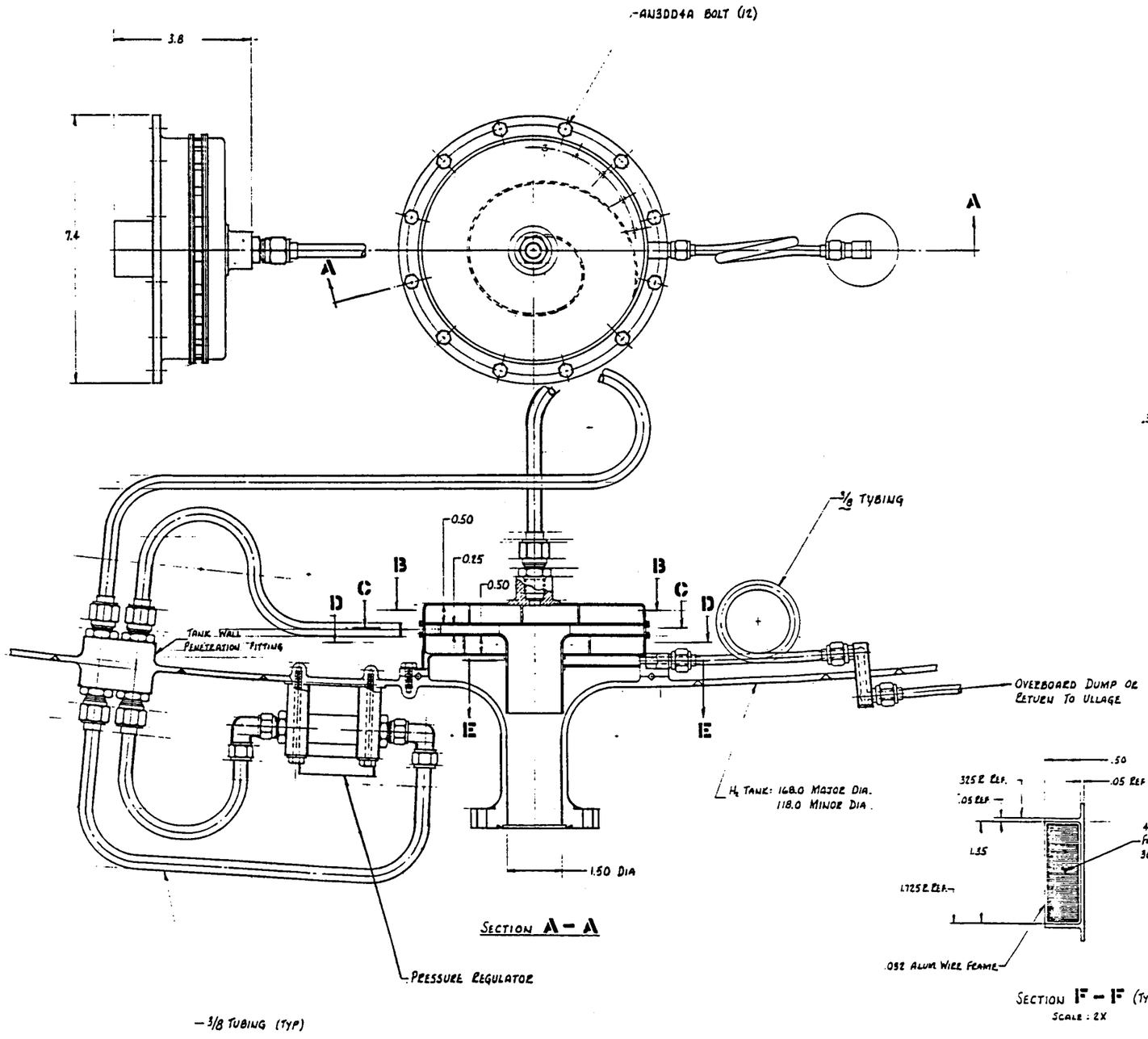

SECTION A – A

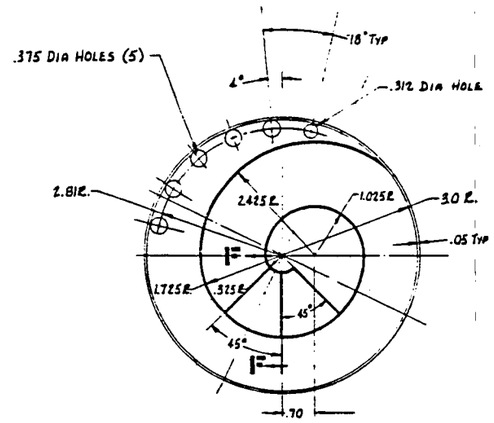

SECTION B – B
ROTATED 64° CCW

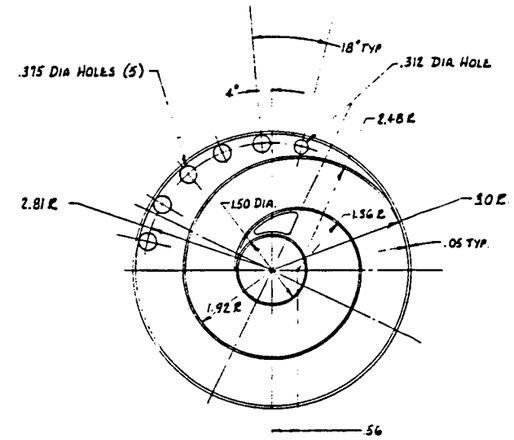

SECTION D – D
ROTATED 64° CCW

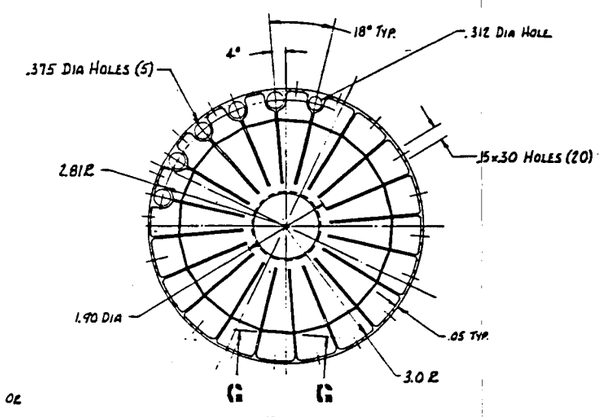

SECTION C – C
ROTATED 64° CCW

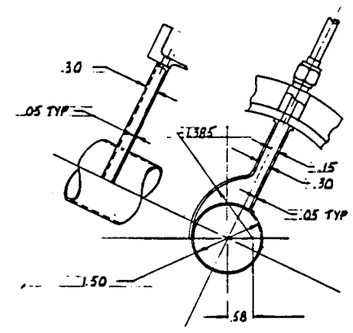

SECTION E – E
ROTATED 64° CCW

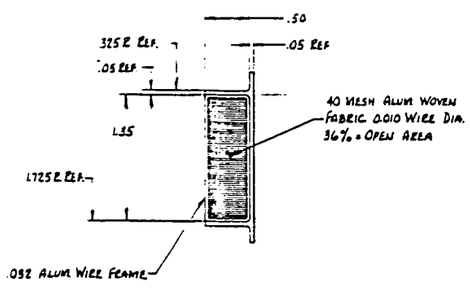

SECTION F – F (TYP 3 PLCS)
SCALE : 2X

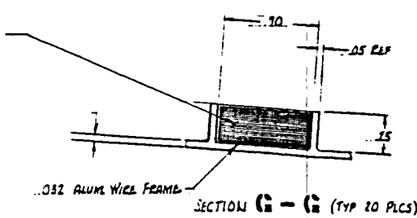

SECTION G – G (TYP 20 PLCS)
SCALE : 3X

1. MAT'L: 6061 ALUM. PLATE
2. FINISHED WALL THICK. .050 TYP
3. MPSP = 0.5 PSI
4. ASSEMBLY TO BE DIP BRAZED

Figure 6-6. LH_2 Thermal Subcooler

DRAWN BY VASQUEZ 10-1-81	PRELIMINARY DESIGN DRAWING	
	H_2 SUB-COOLER	
GENERAL DYNAMICS Convair Division San Diego, California	CODE IDENT. 14170	DRAWING NO.
	SCALE FULL (1.07)	SHEET 1 OF 1

and, consequently, be in thermal contact with only a portion of the total heat transfer area. This would reduce the overall subcooler heat exchanger effectiveness.

6.4.2 SYSTEM WEIGHT PENALTIES. Total system penalties include hardware (pressurization system), helium supply system, vent mass and vapor residuals, and thermal subcooler weights.

The number and weights of the pressurization system components is given in Table 6-2 and totals 27 kg (59.6 lb).

Table 6-6 gives helium supply system weights for LO_2 tank pressurization. Weight totals are 2.9 and 5.6 kg (6.4 and 12.3 lb) for the design engine NPSP requirements. These totals are 8.6 to 16.8 kg (19 to 37 lb) lower than System 2 totals.

Thermal subcooler system weights are tabulated in Table 6-7. Weight totals are 3.5 and 4.2 kg (7.7 and 9.2 lb) for the design engine NPSP requirements. These totals do not include cold-side and hot-side propellant losses for each engine start, which are expected to be small.

System 3 component and total weight penalties are given in Figure 6-7. Ventage and vapor residual masses are not significantly different from the System 1 and 2 predictions. Weight totals for the low and moderate NPSP conditions are 233 and 240 kg (514 and 528 lb), respectively. These totals are only about 13.6 kg (30 lb) lower than the System 2 weight penalties.

6.5 THERMAL CONDITIONING SYSTEM 4

This is the most technologically advanced of the four thermal conditioning systems. The hydrogen subcooler will provide NPSP for both engine start and steady-state operation. Coolant vapor will be returned to the ullage (instead of being dumped overboard) where it will serve as pressurant to provide a portion of the total engine NPSP required. Weight penalties are expected to be the lowest of the four thermal conditioning systems.

6.5.1 SYSTEM DESIGN. A preliminary design drawing of System 4 is given in Figure 6-8. This schematic is similar to that of System 3 except that the autogenous pressurization has been deleted and a pump has been added to return coolant to the tank ullage.

The vehicle-mounted hardware is described by Table 6-2 and Figure 6-8. Only the LO_2 tank pressurization solenoid valves and orifices remain. The thermal subcooler design is the same as described for System 3, except for the return-to-ullage pump and tubing requirements.

6.5.2 SYSTEM WEIGHT PENALTIES. System 4 weight penalties (individual and total) are given in Figure 6-9. Pressurization system hardware weights were obtained from Table 6-2. Helium supply system weights for LO_2 tank pressurization are the same as for System 3 (Table 6-6). Thermal subcooler weights (Table 6-8) are 5.3 and 6.0 kg (11.7 and 13.2 lb). Again, these

Table 6-6. System 3 Helium Supply Weights

	Low Engine NPSP		Moderate Engine NPSP	
	LO_2 Tank	LH_2 Tank	LO_2 Tank	LH_2 Tank
Mission Helium Usages, kg (lb)	0.5 (1.1)	0	1.0 (2.1)	0
Initial Helium Mass,(1) kg (lb)	0.6 (1.3)		1.1 (2.5)	
Helium Bottle Weight(1) kg (lb)	2.1 (4.6)		4.0 (8.8)	
Bottle Supports(2) kg (lb)	0.2 (0.5)		0.5 (1.0)	
Total Weight kg (lb)	2.9 (6.4)		5.6 (12.3)	

(1) From Table 6-5.

(2) Supports = 0.11 x Bottle weight

Table 6-7. Hydrogen Thermal Subcooler Weights (Coolant Dump Configuration)

	Component Weights, kg (lb)	
	3.4 kpa (0.5 psid)	6.9 kpa (1.0 psid)
Subcooler	0.8 (1.7)	1.5 (3.2)
Coolant line	0.6 (1.3)	0.6 (1.3)
Tank penetration fitting	0.1 (0.3)	0.1 (0.3)
Regulator to coolant lines	0.3 (0.7)	0.3 (0.7)
Tubing, fittings, etc.	0.8 (1.8)	0.8 (1.8)
Regulator	0.9 (1.9)	0.9 (1.9)
Totals	3.5 (7.7)	4.2 (9.2)

NOTES:

1. Estimated coolant dump masses for engine start were found to be insignificant.
2. A penalty was not assessed for hot-side mass losses during each engine chilldown and start transient. It is expected that these quantities are the same with or without a subcooler.

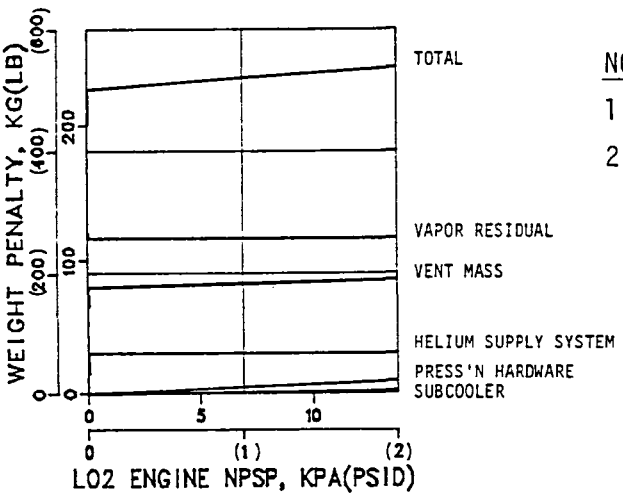

NOTES:

1. LH_2 NPSP = 1/2 x (LO_2 NPSP)
2. A SHARP WEIGHT PENALTY REDUCTION OCCURS BETWEEN NEAR-ZERO AND ZERO NPSP

Figure 6-7. Thermal Conditioning System 3 Weight Penalties

totals do not include cold-side and hot-side engine start propellant losses, which are expected to be small. Ventage and vapor residual masses are similar to those predicted for System 3.

System 4 weight penalty totals are the lowest of the four thermal conditioning systems analyzed during Task IV. The totals of 219 and 2.28 kg (482 and 503 lb), respectively, for the low and moderate NPSP conditions are about 10.9 kg (24 lb) less than the System 3 weight penalties.

6.6 THERMAL CONDITIONING SYSTEMS COMPARISON

A weight penalty comparison of the four thermal conditioning systems is given in Figure 6-10. The new technology systems (3 and 4) show a lower weight penalty over the moderate-to-low NPSP range, as expected. What was not expected however, was the small weight difference between the state-of-the art systems and new technology systems. For example, the weight difference between Systems 2 and 4 is predicted to be 25.9 to 28.6 kg (57 to 63 lb) in the low-to-moderate NPSP range.

Considering the development costs and risks that would be associated with the introduction of a thermal subcooler to replace LH_2 tank pressurization, the potential weight improvement does not appear to be substantial. Furthermore, it is expected that the weight differential between systems will be even less than shown in Figure 6-10 because the general tendency is for a system weight increase between conceptual design and flight hardware. Consequently, there appears to be little advantage in developing a new thermal conditioning system.

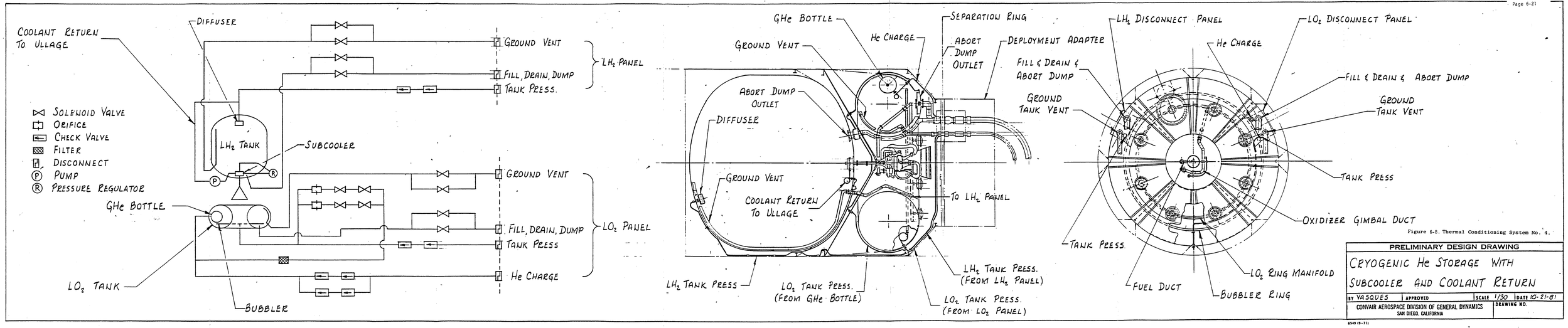

Figure 6-8. Thermal Conditioning System No. 4.

PRELIMINARY DESIGN DRAWING			
CRYOGENIC He STORAGE WITH SUBCOOLER AND COOLANT RETURN			
BY VASQUES	APPROVED	SCALE 1/30	DATE 10-21-81
CONVAIR AEROSPACE DIVISION OF GENERAL DYNAMICS SAN DIEGO, CALIFORNIA			DRAWING NO.

6549 (9-73)

This Page Intentionally Left Blank

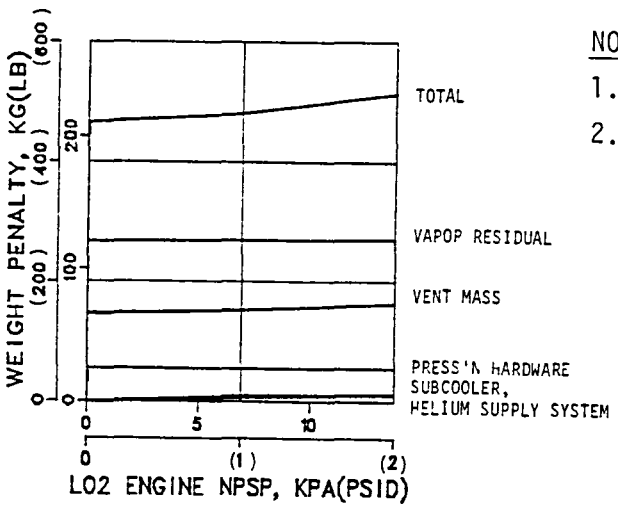

NOTES:

1. LH_2 NPSP = 1/2 x (LO_2 NPSP)
2. A SHARP WEIGHT PENALTY REDUCTION DOES OCCUR BETWEEN NEAR-ZERO AND ZERO NPSP

Figure 6-9. Thermal Conditioning System 4 Weight Penalties

Table 6-8. Hydrogen Thermal Subcooler Weights (Coolant Return-to-Ullage)

	Component Weights, kg (lb)	
	3 4 kpa (0 5 psid)	6 9 kpa (1 0 psid)
Subcooler	0 8 (1 7)	1 5 (3 2)
Coolant line	0 7 (1 6)	0 7 (1 6)
Tank penetration fitting	0 1 (0 3)	0 1 (0 3)
Regulator to coolant line	0 3 (0 7)	0 3 (0 7)
Tubing, fittings, etc	0 9 (2 0)	0 9 (2 0)
Regulator	0 9 (1 9)	0 9 (1 9)
Pump	1 6 (3 5)	1 6 (3 5)
Totals	5 3 (11 7)	6 0 (13 2)

NOTES:

1. Estimated coolant dump masses for engine start were found to be insignificant.
2. A penalty was not assessed for hot-side mass losses during each engine chilldown and start transient. It is expected that these quantities will be the same without or without a subcooler.

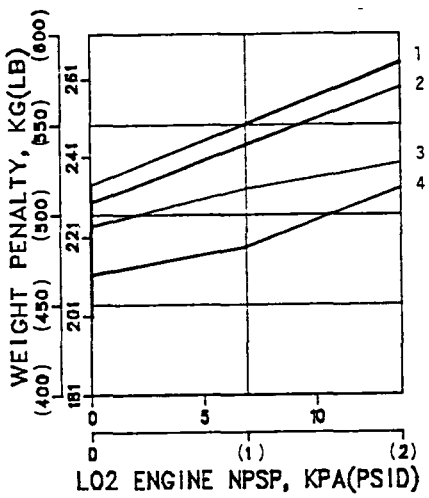

THERMAL CONDITIONING SYSTEMS*
(ENGINE START/ENGINE BURN)

LH_2 TANK

1. HELIUM (AMBIENT)/AUTOGENOUS
2. HELIUM (CRYO)/AUTOGENOUS
3. SUBCOOLER (COOLANT DUMP)/ AUTOGENOUS
4. SUBCOOLER/SUBCOOLER (COOLANT RETURN TO ULLAGE)

* LO_2 TANK EMPLOYS BUBBLER/ BUBBLER

Figure 6-10. Thermal Conditioning Systems Weight Penalty Comparison

An alternative to a new thermal conditioning system is to allocate development funds into a zero NPSP engine system. The weight improvement over System 2 would be 43 to 58 kg (96 to 128 lb). The resulting performance gain would have to be traded against the costs and risks of a zero NPSP engine system.

Table 6-9. LTPS Fill, Dump, Drain and Ground Vent System Weights

Hydrogen System		Oxygen System	
Component(s)	Weight,kg(lb)	Component(s)	Weight,kg(lb)
Fill, Drain and Dump		Fill, Drain and Dump	
Outlet Fitting	0.7 (1.6)	Outlet Fitting & Joint	1.0 (2.2)
Flex Joints (3)	4.5 (9.9)	Flex Joints (5)	4.2 (9.3)
Duct Fittings (4)	1.5 (3.4)	Duct Fittings, Ells,etc.	0.4 (0.8)
Duct Sections	5.3 (11.7)	Duct Sections	1.6 (3.5)
Duct Insulation	1.8 (4.0)	Flanges (4)	2.5 (5.6)
Wiring	0.9 (2.0)	Wiring	1.4 (3.0)
Collars,Links, etc.	1.6 (3.5)	Clips,Bolts, etc.	1.1 (2.5)
Valves	10.0 (22.0)	Valves	10.0 (22.0)
Disconnect	6.0 (13.2)	Disconnect	6.0 (13.2)
Subtotal	32.3 (71.3)	Subtotal	28.2 (62.1)
Ground Vent		Ground Vent	
Outlet Fitting	0.5 (1.1)	Outlet Fitting	0.5 (1.1)
Joint/Flange Assy.	1.1 (2.4)	Joint/Flange Assy.	1.1 (2.4)
Duct Sections	4.6 (10.1)	Duct Sections	3.0 (6.6)
Wiring	0.9 (2.0)	Wiring	0.9 (2.0)
Flex Joints (3)	2.0 (4.5)	Flex Joints (3)	2.0 (4.5)
Duct Supports	0.7 (1.6)	Duct Supports	0.2 (0.5)
Valves (2)	5.0 (11.0)	Valves (2)	2.7 (6.0)
Disconnect	2.7 (6.0)	Disconnect	2.7 (6.0)
Flanges/Seals (4)	3.3 (7.2)		
Subtotal	20.8 (45.9)	Subtotal	13.1 (29.1)
LTPS Totals	53.1 (117.2)		41.3 (91.2)

NOTES

1. This is vehicle-mounted hardware.
2. Weights are independent of thermal conditioning system.

7

LTPS ABORT PRESSURIZATION REQUIREMENTS

In Task II we analytically determined helium pressurant mass requirements to expel LTPS propellants and perform tank inerting during Return-to-Launch-Site (RTLS) emergency operating conditions for Shuttle. Analyses were conducted for LTPS Configurations 1 and 2. Helium pressurization for propellant expulsion was the only technique considered for this analysis due to the desire to inert the tanks following propellant expulsion. Pressurant mass requirements were determined for tank pressure increases of 14, 28 and 55 kpa (2, 4 and 8 psid) during propellant expulsion, and for two re-pressurization cycles following each of two vent cycles performed during tank inerting operations.

7.1 ABORT GUIDELINES AND REQUIREMENTS

During this task we employed guidelines and ground rules established or identified from previous GDC studies. In particular, we relied upon the substantial data accumulated during the Shuttle/Centaur study (Reference 7-1) dealing with design, interface, operational and safety requirements imposed on the Centaur fluids systems while in the Orbiter cargo bay (Figure 7-1). Certain Centaur subsystems and support systems were selected for this study on the basis that they were representative of LTPS subsystems. Analysis techniques and computer programs developed or modified for the Shuttle/Centaur abort dump analysis were also used for this study.

7.1.1 LTPS/SHUTTLE ABORT MODES. The LTPS must be designed for compatibility with all Shuttle abort modes that occur before vehicle deployment. For these aborts, methods of safely operating the LTPS and subsequently disposing of propellants before landing must be devised. Shuttle aborts may be divided into two categories characterized by their impact on LTPS propellant dump design requirements.

a. Return-to-Launch-Site (RTLS) Abort. For Shuttle aborts which occur between 150 and 272 seconds after launch, the RTLS mode may be used. In this mode, the Orbiter reverses its direction of flight at high altitude by rotating in pitch to apply retrograde thrust using the main engines. After entering the atmosphere, the Orbiter glides back to the launch site. Propellants can be dumped during the retrograde thrusting period where ample acceleration for settling is provided (1 to 3g as shown by Figure 7-2) by the three main Shuttle engines (SSMEs) with the gradual g increase due to consumption of propellants from the external tank.

b. Orbital Abort. One of three orbital abort modes defined below can be used if the RTLS abort time has been exceeded or is less desirable:

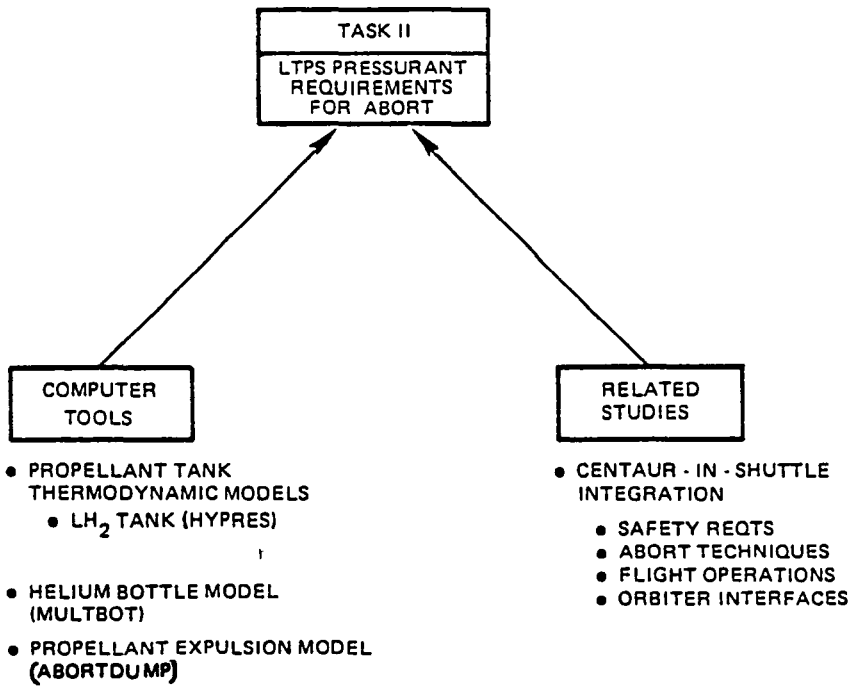

Figure 7-1. Our Centaur-in-Shuttle Study Resolved All Interface Problems Related to Centaur/Shuttle Abort

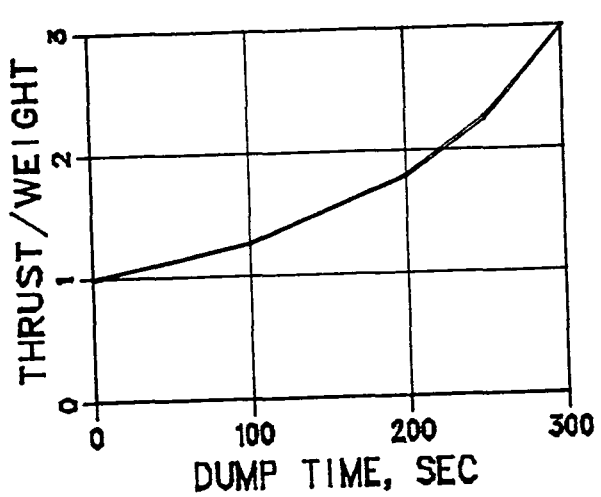

Figure 7-2. Propellant Settling During RTLS Abort Will Be Provided by SSME Thrust

1) Abort-Once-Around (AOA). 240 seconds after launch to start of second OMS burn. The Orbiter continues to slightly less than orbital velocity, reenters and lands at the end of the first orbit.

2) Abort-to-Orbit (ATO). 240 seconds after launch to start of second OMS burn. The Orbiter proceeds to orbit utilizing the SSMEs and Orbital Maneuvering System (OMS).

3) Abort-from-Orbit (AFO). Anytime after injection using the OMS to provide the de-orbit impulse burn.

Of the Shuttle abort modes, RTLS was the only one considered for this study because it would establish the maximum helium requirements due to the limited time available for dumping propellants.

7.1.2 ANALYTICAL TOOLS. Three computer programs used in establishing the Centaur fluids system design concepts were used for the LTPS abort analysis. A brief description and the function of each program are given below.

MULTBOT. The program performs a thermodynamic analysis of the helium bottle(s) blowdown process. Environmental heating and bottle-to-helium heat exchange effects are considered as temperature and pressure histories are determined for the helium expulsion process. Supply helium temperatures will decay during abort dump and this fact must be considered in determining pressurant requirements.

HYPRS. This program describes the thermodynamic state of propellants and ullage during an outflow, venting or pressurization process for the propellant tanks. The analysis includes the influence of tank heating and liquid-ullage coupling. MULTBOT is included as a subroutine so that helium conditions during pressurization reflect the bottle blowdown process.

ABORTDUMP. This program was developed to size the LO_2 and LH_2 dump systems for Shuttle/Centaur RTLS abort. An iterative analysis is performed in which a flow rate is determined that satisfies the requirement for sonic flow at the dump line exit for a given propellant condition at the tank outlet. Two-phase flow generally occurs upstream of the dump line exit. The computer program incorporates realistic, experimentally devised loss coefficients for ducting bends, gimbal joints, flex sections and valves as well as the physical properties for liquid and vaporized propellants. The program was modified to perform abort dump analyses using methane propellant.

7.1.3 SHUTTLE OPERATIONAL AND SAFETY REQUIREMENTS. The Shuttle/Centaur study results have provided a thorough understanding of Shuttle imposed interface, operational and safety requirements. Safety clearly has a great influence on vehicle fluid systems design. This is illustrated by Figures 7-3 and 7-4 which represent the helium pressurization and propellant dump systems of Centaur and its integrated support system (CISS) integrated with the Orbiter. The fluid system valve redundancy indicated by these figures was necessary to satisfy the STS safety requirements specified in NASA document NHB 1700.7. These systems and other Centaur fluid systems have been successfully subjected to the

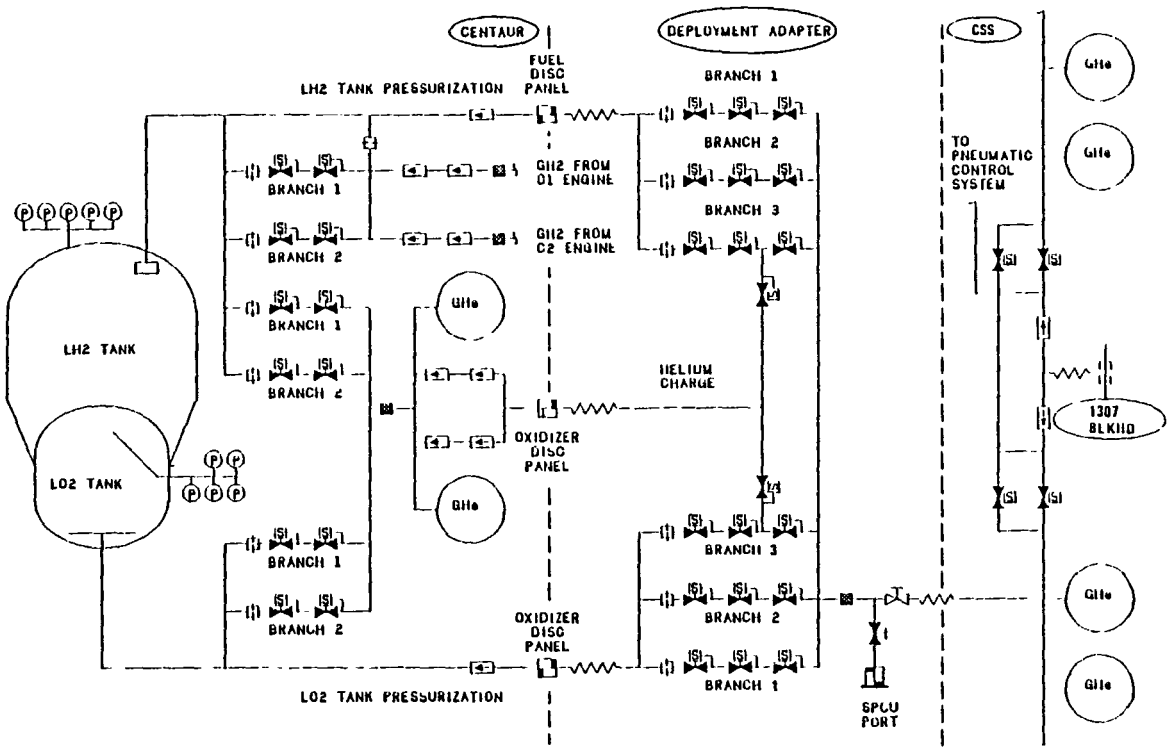

Figure 7-3. Abort Dump Helium Pressurization System for Shuttle/Centaur.

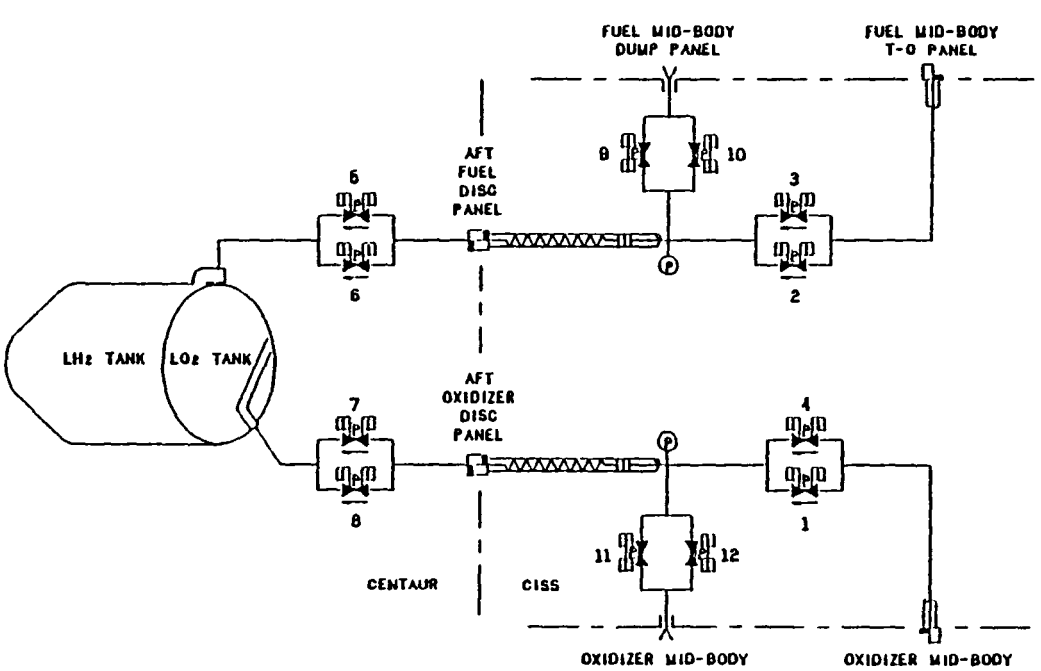

Figure 7-4. Abort Propellant Dump System for Shuttle/Centaur.

JSC Phase 0 and Phase I safety review. Consequently, they comply with overall STS safety requirements from initial installation in the cargo bay until deployment in orbit.

7.1.4 RETURN TO LAUNCH SITE (RTLS) ABORT REQUIREMENTS. Our Centaur analysis reflected compliance with STS operational and safety requirements specified in NASA document NHB 1700.7 and interpreted by the JSC safety panel. Specifically we used the latest JSC published abort trajectory having the lowest acceleration (Figure 7-5) which is based on an RTLS abort caused by one SSME out. In performing the Shuttle/Centaur propellant dump analysis it was determined that imposed g forces had a very significant effect on propellant dump times, especially for the LO_2 system, and thus is correspondingly reflected in required tank pressures. Dumping propellant as late as possible during the RTLS abort will result in minimum helium usage due to the higher g levels.

A propellant dump time of 250 seconds was used for this analysis. Until recently a dump time of 300 seconds was acceptable. However, JSC now anticipates an imposed dump time as short as 250 seconds will be required based on their continuing investigation of various failure modes.

A simultaneous dump of tank propellants will be accomplished in conjunction with the 250-second minimum propellant dump time. A simultaneous dump can be safely accomplished while the Orbiter is above 100,000 feet altitude which corresponds to an ambient pressure less than 0.7 kpa (0.1 psia). Extensive testing has demonstrated that a hydrogen-oxygen mixture will not ignite at pressures below 0.7 kpa (0.1 psia). As a result of the Shuttle/Centaur study effort, it is now agreed that a simultaneous dump should be used.

7.1.5 LTPS ABORT DUMP FLUID SYSTEMS. The LTPS abort helium pressurization and propellant dump systems selected for Task II analyses are schematically shown in Figures 7-3 and 7-4, respectively. These fluid systems, selected for the Shuttle/Centaur configuration, are believed to be representative of the equivalent LTPS systems since they are compatible with all Shuttle abort modes.

7.1.5.1 Helium Pressurization System. The pressurization system of Figure 7-3 consists of vehicle-mounted and Shuttle-mounted hardware. The Shuttle-mounted hardware includes pneumatically-actuated solenoid valves, pressurization orifices and helium supply system. A quad-set of solenoid valves provides the two-failure tolerancy required for pressurizing each propellant tank. Helium will be stored in composite bottles (titanium liner, kevlar outer wrap), manifolded and mounted on an LTPS pallet. Lift-off helium pressure and temperature were selected as 27580 kpa (4000 psia) and 300K (540R). The vehicle-mounted hardware includes pressurization tubing, a LH_2 tank helium diffuser and a LO_2 tank bubbler manifold.

7.1.5.2 Abort Propellant Dump System. The dump line configurations used for this study were the same as those identified for the Shuttle/Centaur. These dump lines are shown in Figures 7-6 and 7-7. Various components such as bellows, expansions/contractions, dividing/converging branches and

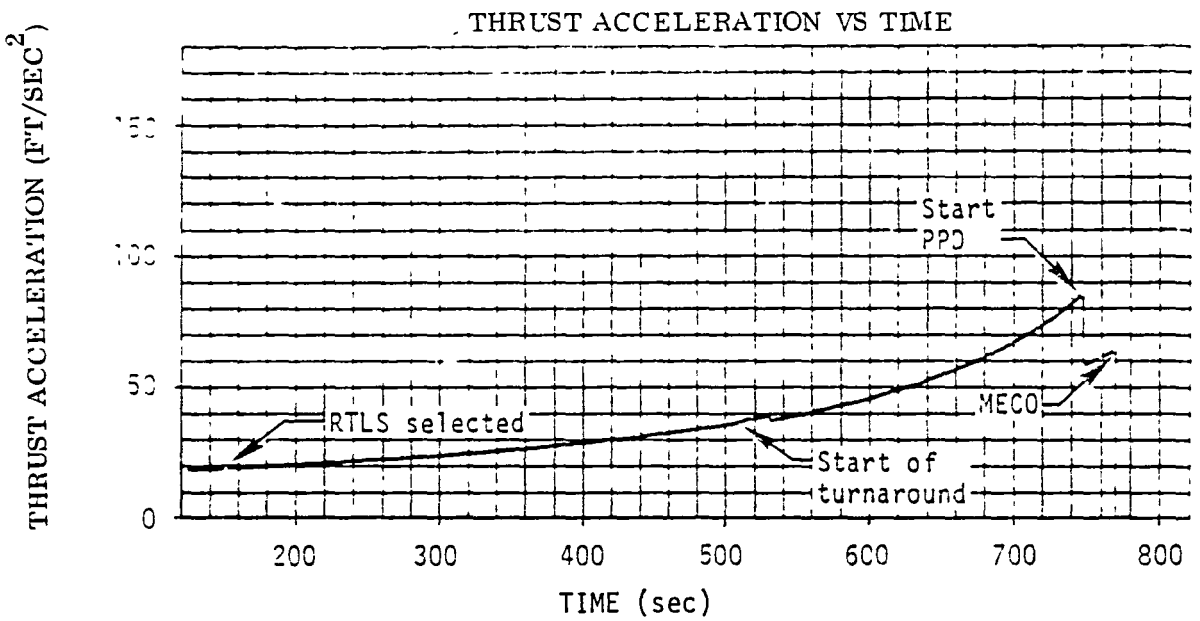

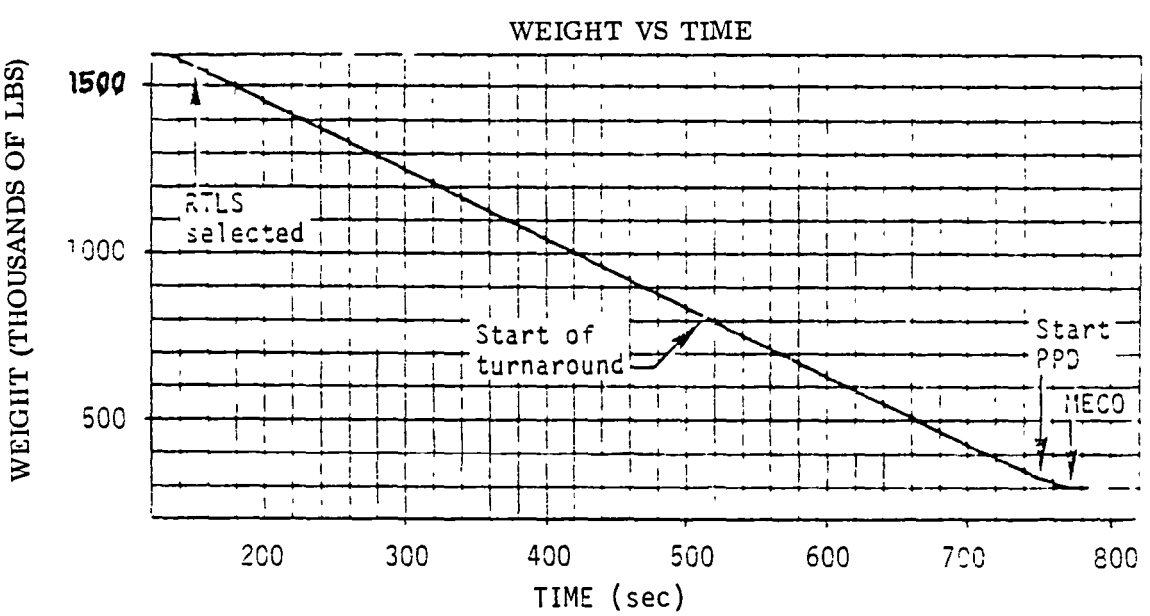

Figure 7-5. Abort Dump Analysis Employed Realistic Shuttle G-levels.

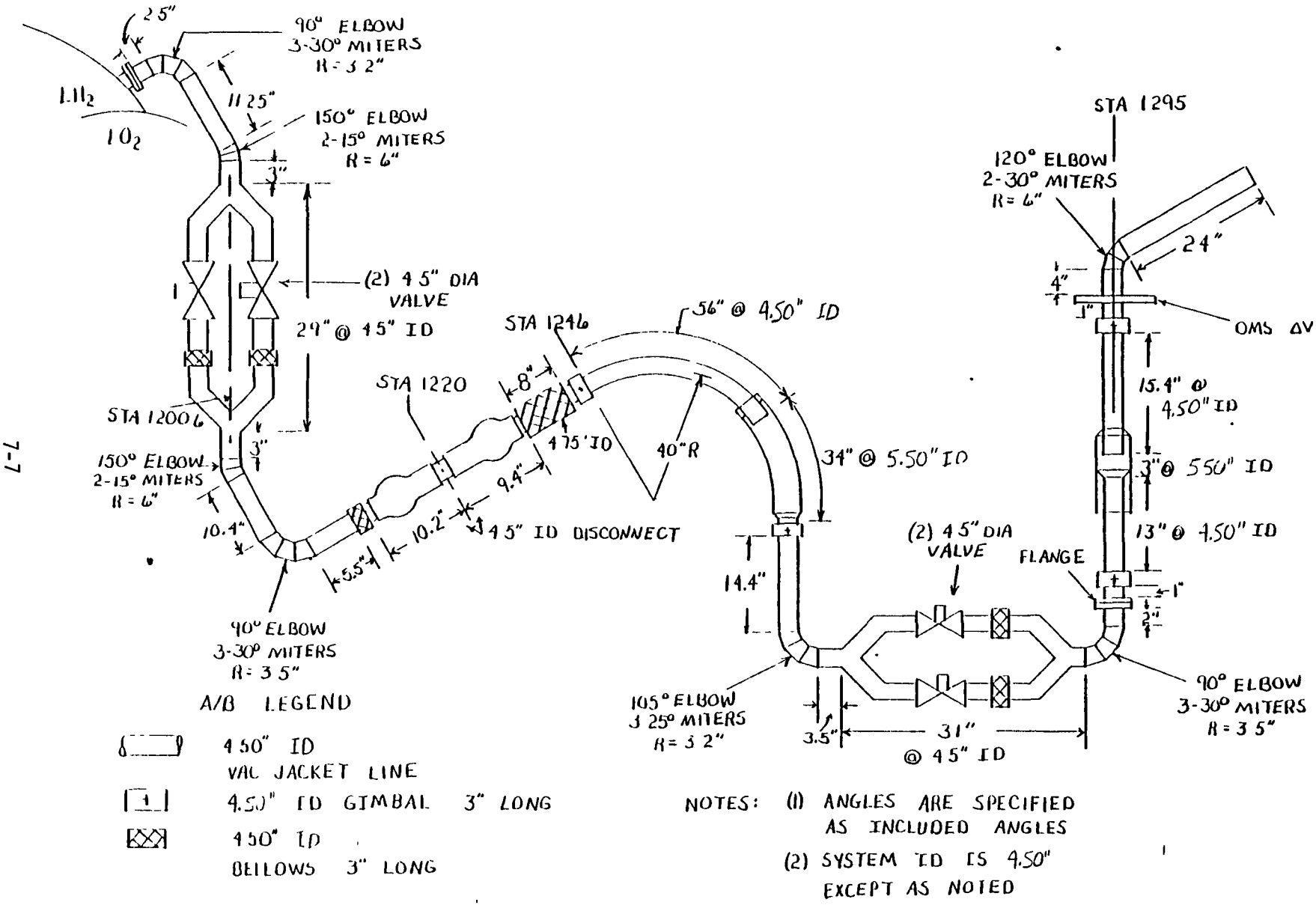

Figure 7-6. Hydrogen Dump Line Schematic

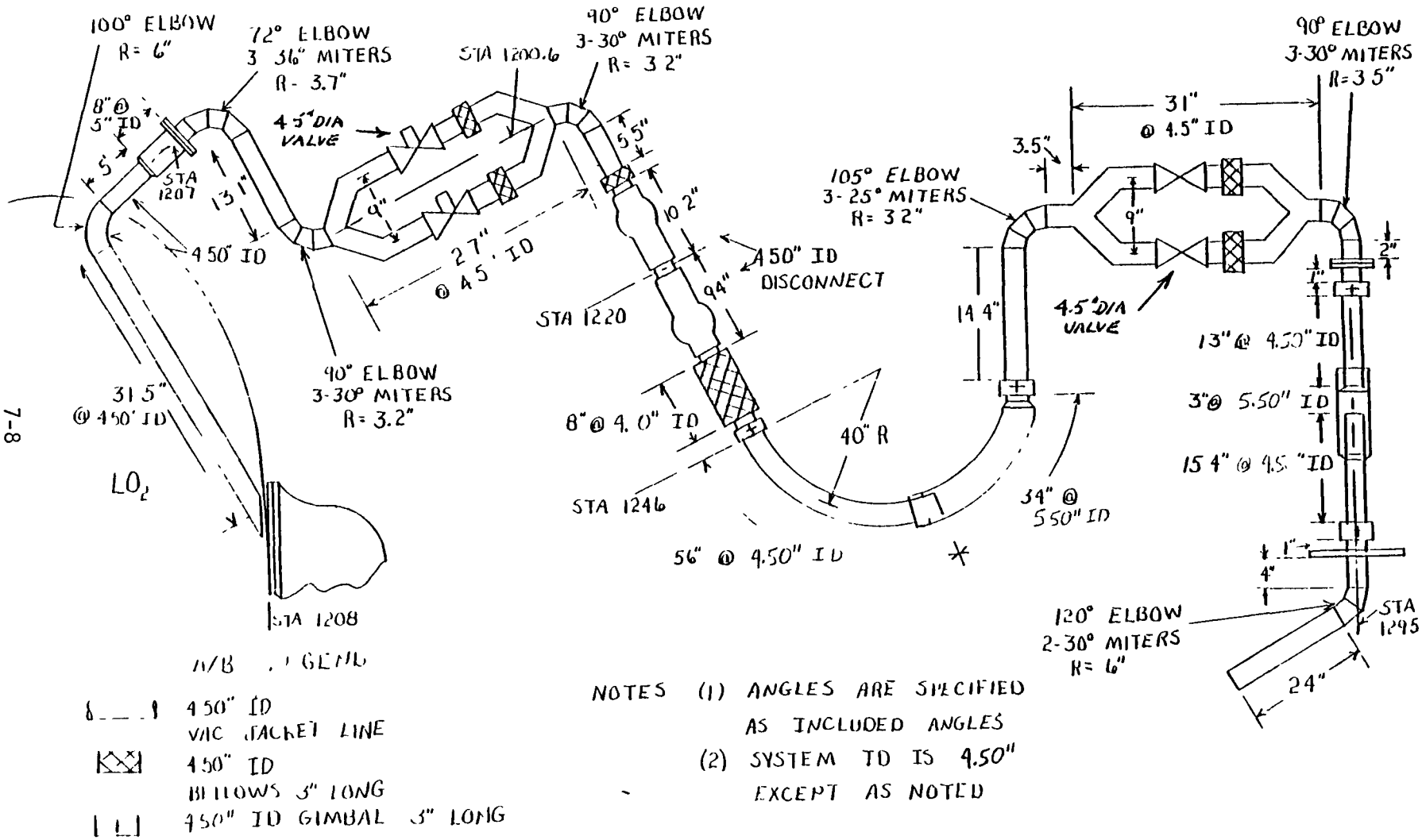

Figure 7-7. Oxygen Dump Line Schematic

numerous bends all contribute to the pressure loss realized by the fluid. Two items are worthy of note. First, the curved sliding tube-within-a-tube allows for vehicle erection out of the Orbiter bay. Secondly, the two flow loops allow for single failure tolerance in both the failed open and failed closed modes.

7.2 ABORT PROPELLANT EXPULSION

Pressurant helium for abort can be determined without considering dump line sizes. That is, helium usages can be calculated for each pressurization ΔP given the requirement that tank propellants will always be dumped in 250 seconds. The obvious outcome will be that more helium (and a heavier supply system) will be required for increased pressurization ΔPs. The missing element in such an analysis is the abort dump line configuration. This was found to be a significant factor in the Shuttle/Centaur dump analysis. It is significant because it represents a complex, large diameter, vacuum-jacketed system that requires redundant valving due to STS safety requirements. It must also accommodate Orbiter relative motion and vehicle-predeployment rotation out of the cargo bay.

It is evident that a smaller dump line will be required if tank pressurization Δ Ps can be increased. Selection of an abort pressurization system, however, must consider size and weight of the abort dump line system in addition to pressurization system size and weight. This approach will enable total system weight optimization similar to that indicated by Figure 7-8.

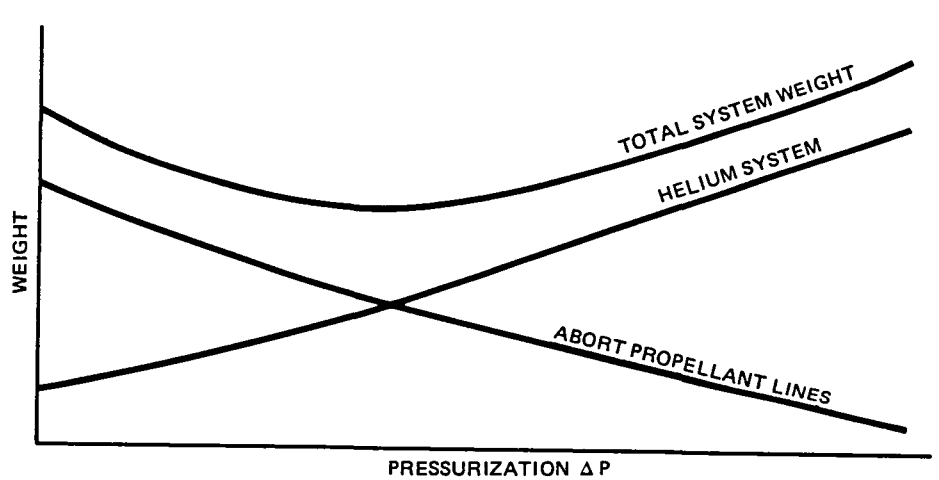

Figure 7-8. Abort Propellant Line Weights Were Included in a Total System Optimization Analysis.

7.2.1 ABORT PRESSURIZATION TECHNIQUE. In earlier studies with Shuttle/Centaur, abort dump pressurization was analyzed for ambient helium injection into the ullage and into the liquid during propellant dump. The approach selected then was to inject helium directly into the hydrogen tank ullage and to inject helium beneath the liquid oxygen surface because each method minimized dump helium mass requirements. Our analysis for LTPS yields the same results. Bubbler pressurization for the liquid methane tank was also selected. Note that these same helium pressurization techniques were also selected for LTPS mission pressurization (Section 2).

An advantage provided by bubbler pressurization is that helium cools propellant as it rises into the ullage. This chilling effect will effectively increase propellant subcooling while maintaining a constant tank pressure. This is illustrated by Figure 7-9 which shows that LO_2 vapor pressure will decay by about 27.6 kpa (4 psia) during propellant dump. Since propellant tank pressures will be maintained at a constant level during dump, it is clear that the propellant will be subcooled by an additional 27.6 kpa (4 psia) at the end of abort. This additional subcooling will serve to increase propellant flow rates during the expulsion period.

7.2.1.1 Helium Mass Requirements. Helium mass usages for propellant tank pressurization during propellant dump were determined using the HYPRS computer program. For all conditions, initial tank pressure (and vapor pressure) was 124 kpa (18 psia). Computer runs were made for tank pressurization ΔPs of 14, 28 and 55 kpa (2, 4 and 8 psid). Tank pressures were maintained constant throughout the 250-second propellant dump period. Helium usages for bubbler injection to the LO_2 and LCH_4 tanks did not exceed 5 kg (11 lb) at the maximum pressurization ΔP, Figure 7-10. LH_2 tank helium usages (for ullage injection) were found to exceed 17.4 kg (40 lb).

The helium supply system weight was calculated using the procedure of Table 7-1. This is a similar procedure to that used for determining LTPS mission helium supply system weights. The resulting system weights (which include helium bottles + supports + initial helium load) are given in Figures 7-11 through 7-13. These totals do not include components such as pressurization lines, solenoid valves and disconnects because such items are required for all systems and do not influence weight optimization.

The Shuttle pallet-mounted helium supply bottles will provide helium for propellant tank inerting and specified purges, as well as for abort dump pressurization. The post-propellant dump helium requirements (discussed in Section 7.3) will influence helium supply temperature during abort dump helium pressurization. LO_2 tank and LCH_4 tank helium usages during dump will not be affected by the post-dump helium demand because pressurant requirements will be the same whether helium enters the liquid at ambient or at liquid temperature. Consequently, helium supply system weights could be determined as a function of tank pressurization ΔP alone, Figures 7-11 and 7-12.

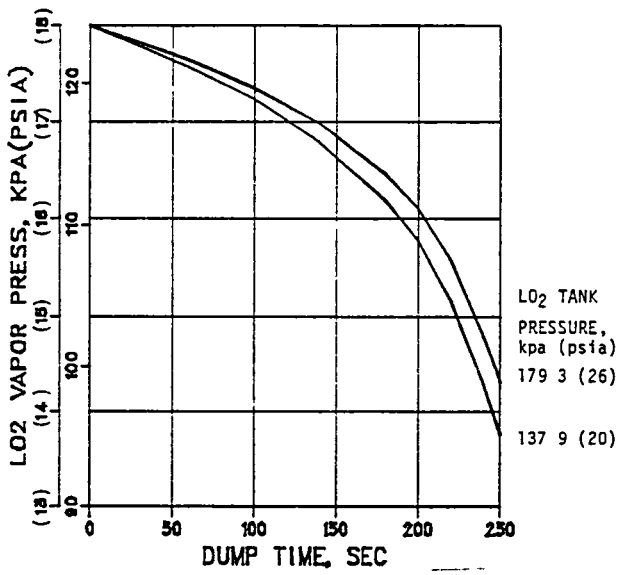

Figure 7-9. Helium Bubbler Pressurization Influence Upon LO_2 Vapor Pressure During Abort Dump

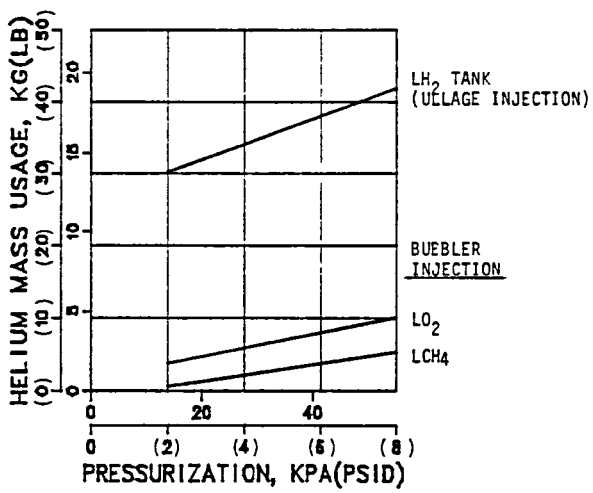

Figure 7-10. Abort Dump Helium Mass Usages

Table 7-1. Procedure for Determining Abort Helium Pressurization System Weight.

Event	Helium Density kg/m^3 (lb/ft^3)	Usable Helium Density kg/m^3 (lb/ft^3)
Pre-launch(1)	39.247 (2.450) ρ_i	N/A
Post-abort Landing(2)	1.185 (0.074) ρ_f	38.061 (2.376) ρ_u

(1) 27580 kpa (4000 psia), 300K (540R)
(2) 690 kpa (100 psia), 278K (500R)

V = helium bottle volume

m_{BTL} = helium bottle mass

ρ_{BTL} = m_{BTL}/V = 253.1 kg/m^3(15.8 lb/ft^3) for titanium liner, kevlar outer wrap

m_s = helium bottle supports

ρ_s = $m_s/V = 0.11 * \rho_{BTL}$

m_u = usable helium mass = $\rho_u * V$

m_i = initial helium mass = $\rho_i * V$

$V = m_u/\rho_u$

m_1 = helium mass for LH_2 and LO_2 tanks pressurization

m_2 = post-abort helium purge mass

m_u = $m_1 + m_2$

M_T = total abort helium pressurization system weight

$$= m_i + m_{BTL} + m_s$$

$$= V * (\rho_i + \rho_{BTL} + 0.11\,\rho_{BTL}) = V * (\rho_i + 1.11\,\rho_{BTL})$$

$$= (m_u/\rho_u)(\rho_i + 1.11\,\rho_{BTL}) = m_u * (\rho_i/\rho_u + 1.11\,\rho_{BTL}/\rho_u)$$

$$= m_u * (1.031 + 7.381) = 8.412\,m_u$$

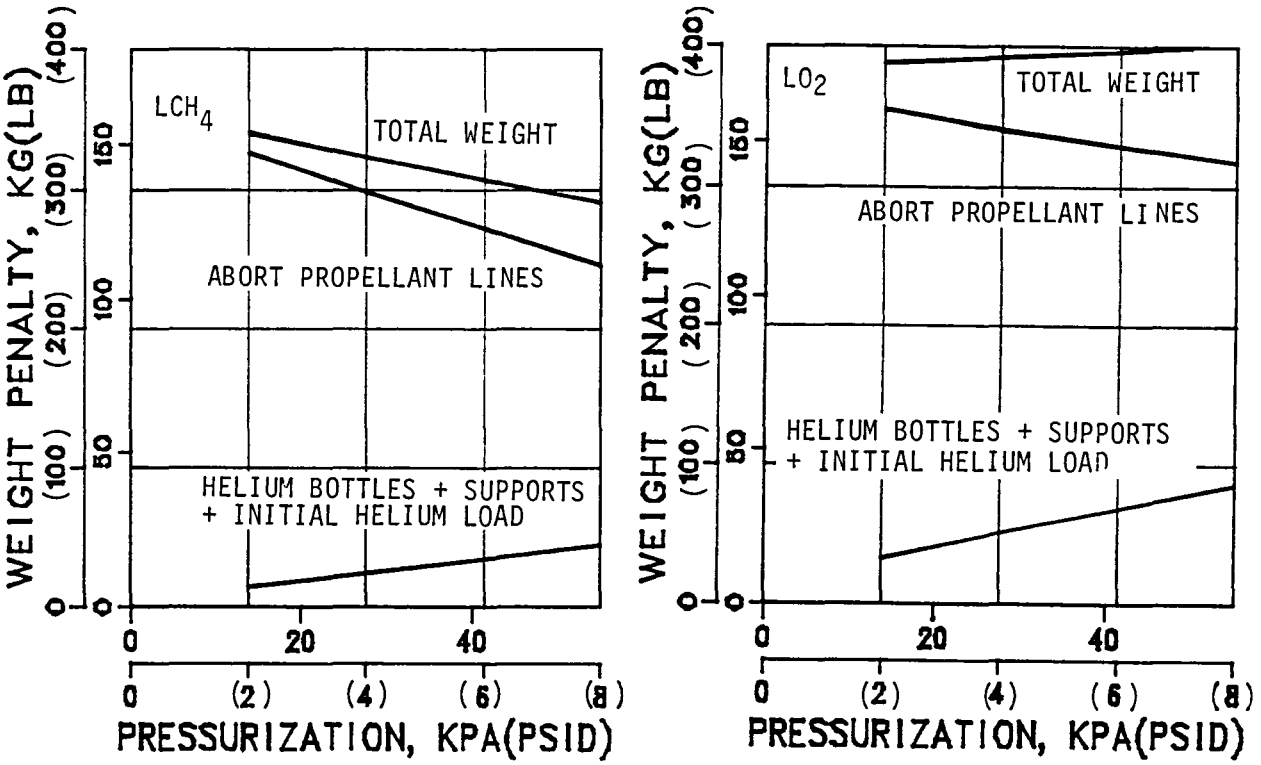

Figure 7-11. LCH_4 and LO_2 Tank Abort Dump System Weight Optimization (Configuration 3)

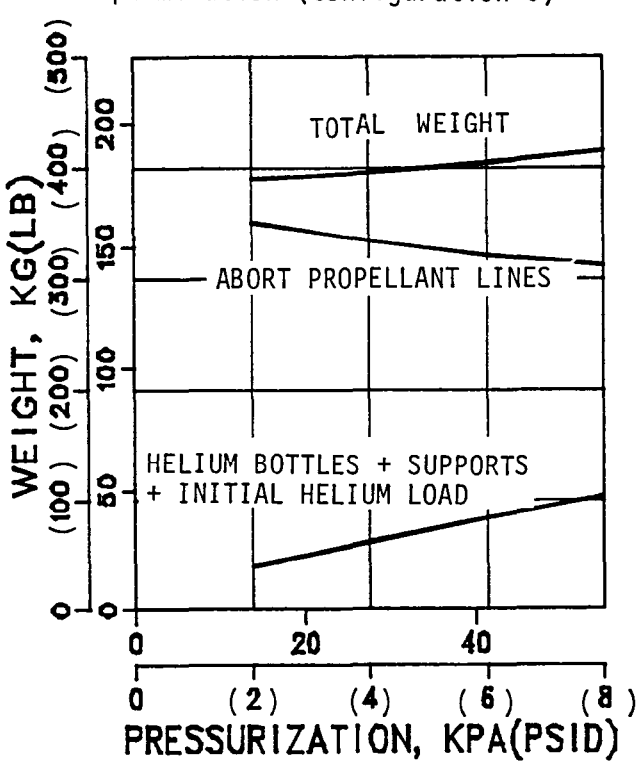

Figure 7-12. LO_2 Abort Dump System Optimization (Configuration 1)

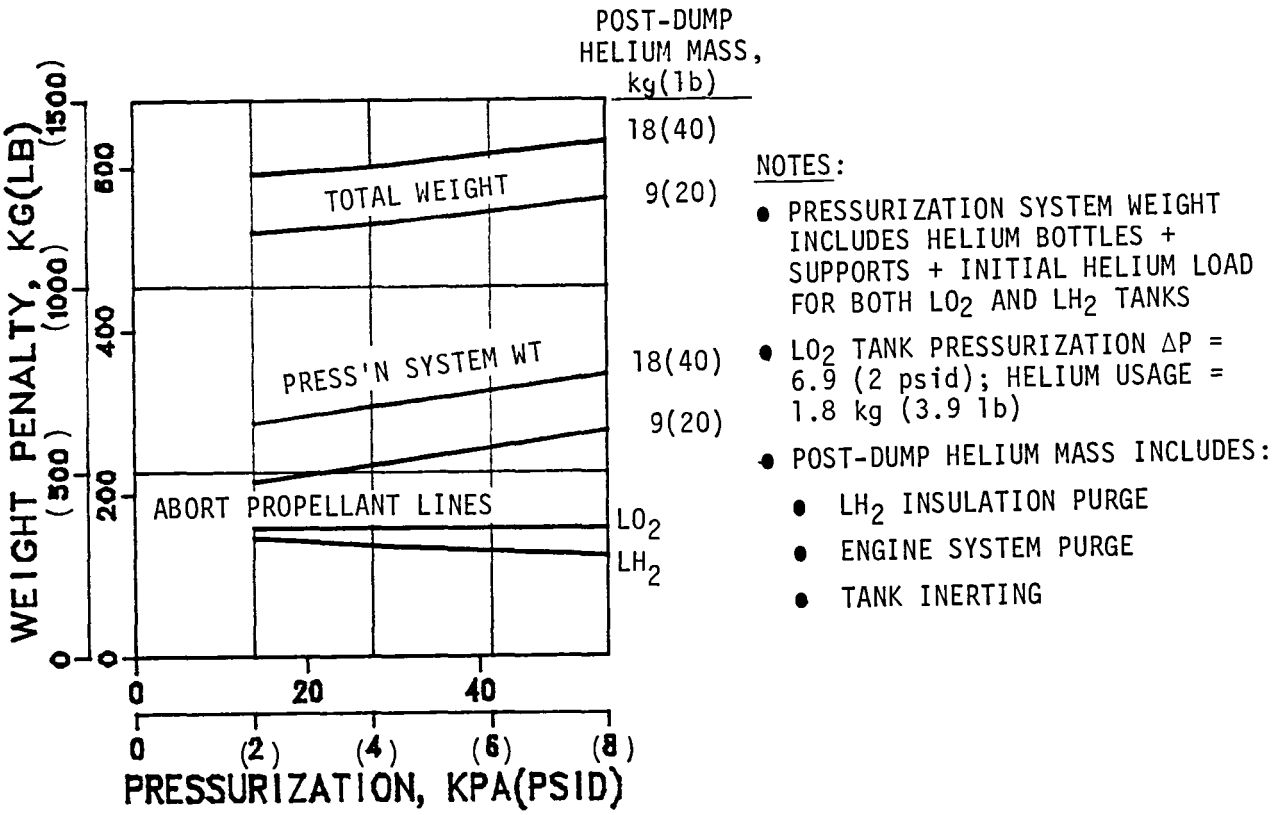

Figure 7-13. LH_2/LO_2 Abort Dump System Optimization (Configuration 1)

LH_2 tank helium mass requirements for propellant dump are a function of tank pressurization ΔP and helium supply temperature. Helium supply temperature will be influenced by LO_2 tank abort pressurization requirements and by post-propellant dump helium requirements. Consequently, these effects must be specified before LH_2 tank helium usages and resulting supply system weights can be calculated. Figure 7-13 gives the LH_2 tank helium supply system weight for known conditions. First, a minimum LO_2 tank pressurization ΔP of 14 kpa (2 psid) was specified because, from Figure 7-12, this represented the minimum system weight. Second, post-dump helium usages of 9 and 18 kpa (20 and 40 lb) were specified to assess this influence upon the helium system weight. Figure 7-13 shows that the helium system weight trend is unaffected by the post-dump helium usages, i.e., weight decreases as LH_2 pressurization ΔP is decreased.

Calculations were performed for vehicle configurations 1 and 3 only. Configuration 1 helium requirements are applicable to Configuration 2 because propellant tank volumes are nearly the same. The different LO_2 tank configurations (toroidal versus elliptical tanks) will affect the dump line routing for each

vehicle configuration. This weight difference was judged to be small relative to the overall dump system weight. Configurations 3 and 4 are identical except for insulation systems which will have no impact upon dump system optimization.

7.2.1.2 Abort Dump Flow Rates. For the given line configurations, propellants will flow at a rate peculiar to the line diameter and initial fluid conditions. As the fluid is dumped into the void of space, the flow rate which is realized is one that must ensure sonic (critical) conditions at the line exit. At these flow rates, the fluid transitions from an initially subcooled fluid to a saturated fluid to a mixture of co-existing liquid/vapor (two-phase fluid) as it continues downstream. In order to predict the resulting flow rates for given initial conditions and line geometry, it is necessary i) to be able to calculate the state, i.e., calculate two thermodynamic properties, in this case pressure and entropy, of the fluid at the exit of the dump line and ii) to be able to determine whether or not critical conditions exist at the line exit for these conditions. Equations for calculating the changes in pressure and entropy in the line are given below:

$$dS = (\dot{w}/\bar{\rho}A)^2 \, (fdx/D + C_D) / 2g_c JT \qquad (7\text{-}1)$$

$$dp = (\dot{w}/A)^2 \, (dA/A + d\rho/\bar{\rho} - fdX/D - C_D)/(\bar{\rho}g_c + \bar{\rho}g/g_c \, dH) \qquad (7\text{-}2)$$

where:

A	=	Pipe cross-sectional area
C_D	=	Pressure loss coefficient
D	=	Pipe diameter
dA	=	Change in A over interval considered
dH	=	Change in position relative to longitudinal axis
dp	=	Change in pressure over interval considered
dS	=	Change in entropy over interval considered
dX	=	Change in mass quality over interval considered
$d\rho$	=	Change in density over interval considered
f	=	Pipe friction factor
g	=	Magnitude of gravity vector
g_c	=	Gravitational constant
G_c	=	Mass flux at critical conditions
J	=	Mechanical/thermal energy conversion
T	=	Temperature
$\dot{w}$	=	Mass flow rate
v	=	Specific volume
ρ	=	Density

The quantities dp and dS are, strictly speaking, differential quantities. Equations 7-1 and 7-2 must then be integrated over a portion of the dump line to yield deltas in pressure and entropy. It is convenient to consider the dump line divided into consecutive intervals, over which the relative changes in density are small. It is then permissible to define an average density, $\bar{\rho}$, over each interval so that the integrations of the above equations are simplified. The calculation of the fluid's final state is then accomplished by a stepwise integration along a constant pressure line and an integration along a constant entropy line.

Once the fluid final state is known, a calculation is made to determine whether or not sonic flow conditions exist. Calculating the so-called critical mass flow rate of a two-phase fluid has been the subject of numerous reports. The diversity of models proposed reflects the uncertainty as to whether i) thermal equilibrium exists between phases, that is, there is sufficient mass transfer between phases to keep the saturation pressure of the liquid and vapor the same; ii) no mass transfer between phases exists at critical flow; or iii) some mass transfer exists between phases but not enough to ensure thermal equilibrium. The homogeneous thermal equilibrium, the frozen flow (Reference 7-2) and Henry's homogeneous, nonequilibrium critical flow models (Reference 7-3) represent respectively the assumptions enumerated above. From the standpoint of ease of calculation and conservatively low predictions of critical flowrates, the homogeneous thermal equilibrium model was chosen for this application. This model calculates critical flow rates in the following manner:

$$G_c^2 = -(dp/dv)_s \cdot g_c \text{ or equivalently}$$

$$= \rho^2 (dp/d\rho)_s \cdot g_c \qquad (7\text{-}3)$$

As was mentioned before, exit fluid conditions were calculated using Equations 7-1 and 7-2 in a step-wise manner. These exit fluid conditions were then used in Equation 7-3 to calculate a critical mass flow rate. Because this flow rate is not, in general, equal to the flow rate assumed in calculating the changes in line pressure and entropy, an iteration is performed on flow rate until the relative change in flow rate is sufficiently small. This logic was put into a computer program called ABORTDUMP, developed for Shuttle/Centaur.

Line diameter requirements. A relationship between dump line weights and tank pressurization was calculated in two stages. First,line sizes were determined that would dump propellants in 250 seconds at a given tank pressure. Then a relationship giving line weights for various line sizes was found. These quantities, when combined, would yield the required information.

The ABORTDUMP computer program was used to calculate mass flow rates for various line diameters and tank pressures. Flow rates were calculated for an initial liquid vapor pressure of 124 kpa (18 psia). LH_2 vapor pressure remained constant throughout propellant dump. LO_2 and LCH_4 vapor pressures decayed during propellant dump, as indicated by Figure 7-9. A one-to-one relationship between tank ΔP and line diameter was generated; results are given in Figure 7-14 for the three propellants.

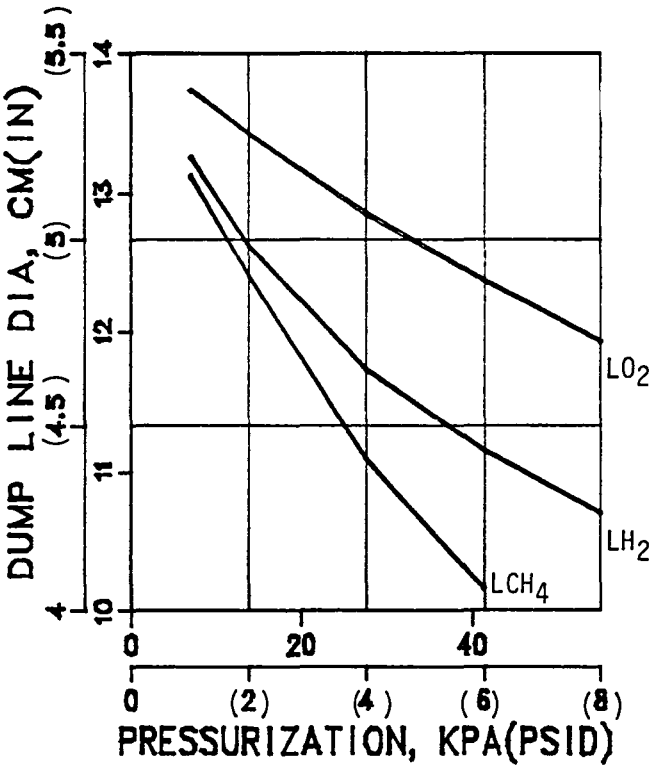

NOTES

- PROPELLANTS ARE DUMPED IN 250 SECONDS
- FLOW ASSUMPTIONS
  - THERMODYNAMIC EQUILIBRIUM
  - SONIC EXIT CONDITIONS (2 - ϕFLOW)
- PROPELLANT QUANTITIES DUMPED

  LO_2 = 15429 kg (34000 lb)

  LH_2 = 2722 kg (6000 lb)

  LCH_4 = 4536 kg (10000 lb)

Figure 7-14. Line Diameter Requirements for Propellant Dump

The Shuttle/Centaur hydrogen and oxygen system dump lines are shown in Figures 7-6 and 7-7. These same systems were assumed for the LTPS configurations. It was also assumed that the LO_2 and LCH_4 systems were identical. A complete list of dump line components and weights is given in Table 7-2. The values in this table assume a nominal line diameter of 11.4 cm (4.5 inches). Component weights for other sizes were taken to be directly proportional to line diameter. The resulting dump line weights versus diameter are summarized in Figure 7-15 for the three propellant systems.

The relationship between dump line weights and pressurization ΔP was obtained by combining the data of Figures 7-14 and 7-15. These relationships are shown in Figures 7-11 through 7-13 for LCH_4, LO_2 and LH_2. As expected, dump line weights increase as tank pressurization ΔP is decreased because a larger line diameter is required for propellant dump in 250 seconds.

7.2.2 DUMP SYSTEM SELECTION. The dump system weights for each propellant were determined by combining abort propellant line weights with helium system weights. It was expected that an optimum system weight would exist within the 14 to 55 kpa (2 to 8 psid) pressure range under study because dump line and helium system weights are, respectively, decreasing and increasing functions of pressurization ΔP. An optimum system weight was not found.

Table 7-2. Weight Tabulation of Abort Dump Line Components for Shuttle/Centaur*

Component	Weight kg (lb)	Quantity
pneumatic ball valves	5.0 (11 0)	4
disconnect unit	2 0 (4 5)	1
disconnect bellows	9 1 (20 0)	1
line bellows	0 54 (1 19)	4
gimbal flex joints	2 15 (4 75)	4
line flanges	0 45 (1 0)	12
telescoping duct	34 0 (75 0)	1
tube-in-tube	0 653(1 44)	1
Y fittings	0 916(2 02)	4
double 90°/60° elbow	1 81 (4 0)	1
90° elbow	0 58 (1 28)	2
reducers	0 124(0 273)	6
LH_2 line, total wt	131 2 (289 5)	1
LO_2 line, total wt.	135 0 (297 7)	1

* These dump line configurations were assumed for LTPS.

1. LH_2 and LO_2 dump lines have identical number of components. Only line lengths and bends are different.
2. Component and line weights are for a 11.4 cm (4.5 in.) diameter line.
3. Total line weights include line, insulation and component weights.

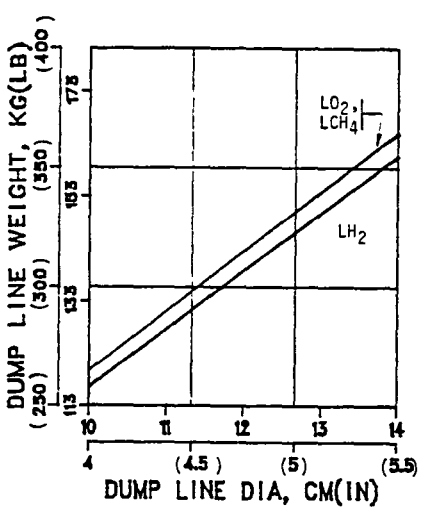

- WEIGHTS WERE LINEARLY SCALED FROM SHUTTLE/CENTAUR LO_2 AND LH_2 DUMP LINE CONFIGURATIONS
- LCH_4 LINE IS ASSUMED IDENTICAL TO THE LO_2 LINE

Figure 7-15. Abort Dump Line Weights

Dump system weights do not include the additional helium mass and storage bottles required for post-propellant dump operations. These weights are treated in Section 7.3. The total abort system weights combining dump system and post-dump system weights are discussed in Section 7.4.

7.2.2.1 Configuration 3 System Selection. Figure 7-11 gives the individual and combined system weight curves versus tank ΔP for LCH_4 and LO_2 dump systems. An optimum weight configuration was not found for either propellant. For LCH_4, total weight decreases linearly with ΔP increase over the pressurization range of interest. It is evident that a ΔP greater than 55 kpa (8 psid) will decrease abort propellant line weight more than the helium supply system weight will be increased. This condition occurs because little helium is required for LCH_4 tank pressurization.

For the LO_2 system, the combined weight decreases linearly with a tank ΔP decrease. Figure 7-11 indicates that system weight will reach a minimum at a tank ΔP less than 14 kpa (2 psid). This total weight slope is opposite from that for LCH_4 because a decrease in tank ΔP will reduce helium supply system weight more than it will increase abort propellant line weights.

The abort dump system selected for vehicle Configuration 3 combines the lowest LO_2 tank pressurization ΔP, 15 kpa (2 psid) with the highest LCH_4 tank pressurization ΔP, 55 kpa (8 psid). The resulting helium usages in combination with post-propellant dump purges, identified in Section 7.3, will be used to determine total helium system weight in Section 7.4.

7.2.2.2 Configuration 1 System Selection. Figures 7-12 and 7-13 give the individual and combined system weights versus tank ΔP for the Configuration 1 LH_2 and LO_2 dump systems. As with Configuration 3, an optimum weight system was not found for Configuration 1. Figure 7-12 gives the LO_2 system data of Figure 7-11. Thus, minimum weight for the LO_2 system will occur at a tank ΔP less than 14 kpa (2 psid). The LH_2 system data of Figure 7-13 exhibits the same trend as the LO_2 system data. Consequently, a minimum weight for this system will also occur at a pressurization ΔP less than 14 kpa (2 psid).

The selected abort dump system for Configuration 1 incorporates the lowest tank pressurization ΔP of 14 kpa (2 psid). The total weight curve of Figure 7-13 includes post-dump helium mass usages as a variable. In Section 7.4 a tabulation of abort system weights is given which includes the calculated helium purge masses.

7.3 POST-PROPELLANT DUMP HELIUM USAGES

Two vent and repressurization cycles will be performed at the completion of propellant dump. This procedure will dilute the propellant vapor concentration in the tank for vehicle "safing" prior to landing. The helium mass required for tank inerting will be stored within the system of manifolded ambient helium supply bottles. Since one purpose of Task II is to determine realistic helium supply system requirements for the RTLS abort, LTPS helium purges were included as part of the abort helium pressurization system requirements. These purges were based upon Shuttle/Centaur estimates for the MLI blanket purge and engine purges.

7.3.1 PROPELLANT TANK INERTING. Analyses were conducted to determine helium mass requirements for propellant tank inerting following the completion of propellant dump. The HYPRS and MULTBOT computer programs were run to evaluate the thermodynamics of this vent and repressurization process. These computer programs were run for the propellant dump pressurization ΔPs selected in Section 7.2. Each computer run was initiated at the beginning of propellant dump and continued through the two vent and repressurization cycles. The sequence of events selected for this RTLS abort mode is given in Table 7-3. This table shows that the first vent will be initiated at the end of propellant dump. It was assumed that tank venting would continue until tank pressure had decayed to 34.5 kpa (5 psia). Helium repressurization would then increase propellant tank pressure up to 103.4 kpa (15 psia). The second vent and repressurization phases were duplicates of the first vent and repressurization phases.

Helium usages for inerting vehicle Configurations 1 and 3 are given in Table 7-4. Slightly more helium is needed for the second repressurization than for the first because helium temperature will be lower during the second repressurization. Because helium will be injected directly into the propellant tank ullage space for all repressurizations, the lower temperatures mean increased helium mass requirements. Note that helium usages for the LH_2 tank are approximately twice that required for the LO_2 and LCH_4 propellant tanks.

7.3.2 HELIUM PURGE REQUIREMENTS. Helium purge requirements for LTPS are taken from Shuttle/Centaur estimates for the LH_2 tank MLI blanket and engine purges. The purges were based upon a 30-minute period, 15 minutes during RTLS and 15 minutes post-landing (GSE helium is available after 15 minutes). The LH_2 tank will require an MLI blanket purge to prevent liquefaction of air on the blanket external surface. Air liquefaction must be prevented in order to avoid potential damage to the cargo-bay liner and components. It was assumed that the LO_2 and LCH_4 tanks would not require MLI system purges because the Centaur LO_2 tank insulation system does not require a helium purge.

The Centaur engine system LH_2 side requires helium purges to minimize the hazard of GH_2 leakage. Although the LTPS engine system is not defined, it was assumed that similar concerns would exist; consequently, the same purge rates were selected for LTPS. LO_2 side engine purges will not be required because oxygen leakage will not constitute a safety hazard. LCH_4 side engine purges will likely be required to minimize the hazards of leakage. Such a determination was beyond the scope of this study. Furthermore, the purge quantity is expected to be less than for the LH_2 side. Thus, both the LO_2 and LCH_4 purges were considered to be zero for Configuration 3.

7.4 TOTAL ABORT DUMP SYSTEM WEIGHT

The total abort dump system weight includes propellant dump lines and a helium system that provides helium throughout the RTLS abort period, including MLI blanket and engine purges until landing plus 15 minutes. A total system weight was determined for vehicle Configurations 1 and 3 using the dump systems selected in Section 7.2, and post-propellant dump helium requirements given in Table 7-4. These abort dump system weights are given in Table 7-5. Note

Table 7-3. Tank Inerting Sequence of Events

Event	Duration (sec)	Initial Pressure kpa (psia)	Final Pressure* kpa (psia)
Propellant dump	250		
First vent	300	103.0 (15.0)	34.5 (5.0)
First repressurization	60	34.5 (5.0)	103.0 (15.0)
Second vent	300	103.0 (15.0)	34.5 (5.0)
Second repressurization	60	34.5 (5.0)	103.0 (15.0)

* Final pressure will be controlled via software to the pressurization or vent valves.

Table 7-4. RTLS Abort Helium Mass Usage Requirement

Requirement	LH_2/LO_2, Configuration 1	LCH_4/LO_2 Configuration 3
Propellant Dump, kg (lb)		
Fuel tank	13.8 (30.5)	2.4 (5.3)
Oxygen tank	1.8 (3.9)	1.8 (4.0)
1st Repress'n,(1) kg (lb)		
Fuel tank	3.3 (7.2)	1.4 (3.0)
Oxygen tank	1.9 (4.2)	1.8 (4.0)
2nd Repress'n,(1) kg (lb)		
Fuel tank	3.4 (7.5)	1.5 (3.2)
Oxygen tank	2.0 (4.4)	2.0 (4.4)
MLI Blanket Purge,(2) kg (lb)	3.1 (6.9)	NA
Engine Purge,(2) kg (lb)	1.0 (2.1)	NA
10% Margin, kg (lb)	3.0 (6.7)	1.1 (2.4)
TOTALS, kg (lb)	33.3 (73.4)	11.9 (26.3)

(1) Repressurization mass usages increase tank pressures from 5 psia to 15 psia.

(2) Purges are based upon Shuttle/Centaur estimates for a 30-minute purge (15 minutes prior to and after landing) of the LH_2 side only. Purges are not required for LO_2 and LCH_4.

Table 7-5. LTPS Abort Dump System Total Weights

Vehicle Configuration	Tank Press'n ΔP kpa (psid)	Total Helium Mass Usage kg (lb)	Helium Bottle Vol Regments $m^3(ft^3)$	Initial Helium Load kg (lb)	Mass of Bottles + Supports kg (lb)	Dump Line Weights kg (lb)	Total System Mass kg (lb)
1	LH_2(1) = 13 8(2 0) LO_2(1) = 13 8(2 0)	33 3(73 4)	0 87(30 9)	34 3(75 7)	245.9(542)	303 9(670)	584 1(1288)
3	LCH_4 = 55 2(8 0) LO_2(1) = 13 8(2 0)	11 9(26 3)	0 31(11 1)	12 3(27 1)	100 2(221)	270 3(596)	384 5(848)

(1) The lightest system weight may occur at a lower tank pressurization ΔP However, space limitations may preclude incorporating a larger line size.

that the total system mass for Configuration 1 is about 50 percent greater than for Configuration 3. This difference is due solely to the liquid hydrogen system that requires considerably more helium for tank pressurization and purges than does the LCH_4 tank.

It should be mentioned that Table 7-5 does not represent the minimum weight abort dump system for either vehicle configuration. The optimum point is represented by lower tank pressurization ΔPs for LO_2 and LH_2, and by a higher ΔP for LCH_4. It is probable, however, that space limitations within the Shuttle Orbiter will preclude incorporating the larger line sizes required to dump propellants at the lower tank ΔPs.

8

TECHNOLOGY EVALUATION

In this section technology requirements were evaluated for each propellant expulsion and thermal conditioning system identified in Sections 6 and 7. A discussion for the analysis, design, test and demonstration required to develop this technology is presented.

8.1 TECHNOLOGY REQUIREMENTS

The technology required for detailed design and development of selected propellant expulsion and thermal conditioning systems was identified. Two of the four selected thermal conditioning systems were state-of-the-art configurations and require no technology plan, although potential problem areas may exist. Hydrogen thermal subcoolers for the two remaining thermal conditioning systems represent new technology. Regarding propellant expulsion during Shuttle abort modes, new technology is not required. Rather, deficiencies may exist in the ability to accurately predict/model certain fluid flow phenomena. Specific technology deficiencies or unresolved problems are described below.

8.1.1 THERMAL CONDITIONING SYSTEMS. A total of five propellant thermal conditioning systems are contained within the four vehicle systems; bubbler pressurization for the LO_2 tank and four (two pressurization and two subcooler) systems for the liquid hydrogen tank.

8.1.1.1 System 1. Liquid oxygen tank helium bubbler pressurization was selected for engine start and engine burn for all thermal conditioning systems. Helium pressurization into the ullage for engine start and autogenous pressurization for engine burn was selected for the liquid hydrogen tank. There are not any apparent technology deficiencies with this helium pressurization system. Substantial empirical data (from flight and ground tests) has been gathered on virtually every phase of pressurization including storage bottle helium blowdown, ullage injection and liquid injection of helium at near zero-g and >1g conditions. Propellant tank pressure control techniques have been developed for the Centaur vehicle which requires sophisticated software capability and high accuracy pressure transducers that are continuously monitored during a mission. Potential problem areas associated with autogenous pressurization include pressure spikes and/or pressure decays following main engine cutoff and propellant stratification. Pressure spikes and pressure decays will be influenced primarily by the interaction of propellant with tank walls and with the ullage mass. However, at the low NPSP levels selected for System 1, pressure spikes and/or decays do not cause a problem.

Propellant stratification can adversely affect main engine NPSP if the stratified liquid layer is expelled during engine firing. Advancing this technology would include studying the influence of tank pressure, ullage temperature and propellant bulk temperature upon the growth of a stratified propellant layer. In-depth studies on propellant stratification have been conducted (References 8-1 through 8-3), with emphasis on conditions having no propellant outflow. Reasonable approximations of stratification are possible with existing analytical methods.

There is a relatively straightforward approach to eliminating any concern with propellant stratification. LH_2 tank pressure can be increased to a higher level shortly before final MECO. This pressure increase will subcool the stratified propellant layer. Furthermore, since only low engine NPSPs are being considered, the pressure rise will not be significant.

8.1.1.2 System 2. This thermal conditioning system is identical to System 1 with the exception of helium storage temperature. Helium will be stored in ambient bottles for System 1 and within the LO_2 tank for System 2. No technology deficiencies or potential problem areas have been identified for storing helium at cryogen temperatures.

8.1.1.3 Systems 3 and 4. LO_2 tank bubbler pressurization has no technology requirements. The LH_2 tank thermal conditioning systems are:

a. System 3: Engine start - Subcooler (coolant dump)
   Engine burn - Autogenous pressurization

b. System 4: Engine start/engine burn - Subcooler (return to ullage)

Both subcooler concepts are the same except that one dumps coolant overboard and the other uses a pump to return coolant to the ullage. This is considered to be a minimal technology difference. Since the subcooler concept is new, performance should be demonstrated through analytical and empirical efforts. The areas of interest relating to subcooler design and performance are:

a. Pressure regulator - Cold-side fluid pressure and temperature must be controlled during operation.

b. Heat exchanger - Heat transfer and fluid flow parameters must be established for subcooler sizing.

c. GH_2 pump - Pump requirements (where applicable) for returning cold-side fluid exhaust to the LH_2 tank ullage must be identified.

d. Engine start transient - Establish procedures through testing to determine NPSP histories of engine flow exiting the subcooler.

e. Engine inlet NPSP controls - Demonstrate through testing that engine NPSP requirements will be satisfied during engine burn.

Each item is discussed below.

Pressure regulator. Cold-side flow control pressure regulators have been employed on zero-g vent systems tested in LH_2 (Reference 8-4) and LO_2 (Reference 8-5). No new technology is required.

Heat Exchanger. During main engine operation LH_2 will be subcooled as it flows through the hot-side of the subcooler heat exchanger to the main engine. At the same time, liquid is throttled as it enters the heat exchanger cold-side and is evaporated as it flows through the system. Design of the heat exchanger hot-side should offer no particular problem because the heat exchange process involves pure liquid flow. For the heat exchanger cold-side, however, uncertainties exist because of the boiling process. Vapor blanketing could occur at the heat transfer surface since there are no phase-separating buoyancy forces to drive the vapor away. One can compensate for the absence of buoyancy in one of several ways. A very large heat exchange surface area can be selected to accept the low heat transfer resulting from vapor blanketing. One can also utilize very small flow passages so that heat exchanger blanketing resistance is kept small by the small passages. Both approaches require a large and/or heavy heat exchanger. The preferred alternative would be to utilize the momentum of the flowing fluids to provide phase distribution control that would deliberately distribute the fluid so that vapor blanketing of a surface is minimized. There is no certainty that the heat exchanger configuration shown in Figure 6-6 will provide adequate phase separation.

GH_2 pump. A pump is needed to return cold-side fluid exhaust to the ullage during operation. The addition of a pump offers a modest weight savings at design NPSP conditions over the option of coolant dump because propellant is returned to the tank. The return-to-ullage option is more complicated, however, because of the pump, its power requirements and the possible need for feedback controls to reduce cold-side flow rate as ullage pressure is increased by the returning vapor.

A review of Figure 6-10 shows that a weight advantage of about 11 kg (24 lb) exists for the return-to-ullage option over coolant dump, at engine NPSP levels less than 6.9 kpa (1.0 psid). Such a weight advantage may not offset the added complexity of a pump, etc. It is suggested, therefore, that emphasis be placed upon subcooler performance during the early stages of technology development. A pump can be added later in the development program. For now, the coolant dump option can be assessed.

Engine start transient. Subcooler tests can be conducted to determine NPSP conditions of engine flow LH_2 exiting the subcooler. These tests would identify the time lag between start of cold-side flow and start of engine (hot-side) flow to provide the required engine NPSP at a minimum propellant engine start loss.

Engine inlet NPSP controls. By employing the coolant dump option, this becomes a test to demonstrate that engine NPSP requirements are satisfied during main engine burn. Propellant tank pressures could decay by 10 to 20 percent during such a flow demonstration.

8.1.2 ABORT EXPULSION SYSTEMS. The greatest uncertainty in designing an abort expulsion system is an accurate determination of cryogen flow rate through the ducting. Ambient pressures will be less than 0.7 kpa (0.1 psia) during the expulsion period; consequently, sonic flow conditions will occur at the exit. It is also likely that the transition from pure liquid flow to two-phase flow will occur upstream of the abort dump line exit. An unknown is whether "shifting" equilibrium or "frozen" equilibrium conditions will exist during the two-phase flow process.

The impact of this two-phase flow uncertainty will be felt in design of the abort pressurization and dump systems. Propellant tank pressure levels or dump line diameters may be increased to compensate for this uncertainty. Either approach will increase abort expulsion system weights. For Shuttle/Centaur, this increase translates to two additional helium bottles for propellant dump, resulting in a weight increase of 41 kg (90 lb). This potential weight penalty is not a major driver for experimentation. Furthermore, it would be preferable to perform tests on a dump line configuration similar to the flight article. Such details for LTPS may be years from being developed. Consequently, a technology plan for two-phase flow experimentation is not recommended.

8.2 TECHNOLOGY PLAN

A technology plan for subcooler development should include two major areas: heat exchanger development and systems tests. A brief description of each is given in Sections 8.2.1 and 8.2.2. However, there may not be sufficient reason to pursue subcooler development, if thermal conditioning system weight reduction is the primary motive. The systems comparisons of Figure 6-10 indicates weight savings of less than 27 kg (60 lb) between state-of-the-art (System 2) and new technology (System 4).

8.2.1 HEAT EXCHANGER DEVELOPMENT. Although subcooler system analysis for this study has employed the subcooler configuration evaluated for high-g vehicle missions and adapted for the LTPS, the opinion now is that a different heat exchanger configuration should be selected. This change of attitude is prompted by the fact that the present configuration does not appear to provide the means for phase distribution control by fluid momentum. There is a heat exchanger, however, that has been tested as part of a zero-g thermodynamic vent system (TVS) that appears to be more suitable for subcooler application.

8.2.1.1 Heat Exchanger Concept. Prototype LH_2 and LO_2 TVS have been developed and tested by GDC, References 8-4 and 8-5. Flow tests have been recently conducted on the LO_2 TVS in support of Shuttle/Centaur TVS development. Heat transfer and pressure loss coefficients were obtained from a series of parametric tests (performed with Freon) designed to provide generalized design data. The heat exchangers of each thermodynamic vent system were designed for a zero-g environment. It is this heat exchanger that is recommended for the LH_2 subcooler. The TVS heat exchangers depend upon curvilinear flow, with the consequent radial force field, to accomplish phase separation in zero gravity. The hot-side fluid passes through a helical duct wrapped onto the outside of the cold-side coil. A schematic diagram of this process is shown in Figure 8-1.

In a straight, forced convection, single tube boiler a wetting fluid enters the tube as a single phase liquid or low quality two-phase mixture and increases in quality along the tube as heat is added. In the present case, the flow within the tube vaporizes completely and some vapor superheating occurs as well.

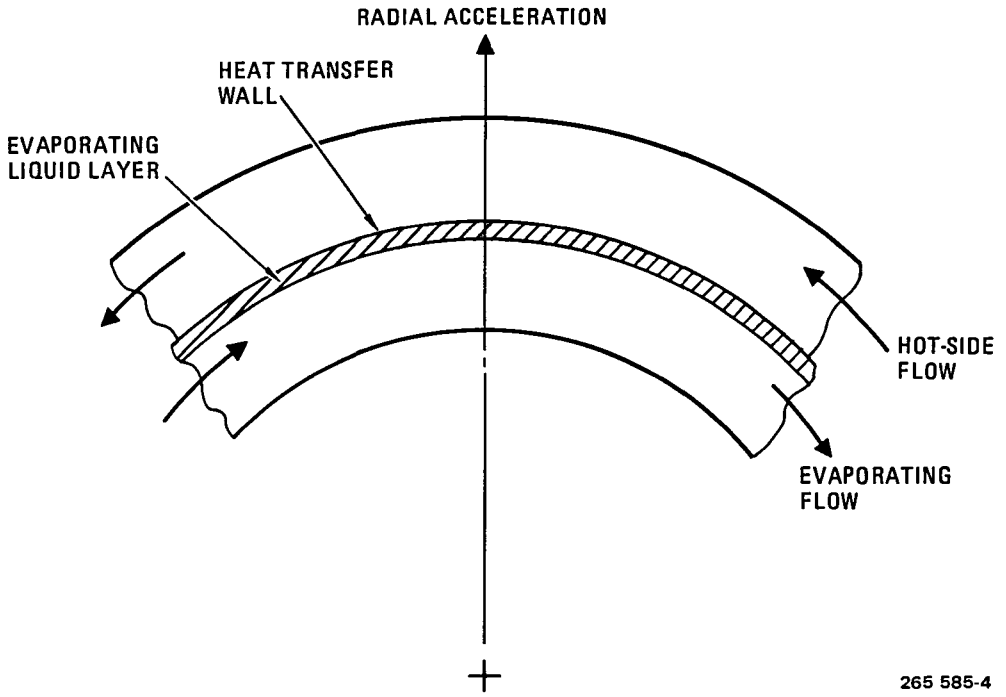

Figure 8-1. Phase Distribution of the Evaporating Process is Affected by Curved Channels

A liquid flow into a straight boiler tube progresses from an all-liquid flow to a low quality bubbly mixture, then to an annular flow with a liquid layer on the wall and vapor in the center. The vapor usually carries some droplets of entrained liquid. At some relatively high quality the annular flow usually ends and the flow consists of a vapor stream with the remaining liquid entrained. In various applications, the quality at which the annular film ends may be as low as 40 percent for a poorly designed system.

Heat transfer to entrained droplets in a vapor flow is very poor. The vapor must superheat above the saturation temperature in order to transfer heat to the droplets, so that the high quality region in a straight once-through boiler is usually long. However, in the curved channels of this heat exchanger, the radial accelerations caused by the coiled tube centrifuge entrained droplets onto the wall so that the vapor remains substantially dry.

It would appear that at all vapor qualities the liquid in the coiled tube would accumulate on the tube wall at the outside of the turn adjacent to the hot-side flow, as shown in Figure 8-2a so that the other three walls would be dry. However, secondary flows in the small diameter tube (compared to the coil radius) distribute some liquid onto the three walls in the lower quality region of the tube, as shown in Figure 8-2b so that all of the surface is effective.

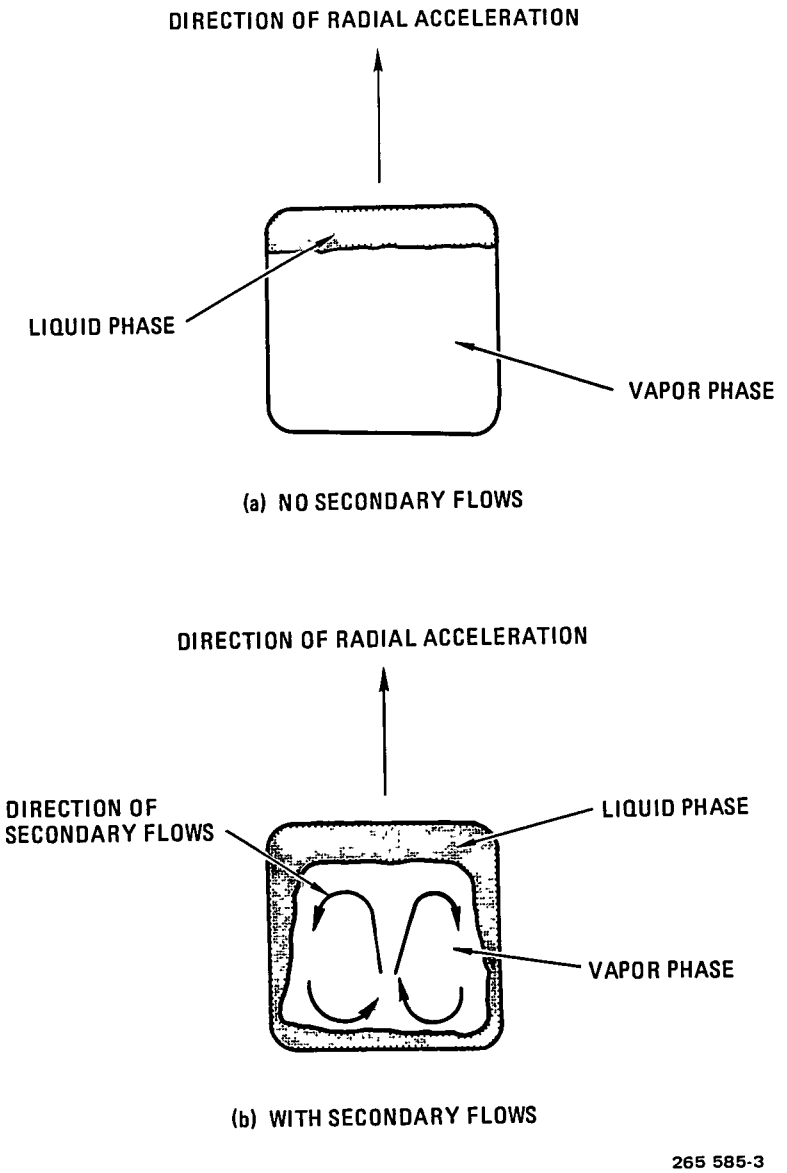

Figure 8-2. Phase Distributions in a Two-Phase Flow in a Curved Channel

The curvilinear flow path does not merely redistribute the liquid and vapor in these heat exchangers. The secondary flows in curved tubes enhance single phase heat transfers, as well as providing phase distribution control. The heat transfer coefficient for an all-liquid flow in the outside passage is more than doubled by secondary flows.

There is substantial test data available (using refrigerants) to demonstrate heat exchanger performance in one-g. It is not possible to provide heat transfer scaling functions for two-phase flows in arbitrary geometries. Therefore, it may not be possible to exactly relate data obtained with a Freon to

performance with hydrogen. The properties of the Freons and hydrogen are quite dissimilar. If vapor velocities or Reynolds numbers are modeled, liquid to vapor density ratios, viscosity ratios, thermal heat capacity rates or some other parameters will be dissimilar. Therefore, despite proof of functioning with refrigerants, ground-based tests with hydrogen would be required to demonstrate heat exchanger performance. Certainly many ground-based tests will be required to qualify a subcooler system.

8.2.1.2 Zero-G Testing. There is the possibility that zero-g testing of this heat exchanger configuration may not be required. Hydrogen heat transfer coefficients have been estimated from Freon tests which indicate cold-side boiling heat transfer coefficients to be an order of magnitude greater than hot-side liquid phase coefficients. It is clear that heat exchanger surface area will be controlled by the hot-side overall conductance so that precise evaluation of the cold-side overall conductance is not required. Consequently, judicious design of the heat exchanger curved channels could eliminate the need for zero-g testing.

8.2.2 SYSTEMS TESTS. Systems tests as a minimum should investigate engine start transients and engine inlet NPSP controls. Tests of this nature are normally not performed until substantial design data is available on the engine feed system and main engine.

8.2.2.1 Engine Start Transient. To establish an engine start sequence of events, it will be necessary to integrate feedline and main engine chilldown requirements with knowledge of the main engine NPSP requirements during the start transient. It is possible that feedline and engine chilldown requirements may be such that the subcooler will be operating at steady-state by main engine start. Otherwise, subcooler flow initiation must be planned to assure steady-state operation by main engine start. Transient tests would have to be performed during actual LTPS engine hot firings.

8.2.2.2 Engine Inlet NPSP Controls. With the coolant dump option, engine NPSP is satisfied by cooling propellant flowing to the engine system. The amount of propellant dumped overboard during engine start will be quite small, so it would be possible to over-size the heat exchanger with little impact on payload capability. For the coolant return-to-ullage option, however, the subcooler must be capable of cold-side flow control. This flow control is needed because main engine propellant NPSP will be a combination of propellant subcooling and tank pressurization (provided by coolant flow to the ullage). At main engine start, coolant flow demand will be a maximum. However, as ullage pressure is increased, due to coolant return to the ullage, coolant flow demand will diminish. A means must be developed for selecting coolant flow rates by continuously monitoring ullage pressures and liquid temperatures so that engine NPSP will be satisfied.

9

SUMMARY OF RESULTS

This study determined preferred techniques for providing abort pressurization and engine feed system net positive suction pressure (NPSP) for low-thrust chemical orbit-to-orbit propulsion systems (LTPS). The relative benefits and weight penalties of each technique and any required technology advances were determined. There were two major study areas: propellant expulsion systems for achieving propellant dump during a return-to-launch-site (RTLS) abort, and thermal conditioning systems for satisfying engine NPSP requirements.

The thermal conditioning techniques considered for providing main engine NPSP during engine start and steady-state operation included:

a. Helium pressurization (ambient and cryogenic temperature).

b. Thermal subcoolers (heat exchangers).

c. Autogenous pressurization for steady-state engine burn with helium pressurization for start-up.

d. Autogenous pressurization for steady-state engine burn with thermal subcoolers for start-up.

Parametric analyses were performed on each thermal conditioning system to obtain pressurant mass, hardware weights, ventage, vapor residuals and other weight penalties associated with each system, as a function of engine NPSP. Total system weight penalties were obtained for two LH_2/LO_2 stages with multi-layer insulation (MLI) and two LCH_4/LO_2 stages, one with MLI and the other with spray-on foam insulation (SOFI).

Major results include the following:

1. A state-of-the-art system, incorporating bubbler (helium injection beneath liquid surface) pressurization for the LO_2 and LCH_4 tanks, showed the lowest system weight penalty over the entire engine NPSP range of 3.4 to 87.1 kpa (0.5 to 12.0 psid).

2. A new technology system incorporating a subcooler for engine NPSP resulted in the lowest weight penalty for the liquid hydrogen tank.

3. For thermal subcoolers, coolant fluid may be dumped overboard, returned to the liquid propellant or returned to the ullage. The latter option resulted in a significantly lower weight penalty.

4. Vent mass penalties due to the higher heating rates of a SOFI system were significantly greater than for the MLI system, up to 1090 kg (2400 lb) greater for the LTPS missions.

Following the parametric analysis, four LH_2/LO_2 systems, listed below, were selected for a preliminary design effort. These systems were designed for engine NPSP levels of 3.4 and 6.9 kpa (0.5 and 1.0 psid), LH_2 and 6.9 and 13.8 kpa (1.0 and 2.0 psid), LO_2. Weight penalties were determined for these design points and for a zero NPSP engine requirement. As expected, System 4 showed the lowest weight penalty. The weight benefit over the state-of-the-art systems was determined to be 18 to 32 kg (40 to 70 lb).

Selected Thermal Conditioning Systems Selected for Preliminary Design

System	LO_2 Tank Engine Start/Engine Burn	LH_2 Tank Engine Start/Engine Burn
1	Bubbler/Bubbler	Helium/Autogenous
2	Same as 1, except for cryogenic storage of helium	
3	Bubbler/Bubbler	Subcooler (coolant dump)/ Autogenous
4	Bubbler/Bubbler	Subcooler/Subcooler (coolant return to ullage)

Propellant dump during Shuttle/LTPS abort modes was studied for purposes of identifying an LTPS propellant expulsion system, which consists of a helium pressurization system and an abort propellant dump system. Helium pressurization for propellant expulsion was the only technique considered for this analysis, due to the requirement to inert the tanks following propellant dump. Pressurant mass requirements were determined for tank pressure increases of 14, 28 and 55 kpa (2, 4 and 8 psid) during propellant expulsion and for two repressurization cycles following each of two vent cycles performed during tank inerting.

Ground rules established or identified from previous GDC Shuttle/Centaur studies were employed during this task. Some of the pertinent ground rules are:

1. Due to its severe time constraint, an RTLS abort mode was selected because it established the worst case conditions for propellant dump and the maximum helium requirements.

2. The defined minimum dump time of 250 seconds for simultaneous dump of propellants was selected.

3. The propellant expulsion system was scaled from established Shuttle/Centaur configurations.

4. Helium was stored in ambient bottles identified for Shuttle/Centaur.

It was expected that a weight optimized system could be identified because of the interrelationship between pressurization system weights and propellant dump system weights. That is, a smaller dump line will decrease dump system weights but it will also increase tank pressurization ΔP levels and pressurization system weights. Analysis results show that the LH_2/LO_2 system is optimized for minimum pressurization ΔP levels, which means increasing dump system line sizes to the maximum diameter possible. For the LCH_4/LO_2 system, the LO_2 side optimized at the minimum tank ΔP while the LCH_4 side optimized at the maximum tank ΔP. Total weights were determined to be 385 kg (848 lb) for the LCH_4/LO_2 system and 584 kg (1288 lb) for the LH_2/LO_2 system.

An assessment was made of propellant expulsion system and thermal conditioning system technology requirements. For design of a propellant expulsion system, the unknown is in an accurate determination of two-phase flow rates through ducting. The unknown is whether "shifting" equilibrium or "frozen" equilibrium conditions will exist as propellant is dumped to ambient pressures less than 0.7 kpa (0.1 psia). No further technology hardware studies were identified as necessary to proceed with LTPS design.

10

CONCLUSIONS AND RECOMMENDATIONS

This study determined preferred techniques for providing abort pressurization and engine feed system net positive suction pressure (NPSP) for low-thrust chemical orbit-to-orbit propulsion systems (LTPS). The relative benefits and weight penalties of each technique and any required technology advances were determined. There were two major study areas: propellant expulsion systems for achieving propellant dump during a return-to-launch-site (RTLS) abort, and thermal conditioning systems for satisfying engine NPSP requirements.

Thermal conditioning techniques considered for providing main engine NPSP during engine start and steady-state operation include a) helium pressurization, b) thermal subcoolers (heat exchangers), and c) autogenous pressurization for steady-state engine burn with helium pressurization or thermal subcoolers for start-up. Parametric analyses were performed to obtain pressurant mass, hardware weights, ventage, and vapor residuals as a function of engine NPSP. Total system weight penalties were obtained for two LH_2/LO_2 stages with multi-layer insulation (MLI) and two LCH_4/LO_2 stages, one with MLI and the other with spray-on foam insulation (SOFI).

Major conclusions include the following:

1. A state-of-the-art system, incorporating bubbler (helium injection beneath liquid surface) pressurization, was found to be the best for LO_2 and LCH_4, regardless of technology. It showed the lowest system weight penalty over the entire engine NPSP range.

2. A new technology system incorporating a subcooler for engine NPSP resulted in the lowest weight penalty for the liquid hydrogen tank. An appreciable weight benefit over state-of-the-art systems was predicted for the high NPSP levels; modest benefits were shown for the low NPSP levels.

3. Vent mass penalties due to the higher heating rates of a SOFI system were significantly greater than for the MLI system. Although there are considerations, such as groundhold, that have not been evaluated, it seems unlikely that the benefits of SOFI could compensate for the vent mass penalty.

Following the parametric analysis, four LH_2/LO_2 systems were selected for a preliminary design effort, two state-of-the-art and two new technology systems. Weight penalties were determined for NPSP levels up to 6.9 kpa (1.0 psid) and 13.8 kpa (2.0 psid), respectively, for the LH_2 and LO_2 sides. An unexpectedly small weight penalty difference of 18 to 32 kg (40 to 70 lb) was found between state-of-the-art and new technology systems.

The only new technology identified for thermal conditioning systems was the heat exchanger portion of the LH_2 thermal subcooler. The key to designing a heat exchanger for this application is in developing a fluid force field to accomplish phase separation in zero gravity to assure that high boiling heat transfer coefficients will be present. There is the possibility that zero gravity testing of this heat exchanger configuration may not be required. Hydrogen cold-side heat transfer coefficients have been estimated to be an order of magnitude greater than hot-side liquid phase coefficients. It is clear that heat exchanger surface area will be controlled by the hot-side overall conductance so that precise evaluation of the cold-side overall conductance is not required. Consequently, judicious design of heat exchanger curved channels could eliminate the need for zero-g testing.

The subject of thermal subcooler systems tests was also addressed. This type of test was not recommended because it was felt that considerable detail was needed on LTPS propellant feed systems, engine system chilldown requirements and start transients before meaningful tests could be defined.

The only candidate for a technology plan is a heat exchanger for zero-g application. It was recommended that LH_2 thermal subcooler development not be pursued because the potential weight gain at low engine NPSPs is not significant. This recommendation is based upon the premise that a low NPSP engine system is an achievable goal.

Propellant dump during Shuttle/LTPS abort modes was studied for purposes of identifying an LTPS propellant expulsion system, which consists of a helium pressurization system and an abort propellant dump system. Helium pressurization for propellant expulsion was the only technique considered for this analysis; no hardware technology areas were identified. An assessment of the propellant expulsion system revealed that the primary uncertainty is whether "shifting" equilibrium or "frozen" equilibrium conditions will exist as propellant is dumped to a near-vacuum condition. An experimental program was not recommended because this uncertainty should not have a major impact upon LTPS performance.

11

SYMBOLS

A	pipe cross-sectional area
dA	change in A over interval considered
A_{SC}	total cold-side heat transfer surface area
C_D	pressure loss coefficient
C_V	constant volume heat capacity
C_P	constant pressure heat capacity
D	pipe diameter
d	hydraulic diameter
ΔE_U	ullage mass internal energy change
f	pipe friction factor
g	magnitude of gravity vector
g_c	gravitational constant
G_c	mass flux at critical conditions
h	heat transfer coefficient
h_{sV}	saturated vapor enthalpy
$h_{s\ell}$	saturated liquid enthalpy
Δh	change in enthalpy
h_{2c}	cold-side fluid enthalpy at subcooler entrance
h_{3c}	cold-side fluid enthalpy at subcooler exit
h_4	enthalpy of coolant returned to the tank
dH	change in position relative to longitudinal axis
J	mechanical/thermal energy conversion

k	thermal conductivity
L	flow distance downstream from entrance
L_f	fin length, root-to-tip
losses	pressure drop within the subcooler
ΔM_{EV}	mass of liquid evaporated into helium bubble
ΔM	mass quantity
$\dot{m}$	liquid flowrate to engine
$\dot{m}_c$	cold-side flowrate
NPSP	required engine inlet net positive suction pressure
P	pressure
P_{Ci}	cold-side inlet pressure
Pr	Prandtl number
dP	change in pressure over interval considered
ΔP	pressurization ΔP
ΔP_{vp}	change in engine flow saturation pressure across the subcooler
$\dot{Q}$	heat transfer rate
$\dot{Q}_r$	required heat removal rate
ΔQ	heat input to ullage
R	gas constant
Re	Reynolds number
dS	change in entropy over interval considered
T	temperature
T_h	average of hot-side inlet and outlet temperatures
T_w	temperature of heat exchanger wall separating hot and cold sides
T_c	temperature of cold-side boiling propellant
ΔT_{wc}	temperature difference between wall and cold-side fluid
V	volume

v	flow velocity
w	fin width
$\dot{w}$	propellant dump flowrate
$\dot{W}_p$	pump power absorbed by coolant
dX	change in mass quality over interval considered
Z	gas compressibility factor
η	ratio of actual heat transferred to heat transferred if entire fin were at root temperature
η_p	pump compression efficiency
ρ	density
$d\rho$	change in density over interval considered
μ	viscosity
σ	surface tension

Subscripts:

B	bubble
HE	helium
L	liquid
ℓC	cold-side liquid properties
U	ullage
V	vapor

12

REFERENCES

1-1. Ketchum, W. J. et al, "Low-Thrust Vehicle Concept Study," GDC-ASP-80-010, September 1980.

1-2. Dergance, R. H. et al, "Low-Thrust Chemical Orbit to Orbit Propulsion System Propellant Management Study," MCR-81-503, June 1981.

1-3. "Centaur-In-Shuttle Integration Study Final Report," Report No. 670-0-80-83, March 1980.

3-1. Blatt, M. H. and J. C. Aydelott, Centaur Propellant Acquisition System, Journal of Spacecraft and Rockets, Vol. 13, No. 9, September 1976.

3-2. Blatt, M. H. and J. C. Aydelott, Centaur Propellant Thermal Conditioning System, AIAA/SAE Thirteenth Propulsion Conference, Orlando, Florida, Paper 77-451, 11 July 1977.

3-3. Kutateladze, S. S., Heat Transfer in Condensation and Boiling, Second Edition, State Scientific and Technical Publications of Literature on Machinery, Moscow, 1952.

7-1. "Centaur-In-Shuttle Integration Study Final Report," Report No. 670-0-80-83, March 1980.

7-2. Smith, R. V., "Critical Two-Phase Flow for Cryogenic Fluids," NBS TN633, January 1973.

7-3. Henry, R. E. and Fauske, H. K., "The Two-Phase Critical Flow of One-Component Mixtures in Nozzles, Orifices and Short Tubes," J. Heat Trans, May 1971.

8-1. Vliet, G., "Stratified Layer Flow Model/A Numerical Approach to Stratification in Liquids Contained in Heated Vessels, Aerophysics Research Report TR 8-30-63-4, November 1963.

8-2. Barakat, H. Z., et al, "Finite Difference Solution of Stratification and Pressure Rise in Containers," Proc. JSME 1967 Semi-International Symposium, September 1967.

8-3. Levy, A. M., et al, "Analytical and Experimental Study of Stratification and Liquid-Ullage Coupling," LMSC 2-05-65-1, August 1965.

8-4. Stark, J. A. and M. H. Blatt, "Cryogenic Zero-Gravity Prototype Vent System," GDC-DDB67-006, October 1967.

8-5. Erickson, R. C., "Space LOX Vent System," CASD-NAS75-021, April 1975.

APPENDIX A

HYPRS COMPUTER PROGRAM

1.1 Description

The HYPRS computer program was originally written to determine thermodynamic conditions within the Centaur hydrogen tank during a mission. The program calculates vapor state, liquid state, helium bottle conditions and tank wall temperatures during engine burn and coast periods. HYPRS has been modified to model any tank configuration and now includes oxygen and methane properties. These changes allowed HYPRS to be used to model all the different OTV vehicle configurations and propellants in this study.

The program is complex and offers many options, both in the type of data entered and the various phenomena which can be modeled. A flow chart of the HYPRS computer program is shown in Figure A-1. Each routine is described below.

1.2 Program HYPRS

HYPRS initializes the derivatives of integration variables, sets up tank segment areas and reads input. Input is accomplished using the NAMELIST convention which is explained in Section 2.

1.3 Subroutine BLEEDS

BLEEDS determines autogenous pressurant gas flow rates from the engines, needed to maintain propellant tank pressure within a prescribed level during engine burn.

1.4 Subroutine BOTLPR

BOTLPR determines the derivatives of helium bottle storage conditions, helium mass flow rates and helium temperature leaving the storage bottle.

1.5 Subroutine BUBBLER

BUBBLER determines the amount of propellant boil-off caused by the bubbler pressurization system. It can calculate the amount of boil-off with either empirical or theoretical equations.

1.6 Subroutine DERIV

DERIV determines the state of the tank fluids during the process specified in the input.

1.7 Subroutine FCONV

FCONV contains equations for calculating free convective heat transfer coefficients at the tank walls.

1.8 Subroutine HEET

HEET determines the heat transferred to the tank from external sources. An energy balance is performed on the tank and fluids to determine tank wall temperature change and net heat input to the ullage and liquid.

1.9 Subroutine HETEMP

HETEMP determines helium temperature change which occurs as it flows from the helium storage bottle to the tank for each pressurization sequence.

1.10 Subroutine INTGRT

INTGRT performs the integration of the state variables using a system of first order differential equations at each time increment.

1.11 Subroutine METHAN

METHAN replaces the hydrogen properties preset in the tables with methane properties.

1.12 Subroutine MIX

MIX forces propellant gas and liquid phases to thermal equilibrium while pressurizing or venting the tank to a desired pressure level.

1.13 Subroutine OXYGEN

OXYGEN replaces the hydrogen properties preset in the tables with oxygen properties.

1.14 Subroutine PLOT

PLOT creates a data file to be used later in a plotting program.

1.15 Subroutine PRINT

PRINT prints out calculated variables and derivatives defining the state of the tank.

1.16 Subroutine STEP

STEP performs one step of integration by the MERSONS modified Runge-Kutta method.

1.17 Subroutine THRMEQ

THRMEQ is an alternate entry into subroutine MIX. It provides the iteration to determine temperature, masses and internal energies at thermal equilibrium.

1.18 Subroutine TPRESS

TPRESS calculates the amount of autogenous pressurant gas required to maintain the desired tank pressure.

1.19 Subroutine VENT

VENT determines the amount of gas to vent overboard if venting is required.

2.1 Namelist Input

Input to this program utilizes the NAMELIST feature of the CYBER 70 Fortran system. Details of the NAMELIST provision can be found in any Fortran manual. A discussion of each namelist input used is given below. A sample computer input file follows the tables containing the input variables.

2.2 Input Arrangement

A mission simulation is accomplished by supplying the necessary input to the following namelist groups: TANK, TNKDIM, GASPRP, CASE, HELIUM, and PHASE. Namelists TANK, CASE, and PHASE input are required for all cases. Whereas HELIUM is used only to provide helium bottle data for a formal bottle blowdown analysis, TNKDIM is input when tank geometry and heat transfer tables are to be input and GASPRP is input when tank gas properties definition is required.

2.2.1 NAMELIST TANK - The first input group of variables namelist TANK includes data which defines the tank wall, its properties and segmentation, heat rate vs time tables and specific heat vs temperature tables. The variables which may be input are defined in Table A-1.

2.2.2 NAMELIST TNKDIM - If TNKDIM=1, as set in namelist TANK, namelist TNKDIM variable values are read into the program. The variables contained in TNKDIM are defined in Table A-2.

2.2.3 NAMELIST GASPRP - If GASPRP=1, as set in namelist TANK, namelist GASPRP variable values are read into the program. The variables contained in GASPRP are defined in Table A-3.

2.2.4 NAMELIST CASE - Data input through namelist CASE define the initial thermodynamic state of the liquid, ullage, and tank walls. Input variables for CASE are defined in Table A-4.

2.2.5 NAMELIST HELIUM - If the flag IREG is set equal to 3 in namelist CASE, namelist HELIUM parameter values are read into the program for a formal helium bottle blowdown analysis. Input for namelist HELIUM are defined in Table A-5.

2.2.6 NAMELIST PHASE - Variables input through namelist PHASE define the particular phase of the mission to be analyzed (e.g., pressurizing prior to engine start, maintaining tank pressure during a burn, venting to a desired level, etc). Input variables for namelist PHASE are defined in Table A-6.

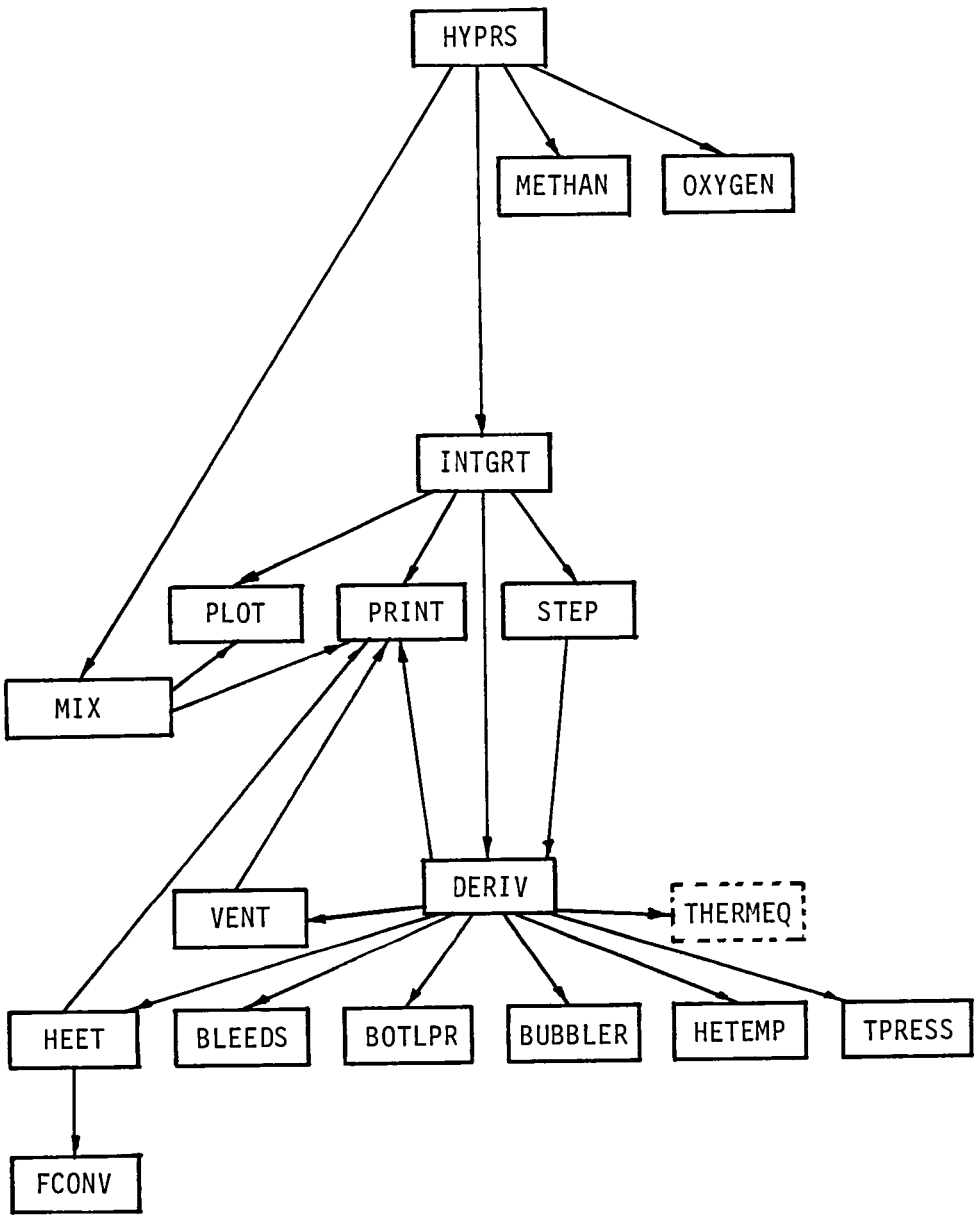

Figure A-1. Flow Chart of Subroutines used by HYPRS.

Table A-1. Namelist TANK Input

Variable Name (Max. Dim.)	Description and Units	Other Sources	Preset Value	Primary Use Subroutine
CW(30)	Tank wall specific heat for each segment, B/lb/R.			HEET
EMISS(30)	Tank wall emissivity for each segment.			HEET
FAW(30)	Wall area factor for each segment for scaling heat flux.	$CASE $PHASE		HEET HYPRS
ICW(30)	Heat input flag for each segment. = -1, Heating values are applied directly to the liquid or ullage. Tank wall energy balance is not calculated. = 0, A constant value of specific heat is used for the energy balance. = 1, The specific heat value from TANK or TNKDIM input, or BLOCKDATA H2TANK is used for energy balance computation for the specified segment. = 6, A specified segment is an insulated common bulkhead which requires the input value of CBLKHD be set to zero. = 7, A specified segment has a radiation shield to which the heat flux is applied.	$TNKDIM		HEET HYPRS
IFLUX(30)	Flag to indicate units of QW. = 0, Heat rate, B/hr = 1, Heat flux, B/hr-ft^2	$TNKDIM		HYPRS
IGSPRP	If greater than zero input $GASPRP.			HYPRS
IQW(30)	Denotes heat flux table to be used for each segment.	$TNKDIM		HYPRS
ITNK	If greater than zero input $TNKDIM.			HYPRS
MW(30)	Wall mass for each segment, lb.	$TNKDIM $PHASE		HEET HYPRS

Table A-1. Namelist TANK Input (Cont'd)

Variable Name (Max. Dim.)	Description and Units	Other Sources	Preset Value	Primary Use Subroutine
NCW	Number of pairs in wall specific heat table.	$TNKDIM	16	HEET
NCWTBS	Number of wall specific heat tables.			HYPRS
NQ	Number of pairs in heating table.			HYPRS
NQSEGS	Number of segments to be input for tank heating.			HYPRS
NQTB	Heating table number (must be .LE. 6)			HYPRS
NQW(5)	Number of pairs in heating table.		24	HYPRS
NQWTBS	Number of heat rate vs. time tables.			HYPRS
QW(30)	Heating rate to tank segment, B/hr.	$TNKDIM		HEET
		$PHASE		HYPRS
RHOW(30)	Wall mass/area at each segment 3 lb/ft^2			HEET
SBOT	Station for tank bottom, in.	$CASE	408.75	HEET
SBOTS(30)	Station for bottom of each heating segment, in.	$TNKDIM		HEET
				HYPRS
STOP	Station defining tank top, in.	$CASE	162.04	HEET
STOPS(30)	Station for top of each heating segment in.	$TNKDIM		HEET
				HYPRS
TBCW(30)	Wall specific heat table, B/lb/R.	$TNKDIM	H2TANK	HEET
TBTCW(30)	Temperature table for wall specific heat table, R	$TNKDIM	H2TANK	HEET
TW(30)	Wall temperature of each segment, R.	$TNKDIM		HYPRS
		$CASE		
VTOT	Total tank volume, ft^3	$CASE		DERIV
		$PHASE	1270.8638	HYPRS
CW(30)	Tank wall specific heat for each segment, B/lb/R.			HEET
EMISS(30)	Tank wall emissivity for each segment.			HEET
FAW(30)	Wall area factor for each segment for scaling heat flux.	$CASE		HEET
		$PHASE		HYPRS

Table A-1. Namelist TANK Input (Cont'd)

Variable Name (Max.Dim.)	Description and Units	Other Sources	Preset Value	Primary Use Subroutine
ICW(30)	Heat input flag for each segment.	$TNKDIM		HEET HYPRS
IFLUX(30)	Heat flux or rate indicator.	$TNKDIM		HYPRS
IGSPRP	If greater than zero input $GASPRP.			HYPRS
IQW(30)	Denotes heat flux table to be used for each segment.	$TNKDIM		HYPRS
ITNK	If greater than zero input $TNKDIM.			HYPRS
MW(30)	Wall mass for each segment, lb.	$TNKDIM $PHASE		HEET HYPRS
NCW	Number of pairs in wall specific heat table.	$TNKDIM	H2TANK	HEET
NCWTBS	Number of wall specific heat tables.			HYPRS
NQ	Number of pairs in heating table.			HYPRS
NQSEGS	Number of segments to be input for tank heating.			HYPRS
NQTB	Heating table number (must be .LE. 6)			HYPRS
NQW(5)	Number of pairs in heating table.		H2TANK	HYPRS
NQWTBS	Number of heat rate vs. time tables.			HYPRS
QW(30)	Heating rate to tank segment, B/hr.	$TNKDIM $PHASE		HEET HYPRS
RHOW(30)	Wall density at each segment, lb/ft^3			HEET
SBOT	Station for tank bottom, in.	$CASE	H2TANK	HEET
SBOTS(30)	Station for bottom of each heating segment, in.	$TNKDIM		HEET HYPRS
STOP	Station defining tank top, in.	$CASE	H2TANK	HEET
STOPS(30)	Station for top of each heating segment, in.	$TNKDIM		HEET HYPRS
TBCW(30)	Wall specific heat table, B/lb/R.	$TNKDIM	H2TANK	HEET
TBTCW(30)	Temperature table for wall specific heat table, R.	$TNKDIM	H2TANK	HEET

Table A-1. Namelist TANK Input (Concluded)

Variable Name (Max.Dim.)	Description and Units	Other Sources	Preset Value	Primary Use Subroutine
TW(30)	Wall temperature of each segment, R.	$TNKDIM $CASE		HYPRS
VTOT	Total tank volume, ft^3	$CASE $PHASE	H2TANK	DERIV HYPRS

Table A-2. Namelist TNKDIM Input

Variable Name (Max.Dim.)	Description and Units	Other Sources	Preset Value	Primary Use Subroutine
AWTBK	Wall area from base of tank to top of bulkhead.			HEET
BTOP	Total bulkhead area, in^2.			HEET
EMISS(N)	Emissivity of tank wall section N.	$PHASE $TANK	5*10.E-10	DERIV
FAW(N)	Section N wall area factor for scaling programmed heat flux.	$PHASE $TANK		DERIV
IAW(N)	Index defining wall area table used for corresponding wall segment.	$TANK		HYPRS
ICW(N)	Heat input flag for section N.	$TANK		HYPRS DERIV
IFLUX(N)	Flag to indicate heat flux or rates.	$TANK		
IQW(N)	For I O heat flux Table 1 will be used for section N.	$TANK		DERIV
LBBK	Bulkhead characteristic length, in.		H2TANK	HEET
MW(N)	Segment N wall mass, lb.	$TANK		DERIV
NAW(N)	Number of entries in tank surface area Table N.	BLKDATA	H2TANK 88, 61	DERIV
NBKA	Number of entries in bulkhead area table.		H2TANK	HEET
NC	NCW = number of entries in wall specific heat table.			NVPRS
NCW(N)	Number of entries in wall specific heat Table N.	$TANK BLKDATA	H2TANK	DERIV
NQ	Number of pairs in heating table.	$TANK		DERIV
NQTB	Heating table number (must be .LT. 6)	$TANK		DERIV
NQW	NQ	$TANK	H2TANK	DERIV
NS	Number of entries in spray flow table.	$CASE	H2TANK	DERIV
NVOL	Number of entries in tank volume table.	BLKDATA	H2TANK 88	DERIV
QW(N)	Heat ratio or flux to segment (N), B/hr or B/hr ft^2	$TANK $PHASE		DERIV

Table A-2. Namelist TNKDIM Input (Cont'd)

Variable Name (Max.Dim.)	Description and Units	Other Sources	Preset Value	Primary Use Subroutine
RADTB	Tank radius table, in.	HEET	TABLE	HEET
SBOTS(N)	Station for bottom of heating segment, in.	$TANK		DERIV
AWTBK	Wall area from base of tank to bottom of bulkhead.			HEET
BTOP	Total bulkhead area, in^2.		138.373	HEET
EMISS(30)	Emmissivity of tank wall section.	$PHASE $TANK	5*10.E-10	DERIV
FAW(30)	Section wall area factor for scaling programmed heat flux.	$PHASE $TANK		DERIV
IAW(30)	Index defining wall area table used for corresponding wall segment.	$TANK		HYPRS
ICW(30)	Heat input flag for each section. = -1, Heating values are applied directly to the liquid or ullage. Tank wall energy balance is not calculated. = 0, A constant value of specific heat is used for the energy balance. = 1, The specific heat value from TANK or TNKDIM input or BLOCKDATA H2TANK is used for energy balance computation for the specified segment. = 6, A specified segment is an insulated common bulkhead which requires the input value of CBLKHD be set to zero. = 7, A specified segment has a radiation shield to which the heat flux is applied.	$TANK		HYPRS
IFLUX(30)	Flag to indicate units of QW = 0, Heat rate, B/hr = 1, Heat flux, B/hr-ft^2			

Table A-2. Namelist TNKDIM Input (Cont'd)

Variable Name (Max.Dim.)	Description and Units	Other Sources	Preset Value	Primary Use Subroutine
IQW(30)	For I > 0 heat flux will be input for each section.	$TANK		DERIV
LBBK	Bulkhead characteristic length, in.		14.028	HEET
MW(30)	Segment wall mass, lb.	$TANK		DERIV
NAW	Number of entries in tank surface area.	BLKDATA	61	DERIV
NBKA	Number of entries in bulkhead area table.		47	HEET
NC	NCW number of entries in wall specific heat table.			NVPRS
NCW	Number of entries in wall specific heat.	$TANK BLKDATA	16	DERIV
NQ	Number of pairs in heating table.	$TANK		DERIV
NQTB	Heating table number (must be .LT.6)	$TANK		DERIV
NQW	NQ	$TANK	24	DERIV
NS	Number of entries in spray flow table.	$CASE	13	DERIV
NVOD	Number of entries in tank volume table.	BLKDATA	104	DERIV
QW(30)	Heat ratio or flux to segment, B/hr or B/hr ft^2	$TANK $PHASE		DERIV
RADTB	Tank radius table, in.	HEET	TABLE	HEET
SBOTS(30)	Station for bottom of heating segment, in.	$TANK		DERIV
SRADTB	Station table for tank radius, in.	HEET	TABLE	HEET
STOPS(30)	Station for top of heating segment, in.	$TANK		DERIV
TBA(300)	Wall surface area table stored sequentially, ft^2	BLKDATA	H2TANK	DERIV
TBCW	Specific heat entries in table, B/lbR	$TANK	H2TANK	DERIV
TBHVOL	Station table for tank table.		H2TANK	
TBKA	Table of bulkhead areas, in^2		H2TANK	
TBKS	Table of bulkhead stations, in.		H2TANK	
TBQ	Heating entries in tank heating tables B/hr or B/hr/ft^2	$TANK	H2TANK	DERIV
TBSA	Station table for wall surface area.		H2TANK	
TBTCW(30)	Temperature table for wall specific heat R.	$TANK	H2TANK	DERIV

Table A-2. Namelist TNKDIM Input (Concluded)

Variable Name (Max.Dim.)	Description and Units	Other Sources	Preset Value	Primary Use Subroutine
TBTQ	Time entries in tank heating table, secs.	$TANK	H2TANK	DERIV
TBVOL(110)	Tank volume table, ft^3		H2TANK	DERIV
TBL	Table length vs. height (TY), in.	$CASE	H2TANK	DIFE3
TW(30)	Segment wall temperature, R.	$TANK		DERIV
TY	Table of liquid height in bulkhead region for determining wall length used in heat transfer determination - in.	$CASE	H2TANK	HEET
XMDOTS(20)	Flow rate values of spray flow, lb/sec.	$CASE	H2TANK	DERIV
XTIMES(20)	Time segment of spray flow table, sec.	$CASE	H2TANK	DERIV

Table A-3. Namelist GASPRP Input

Name (Max.Dim.)	Description and Units	Other Sources	Preset Value	Primary Use Subroutine
ACOND(10)	Array of polynomial coefficients describing propellant gas conductivity, B/hr ft	$PHASE	H2PROP	FCONV
AVISC(10)	Array of polynomial coefficients describing propellant gas viscosity, lb_m/hr ft/R	$PHASE	H2PROP	FCONV
ICN	Number of entries in ACOND(N) table.	$PHASE	6	FCONV
IVN	Number of entries in AVISC(N) table.	$PHASE	6	FCONV
NPG	Number of pressure entries in superheated vapor tables.		9	DERIV
NSAT	Number of entries in saturated vapor properties table.		6	DERIV
NTG	Number of temperature entries in superheated vapor table.		47	DERIV
TBSV(9, 50)	Specific volume table for superheated vapor properties, ft^3/lb		H2PROP	DERIV
*TBTG(9, 50)	Temperature table for superheated vapor properties, R.		H2PROP	DERIV
*TBUG(9, 50)	Internal energy table for superheated vapor properties, B/lb		H2PROP	DERIV
XHFG(10)	Heat of vaporization table for saturated vapor, B/lb		H2PROP	DERIV
XPSAT(10)	Pressure table for saturated vapor properties, psia		H2PROP	DERIV
XSVLIQ(10)	Specific volume table for saturated liquid, ft^3/lb		H2PROP	DERIV
XTSAT(10)	Temperature table for saturated vapor properties, R		H2PROP	DERIV

* To load property values for constant pressure lines load data as follows:

DATA(TBTG(N), N=K, (J-1)*NPG+K, NPG) evaluate indices
K=sequence number of constant pressure line
J=number of entries for constant pressure line
repeat for each constant pressure line.

Table A-4. Namelist CASE Input

Parameter Name (Max.Dim.)	Description and Units	Other Sources	Preset Value	Primary Use Subroutine
ABTL	Internal surface area of helium bottle walls, ft^2	$HELIUM		BOTLPR
ACOND(10)	Polynomial coefficients of propellant gas conductivity = function of temperature, B/hr/R.	$GASPRP	H2PROP	HEET
AL	Liquid surface area, ft^2.			FCONV HEET DERIV
AO(10)	Orifice area, in^2.	$PHASE		HYPRS BOTLPR
ATOPP	Total tank wall area to the top, ft^2		637.979	HEET
AVISC(10)	Polynomial coefficients of propellant gas viscosity function of temperature, lb/hr/ft.	$GASPRP	H2PROP	FCONV
AW(30)	Tank wall area of each segment, ft^2.			HYPRS HEET
BLKHDT	Station at top of intermediate bulkhead, in.			HEET
BTOP	Forward bulkhead area, ft^2.	$TNKDIM	138.373	HEET
CL	Liquid propellant specific heat, B/lb/R.		2.3	HEET, MIX DERIV
CP	Specific heat of vapor at constant pressure B/lb/R.		3.8	FCONV DERIV
CPHE	Specific heat of helium at constant pressure, B/lb/R.		1.24	DERIV, MIX BOTLPR
CPP	Specific heat of hot gas pressurant, B/lb/R.		3.33	TPRESS DERIV
CVHES(90)	Helium specific heat at constant volume table, B/lb/R.	$HELIUM	HEPROP	BOTLPR
DM(10)	Helium mass through each orifice, lb.	$PHASE		HYPRS BOTLPR

Table A-4. Namelist CASE Input (Cont'd)

Parameter Name (Max.Dim.)	Description and Units	Other Sources	Preset Value	Primary Use Subroutine
FAW(30)	Wall area factor for each segment for scaling heat flux.	$TANK $PHASE		HYPRES HEET
FMDOT(10)	Orifice flow factor.	$PHASE		HYPRES BOTLPR
FMDOTS	Spray flow rate modifier.		1.0	DERIV
HCOND	Vapor condensation coefficient.	$PHASE		DERIV
HFG	Latent heat of evaporization at liquid temperature, B/lb.		168.	HEET, TPRESS DERIV, MIX
ICN	Number of entries in ACOND table.	$GASPRP	6	HEET FCONV
IREG	= 1. No pressurization analysis. Orifice data not required. = 2. Call TPRESS to compute helium mass flow, MDOTP, for pressurization. = 3. Call BOTLPR & HETEMP to obtain detailed analysis of helium bottle, orifice flow and helium temperatures entering hydrogen tank. = 4. Call HETEMP to obtain helium temperature entering hydrogen tank. Orifice data not required. = 5 & 6. No pressurization analysis. Orifice data not required.	$PHASE		DERIV HYPRS
ISAVE	Flag for initializing tank conditions. (Not in current use)		1	HYPRS
IVN	Number of entries in AVISC table.	$GASPRP	6	HEET FCONV
KK	Forced convection thermal conductivity factor.			HEET
LOKSEG	Number of wall segments considered during lockup.			HYPRS
LPRINT	Debug printout flag. = 1, Outputs data for debugging purposes.	$HELIUM $PHASE		BOTLPR HETEMP
MBTL	Total mass of helium storage bottles, lb.	$HELIUM		BOTLPR

Table A-4. Namelist CASE Input (Cont'd)

Parameter Name (Max.Dim.)	Description and Units	Other Sources	Preset Value	Primary Use Subroutine
MENISK	Length of TAW and TGRAV tables and meniscus effect flag.	$PHASE		HEET
NCAP	Number of values in TSHCAP and TSHCAPT tables.			HEET
NEQSUP	Number of supports for radiation shield.		1	HYPRS
NS	Number of entries in spray flow tables.	$TNKDIM	H2TANK	DERIV
P	Total tank pressure, psia.			DERIV
				BOTLPR
PBTL	Initial helium pressure in bottle, psia.	$PHASE		HYPRS
		$HELIUM		BOTLPR
PHE	Initial helium partial pressure, psia.			HYPRS
PSATL	Initial propellant vapor pressure, psia.			HYPRS
PU	P			HYPRS
RG	Ullage gas constant based on vapor pressure, $ft\text{-}lb_f/(lbm\text{-}R)$		766.5	HEET
				FCONV
RHE	Helium gas constant, ft lb/lb/R.	$HELIUM	386.	BOTLPR, MIX
SBOT	Station defining bottom of tank, in.		408.75	HEET
SLTOP	Station level of tank sidewall top, in.	$PHASE		HEET
				HYPRS
STANK	Station of liquid in tank at lockup, in.			HYPRS
STOP	Station defining tank top, in.	$TANK	162.04	HEET
			H2TANK	
TAW(40)	Wall area increment table to determine meniscus effect.			HEET
TBTL	Initial temperature of helium and bottle, R.			HYPRS
TGRAV(40)	Gravity potential table to determine meniscus effect.			HEET
TLB(50)	Length vs. height table, in.	$TNKDIM	H2TANK	HEET
TMES2	Spray flow tables time argument for second MES.			DERIV
TSHCAP(30)	Radiation shield heat capacitances = function of temperature.			HEET

TABLE A-4. Namelist CASE Input (Concluded)

Parameter Name (Max.Dim.)	Description and Units	Other Sources	Preset Value	Primary Use Subroutine
TSHCAPT(30)	Temperature for obtaining radiation shield heat capacitance, R.			HEET
TU	Initial ullage temperature R.			ALL
TW(30)	Wall temperature for each segment, R.	$TANK $TNKDIM		HYPRS
TY(50)	Bulkhead region liquid height table for obtaining heat transfer for wall length, in.	$TNKDIM	H2TANK	HEET
VBTL	Helium bottle volume, ft^3.	$HELIUM		HYPRS BOTLPR
VTOT	Total tank volume ft^3.	$TANK $PHASE	1270.8638 H2TANK	HYPRS DERIV
XMDOTS(20)	Spray flow rate table, lb/sec.		H2TANK	DERIV
XML	Initial mass of propellant lb.			HYPRS
XMLMIN	Minimum propellant weight, lb.			INTGRT
XTIMES(20)	Time argument for spray flow table, sec.	$TNKDIM	H2TANK	DERIV

Table A-5. Namelist HELIUM Input

Variable Name (Max.Dim.)	Description and Units	Other Sources	Preset Value	Primary Use Subroutine
ABSOL	Solar absorptivity of helium bottle outer surface.			BOTLPR
ABTL	Internal surface area of helium bottle walls, ft^2.	$CASE	1.0	HYPRS BOTLPR
AORF	Helium supply orifice area, in^2.			HYPRS BOTLPR
CBTL	Specific heat of helium storage bottles, B/lb/R.		1000.	
CD(10)	Helium supply orifice discharge coefficient.	$PHASE		HYPRS BOTLPR
CPH(10)	Pressure argument for CVHES and SPVES tables, psia.			BOTLPR
CPTI(15)	Helium bottle material specific heat table for TCPT, B/lb/R.			BOTLPR
CT(9)	Temperature argument for CVHES and SPVES tables, R.			BOTLPR
CVHES(90)	Helium specific heat at constant volume table, B/lb/R.			BOTLPR
EMMISH	Emissivity of helium bottle.			BOTLPR
FAWBOT	Heat transfer factor from helium bottle wall to gas.			BOTLPR
FRALB	Fraction of helium bottle projected area exposed to albedo radiation.			BOTLPR
FREM	Fraction of helium bottle projected area exposed to earth thermal radiation.	$PHASE		BOTLPR
FRSOL	Fraction of helium bottle projected area exposed to solar radiation.			BOTLPR
G	Acceleration, G/G0.			DERIV, FCONV
HK(10)	Helium thermal conductivity table vs. HT, B/hr/ft/R.			BOTLPR
HM(10)	Helium viscosity table vs. HT, lbm/ft/sec.			BOTLPR
HT(10)	Temperature table for viscosity and conductivity table, R.			BOTLPR
LHEL	Helium bottle characteristic length used in calculating heat transfer coefficient, in.	$PHASE	SQRT (ABTL/TT)	BOTLPR

Table A-5. Namelist HELIUM Input (Cont'd)

Variable Name (Max.Dim.)	Description and Units	Other Sources	Preset Value	Primary Use Subroutine
LPRINT	Debug printout flag.	$CASE		HETEMP
	= 1, outputs data for debugging purposes.	$PHASE		BOTLPR
MBTL	Total mass of helium storage bottles, lb.	$CASE	10. E+10	BOTLPR
MCT	Number of entries in CT table.			HYPRS
MP	Number of entries in CPH table.			BOTLPR
NP	Number of entries in XP table.			BOTLPR
				HYPRS
NT	Number of entries in XT table.			BOTLPR
				HYPRS
PBTL	Initial pressure of helium in bottle, psia.	$CASE		
		$PHASE		BOTLPR
PR	Prandtl number of helium gas in bottle.	$CASE		FCONV
				BOTLPR
QEXT		$PHASE		BOTLPR
RHE	Helium gas constant, ft-lb/lb/R.	$CASE		DERIV, HEET
				TPRESS
				BOTLPR, MIX
SPVES(90)	Helium specific volume vs. CPH and CT table, ft^3/lb.			BOTLPR
T	TBTL	$PHASE		HYPRS
TBTL	Initial temperature of helium in bottle, R.	$CASE		
		$PHASE	540.	HYPRS
TCPT(15)	Temperature table for helium bottle specific heat, CPT, R.			BOTLPR
TL	Liquid temperature R.			HYPRS
VBTL	Helium bottle volume, in^3.	$CASE	10. E+10	BOTLPR
				HYPRS

Table A-5. Namelist HELIUM Input (Concluded)

Variable Name (Max.Dim.)	Description and Units	Other Sources	Preset Value	Primary Use Subroutine
XN				BOTLPR
XP(15)	Pressure table for helium compressibility factor vs. pressure and temperature, psia.			BOTLPR HYPRS
XT(15)	Temperature table for helium compressibility vs. pressure and temperature, R.			BOTLPR HYPRS
ZZ(125)	Compressibility factor table vs. helium bottle pressure and temperature.			BOTLPR HYPRS

Table A-6. Namelist PHASE Input

Name (Max.Dim.)	Description and Units	Other Sources	Preset Value	Primary Use Subroutine
AFILM	Area of liquid film and ullage gas interface, ft^2			DERIV
ALIQ	Area of liquid ullage gas interface excluding film. Use during low g coast when liquid surface is not planar, ft^2			
AO(10)	Pressurization line orifice areas, in^2	$CASE	10*0.	BOTLPR HYPRS
AOGAS	Area of the variable orifice when wide open, in^2			DERIV
AQAB	Area of the tank for use with QAB, ft^2		500.	HEET
BLKHDT	Station level of top of intermediate bulkhead, in.	$CASE		HEET
BTIME	Beginning time of pressurization, sec.			HETEMP
CD(10)	Orifice discharge coefficient.	$HELIUM		BOTLPR HYPRS
CNQFLG	Liquid-gas heat transfer factor.			HEET
CONHP	Helium mass flow factor.			TPRESS
CONQBO	Fraction of heat producing vapor coefficient.			DERIV
CONQLG	Liquid gas heat transfer correction factor.		1.0	HEET
CONQSP	Correction factor for standpipe heat transfer from helium to LO_2.			DERIV
CONSAT	Saturation pressure constant.			DERIV
CONTV	Constant to specify vent temperature.			VENT
DEADWT	Vehicle non-propellant weight, lb.		1.	HEET
DELP	Delta pressure for pressurization sequence, psia.			HYPRS
DELT	Tank pressurization time, secs.			HYPRS
DM(10)	Helium mass per orifice, lb.	$CASE	2*1000.	BOTLPR HYPRS
DTHE(20)	Helium mass vs. temperature table, R.			HETEMP
DTIME	Calculation step size, sec.		1.0	DERIV HYPRS

Table A-6. Namelist PHASE Input (Cont'd)

Name (Max.Dim.)		Other Sources	Preset Value	Primary Use Subroutine
EMSI	Emissivity of the radiation shield internal surface.		.0001	HEET
EMSO	Emissivity of the radiation shield outer surface.		.0001	HEET
EPSA	Maximum allowable absolute error in INTGRT.		.01	INTGRT HYPRS
EPSP	Allowable relative error in pressure iteration.		.0001	DERIV
ERSR	Maximum allowable relative error in INTGRT.		-1.	INTGRT DERIV
F	Total thrust contributing to the gravity field, lb.		1.	
FAW(30)	Wall area factor of each segment available for scaling the programmed heat flux.	$CASE $TANK		HEET HYPRS
FDRY(30)	Factor for modifying the heat flux on the dry portion of a segment.			HEET HYPRS
FFAW	Empirical gas heat correction factor.		1.3333	HEET
FMDOT(10)	Orifice flow factor.	$CASE		BOTLPR HYPRS
FPG	Fraction of propellant vapor pressure to total pressure.		0.	DERIV
FQFE	Fraction of internal heat transfer from the tank wall due to evaporation.			HEET
FQLIQ	Fraction of heat transfer to the liquid which does not produce vapor.		1.0	DERIV
FQSUP	Support structure heat transfer factor.		1.0	HYPRS
FQUENV	Fraction of heat released by the tank wall which produces vapor.			HEET
FREM	Fraction of helium bottle projected area exposed to earth thermal radiation.	$HELIUM		BOTLPR
FSET	Settling thrust for venting, lb.		100.	VENT
HAMS	Spray heat transfer parameter.			DERIV
HCOND	Coefficient for determining vapor condensation.	$CASE		DERIV

Table A-6. Namelist PHASE Input (Cont'd)

Name (Max.Dim.)	Description and Units	Other Sources	Preset Value	Primary Use Subroutine
HEUSE	Constant helium flow rate in addition to that calculated for the LO_2 tank.			BOTLPR
HMAX	Maximum integration step size.			INTGRT
IBUG1	.GT.O debugging output of current values of wall heat transfer parameters.		0	HEET
IBUG2	.GT.O debugging output of current values of wall heat transfer, and gas and liquid heat content.		0	HEET DERIV
IBUG3	.GT.O debugging output of H_2 and He state variables.		0	HEET
IBURP	= 1, Tank pressurization calculations. = 2, No tank pressurization calculations.			DERIV
IFLOW	Vent flag. = 0, No venting. = 1, Venting allowed. = 2, Venting in process.			VENT DERIV
IHTOUT	.GT.1, output wall segment heat values.			HEET FCONV
IMIX	Total ullage thermodynamic equilibrium calculation flag. = 0, No mixing. Ullage is not brought to thermodynamic equilibrium. = 1, Mixing. Ullage is brought to thermodynamic equilibrium.		0	DERIV HYPRS
INVERT	Flag for defining propellant re-orientation. = -1, Forward-to-aft orientation. = 0, No re-orientation. = 1, Aft-to-forward orientation.		0	DERIV HYPRS
IPLOT	Flag to saving data for plotting. (Not currently in use).			HYPRS

Table A-6. Namelist PHASE Input (Cont'd)

Name (Max.Dim.)	Description and Units	Other Sources	Preset Value	Primary Use Subroutine
IQT	Flag for use of REQSUP tables.			HYPRS
IQUEN	Wall quench flag. = 1, Wall quench to occur during current calculation step.			DERIV
IREG	Tank pressurization calculation flag. = 1, No pressurization analysis. Orifice data not required. = 2, Call TPRESS to compute helium mass flow, MDOTP, for pressurization. = 3, Call BOTLPR & HETEMP to obtain detailed analysis of helium bottle, orifice flow and helium temperatures entering hydrogen tank. = 4, Call HETEMP to obtain helium temperature entering hydrogen tank. Orifice data not required. = 5 & 6, No pressurization analysis. Orifice data not required	$CASE		DERIV HYPRS
ISPRAY	Flag for spray calculations. = 1, Calculate spray mass flow rate, MDOTS, and spray heating rate, QGS. = 2, No spray calculations.		2	DERIV HYPRS
ITERMEQ	= 1, Call THRMEQ to force propellant and liquid phases to thermal equilibrium.			DERIV
LFILM	Flag set to 1 when liquid film covers the tank wall.			DERIV HEET
LHEL	Helium bottle characteristic length, in.	$HELIUM		BOTLPR HYPRS
LIQOUT	Flag to determine propellant outflow temperature, TLOUT.		-1	DERIV
LPRINT	Degub printout flag. [.LE.O, TLOUT = TM(5) [.GT.O, TLOUT = TSATLB	$CASE $HELIUM		BOTLPR HETEMP

Table A-6. Namelist PHASE Input (Cont'd)

Name (Max.Dim.)	Description and Units	Other Sources	Preset Value	Primary Use Subroutine
MDOTL	Liquid (LH_2) outflow rate, lb/sec.			DERIV
MDOTTV	Vent mass flow table, lb/sec.			VENT
MENISK	Length of TAW and TGRAV tables and meniscus effect flag.	$CASE		HEET
MW(30)	Wall segment mass, lb.	$TANK		HEET
		$TNKDIM		HYPRS
NEXT	Flag to start new case. = 1, 2, or 3 Input $CASE		4	HYPRS
	= 4 Input $PHASE			
	= 5 Stop			
NITOUT	Number of integration steps between detailed printout.			HYPRS
NQS	Number of segments for tank heating input.			HEET/HYPRS
				PRINT
NUPNT	Flag to denote new point.			DERIV
PBOTL	Initial helium bottle pressure, psia.	$CASE		BOTLPR
		$HELIUM		HYPRS
PCRACK	Vent valve cracking pressure, psia.			DERIV
PMIX	Minimum pressure from a propellant tank mix to thermodynamic equilibrium, psia.			MIX
PRESET	Vent valve reseat pressure, psia.			DERIV
PTV(10)	Vent pressure table for vent flow determination, psia.			VENT
PVARYO	Pressure desired for tank pressurization, psia.		99.	BOTLPR
				DERIV/HYPRS
PVLIQ	Liquid vapor pressure, psia.			DERIV/MIX
QAB(30)	Heat absorbed by ullage and liquid, DTU/hr/ft^2			HEET
QEXT	External heat to helium bottle, B/hr.	$HELIUM		BOTLPR
QRS	Heating rate to the thrust barrel radiation shield, B/hr.			HEET
QSUP	Heating rate of equipment support, B/hr.			HYPRS

Table A-6. Namelist PHASE Input (Cont'd)

Name (Max.Dim.)	Description and Units	Other Sources	Preset Value	Primary Use Subroutine
QW(30)	Heat rate, or flux, to each wall segment, B/hr, or B/hr/ft^2	$TANK $TNKDIM		HEET
QWG	Wall to gas heat rate for all wall segments, B/sec.			HEET
QWL	Wall to liquid heat rate for all wall segments, B/sec.			HEET
RBBKHD	Bulkhead heat resistance, R-hr/B.			HEET
REQSUP( )	Equipment support resistance to heat conduction, R-hr/B.			HEET
RRSSUP	Thermal resistance of thrust barrel radiation shield support bracket, R-hr/B.		1000.	HEET
SHCAP	Radiation shield heat capacity, B/ft^2/R.			HEET
SLTOP	Station level of tank sidewall top, in.	$CASE		HEET HYPRS
SWET	Station of non-planar interface where liquid contacts the tank wall, in.			HEET
TBTL	Initial temperature of helium and helium bottle, R.	$CASE $HELIUM	540.	HYPRS
TDRAIN	Time to drain liquid film from the tank wall after main engine or settling thrust, sec.			HYPRS
TEQ(30)	Source temperature for conduction through an equipment support, R.			HEET HYPRS
TFILM	Time when liquid film draining is completed, secs.			DERIV
THEIN	Helium temperature entering the tank, R.			HEET
THIN	Pressurant gas temperature, R.		500.	DERIV
TIME	Initial time, secs.			DERIV HYPRS
TIMEF	Final time, secs.			DERIV HYPRS
TIMES	Time adjustment for entering spray flow tables.			DERIV
TIMREF	End time of settling thrust, sec.			VENT

Table A-6. Namelist PHASE Input (Concluded)

Name (Max.Dim.)	Description and Units	Other Sources	Preset Value	Primary Use Subroutine
TIREF	Settling thrust time on, sec.			VENT
TM(50)	Integration variables.			INTGRT HYPRS
TQAB(30)	Time table for QAB, sec.		10^8	HEET
TTANK	Temperature of liquid being tanked, R.			DERIV
TTV(10)	Time input for vent flow rate determination, sec.			VENT
TVNT	Vented gas temperature, R.		0.	DERIV VENT
VTIME(20)	Array of programmed vent times, sec.	$CASE		HYPRS
WRATIO	Ratio of total burnable propellant to burnable LO_2.			HEET
X	Factor reducing amount of spray entering ullage.			HETEMP HYPRS
XMHE(20)	Helium mass, lb.			

SAMPLE COMPUTER INPUT FILE

The following input file was used to analyze the Helium/Autogenous pressurization system for the hydrogen tank of vehicle configuration 1.

```
IIW10,T777.
A.WAKABAYA 93773 696-0        Y12512666
ATTACH,LGO,P3995HLGO,ID=ICHI93773,MR=1.
LDSET,PRESET=ZERO.
MAP,OFF.
LGO,PL=20000.
C           LOW THRUST OTV STUDY
C           HELIUM/AUTOGENOUS PRESSURIZATION
C           9 BURN MISSION
C           CONFIGURATION 1 HYDROGEN TANK
P$TANK
 EMISS(1)=15*.0001,
 ICW(1)=15*1,
 ITNK=1,
C           THE WALL THICKNESS IS MULTIPLIED BY 1.3 TO ACCOUNT FOR
C           STUCTURAL SUPPORT ADDITIONS.
 MW( 1)=25.36, 23.34, 21.62, 20.22, 19.26, 16.90, 3*37.17, 18.79,
 MW(11)=19.31, 20.32, 21.74, 23.49, 23.53,
 NCW=16,
 NQSEGS=15,
 SBOT=154.25,
 SBOTS( 1)=154.25,144.25,134.25,124.25,114.25,104.25,95.25,83.25,71.25,59.25,
 SBOTS(11)= 49.25, 39.25, 29.25, 19.25, 9.25,
 STOP=0.,
 STOPS( 1)=144.25,134.25,124.25,114.25,104.25,95.25,83.25,71.25,59.25,49.25,
 STOPS(11)= 39.25, 29.25, 19.25, 9.25, 0.0,
C           SPECIFIC HEAT TABLE FOR ALUMINUM TANK
 TBCW( 1)=0.0, .01, .013, .017, .023, .028, .035, .042, .049, .056,
 TBCW(11)=.092, .139, .175, .192, .205, .210,
 TBTCW( 1)=0.0, 35., 45., 55., 65., 75., 85., 95., 105., 115.,
 TBTCW(11)=155., 230., 330., 430., 530., 600.,
 TW( 1)=15*38.,
 VTOT=1470.75,
 $
P$TNKDIM
C           VEHICLE CONFIGURATION 1, HYDROGEN TANK
 AWTBK=629.70,
 NAW=156,
 NRADTB=156,
 NVOL=156,
C           STATION TABLE (INCHES)
 SRADTB(  1)=   154.25,  153.25,  152.25,  151.25,  150.25,  149.25,  148.25,  147.25,
 SRADTB(  9)=   146.25,  145.25,  144.25,  143.25,  142.25,  141.25,  140.25,  139.25,
 SRADTB( 17)=   138.25,  137.25,  136.25,  135.25,  134.25,  133.25,  132.25,  131.25,
 SRADTB( 25)=   130.25,  129.25,  128.25,  127.25,  126.25,  125.25,  124.25,  123.25,
 SRADTB( 33)=   122.25,  121.25,  120.25,  119.25,  118.25,  117.25,  116.25,  115.25,
 SRADTB( 41)=   114.25,  113.25,  112.25,  111.25,  110.25,  109.25,  108.25,  107.25,
 SRADTB( 49)=   106.25,  105.25,  104.25,  103.25,  102.25,  101.25,  100.25,   99.25,
 SRADTB( 57)=    98.25,   97.25,   96.25,   95.25,   94.25,   93.25,   92.25,   91.25,
 SRADTB( 65)=    90.25,   89.25,   88.25,   87.25,   86.25,   85.25,   84.25,   83.25,
 SRADTB( 73)=    82.25,   81.25,   80.25,   79.25,   78.25,   77.25,   76.25,   75.25,
 SRADTB( 81)=    74.25,   73.25,   72.25,   71.25,   70.25,   69.25,   68.25,   67.25,
 SRADTB( 89)=    66.25,   65.25,   64.25,   63.25,   62.25,   61.25,   60.25,   59.25,
 SRADTB( 97)=    58.25,   57.25,   56.25,   55.25,   54.25,   53.25,   52.25,   51.25,
 SRADTB(105)=    50.25,   49.25,   48.25,   47.25,   46.25,   45.25,   44.25,   43.25,
 SRADTB(113)=    42.25,   41.25,   40.25,   39.25,   38.25,   37.25,   36.25,   35.25,
 SRADTB(121)=    34.25,   33.25,   32.25,   31.25,   30.25,   29.25,   28.25,   27.25,
 SRADTB(129)=    26.25,   25.25,   24.25,   23.25,   22.25,   21.25,   20.25,   19.25,
 SRADTB(137)=    18.25,   17.25,   16.25,   15.25,   14.25,   13.25,   12.25,   11.25,
 SRADTB(145)=    10.25,    9.25,    8.25,    7.25,    6.25,    5.25,    4.25,    3.25,
 SRADTB(153)=     2.25,    1.25,     .25,    0.00,
C           STATION TABLE (INCHES)
```

```
TBHVOL(  1)=   154.25,  153.25,  152.25,  151.25,  150.25,  149.25,  148.25,  147.25,
TBHVOL(  9)=   146.25,  145.25,  144.25,  143.25,  142.25,  141.25,  140.25,  139.25,
TBHVOL( 17)=   138.25,  137.25,  136.25,  135.25,  134.25,  133.25,  132.25,  131.25,
TBHVOL( 25)=   130.25,  129.25,  128.25,  127.25,  126.25,  125.25,  124.25,  123.25,
TBHVOL( 33)=   122.25,  121.25,  120.25,  119.25,  118.25,  117.25,  116.25,  115.25,
TBHVOL( 41)=   114.25,  113.25,  112.25,  111.25,  110.25,  109.25,  108.25,  107.25,
TBHVOL( 49)=   106.25,  105.25,  104.25,  103.25,  102.25,  101.25,  100.25,   99.25,
TBHVOL( 57)=    98.25,   97.25,   96.25,   95.25,   94.25,   93.25,   92.25,   91.25,
TBHVOL( 65)=    90.25,   89.25,   88.25,   87.25,   86.25,   85.25,   84.25,   83.25,
TBHVOL( 73)=    82 25,   81.25,   80.25,   79.25,   78.25,   77.25,   76.25,   75.25,
TBHVOL( 81)=    74.25,   73.25,   72.25,   71.25,   70.25,   69.25,   68.25,   67.25,
TBHVOL( 89)=    66.25,   65.25,   64.25,   63.25,   62.25,   61.25,   60.25,   59.25,
TBHVOL( 97)=    58.25,   57.25,   56.25,   55.25,   54.25,   53.25,   52.25,   51.25,
TBHVOL(105)=    50.25,   49.25,   48.25,   47.25,   46.25,   45.25,   44.25,   43.25,
TBHVOL(113)=    42.25,   41.25,   40.25,   39.25,   38.25,   37.25,   36.25,   35.25,
TBHVOL(121)=    34.25,   33.25,   32.25,   31.25,   30.25,   29.25,   28.25,   27.25,
TBHVOL(129)=    26.25,   25.25,   24.25,   23.25,   22.25,   21.25,   20.25,   19.25,
TBHVOL(137)=    18.25,   17.25,   16.25,   15.25,   14.25,   13.25,   12.25,   11.25,
TBHVOL(145)=    10.25,    9.25,    8.25,    7.25,    6.25,    5.25,    4.25,    3.25,
TBHVOL(153)=     2.25,    1.25,      25,    0.00,
C          STATION TABLE (INCHES)
TBSA(  1)=   154.25,  153.25,  152.25,  151.25,  150.25,  149.25,  148.25,  147.25,
TBSA(  9)=   146.25,  145.25,  144.25,  143.25,  142.25,  141.25,  140.25,  139.25,
TBSA( 17)=   138.25,  137.25,  136.25,  135.25,  134.25,  133.25,  132.25,  131.25,
TBSA( 25)=   130.25,  129.25,  128.25,  127.25,  126.25,  125.25,  124.25,  123.25,
TBSA( 33)=   122.25,  121.25,  120.25,  119.25,  118.25,  117.25,  116.25,  115.25,
TBSA( 41)=   114.25,  113.25,  112.25,  111.25,  110.25,  109.25,  108.25,  107.25,
TBSA( 49)=   106.25,  105.25,  104.25,  103.25,  102.25,  101.25,  100.25,   99.25,
TBSA( 57)=    98.25,   97.25,   96.25,   95.25,   94.25,   93.25,   92.25,   91.25,
TBSA( 65)=    90.25,   89.25,   88.25,   87.25,   86.25,   85.25,   84.25,   83.25,
TBSA( 73)=    82.25,   81.25,   80.25,   79.25,   78.25,   77.25,   76.25,   75.25,
TBSA( 81)=    74.25,   73.25,   72.25,   71.25,   70.25,   69.25,   68.25,   67.25,
TBSA( 89)=    66.25,   65.25,   64.25,   63.25,   62.25,   61.25,   60.25,   59.25,
TBSA( 97)=    58.25,   57.25,   56.25,   55.25,   54.25,   53.25,   52.25,   51.25,
TBSA(105)=    50.25,   49.25,   48.25,   47.25,   46.25,   45.25,   44.25,   43.25,
TBSA(113)=    42.25,   41.25,   40.25,   39.25,   38.25,   37.25,   36.25,   35.25,
TBSA(121)=    34.25,   33.25,   32.25,   31.25,   30.25,   29.25,   28.25,   27.25,
TBSA(129)=    26.25,   25.25,   24.25,   23.25,   22.25,   21.25,   20.25,   19.25,
TBSA(137)=    18.25,   17.25,   16.25,   15.25,   14.25,   13.25,   12.25,   11.25,
TBSA(145)=    10.25,    9.25,    8.25,    7.25,    6.25,    5.25,    4.25,    3.25,
TBSA(153)=     2.25,    1.25,     .25,    0.00,
C          AREA TABLE (FT**2)
TBA(  1)=      0.00,    5.16,   10.28,   15.35,   20.39,   25.38,   30.33,   35.23,
TBA(  9)=     40.10,   44.93,   49.72,   54.46,   59.17,   63.84,   68.47,   73.07,
TBA( 17)=     77.62,   82.14,   86.63,   91.08,   95.49,   99.88,  104.22,  108.54,
TBA( 25)=    112.82,  117.07,  121.29,  125.48,  129.64,  133.77,  137.88,  141.95,
TBA( 33)=    146.00,  150.03,  154.02,  158.00,  161.95,  165.88,  169.78,  173.67,
TBA( 41)=    177.53,  181.38,  185.21,  189.02,  192.81,  196.59,  200.36,  204.11,
TBA( 49)=    207.84,  211.57,  215.29,  218.99,  222.69,  226.38,  230.06,  233.74,
TBA( 57)=    237.41,  241.08,  244.75,  248.42,  252.08,  255.75,  259.41,  263.08,
TBA( 65)=    266.74,  270.41,  274.07,  277.74,  281.40,  285.07,  288.73,  292.40,
TBA( 73)=    296.06,  299.73,  303.39,  307.06,  310.72,  314.39,  318.06,  321.72,
TBA( 81)=    325.39,  329.05,  332.72,  336.38,  340.05,  343.71,  347.38,  351.04,
TBA( 89)=    354.71,  358.37,  362.04,  365.70,  369.37,  373.03,  376.70,  380.36,
TBA( 97)=    384.03,  387.70,  391.36,  395.04,  398.71,  402.39,  406.08,  409.78,
TBA(105)=    413.48,  417.20,  420.92,  424.65,  428.40,  432.16,  435.94,  439.73,
TBA(113)=    443.53,  447.36,  451.20,  455.06,  458.94,  462.84,  466.76,  470.71,
TBA(121)=    474.68,  478.67,  482.69,  486.73,  490.80,  494.89,  499.02,  503.17,
TBA(129)=    507.35,  511.57,  515.81,  520.08,  524.39,  528.73,  533.10,  537.51,
TBA(137)=    541.95,  546.43,  550.94,  555.49,  560.07,  564.69,  569.35,  574.05,
TBA(145)=    578.79,  583.57,  588.38,  593.24,  598.14,  603.08,  608.06,  613.08,
TBA(153)=    618.14,  623.25,  628.40,  629.70,
```

```
C           VOLUME TABLE (INCHES)
 TBVOL(  1)=     0.00,     .21,     .85,    1.91,    3.38,    5.25,    7.51,   10.17,
 TBVOL(  9)=    13.20,   16.61,   20.38,   24.52,   29.00,   33.84,   39.00,   44.50,
 TBVOL( 17)=    50.32,   56.46,   62.90,   69.65,   76.69,   84.02,   91.62,   99 50,
 TBVOL( 25)=   107.64,  116.04,  124.69,  133.58,  142.71,  152.07,  161.64,  171.44,
 TBVOL( 33)=   181.43,  191.63,  202.02,  212.59,  223.34,  234.27,  245.35,  256.59,
 TBVOL( 41)=   267.98,  279.51,  291.17,  302.96,  314.87,  326.89,  339.01,  351.24,
 TBVOL( 49)=   363.55,  375.95,  388.42,  400.96,  413.56,  426.21,  438.91,  451.65,
 TBVOL( 57)=   464.43,  477.22,  490.04,  502.86,  515.69,  528.52,  541.35,  554.18,
 TBVOL( 65)=   567.00,  579.83,  592.66,  605.49,  618.32,  631.15,  643.97,  656.80,
 TBVOL( 73)=   669.63,  682.46,  695.29,  708.11,  720.94,  733.77,  746.60,  759.43,
 TBVOL( 81)=   772.26,  785.08,  797.91,  810.74,  823.57,  836.40,  849.22,  862.05,
 TBVOL( 89)=   874.88,  887.71,  900.54,  913.36,  926.19,  939.02,  951.85,  964.68,
 TBVOL( 97)=   977.50,  990.32, 1003.12, 1015.90, 1028.65, 1041.36, 1054.03, 1066.65,
 TBVOL(105)=  1079.20, 1091.69, 1104.11, 1116.44, 1128.69, 1140.84, 1152.89, 1164.82,
 TBVOL(113)=  1176.64, 1188.34, 1199.90, 1211.33, 1222.60, 1233.73, 1244.69, 1255 48,
 TBVOL(121)=  1266.10, 1276.54, 1286.78, 1296.83, 1306.68, 1316.31, 1325.72, 1334.91,
 TBVOL(129)=  1343.86, 1352.57, 1361.03, 1369.24, 1377.18, 1384.86, 1392.25, 1399.37,
 TBVOL(137)=  1406.19, 1412.71, 1418.92, 1424.82, 1430.40, 1435.65, 1440.57, 1445.14,
 TBVOL(145)=  1449.36, 1453.23, 1456.73, 1459.86, 1462.61, 1464.97, 1466.94, 1468.51,
 TBVOL(153)=  1469.67, 1470.41, 1470.73, 1470.75,
C           RADIUS TABLE (INCHES)
 RADTB(  1)=     0.00,   15.35,   21.61,   26.36,   30.30,   33.73,   36.79,   39.56,
 RADTB(  9)=    42.10,   44.45,   46.65,   48.70,   50.63,   52.45,   54.17,   55.80,
 RADTB( 17)=    57.35,   58.83,   60.24,   61.58,   62.86,   64.09,   65.26,   66.38,
 RADTB( 25)=    67.45,   68.48,   69.46,   70.40,   71.30,   72.17,   72.99,   73.78,
 RADTB( 33)=    74.53,   75.25,   75.93,   76.59,   77.21,   77.80,   78.36,   78.89,
 RADTB( 41)=    79.39,   79.87,   80.32,   80.73,   81.13,   81.49,   81.83,   82.15,
 RADTB( 49)=    82.44,   82.70,   82.94,   83.16,   83.35,   83.51,   83.65,   83.77,
 RADTB( 57)=    83.86,   83.93,   83.98,   84.00,   84.00,   84.00,   84.00,   84.00,
 RADTB( 65)=    84.00,   84.00,   84.00,   84.00,   84.00,   84.00,   84.00,   84.00,
 RADTB( 73)=    84.00,   84.00,   84.00,   84.00,   84.00,   84.00,   84.00,   84.00,
 RADTB( 81)=    84.00,   84.00,   84.00,   84.00,   84.00,   84.00,   84.00,   84.00,
 RADTB( 89)=    84.00,   84.00,   84.00,   84.00,   84.00,   84.00,   84.00,   84.00,
 RADTB( 97)=    83.98,   83.94,   83.88,   83.79,   83.68,   83.55,   83.39,   83.21,
 RADTB(105)=    83.00,   82.76,   82.51,   82.22,   81.92,   81.58,   81.22,   80.84,
 RADTB(113)=    80.42,   79.98,   79.51,   79.02,   78.49,   77.94,   77.36,   76.74,
 RADTB(121)=    76.10,   75.42,   74.71,   73.97,   73.19,   72.37,   71.52,   70.63,
 RADTB(129)=    69.70,   68.73,   67.71,   66.65,   65.54,   64.39,   63.17,   61.91,
 RADTB(137)=    60.58,   59.19,   57.73,   56.20,   54.58,   52.88,   51.09,   49.19,
 RADTB(145)=    47.17,   45.02,   42.71,   40.22,   37.51,   34.53,   31.20,   27.40,
 RADTB(153)=    22.90,   17.14,    7.70,    0.00,
 $
P$CASE
C           INITIAL TANK CONDITIONS SPECIFIED
 CPP=3.33, NEQSUP=0., IREG=3,
 P=18.0, PSATL=18.0, PHE=0., XML=5751.3, TU=39., TW(1)=15*39.,
  $
P$HELIUM
C           HELIUM BOTTLE CONDITIONS
 FAWBOT=2., XN=1., RHE=386.3376, G=.025,
 EMMISH=0.1, ABSOL=0.25,
 FREM=1., FRSOL=1., FRALB=0., LHEL=1., T=450., TBTL=450.,
 $
P$PHASE
C           BURN 1 START
C           AUTOGENOUS PRESSURIZATION
C           NPSP=.5 PSI
 CNQFLG=.02, DTIME=10.,
 CONHP=1.,
 CONSAT=.05,
 DEADWT=19748.,
```

```
 DELT=3820.,
 DELNPSH=.5,
 F=500.,
 FPG=.3,
 IFLOW=0,
 IREG=2,
 LIQOUT=1,
 MDOTL=.1623,
 NITOUT=-200,
 QW(1)=15*49.33,
 THIN=500.,
 TIME=0.,
 WRATIO=6.9,
 $
P$PHASE
C           QUENCH WALLS
 FQUENV=1., F=.001, CONSAT=.9999,
 INVERT=1, MDOTL=0.,
 DELT=.1, DTIME=1.,
 $
P$PHASE
C           MIX AFTER QUENCH
 IMIX=1,
 DELT=0.,
 PRESET=0.,
 $
P$PHASE
C           ZERO-G-COAST BETWEEN BURN 1-2
C           THERMODYNAMIC EQUILIBRIUM
C           VENT TANK TO 18 PSIA
 DELT=6014.,
 IFLOW=1,
 IMIX=1,
 IREG=1, INVERT=-1, LFILM=1, TDRAIN=1.E10,
 PRESET=18.,
 $
P$PHASE
C           PRESSURIZE TO NPSP OF 0.5 PSI PPIOR TO ENGINE BURN 2
 AO(1)=.001,
 AOFUEL=.001,
 CD(1)=.6,
 DELT=10., LFILM=0, DTIME=.1,
 DTHE(1)=10*0.,
 FMDOT(1)=1.,
 IFLOW=0,
 IREG=3,
 THEIN=168.,
 XMHE(1)=0., 9*1000000.,
 $
P$PHASE
C           BURN 2 START
C           AUTOGENOUS PRESSURIZATION
C           NPSP=.5 PSI
 DTIME=10.,
 CONSAT=.05,
 DELT=3538.,
 F=500.,
 IFLOW=0,
 IREG=2,
 MDOTL=.1623,
 $
P$PHASE
```

```
C           QUENCH WALLS
 FQUENV=1., F=.001, CONSAT=.9999,
 INVERT=1, MDOTL=0.,
 DELT=.1, DTIME=1.,
 $
P$PHASE
C           MIX AFTER QUENCH
 IMIX=1,
 DELT=0.,
 PRESET=0.,
 $
P$PHASE
C           ZERO-G-COAST BETWEEN BURN 2-3
C           THERMODYNAMIC EQUILIBRIUM
C           VENT TANK TO 18 PSIA
 DELT=6990.,
 IFLOW=1,
 IMIX=1,
 IREG=1, INVERT=-1, LFILM=1, TDRAIN=1.E10,
 PRESET=18.,
 $
P$PHASE
C           PRESSURIZE TO NPSP OF 0.5 PSI PRIOR TO ENGINE BURN 3
 DELT=10., LFILM=0, DTIME=.1,
 IFLOW=0,
 IREG=3,
 $
P$PHASE
C           BURN 3 START
C           AUTOGENOUS PRESSURIZATION
C           NPSP=.5 PSI
 DTIME=10.,
 CONSAT=.05,
 DELT=3277.,
 F=500.,
 IFLOW=0,
 IREG=2,
 MDOTL=.1623,
 $
P$PHASE
C           QUENCH WALLS
 FQUENV=1., F=.001, CONSAT=.9999,
 INVERT=1, MDOTL=0.,
 DELT=.1, DTIME=1.,
 $
P$PHASE
C           MIX AFTER QUENCH
 IMIX=1,
 DELT=0.,
 PRESET=0.,
 $
P$PHASE
C           ZERO-G-COAST BETWEEN BURN 3-4
C           THERMODYNAMIC EQUILIBRIUM
C           VENT TANK TO 18 PSIA
 DELT=8255.,
 IFLOW=1,
 IMIX=1,
 IREG=1, INVERT=-1, LFILM=1, TDRAIN=1.E10,
 PRESET=18.,
 $
P$PHASE
```

```
C           PRESSURIZE TO NPSP OF 0.5 PSI PRIOR TO ENGINE BURN 4
 DELT=10., LFILM=0, DTIME=.1,
 IFLOW=0,
 IREG=3,
 $
P$PHASE
C           BURN 4 START
C           AUTOGENOUS PRESSURIZATION
C           NPSP=.5 PSI
 DTIME=10.,
 CONSAT=.05,
 DELT=3035.,
 F=500.,
 IFLOW=0,
 IREG=2,
 MDOTL=.1623,
 $
P$PHASE
C           QUENCH WALLS
 FQUENV=1., F=.001, CONSAT=.9999,
 INVERT=1, MDOTL=0.,
 DELT=.1, DTIME=1.,
 $
P$PHASE
C           MIX AFTER QUENCH
 IMIX=1,
 DELT=0.,
 PRESET=0.,
 $
P$PHASE
C           ZERO-G-COAST BETWEEN BURN 4-5
C           THERMODYNAMIC EQUILIBRIUM
C           VENT TANK TO 18 PSIA
 DELT=9972.,
 IFLOW=1,
 IMIX=1,
 IREG=1, INVERT=-1, LFILM=1, TDRAIN=1.E10,
 PRESET=18.,
 $
P$PHASE
C           PRESSURIZE TO NPSP OF 0.5 PSI PRIOR TO ENGINE BURN 5
 DELT=10., LFILM=0, DTIME=.1,
 IFLOW=0,
 IREG=3,
 $
P$PHASE
C           BURN 5 STAPT
C           AUTOGENOUS PRESSUPIZATION
C           NPSP=.5 PSI
 DTIME=10.,
 CONSAT=.05,
 DELT=2810.,
 F=500.,
 IFLOW=0,
 IREG=2,
 MDOTL=.1623,
 $
P$PHASE
C           QUENCH WALLS
 FQUENV=1., F=.001, CONSAT=.9999,
 INVERT=1, MDOTL=0.,
 DELT=.1, DTIME=1.,
```

```
 $
P$PHASE
C           MIX AFTER QUENCH
 IMIX=1,
 DELT=0.,
 PRESET=0.,
 $
P$PHASE
C           ZERO-G-COAST BETWEEN BURN 5-6
C           THERMODYNAMIC EQUILIBRIUM
C           VENT TANK TO 18 PSIA
 DELT=12424.,
 IFLOW=1,
 IMIX=1,
 IREG=1, INVERT=-1, LFILM=1, TDRAIN=1.E10,
 PRESET=18.,
 $
P$PHASE
C           PRESSURIZE TO NPSP OF 0.5 PSI PRIOR TO ENGINE BURN 6
 DELT=10., LFILM=0, DTIME=.1,
 IFLOW=0,
 IREG=3,
 $
P$PHASE
C           BURN 6 START
C           AUTOGENOUS PRESSURIZATION
C           NPSP=.5 PSI
 DTIME=10.,
 CONSAT=.05,
 DELT=2602.,
 F=500.,
 IFLOW=0,
 IREG=2,
 MDOTL=.1623,
 $
P$PHASE
C           QUENCH WALLS
 FQUENV=1., F=.001, CONSAT=.9999,
 INVERT=1, MDOTL=0.,
 DELT=.1, DTIME=1.,
 $
P$PHASE
C           MIX AFTER QUENCH
 IMIX=1,
 DELT=0.,
 PRESET=0.,
 $
P$PHASE
C           ZERO-G-COAST BETWEEN BURN 6-7
C           THERMODYNAMIC EQUILIBRIUM
C           VENT TANK TO 18 PSIA
 DELT=16198.,
 IFLOW=1,
 IMIX=1,
 IREG=1, INVERT=-1, LFILM=1, TDRAIN=1.E10,
 PRESET=18.,
 $
P$PHASE
C           PRESSURIZE TO NPSP OF 0.5 PSI PRIOR TO ENGINE BURN 7
 DELT=10., LFILM=0, DTIME=.1,
 IFLOW=0,
 IREG=3,
```

```
 $
P$PHASE
C           BURN 7 START
C           AUTOGENOUS PRESSURIZATION
C           NPSP=.5 PSI
 DTIME=10.,
 CONSAT=.05,
 DELT=2409.,
 F=500.,
 IFLOW=0,
 IREG=2,
 MDOTL=.1623,
 $
P$PHASE
C           QUENCH WALLS
 FQUENV=1., F=.001, CONSAT=.9999,
 INVERT=1, MDOTL=0.,
 DELT=.1, DTIME=1.,
 $
P$PHASE
C           MIX AFTER QUENCH
 IMIX=1,
 DELT=0.,
 PRESET=0.,
 $
P$PHASE
C           ZERO-G-COAST BETWEEN BURN 7-8
C           THERMODYNAMIC EQUILIBRIUM
C           VENT TANK TO 18 PSIA
 DELT=22426.,
 IFLOW=1,
 IMIX=1,
 IREG=1, INVERT=-1, LFILM=1, TDRAIN=1.E10,
 PRESET=18.,
 $
P$PHASE
C           PRESSURIZE TO NPSP OF 0.5 PSI PRIOR TO ENGINE BURN 8
 DELT=10., LFILM=0, DTIME=.1,
 IFLOW=0,
 IREG=3,
 $
P$PHASE
C           BURN 8 START
C           AUTOGENOUS PRESSURIZATION
C           NPSP=.5 PSI
 DTIME=10.,
 CONSAT=.05,
 DELT=2230.,
 F=500.,
 IFLOW=0,
 IREG=2,
 MDOTL=.1623,
 $
P$PHASE
C           QUENCH WALLS
 FQUENV=1., F=.001, CONSAT=.9999,
 INVERT=1, MDOTL=0.,
 DELT=.1, DTIME=1.,
 $
P$PHASE
C           MIX AFTER QUENCH
 IMIX=1,
```

```
 DELT=0.,
 PRESET=0.,
 $
P$PHASE
C          ZERO-G-COAST BETWEEN BURN 8-9
C          THERMODYNAMIC EQUILIBRIUM
C          VENT TANK TO 18 PSIA
 DELT=22279.,
 IFLOW=1,
 IMIX=1,
 IREG=1, INVERT=-1, LFILM=1, TDRAIN=1.E10,
 PRESET=18.,
 $
P$PHASE
C          PRESSURIZE TO NPSP OF 0.5 PSI PRIOR TO ENGINE BURN 9
 DELT=10., LFILM=0, DTIME=.1,
 IFLOW=0,
 IREG=3,
 $
P$PHASE
C          BURN 9 START
C          AUTOGENOUS PRESSURIZATION
C          NPSP=.5 PSI
 DTIME=10.,
 CONSAT=.05,
 DELT=11000.,
 F=500.,
 IFLOW=0,
 IREG=2,
 MDOTL=.1623,
 NEXT=5,
 $
```

National Aeronautics & Space Administration
Lewis Research Center
21000 Brookpart Road
Cleveland, Ohio 44135

		M S	Copies
Attn	Communications & Propulsion	500-306	1
	E A Bourke	501-5	2
	Technical Utilization Office	3-19	1
	Technical Report Control Office	5-5	1
	AFSC Liaison Officer	501-3	2
	Library	60-3	2
	Office of Rel & Quality Assurance	500-211	1
	J C Aydelott, Project Manager	501-6	20
	L J Ross	3-7	1
	D A Petrash	501-5	1
	R J Priem	501-6	1
	T H Cochran	501-7	1
	S H Gorland	501-8	1
	G R Smolak	501-6	1
	E P Symons	501-6	1
	T L Labus	501-7	1

National Aeronautics and Space Administration
Headquarters
Washington, D C 20546

Attn	RS-5/Director, Space Systems Division	1
	RT-6/Director, Research & Technology Division	1
	RTP-6/F W Stephenson	1
	ME-7/P N Herr	1
	RST-5/E Gabris	1
	RST-5/M Cuviello	1

National Aeronautics & Space Administration
Goddard Space Flight Center
Greenbelt, Maryland 20771

Attn	Library		1
	A Sherman	713	1

National Aeronautics & Space Administration
John F Kennedy Space Center
Kennedy Space Center, Florida 32899

Attn	Library	1
	DD-MED-41/F S Howard	1
	DF-PED/W H Boggs	1

National Aeronautics & Space Administration
Ames Research Center
Moffett Field, California 94035

Attn	Library		1
	Dr W Brooks	244-7	1

National Aeronautics & Space Administration
Langley Research Center
Hampton, Virginia 23365

Attn	Library	1

National Aeronautics & Space Administration
Johnson Space Center
Houston, Texas 77001

		M S	Copies
Attn	Library		1
	EP2/Z D Kirkland		1
	EP5/W Chandler		1
	EP4/Dale Connelly		1
	ED4/C J LeBlanc		1

National Aeronautics & Space Administration
George C Marshall Space Flight Center
Huntsville, Alabama 35812

Attn	Library	1
	EP43/L Hastings	1
	EP43/A L Worlund	1
	EP41/Dr Wayne Littles	1
	ES63/E W Urban	1

Jet Propulsion Laboratory
4800 Oak Grove Drive
Pasadena, California 91103

Attn	Library		1
	Don Young	507-228	1
	P W Garrison		1

NASA Scientific & Technical Information Facility
P O Box 8757
Balt/Wash. International Airport, Maryland 21240

Attn	Accessioning Department	10

Defense Documentation Center
Cameron Station - Bldg 5
5010 Duke Street
Alexandria, Virginia 22314

Attn.	TISIA	1

National Aeronautics & Space Administration
Flight Research Center
P O. Box 273
Edwards, California 93523

Attn.	Library	1

Air Force Rocket Propulsion Laboratory
Edwards, California 93523

Attn.	LKCC/J E Brannigan	1
	LKDS/R L Wiswell	1
	LKDM/Wayne Pritz	1
	LKCC/R A Silver	1

Aeronautical Systems Division
Air Force Systems Command
Wright Patterson Air Force Base
Dayton, Ohio 45433

Attn	Library	1

	M S	Copies
Air Force Office of Scientific Research Washington, D C 20333 Attn Library		1
Aerospace Corporation 2400 E El Segundo Blvd Los Angeles, California 90045 Attn Library - Documents		1
Beech Aircraft Corporation Boulder Facility Box 9631 Boulder, Colorado 80301 Attn Library		1
R A Mohling		1
S Willen		1
Bell Aerosystem, Inc Box 1 Buffalo, New York 14240 Attn Library		1
J Colt		1
T Hinterman		1
Boeing Company P O Box 3999 Seattle, Washington 98124 Attn Library		1
C L Wilkensen	8K/31	1
T J Kramer	8C/05	1
Chrysler Corporation Space Division P O Box 29200 New Orleans, Louisiana 70129 Attn Library		1
McDonnell Douglas Astronautics Co 5301 Bolsa Avenue Huntington Beach, California 92647 Attn Library		1
E C Cady		1
Missiles and Space Systems Center General Electric Company Valley Force Space Technology Center P O Box 8555 Philadelphia, Pennsylvania 19101 Attn Library		1

	M S	Copies
IIT Research Institute Technology Center Chicago, Illinois 60616 Attn Library		1
Lockheed Missiles & Space Company P O Box 504 Sunnyvale, California 94087 Attn Library		1
G D Bizzell		1
S G DeBrock		1
Battelle Memorial Institute Columbus Labs 505 King Avenue Columbus, Ohio 43201 Attn E Rice		1
Space Division Rockwell International Corp 12214 Lakewood Blvd Downey, California 90241 Attn Library		1
A Jones		1
A F Brux		1
Northrop Research & Technology Center 1 Research Park Palos Verdes Peninsula, California 90274 Attn Library		1
TRW Systems, Inc 1 Space Park Redondo Beach, California 90278 Attn. Tech Lib Doc Acquisitions		1
National Science Foundation, Engr Div 1800 G Street, NW Washington, D C. 20540 Attn Library		1
Florida Institute of Technology M E Department Melbourne, Florida 32901 Attn Dr T E Bowmann		1
RCA/AED P O Box 800 Princeton, New Jersey 08540 Attn Mr Daniel Balzer		1

	M S	Copies
Southwest Research Institute Department of Mechanical Sciences P O Drawer 28510 San Antonio, Texas 78284 Attn H Norman Abramson		1
Franklin Dodge		1
McDonnell Douglas Astronautics Co - East P O Box 516 St Louis, Missouri 63166 Attn G Orton		1
W Regnier		1
Xerox Electro-Optical Systems 300 North Halstead Pasadena, California 91107 Attn Robert Richter		1
Science Applications, Inc 1200 Prospect Street P O Box 2351 La Jolla, California 92038 Attn M Blatt		1
Martin Marietta Denver Aerospace P O Box 179 Denver, Colorado 80201 Attn Library		1
D A Fester		1
R N Eberhardt		1

End of Document